Status of petrale sole (*Eopsetta jordani*) along the U.S. West Coast in 2023

by

Ian G. Taylor[1]
Vladlena Gertseva[1]
Nick Tolimieri[1]

[1]Northwest Fisheries Science Center, U.S. Department of Commerce, National Oceanic and Atmospheric Administration, National Marine Fisheries Service, 2725 Montlake Boulevard East, Seattle, Washington 98112

December 2023

Please cite this publication as

Taylor, I.G., V. Gertseva, N. Tolimieri. 2023. Status of petrale sole (*Eopsetta jordani*) along the U.S. West Coast in 2023. Pacific Fishery Management Council, Portland, Oregon. 174 p.

Contents

One-page summary

- This assessment reports the status of petrale sole (*Eopsetta jordani*) off the U.S. West Coast using data through 2022.
- Petrale sole is a commercially value flatfish primarily caught using bottom trawl gear.
- The most recent full stock assessments was in 2013 which was updated in 2015 and 2019.
- All data series have been extended with new data from 2019–2022 and historical data have been updated, including substantial changes to the time series of historical catch landed in Washington.
- The model has been simplified by combining Winter and Summer subsets of the fleets and removing indices of fishery catch per unit effort with little impact on the model results. There are 267 estimated parameters in the current assessment vs 304 in the 2019 update.
- Model estimates are substantially similar to previous assessments although the addition of a fecundity relationship changes the units of spawning output from biomass in metric tons to trillions of eggs. Estimates of the fraction of unfished spawning output in 2019 increased slightly from 0.387 to 0.4.
- Estimates of current (2023) fraction of unfished is 0.336, above the target reference point of 0.25 and an overfished threshold of 0.125. However, the biomass is estimated to be declining due to below-average recruitments in recent years.
- Estimates of recent fishing intensity have been slightly below the limit reference point.
- In general the data on petrale sole are informative due to large sample sizes of length and age data from fisheries and surveys, high frequency of occurrence in the bottom trawl survey, and strong contrast in the data caused by fishing down the stock to a low level followed by rapid rebuilding. Thus, many of the sensitivty analyses show relatively little impact on the results.
- Projections will be completed during the STAR panel and added to this summary.

Executive summary

Stock

This assessment reports the status of petrale sole (*Eopsetta jordani*) off the U.S. West Coast using data through 2022. While petrale sole are modeled as a single stock, the spatial aspects of the coastwide population are addressed through geographic separation of data sources/fleets where possible. There is currently no genetic evidence suggesting distinct biological stocks of petrale sole off the U.S. West Coast. The limited tagging data available to describe adult movement suggests that petrale sole may have some homing ability for deep water spawning sites but also have the ability to move long distances between spawning sites.

Catches

Petrale sole has consistently been the most commercially valuable flatfish targeted in the California Current Ecosystem. It has been caught in the flatfish fishery off the U.S. West Coast since the late 19th century, nearly exclusively by trawl fleets; non-trawl gears contribute only a small fraction of the catches across all years.
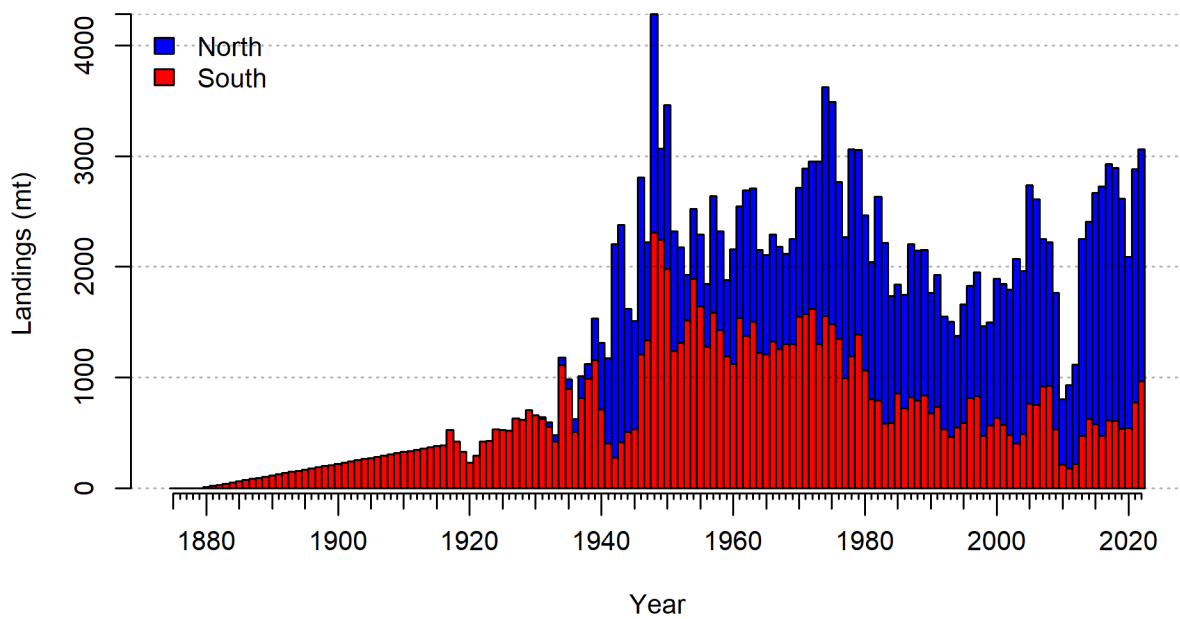
The earliest catches of petrale sole are reported in 1876 in California and 1884 in Oregon. Petrale sole were lightly exploited during the early 1900s, but new gear technology in the 1930s allowed trawling on new grounds and the fishery expanded to greater depths and to Oregon and Washington waters, resulting in larger landings. The petrale sole catches further increased during World War II in response to increased demands. Also, during the "vitamin A rush" in the late 1930s and 1940s it was found that petrale sole has high levels, which contributed to increased catches of this species as well. By the 1950s, the fishery was well developed with the stock showing declines in biomass and catches (Figures i and ii). Also in the 1950s, winter spawning grounds at deeper depths with dense concentrations of petrale sole were discovered, and catches increased accordingly. The rate of decline in spawning biomass accelerated through the 1970s reaching minimums estimated to be generally around or below 10% of the unexploited levels during the 1980s through the early 2000s (Figure iii). Recent annual catches between 1981–2022 range between 803 and 3060 mt per year and the most recent landings are shown in Table i.

Petrale sole are a desirable market species and discarding has historically been low (less than 5%), with most of the discarding due to small sizes.

In this assessment, fishery removals have been divided between two fleets: 1) North and 2) South. Landings for the North fleet are defined as fish landed in Washington and Oregon ports. Landings for the South fleet are defined as fish landed in California ports.

Table i: Recent landings by fleet, total landings summed across fleets, and the total mortality including discards for the model area.

| Year	North (mt)	South (mt)	Total Catch (mt)	Total Dead (mt)
2013	1776.22	477.14	2253.36	2275.27
2014	1783.41	625.33	2408.74	2425.38
2015	2085.62	579.55	2665.17	2680.84
2016	2254.21	473.42	2727.63	2742.78
2017	2313.91	616.71	2930.62	2945.85
2018	2284.80	609.64	2894.44	2905.59
2019	2079.95	536.96	2616.91	2626.94
2020	1548.72	543.41	2092.13	2099.60
2021	2103.03	776.08	2879.11	2888.83
2022	2093.58	966.36	3059.94	3070.05

Figure i: Landings by fleet used in the base model where catches in metric tons by fleet are stacked.

Data and assessment

This assessment uses the stock assessment framework Stock Synthesis (SS3; (Methot and Wetzel 2013)) version 3.30.21.00 released 10 February, 2023. The last full assessment of petrale sole was conducted in 2013 and most recent update assessment in 2019.

The modeling period begins in 1876, assuming an unfished equilibrium state of the stock in 1875. The assessment treats females and males separately due to differences in biology and life history parameters between sexes, and the coastwide population is modeled allowing separate growth and mortality parameters for each sex (a two-sex model). The model also allows for differences in selectivity between sexes.

Types of data that inform the model include catch, length and age frequency data from two commercial fleets, that include 1) North and 2) South. Biological data are derived from both port and on-board observer sampling programs. The AFSC/NWFSC West Coast Triennial Shelf Survey (Triennial Survey) (1980, 1983, 1986, 1989, 1992, 1995, 1998, 2001, and 2004) and the NWFSC West Coast Groundfish Bottom Trawl Survey (WCGBTS) (2003–2019, 2021–2022) relative biomass indices and biological sampling provide fishery independent information on relative trend and demographics of the petrale sole stock.

The definition of fishing fleets changed in this assessment relative to the 2019 assessment. Previously, North and South fleets were additionally divided into seasonal fisheries (Winter and Summer), with fishing year starting in November of previous year. In this assessment, Winter and Summer fisheries are combined within each fleet into annual fisheries with removals corresponding to calendar year.

Growth is assumed to follow the von Bertalanffy growth model, and the assessment explicitly estimates all parameters describing somatic growth. Natural mortality is estimated for both sexes using a meta-analytical prior. Externally estimated life history parameters, including those defining the length-weight relationship, female fecundity and maturity schedule were revised for this assessment to incorporate new information. Recruitment dynamics are assumed to follow the Beverton-Holt stock-recruit function, and recruitment deviations are estimated. Stock-recruitment steepness is fixed at the value generated from meta-analytical study.
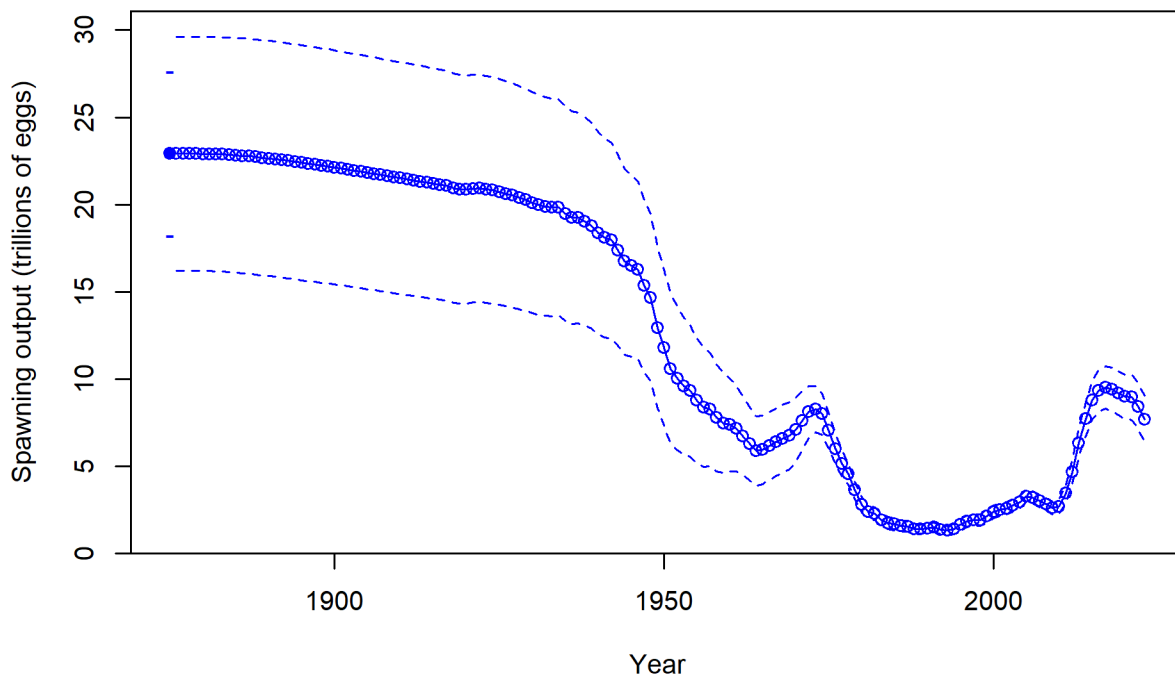
Stock biomass and dynamics

The base model estimate of biomass time series is similar to previous assessments with estimated biomass of ages 3 and older estimated around 42,198 mt in the unfished equilibrium, declining to a minimum of 5,104 mt in 1992, rebuilding quickly to a recent peak of 21,507 mt in 2015 due to 3 years of very high recruitments from 2006 to 2008, and then declining to 15,803 mt in 2023 due to low or average recruitment in the years since.
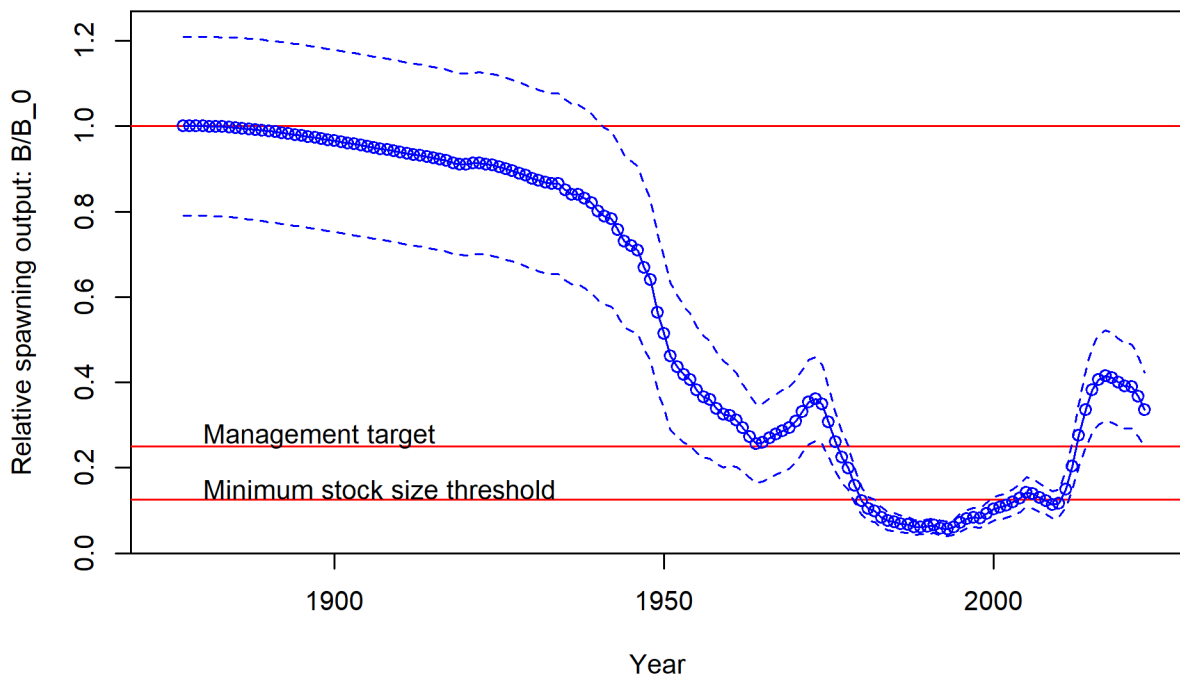
In terms of fraction of unfished spawning output, the minimum was 0.057 in 1993, the recent peak was 0.415 in 2017 and the 2023 estimate is 0.336 (Figure iii, Table ii).

Table ii: Estimated recent trend in spawning output (trillions of eggs) and the fraction unfished and the 95 percent intervals for the model area.

Year	Spawning output (trillions of eggs)	Lower Interval	Upper Interval	Fraction Unfished	Lower Interval	Upper Interval
2013	6.30	5.48	7.12	0.28	0.20	0.35
2014	7.70	6.72	8.68	0.34	0.25	0.43
2015	8.77	7.67	9.87	0.38	0.28	0.48
2016	9.32	8.15	10.48	0.41	0.30	0.51
2017	9.51	8.30	10.72	0.42	0.31	0.52
2018	9.40	8.16	10.64	0.41	0.31	0.52
2019	9.17	7.91	10.44	0.40	0.30	0.50
2020	8.97	7.69	10.25	0.39	0.29	0.49
2021	8.94	7.64	10.24	0.39	0.29	0.49
2022	8.42	7.10	9.73	0.37	0.27	0.46
2023	7.69	6.35	9.02	0.34	0.25	0.42

Figure ii: Estimated time series of spawning output (circles and line: median; light broken lines: 95 percent intervals) for the base model.

Figure iii: Estimated time series of fraction of unfished spawning output (circles and line: median; light broken lines: 95 percent intervals) for the base model.
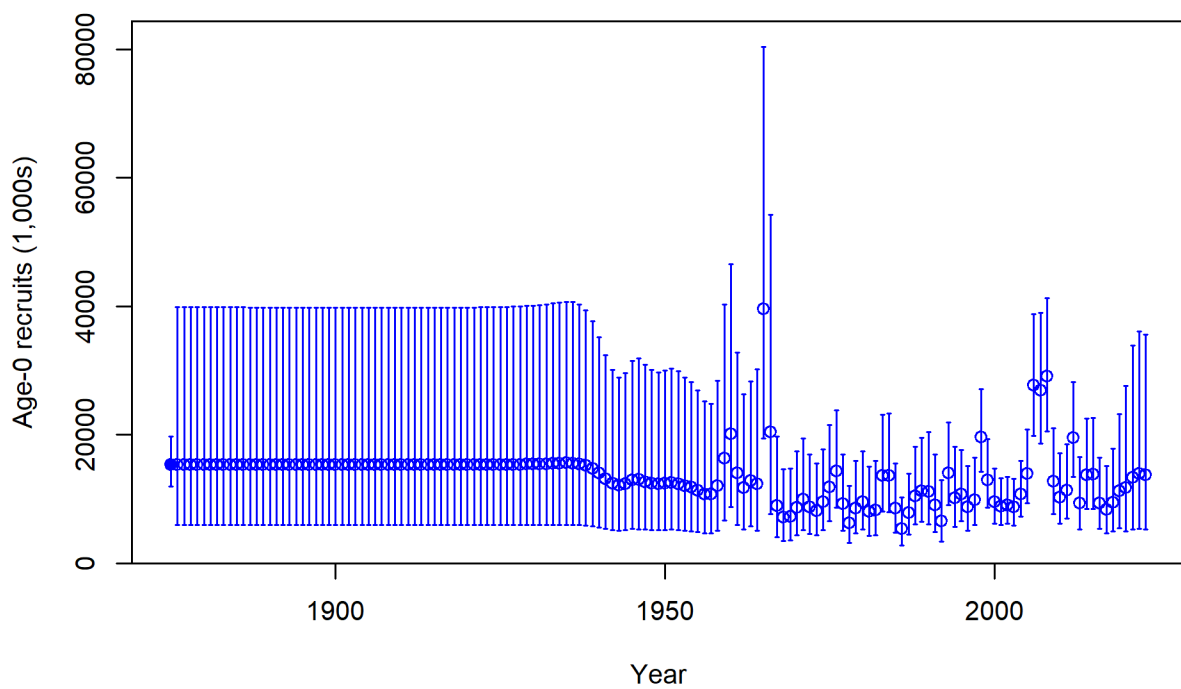
Recruitment

Recruitment dynamics (Figure iv, Table iii) are assumed to follow Beverton-Holt stock-recruit function and the steepness parameter was fixed at the value of 0.8, which is the mean of steepness prior probability distribution, derived from meta-analysis of flatfish stocks. The level of virgin recruitment (R0) is estimated to inform the magnitude of the initial stock size. Annual recruitment is treated as stochastic. "Main" recruitment deviations were estimated for modeled years that had information about recruitment, between 1959 and 2020. We additionally estimated "early" deviations between 1845 and 1958.
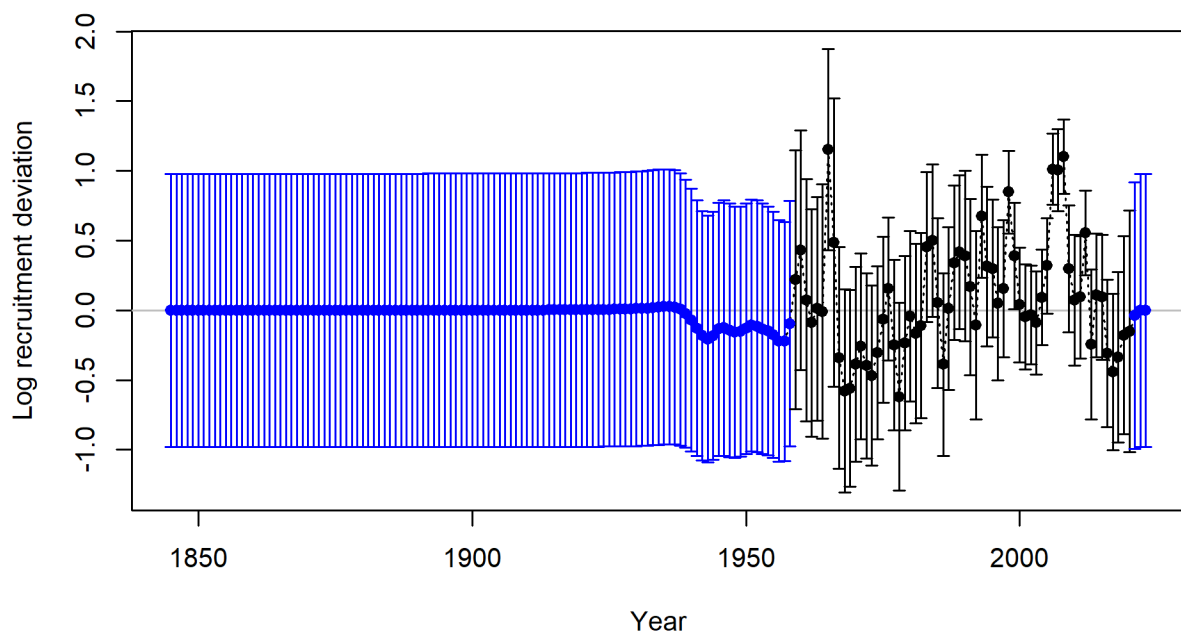
The recruitment time series is punctuated by four large recruitment events in 1965, 2006, 2007, and 2008. The 1965 recruitment was estimated at about 40 million age-0 recruits while the latter three were in the 25–30 million range. The rest of the time series is close to 10 million recruits per year. The recruitment in 2012 was almost 20 million (a positive deviation from the stock-recruit curve of 0.56) but the years since are estimated to have had below-average or close-to-average recruitment, with a low point in 2017 of about 8 million recruits (deviation = -0.44).

Table iii: Estimated recent trend in recruitment (1,000s) and recruitment deviations and the 95 percent intervals for the model area.

Year	Recruit-ment (1,000s)	Lower Interval	Upper Interval	Recruit-ment Devia-tions	Lower Interval	Upper Interval
2013	9321.94	5255.42	16535.05	-0.24	-0.78	0.29
2014	13734.50	8398.55	22460.61	0.11	-0.34	0.55
2015	13832.00	8463.06	22606.98	0.09	-0.35	0.54
2016	9356.73	5330.66	16423.54	-0.31	-0.84	0.22
2017	8356.41	4627.47	15090.23	-0.44	-1.00	0.12
2018	9426.22	4990.68	17803.90	-0.34	-0.95	0.27
2019	11209.00	5427.01	23151.20	-0.18	-0.89	0.53
2020	11693.60	4949.64	27626.29	-0.15	-1.02	0.71
2021	13307.30	5224.16	33897.20	-0.04	-0.99	0.92
2022	13890.30	5344.69	36099.46	0.00	-0.98	0.98
2023	13694.70	5267.81	35602.06	0.00	-0.98	0.98

Figure iv: Estimated time series of age-0 recruits (1000s) for the base model with 95 percent intervals.

Figure v: Estimated time series of recruitment deviations.
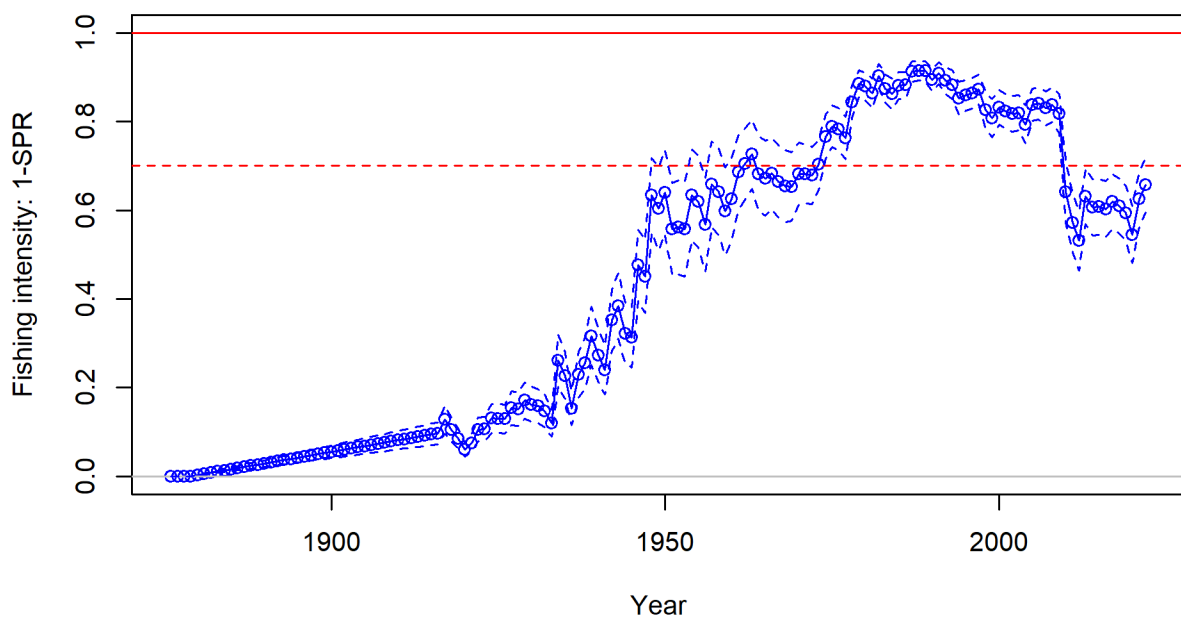
Exploitation status

Two measures of exploitation are fishing intensity and exploitation rate. Fishing intensity is defined here as 1 - SPR, where SPR is the equilibrium spawning output at a given combination of F and selectivity relative to spawning output at unfished equilibrium. Using the units of 1-SPR means that more intense fishing is associated with a higher value. The value of 1-SPR in the absence of fishing is 0 and the maximum is 1.0 if all spawning fish are being killed before spawning. The Pacific Fishery Management Council (PFMC) has chosen an SPR target of 0.3 for petrale sole so harvest which leads to SPR below 0.3, or fishing intensity (1-SPR) greater than 0.7 would be overfishing. Exploitation rate is defined as the catch relative to age 3+ biomass. This metric is included because interpretation is simple, but it is not used as a basis for management.

The estimated time series of exploitation (Figures vi and vii, Table iv) shows an accelerating increase in fishing intensity and exploitation rate with a peak around 1990 when the 1-SPR increased to 0.91 and the exploitation rate was close to 0.4. These rates are estimated to have declined slowly up to the point where the overfishing declaration led to dramatic decrease in catch in 2010, when 1-SPR fell below the reference point to about 0.64. The fishing intensity has increased since that time due to the rebuilding of the stock, but is estimated to have remained below the reference point in the years since.

Table iv: Estimated recent trend in the 1-SPR (where SPR is the spawning potential ratio) and the exploitation rate, along with the 95 percent intervals associated with each of those quantities for the model area .

Year	1-SPR	Lower Interval	Upper Interval	Exploita- tion Rate	Lower Interval	Upper Interval
2013	0.63	0.57	0.69	0.11	0.10	0.13
2014	0.61	0.54	0.67	0.12	0.10	0.13
2015	0.61	0.54	0.67	0.12	0.11	0.14
2016	0.60	0.54	0.67	0.13	0.11	0.14
2017	0.62	0.56	0.68	0.14	0.12	0.16
2018	0.61	0.55	0.67	0.14	0.12	0.16
2019	0.59	0.53	0.66	0.13	0.12	0.15
2020	0.55	0.48	0.61	0.11	0.10	0.13
2021	0.63	0.56	0.69	0.16	0.14	0.18
2022	0.66	0.60	0.72	0.18	0.15	0.21

Figure vi: Estimated time series of the fishing intensity (1 - SPR), where SPR is the spawning potential ratio, with approximate 95% asymptotic intervals. The horizontal line at 0.7 corresponds to SPR = 0.3, the management reference point for petrale sole. The horizontal line at 1.0 corresponds to SPR = 0 (all spawning fish removed from the population).
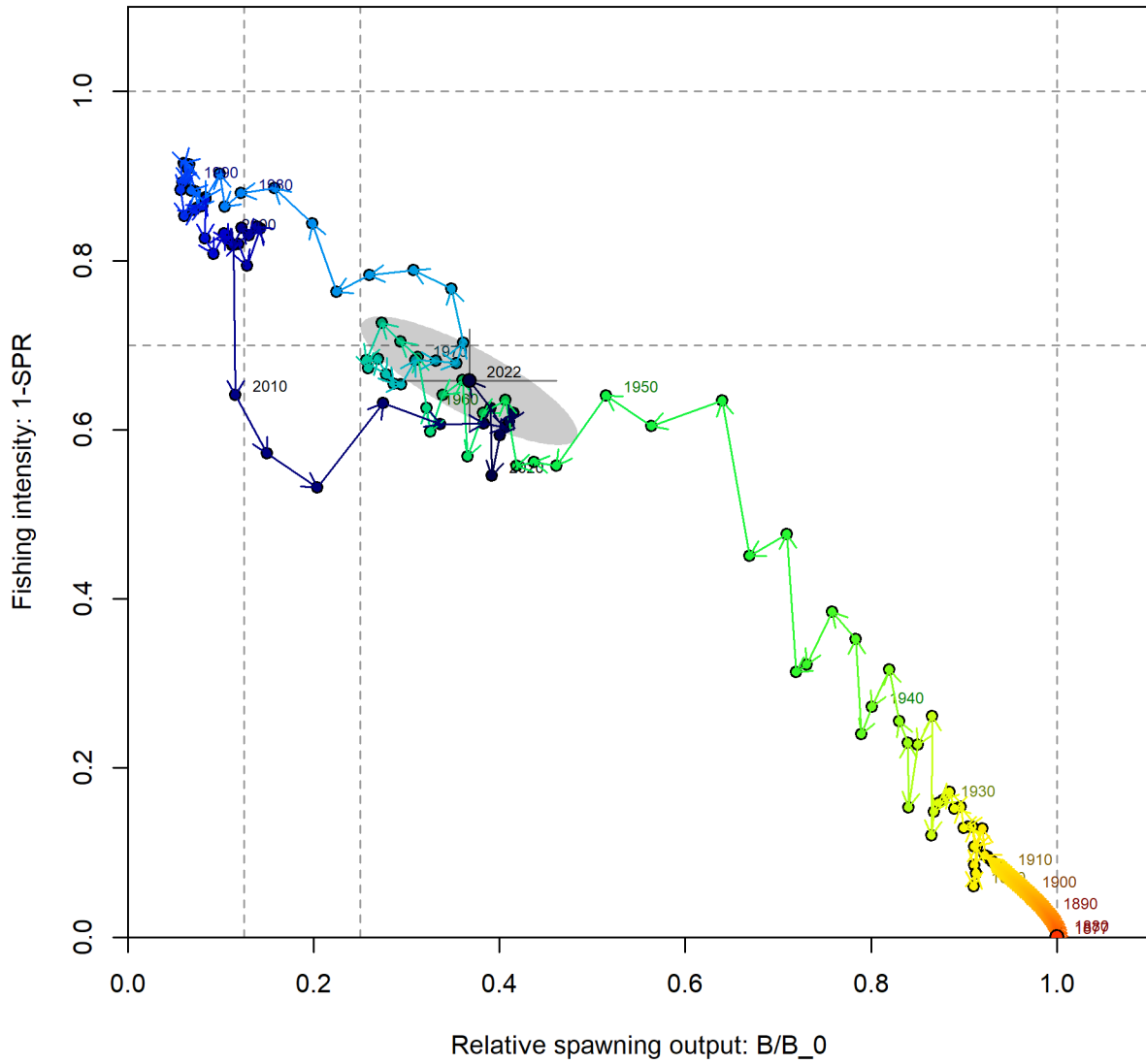
Ecosystem considerations

Haltuch et al. (2020) examined the relationship between petrale sole recruitment and oceanographic drivers based on model output from a Regional Ocean Modeling System (ROMS) model for the California Current Ecosystem (Neveu et al. 2016). The results suggested that ROMS output might be useful as the basis for an environmental index of recruitment for petrale sole, to allow for better model precision and near-term forecasting. However, the ROMS model used by Haltuch et al. (2020) was consistent in structure and inputs for 1980–2010. In 2011, the model was updated, and from 2011 forward, ROMS outputs exhibit distinct discontinuities with 1980–2010 period, showing changes in scale and trend across the 2010/2011 boundary for multiple drivers used to inform the index by Haltuch et al. (2020). Appendix A of this report illustrates the discontinuities in ROMS products over the 2010/2011 boundary and discusses potential reasons for why the ROMS time series changed after the model was updated in 2011.
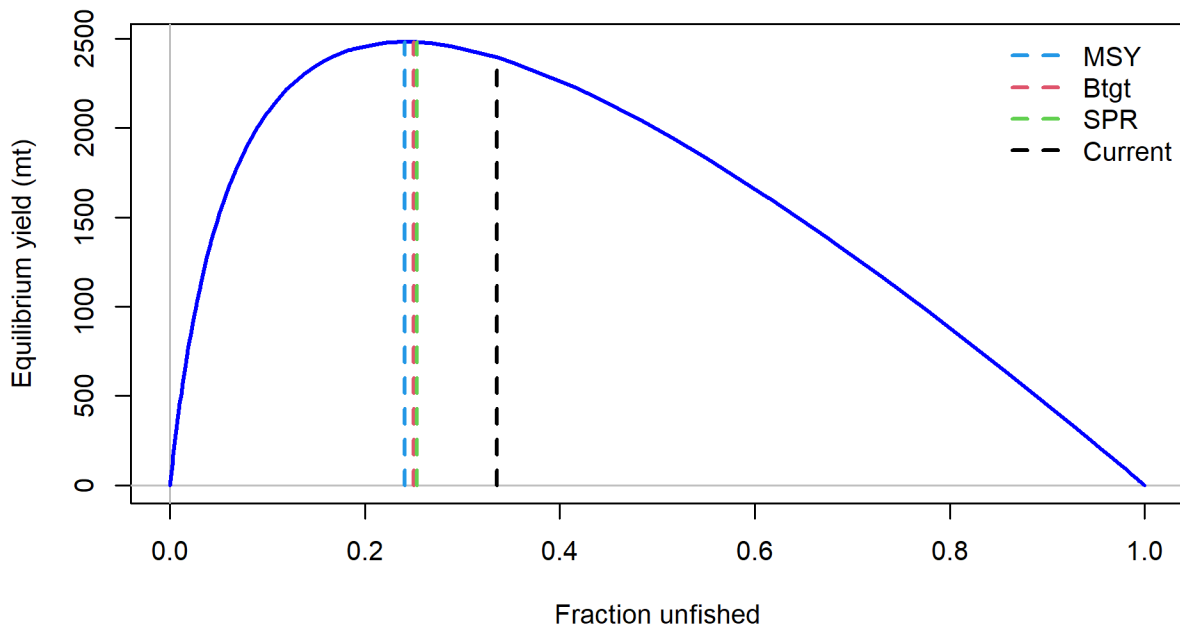
Due to discontinuity in ROMS models between periods before and after 2011, the index developed by Haltuch et al. (2020) could not be used for this stock assessment. However, an alternative oceanographic model products by Copernicus Marine Environment Monitoring Service (CMEMS) (https://marine.copernicus.eu/) and Mercator Ocean International (MOI) (https://www.mercator-ocean.eu/) were investigated to test if this modelling framework could be used to produce an environmental index of petrale sole recruitment. This new effort is ongoing, and has not yet been published or reviewed by the Scientific and Statistical Committee (SSC) of the PFMC. Appendix A of this report describes the most recent, preliminary efforts in developing a new environmental index of petrale sole recruitment based on CMEMS products. In this assessment, we explore the impact of the current CMEMS-based environmental index of petrale sole recruitment via sensitivity analysis.

Reference points

Unfished spawning stock output for petrale sole is estimated to be 22.9 trillion eggs (95% confidence interval: 18–28 trillion eggs). The management biomass target for petrale sole is defined as 25% of the unfished spawning output ($B_{25\%}$), which is estimated by the model to be 5.7 trillion eggs (95% confidence interval: 4.5–6.9 trillion eggs), which corresponds, in a theoretical equilibrium state, to an exploitation rate (catch / age 3+ biomass) of 0.18 (Figure viii, Table v). This harvest rate provides an equilibrium yield of 2481 mt at $B_{25\%}$ (95% confidence interval: 2120–2841 mt). Catch limits are determined by an SPR = 30% reference point which is associated with equilibrium exploitation rate of 0.17. The model estimate of maximum sustainable yield (MSY) is 2482 mt (95% confidence interval: 2121–2842 mt). The estimated spawning stock output at MSY is 5.5 trillion eggs (95% confidence interval: 4.3–6.7 trillion eggs). The exploitation rate corresponding to the estimated F_{MSY} proxy of SPR = 29% is 0.18.

Figure vii: Phase plot of estimated 1-SPR versus fraction unfished for the base model.

Figure viii: Equilibrium yield curve for the base case model. Values are based on the most recent fishery selectivities and retention curves and with steepness fixed at 0.80.

Table v: Summary of reference points and management quantities, including estimates of the 95 percent intervals for the model area.

	Estimate	Lower Interval	Upper Interval
Unfished Spawning output (trillions of eggs)	22.91	18.08	27.73
Unfished Age 3+ Biomass (mt)	42197	34891	49503
Unfished Recruitment (R0)	15357	11505	19208
Spawning output (trillions of eggs) (2023)	7.69	6.35	9.02
Fraction Unfished (2023)	0.34	0.25	0.42
Reference Points Based SO25%			
Proxy Spawning output (trillions of eggs) SO25%	5.73	4.52	6.93
SPR Resulting in SO25%	0.30	0.30	0.30
Exploitation Rate Resulting in SO25%	0.18	0.16	0.19
Yield with SPR Based On SO25% (mt)	2480	2120	2841
Reference Points Based on SPR Proxy for MSY			
Proxy Spawning output (trillions of eggs) (SPR30)	5.80	4.58	7.03
SPR30	0.30	NA	NA
Exploitation Rate Corresponding to SPR30	0.17	0.16	0.19
Yield with SPR30 at SO SPR (mt)	2479	2119	2840
Reference Points Based on Estimated MSY Values			
Spawning output (trillions of eggs) at MSY (SO MSY)	5.52	4.32	6.72
SPR MSY	0.29	0.28	0.30
Exploitation Rate Corresponding to SPR MSY	0.18	0.16	0.20
MSY (mt)	2481	2121	2842

Management performance

In the last ten years total dead catches (including estimated dead discards) have been below the annual catch limit, although the attainment has been greater than 90% in many of those years.

Table vi: Recent trend in the overfishing limits (OFLs), the acceptable biological catches (ABCs), the annual catch limits (ACLs), the total landings, and total mortality (mt). The 'Total dead' values may differ from Groundfish Expanded Mortality Multi-Year (GEMM) estimates because the discard mortality is computed within the model based on estimated retention curves.

Year	OFL	ABC	ACL	Land-ings	To-tal.dead	Dead.ACL
2013	2711	2592	2592	2253	2275	0.88
2014	2774	2652	2652	2409	2425	0.91
2015	2946	2816	2816	2665	2681	0.95
2016	3044	2910	2910	2728	2743	0.94
2017	3280	3136	3136	2931	2946	0.94
2018	3152	3013	3013	2894	2906	0.96
2019	3042	2908	2908	2617	2627	0.90
2020	2976	2845	2845	2092	2100	0.74
2021	4402	4115	4115	2879	2889	0.70
2022	3936	3660	3660	3060	3070	0.84

Unresolved problems and major uncertainties

Uncertainty in this assessment model is explicitly captured in the asymptotic confidence intervals reported throughout this assessment for key parameters and management quantities. These intervals reflect the uncertainty in the model fit to the data sources included in the assessment, but do not include uncertainty associated with alternative model configurations or fixed parameters. To explore uncertainty associated with alternative model configurations and evaluate the responsiveness of model outputs to changes in key model assumptions, a variety of sensitivity runs were performed, including runs with different assumptions model structure and treatment of data, life-history parameters, stock-recruitment parameters, and many others. The uncertainty in natural mortality, stock-recruit steepness and the unfished recruitment level was also explored through likelihood profile analysis. Additionally, a retrospective analysis was conducted where the model was run after successively removing data from recent years, one year at a time.

Main life history parameters, such as natural mortality and stock-recruit curve steepness, generally contribute significant uncertainty to stock assessments. Steepness in this assessment was fixed at 0.8, which is meta-analytical steepness prior for Pleuronectidae. When estimated, steepness was approaching the upper parameter bound of 1, which was considered unrealistic as it was associated with less plausible estimates natural mortality around 0.10 (compared to base model estimates of 0.14 for females). Steepness likelihood profile illustrated that the starting and ending biomass and associated fraction unfished show almost no change across a wide range of steepness values. Natural mortality was estimated for both sexes using meta-analytical prior, but likelihood profile showed that the starting and ending biomass as well as associated fraction unfished are more sensitive to the changes in natural mortality than in steepness. In past several assessments, natural mortality was used as major axis of uncertainty.

Decision table and projections

The base model estimate for 2023 spawning depletion is 33.6%. The primary axis of uncertainty about this estimate used in the decision table is based on female natural mortality. Female natural mortality in the assessment model is estimated within the model, which includes a meta-analytical prior based on the maximum age of 32 years. The estimate in the base model is $M = 0.142$. The natural mortality value for the low state of nature is $M = 0.072$ and for high state of nature is $M = 0.219$. These alternative states were calculated as follows:

1. Low and high values for Spawning Output in 2023 were calculated as the 12.5% and 87.5% quantiles of a lognormal distribution with mean equal to the base model estimate and log standard deviation equal to the `Pstar_sigma` reported by r4ss: 0.0884. This is a log-scale calculation of $\sqrt{(log((SD/x)^2 + 1))}$ where $SD = 0.6807$ is the asymptotic estimate of the standard deviation and $x = 7.686$ is the point estimate and is very similar to the non-log CV (0.0886). The resulting low and high values for 2023 Spawning Output are 6.942 and 8.508.
2. The female natural mortality values associated with these low and high spawning output values were calculated using a linear model fit to the spawning output associated with the profile over female M: $SO_{2023} = 6.181 + 10.605M$. Inverting this relationship to calculate M provided the estimates of 0.072 and 0.219 around the point estimate of 0.142.

Twelve-year forecasts for each state of nature were calculated for two catch scenarios. One uses the default harvest control rule $P^* = 0.45$, and the other is based on harvest control rule with a lower $P^* = 0.40$. In each case the 2023 and 2024 catches are fixed at the ACLs which have been set for that year with estimated fleet allocation provided by the GMT. The alternative states of nature (Low, Base, and High) are provided in the columns of the Decision Table, with Spawning Output and Fraction of unfished provided for each state.

Table vii: Projections of estimated OFL (mt), ABC (mt), resulting ACLs (mt) based on the 25-5 rule and applied buffers, and estimated spawning output in trillions of eggs, and spawning output relative to unfished for 2025-2034, with assumed removals in 2023 and 2024 based on recommended values from the Groundfish Management Team.

Year	Adopted OFL (mt)	Adopted ABC (mt)	Adopted ACL (mt)	Assumed catch (mt)	OFL (mt)	Buffer	ABC	ACL	Spawn. Output	Frac. Unfished
2023	3763	3485	3485	3485	-	-	-	-	7.69	0.336
2024	3563	3285	3285	3285	-	-	-	-	6.70	0.293
2025	-	-	-	-	2518	0.935	2354	2354	5.85	0.255
2026	-	-	-	-	2424	0.930	2255	2238	5.56	0.243
2027	-	-	-	-	2422	0.926	2242	2217	5.48	0.239
2028	-	-	-	-	2475	0.922	2282	2263	5.55	0.242
2029	-	-	-	-	2549	0.917	2337	2334	5.69	0.248
2030	-	-	-	-	2618	0.913	2390	2390	5.85	0.255
2031	-	-	-	-	2672	0.909	2429	2429	5.99	0.261
2032	-	-	-	-	2709	0.904	2449	2449	6.09	0.266
2033	-	-	-	-	2733	0.900	2460	2460	6.16	0.269
2034	-	-	-	-	2749	0.896	2463	2463	6.20	0.271

Table viii: Decision table with 10-year projections. 'Mgmt' refers to the three management scenarios (A) the default harvest control rule $P^* = 0.45$, (B) harvest control rule with a lower $P^* = 0.40$. In each case the 2023 and 2024 catches are fixed at the ACLs which have been set for that year with estimated fleet allocation provided by the GMT. The alternative states of nature ('Low', 'Base', and 'High' as discussed in the text) are provided in the columns, with Spawning Output ('Spawn', in trillions of eggs) and Fraction of unfished ('Frac') provided for each state.

Mgmt	Year	Catch	Low Spawn M=0.072	Low Frac M=0.072	Base Spawn M=0.142	Base Frac M=0.142	High Spawn M=0.219	High Frac M=0.219
A	2023	3485	6.86	0.195	7.69	0.336	8.53	0.528
	2024	3285	6.03	0.172	6.70	0.292	7.41	0.458
	2025	2354	5.27	0.150	5.85	0.255	6.49	0.401
	2026	2238	4.97	0.141	5.56	0.243	6.17	0.382
	2027	2217	4.83	0.137	5.48	0.239	6.08	0.376
	2028	2263	4.78	0.136	5.55	0.242	6.14	0.380
	2029	2334	4.79	0.136	5.69	0.248	6.28	0.388
	2030	2390	4.80	0.137	5.85	0.255	6.43	0.398
	2031	2429	4.79	0.136	5.99	0.261	6.55	0.405
	2032	2449	4.75	0.135	6.09	0.266	6.62	0.409
	2033	2460	4.68	0.133	6.16	0.269	6.67	0.412
	2034	2463	4.59	0.131	6.20	0.271	6.69	0.414
B	2023	3485	6.86	0.195	7.69	0.336	8.53	0.528
	2024	3285	6.03	0.172	6.70	0.292	7.41	0.458
	2025	2198	5.27	0.150	5.85	0.255	6.49	0.401
	2026	2117	5.05	0.144	5.63	0.246	6.24	0.386
	2027	2115	4.96	0.141	5.61	0.245	6.19	0.383
	2028	2169	4.96	0.141	5.72	0.250	6.29	0.389
	2029	2226	5.01	0.143	5.90	0.258	6.46	0.400
	2030	2279	5.07	0.144	6.09	0.266	6.63	0.410
	2031	2318	5.12	0.146	6.27	0.274	6.77	0.419
	2032	2345	5.13	0.146	6.41	0.280	6.88	0.425
	2033	2356	5.12	0.146	6.52	0.285	6.94	0.429
	2034	2360	5.08	0.145	6.60	0.288	6.98	0.432

Scientific uncertainty

The model estimated uncertainty around the 2023 spawning output for is $\sigma = 0.09$. The uncertainty around the OFL is $\sigma = 0.14$. These values are lower than for many West Coast groundfish stocks for several reasons: large petrale sole sample sizes of length and age data from fisheries and surveys, high frequency of occurrence in the WCGBTS thanks to petrale sole primarily residing in trawlable habitat within the scope of the survey, and strong contrast in the data caused by fishing down the stock to a low level followed by rapid rebuilding. Nevertheless, these σ values surely underestimate the overall uncertainty as they do not incorporate the model structural uncertainty and do not account for any time-varying dynamics other than recruitment.

The estimated uncertainty values are lower than the Category 1 default $\sigma = 0.5$, so all projections will use the default σ.

Research and data needs

Progress on a number of research topics and data issues would substantially improve the ability of this assessment to reliably and precisely model petrale sole population dynamics in the future:

1. Continue research toward better understanding of how climate forcing impacts density-independent survival during petrale sole early life stages and further development of environmental recruitment index. Such index can provide additional information on recruitment, not captured by other sources, in most recent years when youngest cohorts may be not yet selected by either surveys or fisheries.

2. The extent of spatial, temporal, and density dependent variability on productivity processes such as growth, recruitment, and maturity is currently unknown and would benefit from further research. It would allow to better understand patterns we see in data and account for potential spatio-temporal variability in life history parameters in the model.

3. Studies on stock structure and movement of petrale sole indicating transboundary movement of petrale sole between U.S. and Canadian waters. Within the scope of this assessment, we explored including multiple data sources from British Columbia waters to the base model via sensitivity analysis. Further studies of transboundary movement of petrale sole between U.S. and Canadian waters would be beneficial for understanding the extent of petrale sole movements and to help lay the groundwork for future collaborative effort between U.S. and Canada and potential transboundary assessment.

4. The analytical solution for catchability (i.e., observed / predicted biomass) for the WCGBTS is above 1.0 in the base model. This was also the case in previous assessments of petrale sole and other flatfish assessments. Further research into flatfish habitat use and behaviors in response to survey gear will enhance the interpretation of catchability values for petrale sole off the West Coast.

5. Exploration of fine-scale differences in sex-specific spatial distribution or behavior that could lead to the differences in estimated selectivity would be helpful, as would investigating the possibility of environmental sex determination in petrale sole.

6. The observed age data from the most recent few years in all sources shows slightly-older-than-expected distributions of ages. This could be a function of some unmodeled process related to time-varying growth, ageing error, or recruitment. As more ageing is conducted in the years ahead, it will be easier to determine the most likely drivers of this pattern and explore ways to improve the fit to these data.

1 Introduction

1.1 Basic Information

Petrale sole (*Eopsetta jordani*) is a right-eyed flounder in the family Pleuronectidae ranging from the western Gulf of Alaska to the Coronado Islands, northern Baja California (Kramer et al. 1995; Love et al. 2005) with a preference for soft substrates at depths ranging from 0–550 m (Love et al. 2005). Common names include brill, California sole, Jordan's flounder, cape sole, round nose sole, English sole, soglia, petorau, nameta, and tsubame garei (Smith 1937; Gates and Frey 1974; Eschmeyer and Herald 1983; Love 1996). In northern and central California petrale sole are dominant on the middle and outer continental shelf. Pacific Fisheries Information Network (PacFIN) fishery logbook data show that a majority of the catches of petrale sole being taken between 70–220 m during March through October, and between 290–440 m during November through February.

There is little information regarding the stock structure of petrale sole off the U.S. West Coast. No genetic research has been undertaken for petrale sole and there is no other published research indicating separate stocks of petrale sole within U.S. waters. Tagging studies show adult petrale sole can move as much as 500 km, having the ability to be highly migratory with the possibility for homing ability (Alverson and Chatwin 1957). Juveniles show little coastwide or bathymetric movement while studies suggest that adults generally move inshore and northward onto the continental shelf during the spring and summer to feeding grounds and offshore and southward during the fall and winter to deep water spawning grounds (Horton 1989; Love 1996). Adult petrale sole can tolerate a wide range of bottom temperatures (Perry et al. 1994).

Tagging studies indicate some mixing of adults between different spawning groups. DiDonato and Pasquale (1970) reported that five fish tagged on the Willapa Deep grounds during the spawning season were recaptured during subsequent spawning seasons at other deepwater spawning grounds, as far south as Eureka (northern California) and the Umpqua River (southern Oregon). However, Pedersen (1975) reported that most of the fish (97%) recaptured from spawning grounds in winter were originally caught and tagged on those same grounds.

Mixing of fish from multiple deep water spawning grounds likely occurs during the spring and summer when petrale sole are feeding on the continental shelf. Fish that were captured, tagged, and released off the northwest Coast of Washington during May and September were subsequently recaptured during winter from spawning grounds off Vancouver Island (British Columbia, 1 fish), Heceta Bank (central Oregon, 2 fish), Eureka (northern California, 2 fish), and Halfmoon Bay (central California, 2 fish) (Pederson, 1975). Fish tagged south of Fort Bragg (central California) during July 1964 were later recaptured off Oregon (11 fish), Washington (6 fish), and Swiftsure Bank (southwestern tip of Vancouver Island, 1 fish) (D. Thomas, California Department of Fish and Game, Menlo Park, CA, cited by Sampson and Lee (1999)).

The highest densities of spawning adults off of British Columbia, as well as of eggs, larvae and juveniles, are found in the waters around Vancouver Island. Adults may utilize nearshore areas as summer feeding grounds and non-migrating adults may stay there during winter (Starr and Fargo 2004).

A recent analysis using an individual-based model coupled with a hydrodynamic model estimated variable but significant transboundary movement of early life stage petrale sole between the U.S. and Canada (Santa Cruz et al. 2023). Tagging studies have also documented limited transboundary movement of adults (Pedersen 1975).

Past assessments completed by Demory (1984), Turnock et al. (1993), and Sampson and Lee (1999) considered petrale sole in the Columbia and U.S.-Vancouver International North Pacific Fishery Commission (INPFC) areas a single stock. Sampson and Lee (1999) assumed that petrale sole in the Eureka and Monterey INPFC areas represented two additional distinct socks. The 2005 petrale sole assessment assumed two stocks, northern (U.S.-Vancouver and Columbia INPFC areas) and southern (Eureka, Monterey and Conception INPFC areas), to maintain continuity with previous assessments. Three stocks (West Coast Vancouver Island, Queen Charlotte Sound, and Heceta Strait) are considered for petrale sole in the waters off British Columbia, Canada (Starr and Fargo 2004). The 2009, 2011, 2013, 2015 and 2019 assessments in the U.S. integrate the previously separate north-south assessments to provide a coastwide status evaluation. The decision to conduct a single-area assessment is based on strong evidence of a mixed stock from tagging studies, a lack of genetic studies on stock structure, a lack of evidence for differences in growth between the areas, and from examination of the fishery size-at-age data, as well as confounding differences in data collection between Washington, Oregon, and California.

This assessment provides a coastwide status evaluation for petrale sole using data through 2022. The U.S.-Canadian border is the northern boundary for the assessed stock, although the basis for this choice is due to political and current management needs rather than the population dynamics (Figure 1). Given the lack of clear information regarding the status of distinct biological populations, this assessment treats the U.S. Petrale sole resource from the Mexican border to the Canadian border as a single coastwide stock. Fishing fleets are separated geographically to account for spatial patterns in catch given the coastwide assessment area.

1.2 Life History

Petrale sole spawn during the winter at several discrete deepwater sites (270–460 m) off the U.S. West Coast, from November to April, with peak spawning taking place from December to February (Harry 1959; Best 1960; Gregory and Jow 1976; Castillo et al. 1993; Reilly et al. 1994; Love 1996). Females spawn once each year and fecundity varies with fish size, with one large female laying as many as 1.5 million eggs (Porter 1964). Petrale sole eggs are planktonic, ranging in size from 1.2 to 1.3 mm, and are found in deep water habitats at water temperatures of 4–10 degrees C and salinities of 25–30 ppt (Best 1960; Ketchen and Forrester 1966; Alderdice and Forrest 1971; Gregory and Jow 1976). The duration of the egg stage can range from approximately 6 to 14 days (Alderdice and Forrest 1971; Love 1996). The most favorable conditions for egg incubation and larval growth are 6–7 degrees C and 27.5–29.5 ppt (Ketchen and Forrester 1966; Alderdice and Forrest 1971; Castillo 1995).

Adult petrale sole achieve a maximum size of around 50 cm and 63 cm for males and females, respectively (Best 1963; Pedersen 1975). The maximum length reported for petrale sole is 70 cm (Eschmeyer and Herald 1983; Love et al. 2005) while the maximum observed break-and-burn age is 31 years (Haltuch et al. 2013b).

1.3 Ecosystem Considerations

Petrale sole juveniles are carnivorous, foraging on annelid worms, clams, brittle star, mysids, sculpin, amphipods, and other juvenile flatfish (Casilla et al. 1998; Pearsall and Fargo 2007). Predators on juvenile petrale sole include adult petrale sole as well as other larger fish (Casilla et al. 1998) while adults are preyed upon by marine mammals, sharks, and larger fishes (Trumble 1995; Love 1996; Casilla et al. 1998).

Adult petrale sole are found on sandy and sand-mud bottoms (Eschmeyer and Herald 1983) and are one of

2

the ambushing flatfishes. They have diverse diets that become more piscivorous at larger sizes (Allen et al. 2006), foraging for a variety of invertebrates including, crab, octopi, squid, euphausiids, and shrimp, as well as anchovies, hake, herring, sand lance, and other smaller rockfish and flatfish (Kravitz et al. 1977; Birtwell et al. 1984; Reilly et al. 1994; Love 1996; Pearsall and Fargo 2007). In Canadian waters evidence suggests that petrale sole tend to prefer herring (Pearsall and Fargo 2007). On the continental shelf petrale sole generally co-occur with English sole, rex sole, Pacific sanddab, and rock sole (Kravitz et al. 1977).

There are several aspects of the California current ecosystem that may impact petrale sole population dynamics. Castillo (1992) and Castillo et al. (1995) suggest that density-independent survival of early life stages is low and show that offshore Ekman transportation of eggs and larvae may be an important source of variation in year-class strength in the Columbia INPFC area. The effects of the Pacific Decadal Oscillation (PDO) on California current temperature and productivity (Mantua et al. 1997) may also contribute to non-stationary recruitment dynamics for petrale sole. The prevalence of a strong late 1990s year-class for many West Coast groundfish species suggests that environmentally driven recruitment variation may be correlated among species with relatively diverse life history strategies.

Over the past several years, progress has been made in understanding how large-scale climate forcing drives regional changes and impacts density-independent survival during petrale sole early life stages. Haltuch et al. (2020) examined the relationship between petrale sole recruitment and oceanographic drivers based on model output from a Regional Ocean Modeling System (ROMS) model for the California Current Ecosystem (Neveu et al. 2016). Four oceanographic variables explained 73% of the variation in in the recruitment deviations.

Recruitment deviations were: 1. positively correlated with degree days during the female precondition period, 2. positively correlated with mixed-layer depth during the egg stage, 3. negatively correlated with cross-shelf transport during the larval stage, and 4. negatively correlated with cross-shelf transport during the benthic juvenile stage.

However, the consistent ROMS data set only covered the period 1980–2010 and the index could not be extended successfully. Appendix A of this report explains the challenges associated with extending the previous index and describes a new effort to extend this analysis and provide a new environmental index of petrale sole recruitment based on CMEMS products. A brief summary of the data sources is also provided under Environmental and Ecosystem Data (Section 2.4).

1.4 Historical and Current Fishery Information

Petrale sole have been caught in the flatfish fishery off the U.S. West Coast since the late 19th century. The fishery first developed off of California where, prior to 1876, fishing in San Francisco Bay was by hand or set lines and beach seining (Scofield 1948). By 1880 two San Francisco based trawler companies were running a total of six boats, extending the fishing grounds beyond the Golden Gate Bridge northward to Point Reyes (Scofield 1948). Steam trawlers entered the fishery during 1888 and 1889, and four steam tugs based out of San Francisco were sufficient to flood market with flatfish (Scofield 1948). By 1915 San Francisco and Santa Cruz trawlers were operating at depths of about 45–100 m with catches averaging 10,000 lbs per tow or 3,000 lbs per hour (Scofield 1948). Flatfish comprised approximately 90% of the catch with 20–25% being discarded as unmarketable (Scofield 1948). During 1915 laws were enacted that prohibited dragging in California waters and making it illegal to possess a trawl net from Santa Barbara County southward (Scofield 1948). By 1934 twenty 56–72 foot diesel engine trawlers operated out of San Francisco fishing between about 55 and 185

m (Scofield 1948). From 1944–1947 the number of California trawlers fluctuated between 16 and 46 boats (Scofield 1948). Although the flatfish fishery in California was well developed by the 1950s and 1960s, catch statistics were not reported until 1970 (Heimann and Carlisle 1970). In this early California report, petrale sole landings during 1916 to 1930 were not separated from the total flatfish landings.

The earliest trawl fishing off Oregon began during 1884–1885, and the fishery was solidly established by 1937. Initially trawlers stayed close to the fishing grounds adjacent to Newport and Astoria, operating at about 35–90 m between Stonewall Bank and Depoe Bay. Fishing operations gradually extended into deep water. For example, Newport-based trawlers were commonly fishing at about 185 m in 1949, at about 185–365 m by 1952, and at about 550 m by 1953.

Alverson and Chatwin (1957) describe the history of the petrale sole fishery off of Washington and British Columbia with fishing grounds ranging from Cape Flattery to Destruction Island. Petrale sole catches off of Washington were small until the late 1930s with the fishery extending to about 365 m following the development of deepwater rockfish fisheries during the 1950s.

The petrale sole catches further increased rapidly during World War II in response to increased demands (Harry and Morgan, 1961). Also, during the "vitamin A rush" in the late 1930s and 1940s it was found that petrale sole has high levels, which contributed to increased catches of this species as well. By the 1950s, the fishery was well developed with the stock showing declines in biomass and catches (Figures 3 and 13). Also in the 1950s, winter spawning grounds at deeper depths with dense concentrations of petrale sole were discovered, and catches increased accordingly (e.g., Alverson and Chatwin (1957); Ketchen and Forrester (1966)).

Both historical and current petrale sole fisheries have primarily relied upon trawl fleets, and petrale sole have been harvested almost exclusively by bottom trawls in the U.S. West Coast groundfish fishery. The rate of decline in spawning biomass accelerated through the 1970s reaching minimums estimated to be generally around or below 10% of the unexploited levels during the 1980s through the early 2000s. Recent annual catches between 1981–2022 range between 803 and 3060 mt per year (Table 1).

Petrale sole are a desirable market species and discarding has historically been low (less than 5%), with most of the discarding due to small sizes.

Fishery removals are divided between two fleets: 1) North, and 2) South. Landings for the North fleet are defined as fish landed in Washington and Oregon ports. Landings for the South fleet are defined as fish landed in California ports.

1.5 Summary of Management History and Performance

Beginning in 1983 the Pacific Fishery Management Council (PFMC) established coastwide annual catch limits (ACLs) for the annual harvests of petrale sole in the waters off the U.S. West Coast. The first assessment of West Coast petrale sole occurred in 1984 (Demory 1984). Based on the 1999 assessment a coastwide ACL of 2,762 mt was specified and remained unchanged between 2001 and 2006.

The 2005 assessment of petrale sole stock assessment split the stock into two areas, the northern area that included U.S.-Vancouver and Columbia INPFC areas and the southern area that included the Eureka,

Monterey and Conception INPFC areas (Lai et al. 2005). While petrale sole stock structure is not well understood, catch per unit effort (CPUE) and geographical differences between states were used to support the use of two separate assessment areas. In 2005 petrale sole were estimated to be at 34 and 29% of unfished spawning stock biomass in the northern and southern areas, respectively. In spite of different models and data, the biomass trends were qualitatively similar in both areas, providing support for a coastwide stock. This assessment estimated that petrale sole had historically been below the Pacific Council's minimum stock size threshold of 25% of unfished biomass from the mid-1970s until just prior to the completion of the assessment, with estimated harvest rates in excess of the target fishing mortality rate implemented for petrale sole at that time (F40%). However, the 2005 stock assessment determined that the stock was in the precautionary zone and was not overfished (i.e., the spawning stock biomass was not below 25% of the unfished spawning stock biomass). Based on the 2005 stock assessment results, ACLs were set at 3,025 mt and 2,919 mt for 2007 and 2008, respectively, with an ACT of 2,499 mt for both years.

In comparison to the 1999 assessment of petrale sole, the 2005 assessment represented a significant change in the perception of petrale sole stock status. The stock assessment conducted in 1999 (Washington-Oregon only) estimated the spawning stock biomass in 1998 at 39% of unfished stock biomass. Although the estimates of 1998 spawning-stock biomass were little changed between the 1999 and 2005 (Northern area) assessments, the estimated depletion in the 2005 assessment was much lower. The change in status between the 1999 and 2005 analyses was due to the introduction of a reconstructed catch history in 2005, which spanned the entire period of removals. The 1999 stock assessment used a catch history that started in 1977, after the bulk of the removals from the fishery had already taken place. Thus the 1999 stock assessment produced a more optimistic view of the petrale stock's level of depletion.

The 2009 coastwide stock assessment estimated that the petrale sole stock had declined from its 2005 high to 11.6% of the unfished spawning stock biomass (Haltuch and Hicks 2009). The stock's estimated decline in status between the 2005 and 2009 assessments was driven primarily by a significant decline in the trawl-survey index over that period. The 2011 assessment concluded that the stock status continued to be below the target of 25% of unfished biomass. The petrale sole was declared overfished based on newly adopted management targets (target spawning output for flatfish stocks defined as 25% and overfished threshold of 12.5% of unfished spawning output) resulting in a rebuilding plan and catch restrictions for petrale sole. The stock was declared rebuilt based on the results of the 2015 update stock assessment which estimated the coastwide biomass at 30.7% of unfished spawning stock output (Stawitz et al. 2015).

1.6 Fisheries off Canada and Alaska

The Canadian fishery developed rapidly during the late 1940s to mid-1950s following the discovery of petrale sole spawning aggregations off the West Coast of Vancouver Island (Anon 2001). Annual landings of petrale sole in British Columbia peaked at 4,800 mt in 1948 but declined significantly after the mid-1960s (Anon 2001). By the 1970s, analysis conducted by Pederson (1975) suggested that petrale sole abundance was low and abundance remained low into the 1990s. In the early 1990s vessel trip quotas were established to try to halt the decline in petrale sole abundance (Anon 2001). Winter quarter landings of petrale sole were limited to 44,000 lb per trip during 1985–91; to 10,000 lb per trip during 1991–95; and to 2,000 lb per trip in 1996. Biological data collected during 1980–1996 showed a prolonged decline in the proportion of young fish entering the population (Anon 2001). Therefore, no directed fishing for petrale sole was permitted in Canada starting in 1996 due to a continuing decline in long term abundance (Fargo 1997; Anon 2001). As of 2005 petrale sole off of British Columbia were treated as three "stocks" and were still considered to be at low levels.

The recent assessments for the Canadian stocks have been based on catch histories and limited biological data. However, a new stock assessment is currently being conducted by Fisheries and Oceans Canada (DFO) for petrale sole in Canadian waters although results are not expected to be available until months after the completion of this one (pers. comm. M. Mazur, DFO).

In Alaska petrale sole are not targeted in the Bering Sea/Aleutian Island fisheries and are managed as a minor species in the "Other Flatfish" stock complex.

2 Data

Data comprise the foundational components of stock assessment models. The decision to include or exclude particular data sources in an assessment model depends on many factors. These factors often include, but are not limited to, the way in which data were collected (e.g., measurement method and consistency); the spatial and temporal coverage of the data; the quantity of data available per desired sampling unit; the representativeness of the data to inform the modeled processes of importance; timing of when the data were provided; limitations imposed by the Terms of Reference; and the presence of an avenue for the inclusion of the data in the assessment model. Attributes associated with a data source can change through time, as can the applicability of the data source when different modeling approaches are explored (e.g., stock structure or time-varying processes). Therefore, the specific data sources included or excluded from this assessment should not necessarily constrain the selection of data sources applicable to future stock assessments for petrale sole. Even if a data source is not directly used in the stock assessment they can provide valuable insights into biology, fishery behavior, or localized dynamics.

Data from a wide range of programs were available for possible inclusion in the current assessment model. Descriptions of each data source included in the model (Figure 2) and sources that were explored but not included in the base model are provided below. Data that were excluded from the base model were explicitly explored during the development of this stock assessment or have not changed since their past exploration in a previous petrale sole stock assessment. In some cases, the inclusion of excluded data sources were explored through sensitivity analyses (see Section 3.4.2).

2.1 Fishery-Dependent Data

Fishery removals in this assessment were divided between two fleets: 1) North and 2) South. Landings for Washington and Oregon are summed into a single North fleet (consistent with previous several assessments) due to the fact that vessels commonly fish and land in each other's waters and ports. Landings for the South feet are defined as fish landed in California ports.

The landings of petrale sole are made primarily by groundfish bottom trawl gear; landings by gear types other than bottom trawl have been inconsequential, averaging less than 2.5% of the coastwide landings. All non-trawl landings are included along with the trawl landings. Recreational catch is inconsequential and not accounted for in this assessment.

2.1.1 Commercial Fishery Landings

2.1.1.1 Recent Landings Recent commercial landings of petrale sole (1981–2022 for California and Washington; 1987–2022 for Oregon) were obtained from PacFIN, a regional fisheries database that manages fishery-dependent information in cooperation with West Coast state agencies and National Marine Fisheries

Service (NMFS). Catch data were extracted from PacFIN on June 12, 2023, by state and then combined into the fishing fleets used in the assessment. Time series of recent landings by fleet and state are reported in Table 1 and shown in Figures 3 to 5.

2.1.1.2 Historical Landings Historical landings of petrale sole were reconstructed by state, by year.

The Washington historical landings (1938–1980) were provided by Washington Department of Fish and Wildlife, who recently conducted historical catch reconstruction for petrale sole (pers. comm. T. Tsou and G. Lippert, Washington Department of Fish and Wildlife (WDFW)). The new reconstruction of Washington historical landings utilizes several historical sources, including Alverson and Chatwin (1957), who reported petrale sole landings in Washington ports for the 1938-1947 period, and Ward et al. (1969), who reported petrale sole landings for the 1948-1969 period. Both sources reported Washington petrale sole landings that were caught off the United States and Canada. Alverson and Chatwin (1957), however, also reported Washington landings by area of catch for a subset of years (1948-1955) that were informed by historical tagging study. Washington petrale sole landings caught off U.S. west coast from Alverson and Chatwin (1957) were used for the period between 1948 and 1955 by year, and an average proportion of landings caught off U.S. west coast across 1948-1955 period (11.6%) was used to apportion the petrale sole Washington landings between U.S. and Canada for the rest of years within the 1938-1969 period. For 1970-1980, Washington landings are from area-specific fish receiving tickets (pers. comm. T. Tsou, WDFW). A linear interpolation was applied between landings in 1938 and zero landings in 1930.

The Oregon historical landings (1896–1986) were obtained from Oregon historical catch reconstruction, conducted by Oregon Department of Fish and Wildlife in collaboration with NWFSC (Karnowski et al. 2014).

The California historical landings were informed by several sources. Landings from the most recent "historical" period (between 1969 and 1980) were available from the CalCOM database for the California Cooperative Survey (CalCOM) database. Earlier landing records (between 1931 and 1968) were reconstructed by the Southwest Fisheries Science Center (Ralston et al. 2010). Ralston et al. (2010) included only catches made in waters off California and landed in California ports, therefore Ralston et al. (2010) estimates were supplemented by catches landed in California, but made in waters off Oregon and Washington, provided by the SWFSC (pers. comm. E.J. Dick, SWFSC). The earliest California landings were obtained from California Department of Fish and Game (CDFW) Fish Bulletins for 1916–1930 landings (Heimann and Carlisle 1970) as reconstructed by Lai et al. (2005) and used in previous assessments. The California fishery began in 1876, but no landings data are available from 1876–1915. Therefore, consistent with previous petrale sole assessments, a linear interpolation between landings of 1 ton in 1879 and the landings recorded for 1916 were used to filling this period.

Comparison of petrale sole historical landings by state and fleet between this and 2019 assessment is provided in Figure 5. Historical Oregon and California landings did not change. Slight discrepancies between California landings used in the 2019 and 2023 assessments in Figure 5 are caused by the fact that fishing year in 2019 model was defined from November of previous year to October of current year, since North and South fleets were further divided into Winter and Summer fisheries. We did not have access to original annual landings used in 2013 full assessment and then in 2019 update assessment, and therefore comparison between California landings used in the 2019 and 2023 assessments in Figure 5 is approximate, but still able to illustrate that California landings did not change. The noticeable difference in this assessment from 2019 model is in Washington landings. This year Washington Department of Fish and Wildlife completed historical catch

reconstruction of petrale sole, and newly estimated landings are lower than those used in previous assessment. Historical landings in 2013 assessment were based on preliminary estimates and might have included catches from Puget Sound and Canadian waters (pers. comm. T. Tsou, WDFW). New Washington historical landings are more consistent with history of commercial removals on the U.S. West Coast and represent improvement to the assessment.

2.1.2 Discard

Data on discards of petrale sole are available from two different data sources. In 2002, the West Coast Groundfish Observer Program (WCGOP) was implemented on the West Coast of the United States, which began with gathering bycatch and discard information for the limited entry trawl and fixed gear fleets. Observer coverage has expanded to include the California halibut trawl, the nearshore fixed gear and pink shrimp trawl fisheries.

Since 2011, trawl fisheries have been managed with catch shares under a system of annual individual fishing quotas (IFQs) for the shoreside sector (i.e., vessels delivering to shoreside processors) and harvest cooperatives for the at-sea hake sectors (catcher-processors who catch and process hake at sea; and Motherships, factory processors that take delivery of hake from catcher vessels at sea). Constant monitoring of catch using observers or electronic monitoring (EM) is required to participate in the trawl catch share fishery.

Table 11 shows the discard ratios (discarded/(discarded + retained)) of petrale sole from WCGOP based on observer observations. The discarding rate of petrale sole within this data-set has always been relatively low. Discard rates were obtained for both the catch share and the non-catch share sector for petrale sole.

The vast majority of removals was made within the catch share fleet, and therefore, discard rates from the catch share sector was used for the periods after 2011. Coefficients of variation were calculated for the pre-catch share years by bootstrapping vessels within ports because the observer program randomly chooses vessels within ports to be observed. The coefficient of variation of discarding in the catch share fleet, given nearly 100% observer coverage, was considered low and a value of 0.015 was assumed.

The historical source (often referred to as the Pikitch data) comes from a study by Ellen Pikitch that collected trawl discards from 1985–1987 (Pikitch et al. 1988). The study was conducted off the coast of Washington and Oregon with no participating vessels fishing off the coast of California (Pikitch et al. 1988; Rogers and Pikitch 1992). Therefore, this source of discard data is only relevant to North fleet. Participation in the study was voluntary and included vessels using bottom, midwater, and shrimp trawl gears. Observers of normal fishing operations on commercial vessels collected the data, estimated the total weight of the catch by tow, and recorded the weight of species retained and discarded in the sample. The discard ratios (discarded/(discarded + retained)) from the Pikitch data were obtained from NWFSC (pers. comm. J. Wallace, NWFSC), and are also shown in Table 11.

WCGOP provided estimates of discard mean body weight, and these data were used in this assessment for each fishing fleet. The mean body weight of discarded fish are shown in Figures 45 and 46.

2.1.3 Fishery Length and Age Data

The fishery length and age data for North fleet were obtained from PacFIN Biological Data System (BDS) database and contained data from Oregon and Washington. For South fleet, length and age data were

obtained from PacFIN BDS database and also from the CalCOM. The latter were provided by California Department of Fish and Wildlife (CDFW) (pers.comm. B. Erwin, Pacific States Marine Fisheries Commission (PSMFC)) as the CalCOM samples for flatfish collected before 1990 are not included in PacFIN at this time. The fishery length and age samples were collected by port samplers.

Length bins from 12 to 62 cm in 2 cm increments were used to summarize the length frequency of the catches in each year. The first length bin includes all observations less than 14 cm and the last bin includes all fish 62 cm and longer. Age distributions included bins from age 1 to age 17, with the first bin including all fish ages 0 and 1 and the last bin including all fish age 17 and above.

Commercial length-frequency distributions were developed for each fleet and year, for which observations were available. Females and males distributions were treated separately, to track sex-specific differences. For each fleet, the raw observations (compiled from the PacFIN and CalCOM databases) were expanded to the trip level, to account for differences in samples sizes relative catch weights among trips (first stage expansion). The expanded length observations were then further expanded to state level, to account for differences in sampling intensity of petrale sole landings among states combined into a single fleet (second stage expansion). The expansion algorithm can be illustrated with the following equation:

$$N_{b,j,y} = \sum_{s=1}^{s=k} \sum_{t=1}^{t=n} L_{b,j,t} \cdot \left(\frac{LC_t}{SC_t} \right) \cdot \left(\frac{LC_{s,y}}{SC_{s,y}} \right)$$

Were $N_{b,j,y}$ is the number of lengths in each length bin (b) by sex (j) and year (y) within each fleet. $L_{b,j,t}$ represents an individual length sample by bin (b) and sex (j) within an individual fishing trip (t). As the first stage expansion, $L_{b,j,t}$ was multiplied by the ratio of landed catch (LC_t) within that trip (t) to portion of catch sampled for lengths (SC_t) within the same trip (t). In the second stage expansion, the individual length sample ($L_{b,j,t}$) was multiplied by the ratio of landed catch ($LC_{s,y}$) within individual state (s) and year (y) to catch weights sampled for lengths ($SC_{s,y}$) within the same state (s) and year (y). As the final step, the expanded length samples from the same size bin and sex were summed across all trips and states (combined into a single fleet) within a single year, to obtain the total number of lengths in each length bin by sex, year and fleet ($N_{b,j,y}$). The same calculations were repeated for each length bin (26 bins total), to develop sex specific length frequencies for each fishing fleet by year. Since coastwide catches in the assessment model were divided between South (California) and North (Oregon-Washington) fleets, the second stage expansion of length samples was relevant to only North fleet.

Age frequencies were computed in the same manner, except that age observations for Washington and Oregon were not combined due to ageing error considerations.

The filtering and cleaning of the PacFIN data and the length and age composition expansion was conducted using the {PacFIN.Utilities} package in R (Johnson and Wetzel 2023). The filtering steps included removing samples with missing vital information and removing ages for fish which fell more than 4 standard deviations from an estimated growth curve (fewer than 1 in 500 ages).

All petrale sole PacFIN samples from Oregon prior to 1987, a total of 37,348 samples starting in 1966, have SAMPLE_METHOD = "S", indicating "special request" rather than random sampling. This categorization was apparently made due to lack of documentation on how these samples were taken and processed (pers. comm. A. Whitman, ODFW). Exploration of the impact of including or excluding these samples indicated

that the combination of differences in lengths observed in Washington and Oregon, combined with gaps in the years when samples were available from Washington during the 1966–1986, resulted in discontinuities in the length comps which the model could not fit well. Including all the early (1966–1986) Oregon special project samples resulted in more plausible estimates of recruitment so that choice was made for the base model. Excluding these samples was the subject of a sensitivity analysis (Section 3.4.2).

As discussed under "Ageing Precision and Bias" (Section 2.3.6), the age estimation comes from two labs, the Cooperative Aging Project (CAP) lab and WDFW, using a combination of surface and break and burn ages. The analysis of ageing precision conducted in 2013 (Haltuch et al. 2013b) estimated 7 ageing error matrices of which the two groups with highest variability were "CAP Surface Pre-1990" and "WDFW Surface" (Tables 7 and 8). Concerns over the reliability of those early surface age estimates (including consistent underestimation of ages using surface methods) and their potential impacts on estimated selectivity and growth, were raised in multiple previous petrale sole assessments. The age compositions associated with these ageing errors were not fit well by any models explored during the assessment process so those two groups with the highest imprecision were excluded from the likelihood in the base model.

Length and age data collected from commercial landings for each fleet are summarized by the number of trips and fish sampled by year (Tables 2 and 3). Figures 29 and 36 show plots of the commercial length and age composition data across time for each fishery fleet.

The input sample sizes for length and age frequency distributions by year were calculated as a function of the number of trips and number of fish via the Stewart Method (pers.comm. I. Stewart, International Pacific Halibut Commission (IPHC)). The method is based on analysis of the input and model derived effective sample sizes from West Coast groundfish stock assessments. A piece-wise linear regression was used to estimate the increase in effective sample size per sample based on fish-per-sample and the maximum effective sample size for large numbers of individual fish. The resulting equations are:

$$\text{Input N} = N_{\text{trips}} + 0.138 * N_{\text{fish}} \text{ if } N_{\text{fish}}/N_{\text{trips}} \text{ is} < 44,$$

$$\text{Input N} = 7.06 * N_{\text{trips}} \text{ if } N_{\text{fish}}/N_{\text{trips}} \text{ is} \geq 44.$$

Discard length composition data for both fleets were available from WCGOP, and for North fleet from Pikitch study as well. WCGOP length composition data were not sex-specific. WCGOP raw observations were expanded to the haul level, to account for differences in catch among hauls. Pikitch data (although available by sex) were very limited (32 fish sampled for length), and were included in the assessment as females and males combined.

No age data were available for discarded fish.

2.2 Fishery-Independent Data

Data from two fishery-independent surveys were used in this assessment., which included one historical survey (the Triennial Survey) and one current survey (the WCGBTS). Three sources of information are produced by these surveys: indices of relative abundance, length-frequency distributions, and age-frequency distributions.

2.2.1   AFSC/NWFSC West Coast Triennial Shelf Survey

2.2.1.1   Survey Description   The Triennial Survey was first conducted by the Alaska Fisheries Science Center (AFSC) in 1977, and the survey continued until 2004 (Weinberg et al. 2002).

Its basic design was a series of equally-spaced east-to-west transects across the continental shelf from which searches for tows in a specific depth range were initiated. The survey design changed slightly over time. In general, all of the surveys were conducted in the mid summer through early fall. The 1977 survey was conducted from early July through late September. The surveys from 1980 through 1989 were conducted from mid-July to late September. The 1992 survey was conducted from mid-July through early October. The 1995 survey was conducted from early June through late August. The 1998 survey was conducted from early June through early August. Finally, the 2001 and 2004 surveys were conducted from May to July.

Haul depths ranged from 91-457 m during the 1977 survey with no hauls shallower than 91 m. Due to haul performance issues and truncated sampling with respect to depth, the data from 1977 were omitted from this analysis. The surveys in 1980, 1983, and 1986 covered the U.S. West Coast south to 36.8°N latitude and a depth range of 55-366 m. The surveys in 1989 and 1992 covered the same depth range but extended the southern range to 34.5°N (near Point Conception). From 1995 through 2004, the surveys covered the depth range 55-500 m and surveyed south to 34.5°N. The distribution of petrale sole in the survey relative to these limits is shown in Figure 7.

In 2004, the final year of the Triennial Survey series, the Northwest Fisheries Science Center (NWFSC) Fishery Resource and Monitoring Division (FRAM) conducted the survey following similar protocols to earlier years. Although the protocol was similar, subtle differences in how it had been implemented prior to 2004 may have contributed to a large difference in estimated biomass between 2001 and 2004, where few of the West Coast groundfish stock assessments have been able to match the observed increase in 2004 relative to the previous years.

2.2.1.2   Index of Abundance   Geostatistical models of biomass density were fit to survey data using Template Model Builder (TMB) (Kristensen et al. 2016) via the R package Species Distribution Models with (`sdmTMB`) (Anderson et al. 2022b). These models can account for latent spatial factors with a constant spatial Gaussian random field and spatiotemporal deviations to evolve as a random walk Guassian random field (Thorson et al. 2015). Tweedie, delta-binomial, delta-gamma, and mixture distributions, which allow for extreme catch events, were investigated. Results are only shown for the distribution that led to the best model diagnostics, e.g., similar distributions of theoretical normal quantiles and model quantiles, high precision, lack of extreme predictions that are incompatible with the life history, and low Akaike information criterion (AIC). Estimates of biomass from this best model were predicted using a grid based on available survey locations. Code to reproduce the analysis is available at https://github.com/pfmc-assessments/indexwc.

In this assessment, a single Triennial Survey index (1980–2004) was developed. Sensitivity analysis was conducted to evaluate impact of using a single abundance index versus two indices with a split in 1995 (to account for change in spatial coverage and survey timing), as well as using a single index but estimating a separate catchability parameter for the period from 1995 forward, and others. All sensitivity runs resulted in virtually identical results, and the most parsimonious approach (a single survey index) was retained for the base model (Section 3.4.2).

The data were truncated to latitudes north of 37°N latitude and to depths less than 366 m prior to modeling, to only include survey area consistent in spatial coverage among years. The prediction grid was also truncated to only include available survey locations in depths between 55–366 m to limit extrapolating beyond the modeled area and edge effects. The model used a delta model with a lognormal distribution for the catch-rate component. The lognormal error structure was used because it is able to better account for extreme catch events observed for petrale sole in both surveys. A logit-link was used for encounter probability and a log-link for positive catch rates. The response variable was catch (mt) with an offset of area (km^2) to account for differences in effort. Fixed effects were estimated for each year. No other covariates were modelled. Vessel-year effects, which have traditionally been included in index standardization for this survey, were not included as the estimated variance for the random effect was close to zero. Vessel-year effects were more prominent when models did not include spatial effects and were included for each unique combination of vessel and year in the data to account for the random selection of commercial vessels used during sampling (Helser et al. 2004; Thorson and Ward 2014).

Spatial and spatiotemporal variation was included in the encounter probability and the positive catch rate model. Spatial variation was approximated using 500 knots, where more knots led to non-estimable standard errors because the positive encounters are too sparse to support the dense spatiotemporal structure.

The estimated distribution of petrale sole density for 2004 is shown in Figure 6.

2.2.1.3 Length Compositions

Length bins from 12 to 62 cm in 2 cm increments were used to summarize the length frequency of the survey catches in each year. Table 4 shows the number of lengths taken by the survey.

Prior to 1989, only limited length samples were collected and those samples were limited to the Northern area of the survey; therefore, length samples from years prior to 1989 are not used in the assessment. Less than a half percent of all length samples were collected in depths deeper than 350 m. Therefore, truncation of data to depths less than 350 m (for development of a single abundance index) did not impact length composition samples.

Length compositions were separated into males and females. These length compositions were expanded to account for subsampling tows, with further expansion based upon the stratification by depth and latitude. The stratifications for length data expansions are provided in Table 10.

The input sample sizes for length composition data for all fishery-independent surveys were calculated based on Stewart and Hamel (2014) as Input $N_y = 3.09 * N_{tow}$ where the 3.09 value was estimated for a group of 8 flatfish species including petrale sole.

There are no petrale sole age data from the Triennial Survey, and the Triennial Survey sampling manual does not mention collecting age structures from flatfish species.

Processing of length and age data from both surveys was conducted using the {nwfscSurvey} package in R (Wetzel et al. 2023).

2.2.2 NWFSC West Coast Groundfish Bottom Trawl Survey

2.2.2.1 Survey Description The WCGBTS is based on a random-grid design; covering the coastal waters from a depth of 55–1,280 m (Bradburn et al. 2011). This design generally uses four industry-chartered vessels per year assigned to a roughly equal number of randomly selected grid cells and divided into two 'passes' of the coast. Two vessels fish from north to south during each pass between late May to early October. This design therefore incorporates both vessel-to-vessel differences in catchability, as well as variance associated with selecting a relatively small number (approximately 700) of possible cells from a very large set of possible cells spread from the Mexican to the Canadian borders.

The WCGBTS commonly encounters petrale sole along the U.S West Coast, except south of Point Conception (Figure 6). They occur in about 75% of tows shallower than 200 m. with few observations beyond 450 m. (Figure 8). Petrale sole occur throughout the surveyed latitudes with lower densities in southern California, a peak around the San Francisco area (37°N latitude, Figure 9) and a general increase in presence with increasing latitude.

2.2.2.2 Index of Abundance Geostatistical models of biomass density were fit to survey data using TMB (Kristensen et al. 2016) via the R package `sdmTMB` (Anderson et al. 2022b), as in case of Triennial Survey.

The data were truncated to depths less than 675 m prior to modeling given that there were zero positive encounters in depths deeper than 675 m. The prediction grid was also truncated to only include available survey locations in depths between 55–675 m to limit extrapolating beyond the data and edge effects.

The model used a delta model with a lognormal distribution for the catch-rate component. The model used a delta model with a lognormal distribution for the catch-rate component. The lognormal error structure was used because it is able to better account for extreme catch events observed for petrale sole in both surveys; most recently extreme catch events occurred within the WCGBTS in 2021 and also in 2014. A logit-link was used for encounter probability and a log-link for positive catch rates. The response variable was catch (mt) with an offset of area (km^2) to account for differences in effort. Fixed effects were estimated for each year. The following additional covariates were included: pass. Vessel-year effects, which have traditionally been included in index standardization for this survey, were not included as the estimated variance for the random effect was close to zero. Vessel-year effects were more prominent when models did not include spatial effects and were included for each unique combination of vessel and year in the data to account for the random selection of commercial vessels used during sampling (Helser et al. 2004; Thorson and Ward 2014).

Spatial and spatiotemporal variation was included in the encounter probability and the positive catch rate model. Spatial variation was approximated using 500 knots, where more knots led to non-estimable standard errors because the positive encounters are too sparse to support the dense spatiotemporal structure.

The estimated distribution of petrale sole density for 2004 is shown in Figure 6.

2.2.2.3 Length and Age Compositions Length bins from 12 to 62 cm in 2 cm increments were used to summarize the length frequency of the survey catches in each year. The first length bin includes all observations less than 14 cm and the last bin includes all fish larger than 62 cm. Table 5 shows the number of lengths taken by the survey.

Length compositions were separated into males and females. These length compositions were expanded to account for subsampling tows, with further expansion based upon the stratification by depth and latitude. The stratifications for length data expansions are provided in Table 9.

Age distributions included bins from age 1 to age 17, with the last bin including all fish of greater age. Table 6 shows the number of ages taken by the survey. Age distributions were included in the model as conditional-age-at-length (CAAL) observations. The marginal WCGBTS age-compositions were also included, but only for easier viewing of strong cohorts. The conditional-age-at-length data were not expanded and were binned according to length, age, sex, and year.

The input sample sizes for length and marginal age-composition data for all fishery-independent surveys The input sample sizes for length composition data for all fishery-independent surveys were calculated based on Stewart and Hamel (2014) as Input $N_y = 3.09 * N_{tow}$ where the 3.09 value was estimated for a group of 8 flatfish species including petrale sole.

The input sample size of CAAL data was set at the number of fish at each length by sex and by year. The marginal age compositions were only used for comparing the implied fits while the CAAL data were used in the likelihood.

2.2.3 Fishery-independent data sources considered but not used

2.2.3.1 AFSC Slope Survey The AFSC Slope Survey (Slope Survey) operated during the months of October to November aboard the R/V Miller Freeman. Partial survey coverage of the U.S. West Coast occurred during the years 1988–1996 and complete coverage (north of 34°30'S Lat.) during the years 1997 and 1999–2001. Typically, only these four years that are seen as complete surveys are included in assessments. This survey was considered, but similarly to the past assessments not included in the model because the frequency of petrale sole occurrence was too low. Survey spatial coverage did not align well with range of petrale sole depth range, and the survey data was not sufficient to develop an informative index.

2.2.3.2 NWFSC Slope Survey The NWFSC also operated a Slope Survey during the years 1998–2002. However, this survey was not included in this assessment because the frequency of petrale sole occurrence was too low. Survey spatial coverage did not align well with range of petrale sole depth range, and the survey data was not sufficient to develop an informative index.

2.3 Biological Data

2.3.1 Natural Mortality

The instantaneous rate of natural mortality for a wild fish population is notoriously difficult to estimate. One accepted method is to examine the age distribution of an unexploited or lightly exploited stock. This method cannot readily be applied to petrale sole given the long history of exploitation off the U.S. West Coast. Ketchen and Forrester (1966) estimated that the natural mortality coefficients were 0.18-0.26 yr^{-1} for males and 0.19-0.21 yr^{-1} for females based on a catch curve analysis of 1943–1945 Washington trawl data from Swiftsure Bank, off the southwest corner of Vancouver Island. However, petrale sole catches were relatively high during mid-1940s through the 1950s. Starr and Fargo (2004) estimated the instantaneous rate of natural mortality (M) using Hoenig's method (Hoenig 1983) estimating M values of 0.22 and 0.15 yr^{-1} were estimated given maximum ages of 20 and 30 years, respectively.

An archived set of commercial samples, collected from Northern California between the late 1950s and early 1980s, recently found that multiple samples were aged between 20–31 years old, suggesting a similar range of M values for U.S. West Coast petrale sole. U.S. stock assessments prior to 2009 and current British Columbia stock assessments assumed a value of $M = 0.2$ yr^{-1} for both sexes. The 2013 stock assessment used a meta-analysis value produced the following normal prior distributions for females (mean = 0.151, sd = 0.16) and males (0.206, sd = 0.218) based on Hamel (2015) with maximum age for females and males of 32 and 29 years, respectively.

Hamel (2015), recently updated by Hamel and Cope (2022), represents the current method for developing a prior on natural mortality for West Coast groundfish stock assessments. This method combines meta-analytic approaches relating the natural mortality rate to other life-history parameters to develop a general prior on M for many fish species. The updated approach modifies work done by Then et al.(2015) who estimated M and recommended M estimates based on maximum age alone. Hamel (2022) re-evaluated the data used by Then et al. (2015) by fitting the one-parameter A_{max}, model under a log-log transformation and also reduced the variance around the estimate. The resulting equation for the point estimate (i.e., the median, in real space) for M, is:

$$M = \frac{5.4}{A_{\mathrm{max}}}$$

where A_{max} is the maximum age of the focal species. The above is also the median of the prior. The prior is defined as a lognormal distribution with mean (in log space) $ln(5.4/A_{\mathrm{max}})$ and SE = 0.31.

Maximum age was assumed to be 32 and 29 years for females and males, respectively, consustent with several previous assessments. Using the Hamel and Cope (2022) approach above, the median of the prior for females in regular space is 0.169 and for males is 0.186.

2.3.2 Maturation and Fecundity

A new maturity ogive was developed for this assessment (pers. comm. M. Head, NWFSC) based on an analysis of 553 ovary samples collected from 2015 to 2021 by port samplers in Washington and Oregon as well as on board the WCGBTS (Figures 19 and 20). Very little difference in biological and functional maturity was observed and there was evidence of only a minimal amount of skip spawning. The estimated length at 50% maturity was 35.45, which was similar to the 33.1 cm used in the previous assessment which was based on samples from a narrower geographic range (Hannah et al. 2002).

A fecundity relationship published in 2019 (Lefebvre et al. 2019) was used as a sensitivity analysis in the previous assessment and has been adopted for the base model in this one. The relationship shows a slightly faster increase in the number of eggs per unit length than when fecundity was assumed proportional to body weight. The addition of this fecundity relationship means that spawning output is reported in trillions of eggs rather than metric tons of spawning biomass. A comparison of the fecundity and weight-length relationships is provided in Figure 21.

2.3.3 Sex Ratio

The fraction of the smallest and youngest petrale sole observed in the WCGBTS (less than 35 cm or younger than age 5) identified as female is less than 50%. No study on what determines phenotypic sex for petrale sole has been conducted, but environmental sex determination (ESD) has been established for many other flatfish,

where environmental factors can influence phenotypic sex in the female genotype, resulting in male-skewed sex ratios (Luckenbach et al. 2009; Honeycutt et al. 2019). The sex ratio of larger and older fish is skewed toward females presumably due to lower natural mortality.

As a part of this assessment, we explored multiple model formulations with age-0 fraction female estimated internally. However, in many of those formulations, age-0 fraction female was estimated above 50% due to confounding with sex-specific selectivity. The reasonable estimate of age-0 fraction female was achieved only when a single selectivity curve was assumed for the females and males in the WCGBTS, which deteriorated fit to length composition data. Furthermore, the length and age bins which are skewed male in the WCGBTS contain so few fish relative to larger sizes, that the influence of a sex ratio estimate different from 50% was minimal. The value of estimated age-0 fraction female in that model run was 0.48, and it was assumed reasonable to continue to use a 50% sex ratio at birth between females and males, consistent with previous assessments.

2.3.4 Length-Weight Relationship

The weight-length relationship for petrale sole was estimated outside of the assessment model by fitting biological data to the standard power function, $W = aL^b$ using the R function `PacFIN.Utilities::getWLpars()` (where W is weight in kilograms and L is length in centimeters). The function estimates the relationship on a log-log scale and then uses the estimated standard deviation of the observed weights around the expected value to calculate the median weight at each length from the resulting lognormal distribution.

The parameters were estimated using data from the WCGBTS, where 21,704 fish collected between 2003 and 2022 had both weight and length available of which 57.6% were female, 42.3% were male, and 0.1% were unsexed. The resulting relationships were $W = 0.000002035 * L^{3.478}$ for females and $W = 0.000003043 * L^{3.359}$ for males. These relationships are very similar to those used for the previous assessment (Wetzel 2019a).

2.3.5 Growth (Length-at-Age)

The length-at-age was estimated for male and female petrale sole via 5 von Bertalanffy parameters, with independent parameters for length at age 17 (L_at_Amax) for females and males, independent k parameters, and a shared parameter for length at age 1 for both females and males. Variability in length at age was estimated via 2 parameters for each sex controlling the standard deviation of length-at-age as a piecewise linear function of length with breaks points at lengths associated with the two reference ages: 1 and 17. This differs from the 2019 assessment which parameterized variability in length-at-age as a CV rather than standard deviation, and used age 2 as the first reference age. The changes resulted in smoother changes in the distributions of length-at-age and avoided a bulge in the variability at young ages that was present in the 2019 model.

2.3.6 Ageing Precision and Bias

Historically, petrale sole otoliths have been read by multiple ageing labs using surface and break and burn methods, and double-read data from the Cooperative Aging Project (CAP) and the Washington Department of Fish and Wildlife (WDFW), as well information from a bomb radiocarbon age validation study for petrale sole off the U.S. West Coast Haltuch et al. (2013a), were used to generate multiple ageing error matrices, to incorporate ageing bias and imprecision into the assessment model.

The ageing error matrices used in the previous assessment were retained for this analysis (Tables 7 and 8). Ageing error was explored in the last full assessment including extensive model selection. A qualitative examination of the new break and burn double reads showed no evidence that the ageing estimation had changed over time relative to the samples included in the previous analysis. Furthermore, a new TMB-based ageing error software has been developed (pers. comm. A. Punt, University of Washington), but has not yet been fully explored or documented. Therefore, revision of the ageing error matrices has been left as a research project to be completed in time for the next full assessment.

2.4 Environmental and Ecosystem Data

Over the past several years, progress has been made in understanding how large-scale climate forcing drives regional changes and impacts density-independent survival during petrale sole early life stages. Haltuch et al. (2020) examined the relationship between petrale sole recruitment and oceanographic drivers based on model output from a Regional Ocean Modeling System (ROMS) model for the California Current Ecosystem (Neveu et al. 2016). The results suggested that ROMS output might be useful as the basis for an environmental index of recruitment for petrale sole, to allow for better model precision and near-term forecasting. However, the ROMS model used by Haltuch et al. (2020) was consistent in structure and inputs for only 1980–2010. In 2011, the model was updated, and from 2011 forward, ROMS outputs exhibit distinct discontinuities with the 1980–2010 period, showing changes in scale and trend across the 2010/2011 boundary for multiple drivers used to inform the index by Haltuch et al. (2020). Appendix A of this report illustrates the discontinuities in ROMS products over the 2010/2011 boundary and discusses potential reasons for why the ROMS time series changed after the model was updated in 2011.

Due to discontinuity in ROMS models between periods before and after 2011, the index developed by Haltuch et al. (2020) could not be used for this stock assessment. However, alternative oceanographic model products by Copernicus Marine Environment Monitoring Service (CMEMS) (https://marine.copernicus.eu/) and Mercator Ocean International (MOI) (https://www.mercator-ocean.eu/) were investigated to test if these modeling frameworks could be used to produce an environmental index of petrale sole recruitment. This new effort is ongoing, and has not yet been published or reviewed by the SSC of the PFMC. Appendix A of this report describes the most recent, preliminary efforts in developing a new environmental index of petrale sole recruitment based on CMEMS products. In this assessment, we explore the impact of the current CMEMS-based environmental index of petrale sole recruitment via sensitivity analysis.

3 Assessment Model

3.1 Summary of Previous Assessments and Reviews

3.1.1 History of Modeling Approaches

Early stock assessments assessed petrale sole in only the combined U.S.-Vancouver and Columbia INPFC areas, i.e., petrale sole in these areas were treated as a unit stock, using time series of data that began during the 1970s (Demory 1984; Turnock et al. 1993). The first assessment used stock reduction analysis and the second assessment used the length-based Stock Synthesis model. The third petrale sole assessment utilized the hybrid length-and-age-based Stock Synthesis 1 model, using data from 1977–1998 (Sampson and Lee 1999). During the 1999 stock assessment an attempt was made to include separate area assessments for the Eureka and Monterey INPFC areas but acceptable models could not be configured due to a lack of data (Sampson and Lee 1999).

The 2005 petrale sole assessment was conducted as two separate stocks, the northern stock encompassing the U.S. Vancouver and Columbia INPFC areas and the southern stock including the Eureka, Monterey and Conception INPFC areas, using Stock Synthesis 2, a length-age structured model. Both the northern- and southern-area models specified the fishing year as beginning on November 1 and continuing through October 31 of the following year, with a November-February winter fishery and a March-October summer fishery. Landings prior to 1957 were assumed to have been taken during the summer season in years where monthly data were not available to split the catches seasonally. The complete catch history was reconstructed for petrale sole for the 2005 stock assessment, with the northern area model starting in 1910 and the southern area model in 1876. In 2005, the STAR panel noted that the petrale sole stock trends were similar in both northern and southern areas, in spite of the different modeling choices made for each area, and that a single coastwide assessment should be considered.

The 2009 and 2011 assessments treated petrale sole as a single coastwide stock, with the fleets and landings structured by state (WA, OR, CA) area of catch. During the 2011 STAR panel concerns were raised regarding the difficulty of discriminating landings from Washington and Oregon waters, particularly in light of the Oregon historical landings reconstruction that includes a summary of data by port of landing but not by catch area, due to the fact that the Oregon and Washington vessels commonly fish in each other's waters and land in each other's ports. The availability of the historical comprehensive landings reconstruction for Oregon by port of landing lead the STAR panel to recommend combining the Washington and Oregon fleets within the coastwide stock assessment using port of landing rather than catch area.

Starting with the 2013 stock assessment, the coastwide stock assessment now summarizes petrale sole landings by the port of landing and combines Washington and Oregon into a single fleet (Haltuch et al. 2013b). The 2015 and 2019 update assessments (Stawitz et al. 2015; Wetzel 2019a) use the same approach as required by the terms of reference for updates. This assessment as well models the resource as a single coastwide stock, with two fishing fleets, North (Washington and Oregon) and South (California).

3.1.2 Most Recent STAR Panel and SSC Recommendations

The most recent STAR panel for petrale sole was for the 2013 full assessment. The STAR panel report from the 2013 full assessment identified a number of recommendations for the next assessment. Below, we list the 2013 STAR panel recommendations and explain how these recommendations were taken into account in this assessment.

1. The states of California and Oregon have completed comprehensive historical catch reconstructions. Washington historical data are not yet available. Completion of Washington historical catch reconstruction would provide a better catch series.

Response: This year Washington Department of Fish and Wildlife completed historical catch reconstruction of petrale sole (pers. comm. T. Tsou, WDFW). These newly estimated landings were used in this assessment. These newly estimated landings are lower than those used in previous assessment. We were not able to locate the source of Washington historical landings used in 2013 (and following update assessments), but historical landings in 2013 assessment were based on preliminary estimates and might have included catches from Puget Sound and Canadian waters (pers. comm. T. Tsou, WDFW). New Washington historical landings are more consistent with history of commercial removals on the U.S. West Coast and represent improvement to the assessment.

2. Update both the maturity and fecundity relationships using samples with wider geographic coverage to include California, and from more recent years for petrale sole would be beneficial.

Response: This assessment uses updated maturity and fecundity estimated. Updated maturity parameters were calculated from data collected within the WCGBTS (pers. comm. M. Head, NWFSC). Updated fecundity parameters were informed by Lefebvre et al. (2019)

3. Studies on stock structure and movement of petrale sole indicating transboundary movement of petrale sole between U.S. and Canadian waters, particularly with regard to the winter-summer spawning migration. It will be informative to include a time-series plot of fishery catch from Canadian waters in future assessment.

Response: Incorporation of fishery catches as well as index on abundance from Canadian waters were explored in this assessment via sensitivity analysis, and results are presented later in this report.

4. Increased collection of commercial fishery age data as well as re-aging any available historical samples from California would help reduce uncertainty. While some recent age data were made available from California, sample sizes could be increased and this data collection needs to continue into the future. Without good age data, the ability to estimate year-class strength and the extent of variation in recruitment is compromised.

Response: Additional age reads from California estimates were generated since 2019, and these ages were included in this assessment.

5. Where possible, historical otolith samples aged using a combination of surface and break-and-burn methods should be re-aged using the break-and-burn method. Early surface read otoliths should also be re-aged using the break and burn method. Historical otoliths aged with a standard method will allow the further evaluation of the potential impacts of consistent under-aging using surface read methods, changes in selectivity during early periods without any composition information, and potential changes in growth.

Response: Although progress has been done in generating additional ages for petrale sole, historical surface-read ages were not re-evaluated. In this assessment, we excluded historical surface-read ages, and conducted sensitivity analysis to evaluate the impact of removing those historical ages to model fits and results.

6. The effect of the implementation of the IFQ (catch shares) program that began during 2011 on fleet behavior, including impacts on discards, fishery selectivity, and fishing locations, would benefit from further study.

Response: In this assessment, additional flexibility is given to the model, through time varying selectivity and retention parameters for the period after 2011, to account for changes in discard rates and fishery selection after IFQ program was implemented.

7. The extent of spatial variability on productivity processes such as growth, recruitment, and maturity is currently unknown and would benefit from further research.

Response: Progress has been made in exploring spatial variability in growth of multiple groundfish species, including petrale sole. Gertseva et al. (2017), for instance, found that detecting spatial growth variability in petrale sole is complicated by the seasonal migrations of fish between shallow northern feeding grounds during warm summer months to southern offshore spawning areas in autumn and winter, and suggested that it could potentially be a sex–area interaction in petrale sole growth. In the early stages of this assessment a two-area spatial model was developed but the additional complexity required by estimating the distribution of annual recruitment among two areas was not supported by the age data available from California so that model was not pursued in depth.

8. The Panel appreciated the delta-GLMM approach to derive an index of stock size from commercial CPUE data. However, there may still be factors other than stock size that affect time-trends in the standardized CPUE indices. The panel recommends:

a. Investigate using effort as an offset in the model. That is, rather than modeling catch/effort = effects, use catch = effort*effects. When a log-link is used then log(effort) can be included as an additive offset, and most GLMM packages include this option. The advantage of this approach is that it is easy to investigate if catch is proportional to effort or not. For example, it may be that CPUE can be higher when effort is low than when effort is high.

b. Include further consideration of the impacts of trip limits on CPUE. Such limits were gradually introduced since 2006 in the winter fisheries and this may impact CPUE. This consideration should involve consultations with fleet members to understand how their fishing behavior was affected by trip limits.

Response: This assessment no longer includes fishery CPUE to inform trend in petrale sole abundance, and, thus, this recommendation is no longer relevant. A lack of influence of fishery CPUEs on model results was illustrated in past and current assessments, indicating that survey data provide sufficient information to monitor changes in abundance.

3.1.3 Response to STAR Panel Requests (not required in draft)

3.2 Model Structure and Assumptions

3.2.1 Model Changes from the Last Assessment and Bridging Analysis

The last full assessment of petrale sole was conducted in 2013 and the most recent update assessment in 2019. The 2019 assessment model was the starting point for this assessment. We retained a number of features of the 2019 assessment and also included a number of improvements related to use of data, model structure and modeling techniques.

Bridging analysis was conducted to illustrate the impact of incremental changes. The results of bridging analysis are shown in Figure 14 to Figure 17. Below, we describe the most important changes made since the last assessment:

1. Upgraded to Stock Synthesis version 3.30.21 (released in February 2023). This is standard practice to capitalize on newly developed features and corrections to older versions as well as improvements in computational efficiency. No discernible differences were produce by this change.

2. Updated historical and current fishery removals, to include most up to date information. This year WDFW completed historical catch reconstruction of petrale sole and newly estimated landings are lower than those used in previous assessment. Historical landings in 2013 assessment were based on preliminary estimates and might have included catches from Puget Sound and Canadian waters (pers. comm. T. Tsou, WDFW). New Washington historical landings are more consistent with history of commercial removals on the U.S. West Coast and represent improvement to the assessment.

3. Removed fishery CPUE time series. This change did not impact the assessment outputs or model fits (Figure 14).

4. Combined Winter and Summer fleets into corresponding annual North and South fleets. The separation of North and South fisheries into the Winter and Summer fleets were primarily motivated by the using the fishery CPUE indices from Winter fisheries, targeting petrale sole spawning aggregations. With removal of CPUE indices from the model, separation into Winter and Summer fleets was no longer needed. Also, Winter and Summer fleets selectivity curves were very similar within respective fisheries. Combining Winter and Summer fleets within North and South fisheries yielded very similar results (Figure 15). Combining seasonal fleets also removed uncertainty associated with separating historical annual catches by season (since fishing year for Winter fleet was defined from November of previous year through the February of the current year). Finally, using annual catches puts assessment in alignment with management system, which operates on a calendar year basis.

5. Recalculated survey abundance indices using sdmTMB geostatistical model. Results did not impact the model output (Figure 14).

6. Switched to a single Triennial Survey index (instead of separating it into two indices for early and late survey periods). The Triennial Survey was separated in past assessments due to change in depth and latitudinal coverage of the Triennial Survey. Using a single index did not impact model results (Figure 14), but provided a longer historical survey trend and simplified the structure of the assessment model.

7. Updated input sample sizes associated with fisheries composition data to using a function of number of trips and number and fish (rather than number of trips, as in previous assessment), to follow current best practices and ensure a consistent treatment of fishery and survey input data (Figure 15).

8. Updated weight-length, maturity and fecundity parameters, to include most up to date and improved information. Updating weight-length parameters did not produce a noticeable change. Model with new maturity parameters had slightly lower scale as length at 50% maturity now is slightly higher (Figure 16 and Figure 17). With new fecundity parameters, the model produces spawning output rather that spawning biomass, and 2019 model 2023 spawning outputs are no longer comparable. However, relative depletion show similar results (Figure 17).

9. Updated spawn-recruit parameters and fixed Beverton-Holt steepness at 0.8, mean of the Myers prior developed based on meta-analysis of flatfish steepness (Myers et al. 1999). When estimated, steepness was approaching the upper parameter bound of 1 (steepness likelihood profile is included in this report). Limiting steepness to 0.8 did not cause a change in model results (Figure 16 and Figure 17), but yielded more reasonable estimates of other life history parameters, including natural mortality.

The list above documents only the most important changes made to this assessment relative to the previous one.

Despite the large number of changes made to data sources and the model configuration, the results of this assessment are consistent with those done previously (Figure 13).

3.2.2 Modeling Platform and Structure

General model specifications (e.g., executable version, model structure, definition of fleets and areas)

3.2.3 Model Parameters

The estimated parameters are summarized in table 13 and all estimated and fixed parameters are shown in Tables 14-21. The total number of parameters is reduced from 304 in 2019 to 267 dur to the simplification of the fleet structure into an annual model without separate selectivity for winter and summer. There are 190 estimated recruitment deviations parameters which are divided as follows: 31 parameters set up the initial age structure in 1876, 147 parameters for the recdevs in 1876 to 2022, and 12 forecast recruitment parameters for the years 2023 to 2035. The recevs in the time series are divided into early, main, and late deviations with the main period covering the years 1959 to 2020. However, the distinction between these periods in Stock Synthesis is only relevant if the main period is a zero-centered vector, which it is not in the base model. Sensitivity analyses are used to explore the impact of relaxing the zero-centering and including all recruitment deviations in the main period.-13

3.2.4 Key Assumptions and Structural Choices

The structure of the base model was selected to balance model realism and parsimony. A large number of alternate model formulations were evaluated during the assessment process. Structural choices were made to be as objective as possible and follow generally accepted methods of approaching similar modeling problems and data issues. The relative effect on assessment results of each of these choices is often unknown; however, extensive efforts were made to evaluate effects of structural choices on model output prior to selecting the base model.

Prior to arriving at the base model, an extensive evaluation of model structure was performed. We explored retaining the four-fleet model with seasonal fisheries of the previous assessment versus two-fleet model with annual fisheries. We also explored a single-fleet model (combining North and South fleets), as well as two-area model, with a single set of growth parameters estimated as well as separate growth parameters estimated for each area. These models produced very similar results, yet the annual two-fleet model was found to be the most appropriate for this assessment. The selected formulation allowed to simplify the model structure and resulted in best fit to data and parameters estimates, which are most consistent with current knowledge of petrale sole, while also accounting for the difference in history of removals among North and South. The simplification of the model allowed to substantially reduce model run time (from several hours to eighteen minutes) and improve final gradient.

As mentioned earlier, the separation of North and South fisheries into the Winter and Summer fleets in past assessments were primarily motivated by the using the fishery CPUE indices from Winter fisheries, targeting petrale sole spawning aggregations. With removal of CPUE indices from the model, separation into Winter and Summer fleets was no longer needed. Winter and Summer fleets selectivity curves were very

similar within respective fisheries, and combining Winter and Summer fleets within North and South fisheries yielded very similar results (Figure 15). Combining seasonal fleets also removed uncertainty associated with separating historical annual catches by season (since fishing year for Winter fleet was defined from November of previous year through the February of the current year). Finally, using annual catches puts assessment in alignment with management system, which operates on a calendar year basis.

Substantial amount of efforts within the assessment was devoted to evaluation of the quality of data available for the assessment, and structural choices were made regarding whether and how specific sources (or their components) should be treated in the model. This included decisions on filtering length and age composition data, treatment of survey indices, and decision on how to best use environmental indices in the model.

We also evaluated various blocking schemes applied to fisheries selectivity parameters to enable reflection of changes associated with management measures applied throughout time, and arrive to model that would allow to best fit to data. Specifically, we implemented blocking for the period after IFQ fishery began, that allowed to reflect changes in discard practices. We also re-evaluation early blocking on retention parameters to ensure that estimation of early discard is informed by sufficient amount of data.

3.3 Base Model Results

As a supplement to the model results figures included in this report and described below, a full set of diagnostic plots created by the {r4ss} package (Taylor et al. 2021) is available at https://pfmc-assessments.github.io/petrale/ along with the Stock Synthesis input files.

3.3.1 Parameter Estimates

Estimated and fixed parameter values are shown in Tables 14-21.

Estimates of key parameters include female $M = 0.142$, male $M = 0.155$. Females were estimated as growing larger than males with female length at age 17 (the second reference age) equal to 47.7 cm compared to 40 cm for males. The L_∞ associated with the estimated growth parameters was 49.5 cm for females and 40.6 cm for males.

3.3.2 Fits to the Data

The model fits the WCGBTS index very well, including a decline from 2005 to 2009 followed by a rapid increase to a plateau in 2013–2017 and a gradual decline to the most recent observations. The observations that fit the least well are 2018 and 2019, which were lower than the years before and after. The absence of a 2020 survey due to the COVID-19 pandemic makes it difficult to determine if those two years were just outliers or if there was some unexplained population dynamics leading to a reduction in available biomass for those years.

When an extra standard deviation parameter was estimated for the WCGBTS, the value was minimal, indicating that the index fits well enough to not require additional tuning.

The fit to length composition data was very good for all fleets when aggregating across years (28). The most visible lack of aggregate fit occurring for discards in the south, where the mode of the observed and expected distributions differed by 2 cm (30 cm vs 28 cm, respectively). However, the tails of the distribution were fit

well. Pearson residuals for the individual years (Figure 30) show short periods with notable residual patterns, such as 1975 and 1982–1983 for the North fleet suggesting unmodeled short-term dynamics in the fleet or population. However, there are not strong patterns within any group of length bin (horizontal stripes within the Pearson plots) indicating a systematic lack of fit.

Expected mean length in each year matches both long-term and short-term trends (Figures 31 to 34). However, a notable lack of fit in this diagnostic is for the 2021 WCGBTS where the largest haul in the history of the survey took place which was dominated by large females, resulting in an outlier in the observed mean lengths.

The fit to the marginal age composition data was good for the North fleet when aggregated across years, but less good for the South (Figure 35). The North fleet has far more age data (Table 23, Figures 36 and 37) due to large gaps in the years with samples from California and smaller sample sizes per year. The years 2018–2022 have the highest sample sizes and are characterized by older than expected fit. Examination of the distributions of ages within each length bin indicates that these fish are older than expected given their lengths.

Fit to the conditional age-at-length (CAAL) data for the WCGBTS was generally good (Figures 38-41), with a few notable clusters of residuals in 2005 (younger than expected fish in the 30–40cm range), 2014 (more young fish in the smaller length bins), and the last few years, where there are more old fish of both sexes in the larger length bins. This pattern of positive residuals for the oldest ages matches the lack of fit to the fishery ages for these years as well. Time varying growth was explored to resolve this lack of fit but did not substantially improve the fit. The likelihood profiles indicate that all the age comps are best fit at smaller natural mortality values than the estimated value which incorporates other data sources. The mean age of the population is estimated to be higher in recent years than at any point since the early 1970s when age data weren't available, so the lack of fit to old ages may be only notable for these recent years because they are the only period with samples of the oldest age bins.

Fit to the discard rates (Figures 42 and 43) and mean body weight of the discards (Figures 45 and 46) was good thanks to consistently low and stable rates and the use of time blocks on the retention parameters to fit the years with significant change. A change in blocking for retention in the South fleet relative to the 2019 assessment (baseing historical period on retention up through 2010 rather than just 2002) resulted in lower and more plausible estimates of discard rates and total discards for the period prior to the availability of observer data for the South fleet (Figure 44).

3.3.3 Population Trajectory

The base model estimate of biomass time series is similar to previous assessments (Figure 13), with estimated biomass of ages 3 and older estimated around 42,198 mt in the unfished equilibrium, declining to a minimum of 5,104 mt in 1992, rebuilding quickly to a recent peak of 21,507 mt in 2015 due to 3 years of very high recruitments from 2006 to 2008, and then declining to 15,803 mt in 2023 due to low or average recruitment in the years since.

In terms of fraction of unfished spawning output (Figure 48), the minimum was 0.057 in 1993, the recent peak was 0.415 in 2017 and the 2023 estimate is 0.336.

The recruitment time series is punctuated by four large recruitment events in 1965, 2006, 2007, and 2008 (Figures 49, 50, and 51). The 1965 recruitment was estimated at about 40 million age-0 recruits while the

latter three were in the 25–30 million range. The rest of the time series is close to 10 million recruits per year. The recruitment in 2012 was almost 20 million (a positive deviation from the stock-recruit curve of 0.56) but the years since are estimated to have had below-average or close-to-average recruitment, with a low point in 2017 of about 8 million recruits (deviation = -0.44).

The precision of the recruitment deviation estimates is highest for the cohorts informed by age data from the WCGBTS which began in 2003 (Figure 51). Therefore the chosen bias adjustment time series has a relative narrow plateau from 2002 to 2015 (Figure 52), where cohorts spawned after that point have been observed for too few years to have as precise an estimate of their year-class strength.

Two measures of exploitation are fishing intensity and exploitation rate. Fishing intensity is defined here as 1 - SPR, where SPR is the equilibrium spawning output at a given combination of F and selectivity relative to spawning output at unfished equilibrium. Using the units of 1-SPR means that more intense fishing is associated with a higher value. The value of 1-SPR in the absence of fishing is 0 and the maximum is 1.0 if all spawning fish are being killed before spawning. The PFMC has chosen an SPR target of 0.3 for petrale sole so harvest which leads to SPR below 0.3, or fishing intensity (1-SPR) greater than 0.7 would be overfishing. Exploitation rate is defined as the catch relative to age 3+ biomass. This metric is included because interpretation is simple, but it is not used as a basis for management.

The estimated time series of exploitation (Figures 53 and 55, Table iv) shows an accelerating increase in fishing intensity and exploitation rate with a peak around 1990 when the 1-SPR increased to 0.91 and the exploitation rate was close to 0.4. These rates are estimated to have declined slowly up to the point where the overfishing declaration led to dramatic decrease in catch in 2010, when 1-SPR fell below the reference point to about 0.64. The fishing intensity has increased since that time due to the rebuilding of the stock, but is estimated to have remained below the reference point in the years since.

3.4 Model Diagnostics

3.4.1 Convergence

A number of tests were performed to verify convergence of the base model, facilitated by the {nwfscDiags} package in R (Wetzel 2023). Following conventional AD Model Builder methods (Fournier et al. 2012), we checked that the Hessian matrix for the base model was positive-definite. There were no difficulties in inverting the Hessian to obtain estimates of variability. We also confirmed that the final gradient is below 0.001. The gradient was even further reduced using `hess_step`, a recent option in ADMB and SS3, allowing to use the Hessian information to fit the true best fit to the data.

To confirm that the reported estimates were from the global best fit, we evaluated the model's ability to recover similar likelihood estimates when initialized from dispersed starting points (jitter option in SS3). Starting parameters were jittered using a setting of 0.05 for 100 iterations. This perturbs the initial values used for minimization with the intention of causing the search to traverse a broader region of the likelihood surface. The majority (62 out of 100) returned to the same objective function value as the base model. The remaining runs exhibited worse fit than the base model. The spread of this search indicates that the jitter was sufficient to search a large portion of the likelihood surface, and that the base model is in a global minimum.

3.4.2 Sensitivity Analyses

We performed a number of sensitivity analyses on the base assessment model, to evaluate the base model's response to change in key parameters and model components.The sensitivity analyses were divided into five groups: indices, composition data, biology, recruitment and environmental index, and the transboundary nature of the stock (Tables 25 to 29 and Figures 58 to 66).

These groups included the following runs:

- Indices
  - Estimating separate catchability parameter and separate selectivity parameters for the late Triennial Survey period.
  - Excluding Triennial Survey 2004 observation.
  - Allowing Triennial Survey selectivity to be dome-shaped.
  - Estimating extra standard deviation for the WCGBTS
  - Including fisheries CPUEs in the model.
- Composition data
  - Tuning the sample sizes using the Dirichlet-Multinomial likelihood.
  - Early surface read ages are included and retuned.
  - Early ages from Oregon marked "special request" are excluded.
- Biology
  - Weight-Length relationship from 2019 assessment.
  - Maturity parameters from 2019 assessment.
  - Estimating age-0 fraction female within the model.
  - Estimating age-0 fraction female with no sex offset on the WCGBTS selectivity parameters.
- Recruitment
  - Incorporating environmental index of petrale sole recruitment based on CMEMS.
  - Using zero-centered recruitment deviations settings.
  - Nor separating early/main/late periods for recruitment deviations.
- Transboundary nature of the stock
  - Adding the West Coast Vancouver Island (WCVI) synoptic bottom trawl survey index to the assessment model.
  - Adding petrale sole catches from British Columbia waters to the North fishing fleet.
  - Adding both index and catches to the base model.

Sensitivities to alternative assumptions regarding treatment of index data had little discernible difference on the population trajectory (Table 25 and Figure 58).

The Dirichlet-Multinomial data weighting method led to weights of 97–99% of the input sample sizes for all composition data other than the WCGBTS which had an applied weight of 74% of the input sample sizes. These weights are far higher than the weights used in the base model calculated using the Francis method and resulted in much more variability in the recruitment time series and relatively less weight applied to the index data. Model runs with the early surface reads included or the early Oregon 'special request' samples excluded similarly led to a less plausible recruitment time series (Table 26 and Figure 59 and 60).

Using weight-length and maturity parameters from 2019 model did not impact model results (Table 27 and

Figure 61). Exploring alternatives for estimating age-0 fraction female were motivated by the explorations of sex ratios discussed in Section 2.3.3. However, the model with fraction female estimated and sex-specific selectivity results in an estimate of 62% female at birth, contrary to the patterns in the data and the patterns in other flatfish indicating confounding with the selectivity parameters. When the sex offset in selectivity was removed for the WCGBTS, the estimate was 47% and the total likelihood was worse by about 30 units of log-likelihood due to degraded fits to the length composition data (Table 27).

Trajectories of all the runs from recruitment sensitivity group were similar (Table 27 and Figure 62). The recruitment estimates in the model with environmental index included, are virtually the same over the most time series, well-informed by the age structure data, but diverge in most recent period, which includes most recent few years, for which youngest cohorts may be not yet selected by either surveys or fisheries (Figures 63 and 64). For those few years, the environmental index becomes more influential, as it can provide additional information, not captured by other sources. This is the expected result from a recruitment index: that it is most influential in the recent years for the cohorts that have not yet been observed in the composition data.

Results of this sensitivity run, therefore, emphasizes the importance of progress in generating an environmental recruitment index and getting it vetted through either peer-review publication or SSC review, so that it might be used with confidence in the assessment.

Studies on stock structure and movement of petrale sole indicating transboundary movement of petrale sole between U.S. and Canadian waters. Addition survey and catches from British Columbia waters to the base model did not cause a conflict among data sources from United States and Canada. The index from the synoptic bottom trawl survey conducted on the West Coast Vancouver Island (WCVI) since 2004 is consistent with the WCGBTS index conducted on the U.S. West Coast (Figure 65). Estimated stock trajectories did not change in any of the alternative runs (Table 29 and Figure 66). As expected, with Canadian catches added, initial spawning output increased.

3.4.3 Retrospective Analysis

A five-year retrospective analysis was conducted by successively removing years of data starting from 2022 (i.e., "Data -1 Years" corresponds to data through 2021 instead of 2022). The estimated spawning output exhibited small changes in the initial equilibrium and the final few years of the model (Figures 67 and 68). These changes are driven primarily by the fit to the WCGBTS, where the combination of the lower observed index in 2018 and 2019 and the absence of a survey in 2020 resulted in the Data-2 through Data-4 retrospectives to a more steeply declining trend at the end of the time series (Figure 69).

3.4.4 Historical Analysis

The second type of retrospective analysis addresses assessment error, or at least in the historical context of the current result, given previous analyses. Figure 13 illustrates the comparison of biomass time series across multiple previous assessments and shows that the base model output follows the same trajectory as previous assessment and estimate stock scale is in the middle range of previous assessments.

3.4.5 Likelihood Profiles

Likelihood profiles were conducted for R_0, steepness, and female natural mortality values separately (Figures 70 - 75). These likelihood profiles were conducted by fixing the parameter at specific values and estimating

the remaining parameters based on the fixed parameter value. The priors for all parameters, including the parameter being profiled, were included in every likelihood model. For example, including the prior on natural mortality across the profiled values of natural mortality provides information on the likelihood contribution of that prior as if it were estimated in the model.

The results of the likelihood profile analysis on R_0 are shown in Figure 70. The negative log-likelihood is optimized at a value of 9.64 for the base model, with the age data best fit at a slightly lower value and hte length comps fit slightly higher. The starting and ending biomass and associated fraction unfished are relatively insensitive to changes in R_0 indicating that other parameters, like natural mortality, are compensating for changes along the profile (Figure 71).

The likelihood profile for steepness shows that the negative log-likelihood for the base model declines with increasing steepness up to an MLE estimate around 0.96 with a flat profile from there up to 1.0 (Figure 72). The model with this steepness value was considered unrealistic as it was associated with less plausible estimates natural mortality around 0.10 (compared to base model estimates of 0.14 for females). Spawner-recruit steepness in the model was fixed at 0.8, which is the Myers prior for Pleuronectidae based on meta-analysis of flatfish steepness (Myers et al. 1999). The starting and ending biomass and associated fraction unfished show almost no change across a wide range of steepness values (Figure 73).

Natural mortality is estimated in this assessment using meta-analytical prior (Hamel 2015; Hamel and Cope 2022). Change in the negative log-likelihood across a range of female natural mortality values is shown in Figure 74. The starting and ending biomass and associated fraction unfished were more sensitive to the changes in female M than the other profile parameters (Figure 75). The dashed line Figure 74 shows the total likelihood without the prior on female M included, but this underestimates the influence of the priors because there remains a prior on male M and the two parameters are highly correlated. Treating male M as an offset or profiling in two dimensions over both M parameters would be good ways to explore the influence of the priors on estimates of M for this model.

4 Management

4.1 Reference Points

Estimated reference points are reported in Table v.

Unfished spawning stock output for petrale sole is estimated to be 22.9 trillion eggs (95% confidence interval: 18–28 trillion eggs). The management biomass target for petrale sole is defined as 25% of the unfished spawning output ($B_{25\%}$), which is estimated by the model to be 5.7 trillion eggs (95% confidence interval: 4.5–6.9 trillion eggs), which corresponds to an exploitation rate (catch / age 3+ biomass) of 0.18. This harvest rate provides an equilibrium yield of 2481 mt at $B_{25\%}$ (95% confidence interval: 2120–2841 mt). Catch limits are determined by an SPR = 30% reference point which is associated with equilibrium exploitation rate of 0.17. The model estimate of maximum sustainable yield (MSY) is 2482 mt (95% confidence interval: 2121–2842 mt). The estimated spawning stock output at MSY is 5.5 trillion eggs (95% confidence interval: 4.3–6.7 trillion eggs). The exploitation rate corresponding to the estimated F_{MSY} proxy of SPR = 29% is 0.18.

4.2 Unresolved Problems and Major Uncertainties

Uncertainty in this assessment model is explicitly captured in the asymptotic confidence intervals reported throughout this assessment for key parameters and management quantities. These intervals reflect the uncertainty in the model fit to the data sources included in the assessment, but do not include uncertainty associated with alternative model configurations or fixed parameters. To explore uncertainty associated with alternative model configurations and evaluate the responsiveness of model outputs to changes in key model assumptions, a variety of sensitivity runs were performed, including runs with different assumptions model structure and treatment of data, life-history parameters, stock-recruitment parameters, and many others. The uncertainty in natural mortality, stock-recruit steepness and the unfished recruitment level was also explored through likelihood profile analysis. Additionally, a retrospective analysis was conducted where the model was run after successively removing data from recent years, one year at a time.

Main life history parameters, such as natural mortality and stock-recruit curve steepness, generally contribute significant uncertainty to stock assessments, and they continue to be a major source of uncertainty in this assessment. These quantities are essential for understanding the dynamics of the stock and determining projected rebuilding. Steepness in this assessment was fixed at 0.8, which is meta-analytical steepness prior for Pleuronectidae. When estimated, steepness was approaching the upper parameter bound of 1, which was considered unrealistic as it was associated with less plausible estimates natural mortality around 0.10 (compared to base model estimates of 0.14 for females). Steepness likelihood profile illustrated that the starting and ending biomass and associated fraction unfished show almost no change across a wide range of steepness values. Natural mortality was estimated for both sexes using meta-analytical prior, but likelihood profile showed that the starting and ending biomass as well as associated fraction unfished are more sensitive to the changes in natural mortality than in steepness. In past several assessments, natural mortality was used as major axis of uncertainty.

4.3 Harvest Projections and Decision Tables

The base model estimate for 2023 spawning depletion is 33.6%. The primary axis of uncertainty about this estimate used in the decision table is based on female natural mortality. Female natural mortality in the assessment model is estimated within the model, which includes a meta-analytical prior based on the maximum age of 32 years. The estimate in the base model is $M = 0.142$. The natural mortality value for the low state of nature is $M = 0.072$ and for high state of nature is $M = 0.219$. These alternative states were calculated as follows:

1. Low and high values for Spawning Output in 2023 were calculated as the 12.5% and 87.5% quantiles of a lognormal distribution with mean equal to the base model estimate and log standard deviation equal to the `Pstar_sigma` reported by r4ss: 0.0884. This is a log-scale calculation of $\sqrt{(log((SD/x)^2 + 1))}$ where $SD = 0.6807$ is the asymptotic estimate of the standard deviation and $x = 7.686$ is the point estimate and is very similar to the non-log CV (0.0886). The resulting low and high values for 2023 Spawning Output are 6.942 and 8.508.

2. The female natural mortality values associated with these low and high spawning output values were calculated using a linear model fit to the spawning output associated with the profile over female M: $SO_{2023} = 6.181 + 10.605M$. Inverting this relationship to calculate M provided the estimates of 0.072 and 0.219 around the point estimate of 0.142.

Twelve-year forecasts for each state of nature were calculated for two catch scenarios. One uses the default harvest control rule P* = 0.45, and the other is based on harvest control rule with a lower P* = 0.40. In each case the 2023 and 2024 catches are fixed at the ACLs which have been set for that year with estimated fleet allocation provided by the GMT. More detailed information for the default P* = 0.45 projection is provided in Table 30. Projections for both catch streams and the alternative states of nature (Low, Base, and High) are provided in the columns of the Decision Table (Table 31), with Spawning Output and Fraction of unfished provided for each state. The states of nature and projections are also illustrated in Figures 76 and 77.

4.4 Evaluation of Scientific Uncertainty

The model estimated uncertainty around the 2023 spawning output for is $\sigma = 0.09$. The uncertainty around the OFL is $\sigma = 0.14$. Both of these values are reported by the {r4ss} package based on the log-scale calculation $\sqrt{(log((SD/x)^2 + 1))}$ where SD is the asymptotic estimate of the standard deviation and x is the point estimate. The resulting σ values are lower than for many West Coast groundfish stocks for several reasons: large sample sizes of length and age data from fisheries and surveys, high frequency of occurrence in the WCGBTS thanks to petrale primarily residing in trawlable habitat within the scope of the survey, and strong contrast in the data caused by fishing down the stock to a low level followed by rapid rebuilding. Nevertheless, these σ values surely underestimate the overall uncertainty as they do not incorporate the model structural uncertainty and do not account for any time-varying dynamics other than recruitment.

The estimated uncertainty values are lower than the Category 1 default $\sigma = 0.5$, so all projections will use the default σ.

4.5 Regional management considerations

Studies on stock structure and movement of petrale sole indicate transboundary movement of petrale sole between U.S. and Canadian waters as discussed in Section 1.1. Within the scope of this assessment, we explored including multiple data sources from British Columbia waters to the base model via sensitivity analysis. Further studies of transboundary movement of petrale sole between U.S. and Canadian waters would be beneficial for understanding of extend of petrale soleto help lay the groundwork for future collaborative effort between U.S. and Canada and potential transboundary assessment.

4.6 Research and Data Needs

Progress on a number of research topics and data issues would substantially improve the ability of this assessment to reliably and precisely model petrale sole population dynamics in the future:

1. Continue research toward better understanding how climate forcing impacts density-independent survival during petrale sole early life stages and further development of environmental recruitment index. Such index can provide additional information on recruitment, not captured by other sources, in most recent years when youngest cohorts may be not yet selected by either surveys or fisheries.

2. The extent of spatial, temporal, and density dependent variability on productivity processes such as growth, recruitment, and maturity is currently unknown and would benefit from further research. It would allow to better understand patterns we see in data and account for potential spatio-temporal variability in life history parameters in the model.

3. Further studies of transboundary movement of petrale sole between U.S. and Canadian waters would be beneficial for understanding the extent of petrale sole movements to help lay the groundwork for future collaborative effort between U.S. and Canada and potential transboundary assessment.

4. The analytical solution for catchability (i.e., observed / predicted biomass) for the WCGBTS is above 1.0 in the base model. This was also the case in previous assessments of petrale sole and other flatfish assessments. Further research into flatfish behaviors in response to survey gear will enhance the interpretation of catchability values for petrale sole off the West Coast.

5. Exploration of fine-scale differences in sex-specific spatial distribution or behavior that could lead to the differences in estimated selectivity would be helpful, as would investigating the possibility of environmental sex determination in petrale sole.

6. The observed age data from the most recent few years in all sources shows slightly-older-than-expected distributions of ages. This could be a function of some unmodeled process related to time-varying growth, ageing error, or recruitment. As more ageing is conducted in the years ahead, it will be easier to determine the most likely drivers of this pattern and explore ways to improve the fit to these data.

5 Acknowledgments

Many people contributed to this assessment. In particular we would like to acknowledge the following:

6 References

Alderdice, D.F., and Forrest, C.R. 1971. Effects of salinity and temperature on embryonic development of the petrale sole(*Eopsetta jordani*). Journal of Fisheries Research Board Canada **28**: 727–744.

Allen, L.G., Pondella, D.J., and Horn, M.H. 2006. The ecology of marine fishes: California and adjacent waters. University of California Press, Los Angeles.

Alverson, D.L., and Chatwin, B.M. 1957. Results from tagging experiments on a spawning stock of petrale sole, *Eopsetta jordani* (Lockington). Journal of Fisheries Research Board Canada **14**: 953–974.

Anderson, S.C., Ward, E.J., English, P.A., and Barnett, L.A. 2022a. sdmTMB: An r package for fast, flexible, and user-friendly generalized linear mixed effects models with spatial and spatiotemporal random fields. bioRxiv. Cold Spring Harbor Laboratory.

Anderson, S.C., Ward, E.J., Philina A. English, and, and Barnett, L.A.K. 2022b. sdmTMB: An r package for fast, flexible, and user-friendly generalized linear mixed effects models with spatial and spatiotemporal random fields. bioRxiv **2022.03.24.485545**. doi:10.1101/2022.03.24.485545.

Anon. 2001. Fish stocks of the Pacific coast. Fisheries; Oceans Canada.

Bartoń, K. 2023. MuMIn: Multi-model inference. Available from https://CRAN.R-project.org/package=MuMIn.

Best, E.A. 1960. Petrale Sole. In: California ocean fisheries resources to the year 1960. California Department of Fish; Game.

Best, E.A. 1963. Movements of petrale sole, *Eopsetta jordani*, tagged off of California. Pacific Marine Fisheries Commission Bulletin **6**: 24–38.

Birtwell, I.K., Wood, M., and Gordon, D.K. 1984. Fish diets and benthic invertebrates in the estuary of the Somass River, Port Alberni, British Columbia. California Manuscript Report of Fisheries; Aquatic Sciences.

Bradburn, M.J., Keller, A.A., and Horness, B.H. 2011. The 2003 to 2008 US West Coast bottom trawl surveys of groundfish resources off Washington, Oregon, and California: Estimates of distribution, abundance, length, and age composition. US Department of Commerce, National Oceanic; Atmospheric Administration, National Marine Fisheries Service.

Burnham, K.P., and Anderson, D.R. 1998. Model selection and inference: A practical information-theoretic approach. Book, Springer-Verlag, New York, NY.

Casilla, E., Crockett, L., deReynier, Y., Glock, J., Helvey, M., Meyer, M., Meyer, B., Schmitt, C., Yoklavich, M., Bailey, A., Chao, B., Johnson, B., and Pepperell, T. 1998. Essential fish habitat West Coast groundfish. National Marine Fishereis Service, Seattle, WA. Available from http://www.nwr.noaa.gov/1sustfsh/efhappendix/page1.html.

Castillo, G.C. 1992. Fluctuations of year-class strength of petrale sole (*Eopsetta jordani*) and their relation to environmental factors. Master's thesis, Oregon State University.

Castillo, G.C. 1995. Latitudinal patterns in reproductive life history traits of northeast Pacific flatfish. *In* Proceedings of the International Symposium on North Pacific Flatfish. Alaska Sea Grant, University of Alaska Fairbanks. pp. 51–72.

Castillo, G.C., Li, H.W., and Golden, J.T. 1993. Environmental induced recruitment variation in petrale sole, *Eopsetta jordani.* Fisheries Bulletin **92**: 481–493.

Demory, R.L. 1984. Progress report on the status of petrale sole in the INPFC Columbia-Vancouver areas in 1984. Pacific Fishery Management Council, 7700 Ambassador Place NE, Suite 200, Portland, OR 97220.

DiDonato, G., and Pasquale, N. 1970. Migration of petrale sole tagged in deep water off the Washington coast. Wash. Dept. Fish. Res. Pap. **3**: 53–61.

Drevillon, M., Fernandez, E., and Lellouche, J.M. 2022. For the global ocean physical multi year product GLOBAL_MULTIYEAR_PHY_001_030. Copernicus Product User Manual **1**(4): 1–25. Journal Article.

Eschmeyer, W.N., and Herald, E.S. 1983. A field guide of Pacific coast fishes North America. Houghton Mifflin CO, Boston, MA.

Fargo, J.J. 1997. Flatfish stock assessments for the West Coast of Canada for 1997 and recommended yield options for 1998. Can. Stock Assess. Sec. Res. Doc.

Fernandez, E., and Lellouche, J.M. 2018. Product user manual for the global ocean physical reanalysis product GLORYS12V1. Copernicus Product User Manual **4**: 1–15. Journal Article.

Gates, D.E., and Frey, H.W. 1974. Designated common names of certain marine organisms of California. Fish Buletin **161**: 55–90.

Gertseva, V., Matson, S.E., and Cope, J. 2017. Spatial growth variability in marine fish: example from Northeast Pacific groundfish. ICES Journal of Marine Science **74**(6): 1602–1613. doi:10.1093/icesjms/fsx016.

Gregory, P.A., and Jow, T. 1976. The validity of otoliths as indicators of age of petrale sole from California. California Department of Fish and Game **62**(2): 132–140.

Haltuch, M.A., Hamel, O.S., Piner, K.R., McDonald, P., Kastelle, C.R., and Field, J.C. 2013a. A California Current bomb radiocarbon reference chronology and petrale sole (*Eopsetta jordani*) age validation. Canadian Journal of Fisheries and Aquatic Sciences **70**(1): 22–31. doi:10.1139/cjfas-2011-0504.

Haltuch, M.A., and Hicks, A.C. 2009. Status of the U.S. Petrale sole resource ien 2008. Pacific Fishery Management Council, Pacific Fishery Management Council, 7700 Ambassador Place NE, Suite 200, Portland, OR 97220.

Haltuch, M.A., Ono, K., and Valero, J.L. 2013b. Status of the U.S. Petrale sole resource in 2012. Pacific Fishery Management Council, Pacific Fishery Management Council, 7700 Ambassador Place NE, Suite 200, Portland, OR 97220.

Haltuch, M.A., Tolimieri, N., Lee, Q., and Jacox, M.G. 2020. Oceanographic drivers of petrale sole recruitment in the california current ecosystem. Fisheries Oceanography **29**(2): 122–136. doi:https://doi.org/10.1111/fog.12459.

Hamel, O.S. 2015. A method for calculating a meta-analytical prior for the natural mortality rate using multiple life history correlates. ICES Journal of Marine Science: Journal du Conseil **72**(1): 62–69. doi:10.1093/icesjms/fsu131.

Hamel, O.S., and Cope, J.M. 2022. Development and considerations for application of a longevity-based prior for the natural mortality rate. Fisheries Research **256**: 106477. doi:https://doi.org/10.1016/j.fishres.2022.106477.

Hannah, R.W., Parker, S.J., and Fruth, E.L. 2002. Length and age at maturity of female petrale sole (*Eopsetta jordani*) determined from samples collected prior to spawning aggregation. U.S. Fish Bulletin **100**: 711–719.

Harry, G. 1959. Time of spawning, length at maturity, and fecundity of the English, petrale, and dover soles (*Parophrys vetulus*, *Eopsetta jordani*, and *Microstomus pacificus*, respectively). Fisheries Commission of Oregon, Research Briefs **7**(1): 5–13.

Harvey, A., C. J. Leising. 2022. 2022-2023 CALIFORNIA CURRENT ECOSYSTEM STATUS REPORT a report of the NOAA california current integrated ecosystem assessment team (CCIEA) to the pacific fishery management council, march 7, 2023. Edited Book.

Heimann, R.F.G., and Carlisle, J.G. 1970. Pacific Fishes of Canada. California Department of Fish and Game Fish Bulletin **149**.

Helser, T.E., Punt, A.E., and Methot, R.D. 2004. A generalized linear mixed model analysis of a multi-vessel fishery resource survey. **70**: 251–264.

Hoenig, J.M. 1983. Empirical use of longevity data to estimate mortality rates. Fishery Bulletin **82**: 898–903.

Honeycutt, J., Deck, C., Miller, S., Severance, M., Atkins, E., Luckenbach, J., Buckel, J.A., Daniels, H.V., Rice, J., Borski, R., and others. 2019. Warmer waters masculinize wild populations of a fish with temperature-dependent sex determination. Scientific Reports **9**(1): 6527. Nature Publishing Group UK London.

Horton, H.F. 1989. Species profile: Life histories and environmental requirements of coastal fishes and invertebrates (Pacific Northwest),. U.S. Fish; Wildlife Service Biological Report.

Jean-Michel, L., Eric, G., Romain, B.-B., Gilles, G., Angélique, M., Marie, D., Clément, B., Mathieu, H., Olivier, L.G., and Charly, R. 2021. The copernicus global 1/12 oceanic and sea ice GLORYS12 reanalysis. Frontiers in Earth Science **9**: 698876. Journal Article.

Johnson, K.F., and Wetzel, C.R. 2023. PacFIN.utilities: Generate fishery composition data from PacFIN data for the NWFSC. Available from https://github.com/pfmc-assessments/PacFIN.Utilities.

Karnowski, M., Gertseva, V.V., and Stephens, A. 2014. Historical Reconstruction of Oregon's Commercial Fisheries Landings. Oregon Department of Fish; Wildlife, Salem, OR.

Keller, A.A., Wallace, J.R., and Methot, R.D. 2017. The northwest fisheries science center's west coast groundfish bottom trawl survey: History design, and description. Report, U.S. Department of Commerce. doi:10.7289/V5/TM-NWFSC-136.

Ketchen, K.S., and Forrester, C.R. 1966. Population dynamics of the petrale sole, *Eopsetta jordani*, in waters off western Canada. Fish. Res. Bd. Canada Bull.

Kramer, D.E., Barss, W.H., Paust, B.C., and Bracken, B.E. 1995. Guide to northeast Pacific flatfishes: Families Bothidae, Cynoglossidae, and Pleuronectidae. Alaska Sea Grant, University of Alaska Fairbanks.

Kravitz, M.J., Pearcy, W.G., and Guin, M.P. 1977. Food of five species of co-occurring flatfishes on Oregon's continental shelf. Fishery Bulletin **74**(4): 984–990.

Kristensen, K., Nielsen, A., Berg, C.W., Skaug, H.J., and Bell, B.M. 2016. TMB: Automatic Differentiation and Laplace Approximation. Journal of Statistical Software **70**: 1–21.

Lai, H.L., Haltuch, M.A., Punt, A.E., and Cope, J. 2005. Stock assessment of petrale sole: 2004. Pacific Fishery Management Council, Pacific Fishery Management Council, 7700 Ambassador Place NE, Suite 200, Portland, OR 97220.

Le Galloudec, O., Law Chune, S., Nouel, L., Fernandez, E., Derval, C., Tressol, M., Dussurget, R., Bairdeau, A., and Tonani, M. 2022. Product user manual for global ocean physical analysis and forecasting product GLOBAL_ANALYSISFORECAST_PHY_001_024. Copernicus Product User Manual **1**(9): 1–41. Journal Article.

Lefebvre, L.S., Friedlander, C.L., and Field, J.C. 2019. Reproductive ecology and size-dependent fecundity in the petrale sole (Eopsetta jordani) in waters of California, Oregon, and Washington. Fishery Bulletin **117**(4): 291–302. doi:10.7755/FB.117.4.2.

Love, M. 1996. Probably more than you want to know about the fishes of the Pacific Coast. Really Big Press, Santa Barbara, California.

Love, M., Mecklenburg, C.W., Mecklenburg, T.A., and Thorsteinson, L. 2005. Resource inventory of marine and estuarine fishes of the West Coast and Alaska: A checklist of north Pacific and arctic ocean species from Baja California to the Alsaka-Yukon border. USGS, Seattle, WA.

Luckenbach, J.A., Borski, R.J., Daniels, H.V., and Godwin, J. 2009. Sex determination in flatfishes: Mechanisms and environmental influences. *In* Seminars in cell & developmental biology. Elsevier. pp. 256–263.

Mantua, N.J., Hare, S.R., Zhang, Y., Wallace, J.R., and Francis, R.C. 1997. A Pacific interdecadal climate oscillation with impacts on salmon production. Bull. Am. Meteorol Soc. **78**: 1069–1080.

Myers, R.A., Bowen, K.G., and Barrowman, N. 1999. Maximum reproductive rate of fish at low population sizes. Canadian Journal of Fisheries and Aquatic Sciences **56**: 2404–2419. Available from http://www.nrcresearchpress.com/doi/pdf/10.1139/f99-201 [accessed 4 October 2016].

Neveu, E., Moore, A.M., Edwards, C.A., Fiechter, J., Drake, P., Crawford, W.J., Jacox, M.G., and Nuss, E. 2016. An historical analysis of the california current circulation using ROMS 4D-var: System configuration and diagnostics. Ocean Modelling **99**: 133–151. Journal Article. doi:10.1016/j.ocemod.2015.11.012.

Pearsall, I.A., and Fargo, J.J. 2007. Diet composition and habitat fidelity for groundfish in Hecete Strait, British Columbia. Canadian Technical Report of Fisheries; Aquatic Sciences.

Pedersen, M.G. 1975. Movements and growth of petrale sole (*Eopsetta jordani*) tagged off Washington and southwest Vancouver Island. Fishery Research Board of Canada Progress Report.

Perry, R.I., Stocker, M., and Fargo, J. 1994. Environmental effects on the distribution of groundfish in Hecate Strait, British Columbia. Canadian Journal of Fisheries and Aquatic Sciences **51**: 1401–1409.

Pikitch, E.K., Erickson, D.L., and Wallace, J.R. 1988. An evaluation of the effectiveness of trip limits as a management tool. Northwest; Alaska Fisheries Center, National Marine Fisheries Service NWAFC Processed Report. Available from https://www.afsc.noaa.gov/Publications/ProcRpt/PR1988-27.pdf [accessed 28 February 2017].

Porter, P. 1964. Notes on fecundity, spawning, and early life history of petrale sole (*Eopsetta jordani*) with descriptions of flatfish larvae collected in the Pacific Ocean off Humboldt Bay, California. Master's thesis, Humboldt State College.

R Core Team. 2023. R: A language and environment for statistical computing. R Foundation for Statistical Computing, Vienna, Austria. Available from https://www.R-project.org/.

Ralston, S., Pearson, D.E., Field, J.C., and Key, M. 2010. Documentation of the California catch reconstruction project. US Department of Commerce, National Oceanic; Atmospheric Adminstration, National Marine.

Reilly, P.N., Wilson-Vandenberg, D., Lea, R.N., Wilson, C., and Sullivan, M. 1994. Recreational angler's guide to the common nearshore fishes of Northern and Central California. California Department of Fish; Game.

Rogers, J.B., and Pikitch, E.K. 1992. Numerical definition of groundfish assemblages caught off the coasts of Oregon and Washington using commercial fishing strategies. Canadian Journal of Fisheries and Aquatic Sciences **49**(12): 2648–2656.

Sampson, D.B., and Lee, Y.W. 1999. An assessment of the stocks of petrale sole off Washington, Oregon, and Northern California in 1998. Pacific Fishery Management Council, 7700 Ambassador Place NE, Suite 200, Portland, OR 97220.

Santa Cruz, F., Parada, C., Haltuch, M., Wallace, J., Cornejo-Guzmán, S., and Curchitser, E. 2023. Petrale sole transboundary connectivity and settlement success: A biophysical approach. Frontiers in Marine Science **10**. doi:10.3389/fmars.2023.1155227.

Scofield, W.L. 1948. Trawling gear in California. California Fish and Game Fish Bulletin **72**: 1–60.

Smith, R.T. 1937. Report on the Puget Sound otter trawl investigations. Master's thesis, University of Washington.

Starr, P.J., and Fargo, J. 2004. Petrale sole stock assessment for 2003 and recommendations for management in 2004. CSAS Res. Doc 2004/036.

Stawitz, C.C., Hurtado-Ferro, F., Kuriyama, P.T., Trochta, J.T., Johnson, K.F., Haltuch, M.A., and Hamel, O.S. 2015. Stock assessment update: Status of the U.S. Petrale sole resource in 2014. Pacific Fishery Management Council, 7700 Ambassador Place NE, Suite 200, Portland, OR 97220.

Stewart, I.J., and Hamel, O.S. 2014. Bootstrapping of sample sizes for length- or age-composition data used in stock assessments. Canadian Journal of Fisheries and Aquatic Sciences **71**(4): 581–588. doi:10.1139/cjfas-2013-0289.

Taylor, I.G., Doering, K.L., Johnson, K.F., Wetzel, C.R., and Stewart, I.J. 2021. Beyond visualizing catch-at-age models: Lessons learned from the r4ss package about software to support stock assessments. Fisheries Research **239**: 105924. Available from https://doi.org/10.1016/j.fishres.2021.105924.

Then, A.Y., Hoenig, J.M., Hall, N.G., and Hewitt, D.A. 2015. Evaluating the predictive performance of empirical estimators of natural mortality rate using information on over 200 fish species. ICES Journal of Marine Science **72**(1): 82–92. doi:10.1093/icesjms/fsu136.

Thorson, J.T. 2019. Guidance for decisions using the Vector Autoregressive Spatio-Temporal (VAST) package in stock, ecosystem, habitat and climate assessments. Fisheries Research **210**: 143–161. doi:10.1016/j.fishres.2018.10.013.

Thorson, J.T., Shelton, A.O., Ward, E.J., and Skaug, H.J. 2015. Geostatistical delta-generalized linear mixed models improve precision for estimated abundance indices for West Coast groundfishes. ICES Journal of Marine Science **72**(5): 1297–1310. doi:10.1093/icesjms/fsu243.

Thorson, J.T., and Ward, E.J. 2014. Accounting for vessel effects when standardizing catch rates from cooperative surveys. Fisheries Research **155**: 168–176. doi:10.1016/j.fishres.2014.02.036.

Tolimieri, N., Haltuch, M.A., Lee, Q., Jacox, M.G., and Bograd, S.J. 2018. Oceanographic drivers of sablefish recruitment in the California Current. Fisheries Oceanography **27**(5): 458–474. doi:10.1111/fog.12266.

Tolimieri, N., Wallace, J., and Haltuch, M. 2020. Spatio-temporal patterns in juvenile habitat for 13 groundfishes in the california current ecosystem. PLoS One **15**(8). Journal Article. doi:10.1371/journal.pone.0237996.

Trumble, S.J. 1995. Abundance, movements, dive behavior, food habits, and mother - pup interactions of harbor seals (*Phoca vitulina richardsi*) near Monterey Bay, California. Master's thesis, California State University Fresno.

Turnock, J., Wilkins, M., Saelens, M., and Wood, C. 1993. Status of West Coast petrale sole in 1993. Pacific Fishery Management Council, 7700 Ambassador Place NE, Suite 200, Portland, OR 97220.

Weinberg, K.L., Wilkins, M.E., Shaw, F.R., and Zimmermann, M. 2002. The 2001 Pacific West Coast bottom trawl survey of groundfish resources: Estimates of distribution, abundance and length and age composition. {NOAA} {Technical} {Memorandum}, U.S. Department of Commerce.

Wetzel, C. 2023. nwfscDiag: Generate standard NWFSC assessment diagnostics. Available from https://github.com/pfmc-assessments/nwfscDiag.

Wetzel, C.R. 2019a. Status of petrale sole (*Eopsetta jordani*) along the U.S. West coast in 2019. Pacific Fishery Management Council, 7700 Ambassador Place NE, Suite 200, Portland, OR.

Wetzel, C.R. 2019b. Status of petrale sole (eopsetta jordani) along the u.s. West coast in 2019. Pacific fishery management council, 7700 ambassador place NE, suite 101, portland, OR 97220. Journal Article.

Wetzel, C.R., Johnson, K.F., and Hicks, A.C. 2023. nwfscSurvey: Northwest fisheries science center survey. Available from https://github.com/pfmc-assessments/nwfscSurvey.

7 Tables

Table 1: Landed catch by fleet and state (mt).

Year	Total	North (OR + WA)	South (CA)	WA	OR
1876	1	0	1	0	0
1877	1	0	1	0	0
1878	1	0	1	0	0
1879	1	0	1	0	0
1880	12	0	12	0	0
1881	22	0	22	0	0
1882	33	0	33	0	0
1883	43	0	43	0	0
1884	54	0	54	0	0
1885	64	0	64	0	0
1886	75	0	75	0	0
1887	85	0	85	0	0
1888	96	0	96	0	0
1889	106	0	106	0	0
1890	117	0	117	0	0
1891	128	0	128	0	0
1892	138	0	138	0	0
1893	149	0	149	0	0
1894	159	0	159	0	0
1895	170	0	170	0	0
1896	181	0	180	0	0
1897	191	0	191	0	0
1898	202	0	201	0	0
1899	212	0	212	0	0
1900	223	0	223	0	0
1901	233	0	233	0	0
1902	244	0	244	0	0
1903	254	0	254	0	0
1904	265	0	265	0	0
1905	275	0	275	0	0
1906	286	0	286	0	0
1907	297	0	296	0	0
1908	307	0	307	0	0
1909	318	0	318	0	0
1910	328	0	328	0	0
1911	339	0	339	0	0
1912	349	0	349	0	0
1913	360	0	360	0	0
1914	370	0	370	0	0
1915	381	0	381	0	0
1916	386	0	386	0	0
1917	526	0	526	0	0
1918	424	0	424	0	0
1919	334	0	333	0	0

Table 1: Landed catch by fleet and state (mt). (*continued*)

Year	Total	North (OR + WA)	South (CA)	WA	OR
1920	231	0	230	0	0
1921	294	0	294	0	0
1922	425	0	425	0	0
1923	427	0	427	0	0
1924	533	0	533	0	0
1925	529	0	528	0	0
1926	522	0	522	0	0
1927	632	0	632	0	0
1928	620	0	620	0	0
1929	708	2	706	0	2
1930	660	1	659	0	1
1931	641	17	624	16	1
1932	598	42	557	33	9
1933	479	54	424	49	5
1934	1180	69	1111	65	4
1935	982	87	895	82	5
1936	626	115	511	98	17
1937	1016	198	818	114	84
1938	1124	135	989	130	4
1939	1535	374	1161	120	254
1940	1317	602	715	146	456
1941	1177	772	405	230	542
1942	2206	1929	277	251	1678
1943	2376	1959	417	313	1646
1944	1621	1112	509	267	845
1945	1508	974	534	290	684
1946	2806	1596	1209	266	1330
1947	2223	886	1337	251	635
1948	4280	1972	2309	780	1192
1949	3069	823	2246	128	695
1950	3461	1481	1980	116	1365
1951	2323	1085	1238	194	891
1952	2177	864	1313	218	647
1953	1928	414	1514	31	383
1954	2526	634	1892	149	485
1955	2294	653	1642	189	464
1956	1849	571	1278	152	420
1957	2640	1052	1588	246	806
1958	2319	891	1428	112	778
1959	1881	687	1194	160	527
1960	2157	1035	1123	130	904
1961	2548	1010	1538	183	827
1962	2691	1311	1379	159	1152
1963	2711	1206	1505	158	1048
1964	2151	927	1224	113	814
1965	2109	902	1208	143	759

Table 1: Landed catch by fleet and state (mt). (*continued*)

Year	Total	North (OR + WA)	South (CA)	WA	OR
1966	2290	962	1328	130	832
1967	2181	926	1256	96	830
1968	2121	817	1304	82	735
1969	2249	949	1300	84	864
1970	2714	1165	1549	172	992
1971	2888	1314	1573	260	1054
1972	2953	1332	1622	325	1007
1973	2951	1646	1305	623	1023
1974	3625	2069	1556	822	1247
1975	3490	2007	1483	801	1206
1976	2764	1413	1351	612	801
1977	2268	1270	998	444	826
1978	3059	1864	1195	845	1019
1979	3055	1666	1389	609	1057
1980	2468	1402	1066	544	858
1981	2041	1236	805	352	884
1982	2630	1839	792	331	1508
1983	2214	1630	584	525	1105
1984	1739	1149	591	460	688
1985	1839	983	857	405	578
1986	1750	1024	726	313	711
1987	2205	1381	824	526	855
1988	2149	1354	795	452	902
1989	2153	1312	841	450	862
1990	1765	1086	678	342	744
1991	1927	1193	735	261	932
1992	1554	1021	532	251	771
1993	1503	1040	464	265	775
1994	1375	826	550	210	616
1995	1659	1066	593	270	797
1996	1829	1010	818	290	720
1997	1948	1114	834	308	806
1998	1463	990	473	308	682
1999	1497	931	566	257	674
2000	1893	1253	640	395	858
2001	1845	1270	575	348	922
2002	1797	1317	480	425	892
2003	2070	1661	408	522	1139
2004	1964	1471	493	517	955
2005	2734	1971	764	535	1436
2006	2610	1858	752	294	1565
2007	2253	1334	919	181	1152
2008	2220	1295	925	177	1118
2009	1767	1237	531	224	1013
2010	803	590	213	84	506
2011	935	757	177	234	523

Table 1: Landed catch by fleet and state (mt). (*continued*)

Year	Total	North (OR + WA)	South (CA)	WA	OR
2012	1118	896	221	217	679
2013	2253	1776	477	390	1386
2014	2409	1783	625	272	1511
2015	2665	2086	580	267	1818
2016	2728	2254	473	313	1941
2017	2931	2314	617	367	1946
2018	2894	2285	610	424	1860
2019	2617	2080	537	406	1673
2020	2092	1549	543	80	1468
2021	2879	2103	776	211	1892
2022	3060	2094	966	134	1959

Table 2: Sample sizes of commercial length composition data by fleet.

Year	Trips North	Fish North	Input N North	Trips South	Fish South	Input N South
1948	0	0	0	8	405	56
1949	0	0	0	10	458	71
1950	0	0	0	0	0	0
1951	0	0	0	0	0	0
1952	0	0	0	0	0	0
1953	0	0	0	0	0	0
1954	0	0	0	0	0	0
1955	1	507	7	0	0	0
1956	2	689	14	0	0	0
1957	4	1053	28	0	0	0
1958	3	2140	21	0	0	0
1959	0	0	0	0	0	0
1960	1	252	7	0	0	0
1961	1	100	7	0	0	0
1962	0	0	0	3	150	21
1963	0	0	0	0	0	0
1964	1	200	7	24	970	158
1965	1	99	7	15	608	99
1966	4	1125	28	53	2248	363
1967	3	485	21	56	2296	373
1968	15	3378	106	100	3913	640
1969	7	1634	49	68	2612	428
1970	14	3581	99	35	1144	193
1971	16	3638	113	49	1699	283
1972	18	4202	127	60	2179	361
1973	8	1715	56	59	2221	365
1974	33	9485	233	63	2106	354
1975	44	7875	311	27	1198	191
1976	7	1971	49	36	1730	254
1977	22	2629	155	54	2555	381
1978	25	3232	176	42	2097	297
1979	29	3009	205	17	846	120
1980	53	5514	374	101	5040	713
1981	46	4596	325	96	4656	678
1982	22	2207	155	64	2930	452
1983	4	413	28	50	2450	353
1984	1	201	7	32	1570	226
1985	6	596	42	25	1225	176
1986	14	1397	99	27	1351	191
1987	22	1105	155	20	1000	141
1988	18	899	127	11	516	78
1989	16	803	113	17	841	120
1990	16	801	113	12	504	82
1991	17	633	104	24	836	139
1992	19	741	121	6	176	30
1993	16	530	89	0	0	0

Table 2: Sample sizes of commercial length composition data by fleet. (*continued*)

Year	Trips North	Fish North	Input N North	Trips South	Fish South	Input N South
1994	15	629	102	0	0	0
1995	8	296	49	0	0	0
1996	6	235	38	0	0	0
1997	21	774	128	0	0	0
1998	39	1697	273	0	0	0
1999	38	1603	259	0	0	0
2000	48	1962	319	0	0	0
2001	36	1489	241	16	478	82
2002	52	2078	339	14	305	56
2003	75	2633	438	40	699	136
2004	61	2357	386	23	588	104
2005	74	2928	478	41	1061	187
2006	96	4466	678	72	1802	321
2007	95	4303	671	153	4358	754
2008	101	4182	678	143	3889	680
2009	98	4080	661	76	1880	335
2010	105	3347	567	60	1620	284
2011	73	2871	469	45	1334	229
2012	76	3012	492	52	1874	311
2013	107	4442	720	73	3447	515
2014	123	4578	755	75	2859	470
2015	124	4419	734	62	2166	361
2016	78	2742	456	71	2599	430
2017	131	4605	766	81	3108	510
2018	142	3988	692	88	3105	516
2019	160	3459	637	90	3556	581
2020	73	1447	273	107	3654	611
2021	109	2080	396	95	2804	482
2022	104	2898	504	36	1345	222

Table 3: Sample sizes of commercial age composition data by year, fleet, and ageing error matrix (Age-Mat) applied to those observations in the model. The AgeMat codes are as follows: C-S1: CAP Surface Pre-1990 (EXCLUDED FROM BASE MODEL), C-S2: CAP Surface, C-C: CAP Combo, C-BB: CAP Break-Burn, W-S: WDFW Surface (EXCLUDED FROM BASE MODEL), W-C: WDFW Combo, W-BB: WDFW Break-Burn. Note that there are repeated years in this table and in the model for years where there are multiple ageing error matrices applied within the same year/fleet combination.

year	North Ntrips	North Nfish	North In-putN	North Age-Mat	South Ntrips	South Nfish	South In-putN	South Age-Mat
1960	1	168	7	W-S	0	0	0	NA
1961	1	100	7	W-S	0	0	0	NA
1964	1	200	7	W-S	0	0	0	NA
1965	1	99	7	W-S	0	0	0	NA
1966	3	525	21	W-S	46	1090	196	C-S1
1967	3	482	21	W-S	13	323	58	C-S1
1968	11	2175	78	W-S	60	1404	254	C-S1
1969	5	496	35	W-S	43	1059	189	C-S1
1970	13	2126	92	W-S	34	835	149	C-S1
1971	12	1997	85	W-S	49	1224	218	C-S1
1972	17	2685	120	W-S	59	1475	263	C-S1
1973	8	1439	56	W-S	54	1384	245	C-S1
1974	26	2660	184	W-S	61	1480	265	C-S1
1975	20	1976	141	W-S	25	649	115	C-S1
1976	6	597	42	W-S	33	825	147	C-S1
1977	2	198	14	W-S	43	1063	190	C-S1
1977	19	1852	134	C-S1	0	0	0	NA
1978	5	695	35	W-S	38	950	169	C-S1
1978	15	1364	106	C-S1	0	0	0	NA
1979	3	295	21	W-S	15	370	66	C-S1
1979	22	2270	155	C-S1	0	0	0	NA
1980	27	2612	191	C-C	62	1545	275	C-S1
1980	18	1745	127	W-S	0	0	0	NA
1981	42	4170	297	C-C	37	927	165	C-S1
1981	2	195	14	W-S	0	0	0	NA
1982	20	1079	141	C-C	25	527	98	C-S1
1983	4	405	28	C-C	17	468	82	C-S1
1984	0	0	0	NA	5	123	22	C-S1
1985	6	489	42	C-C	6	150	27	C-C
1986	13	1234	92	C-C	0	0	0	NA
1987	22	747	125	C-C	0	0	0	NA
1988	18	635	106	C-C	0	0	0	NA
1989	15	651	105	C-C	0	0	0	NA
1990	16	432	76	C-C	11	331	57	C-C
1991	17	353	66	C-C	8	245	42	C-C
1992	19	737	121	C-C	0	0	0	NA
1993	16	530	89	C-C	0	0	0	NA
1994	15	628	102	C-C	0	0	0	NA
1995	8	295	49	C-C	0	0	0	NA
1996	6	232	38	C-C	0	0	0	NA
1997	20	733	121	C-C	0	0	0	NA

Table 3: Sample sizes of commercial age composition data by year, fleet, and ageing error matrix (Age-Mat) applied to those observations in the model. The AgeMat codes are as follows: C-S1: CAP Surface Pre-1990 (EXCLUDED FROM BASE MODEL), C-S2: CAP Surface, C-C: CAP Combo, C-BB: CAP Break-Burn, W-S: WDFW Surface (EXCLUDED FROM BASE MODEL), W-C: WDFW Combo, W-BB: WDFW Break-Burn. Note that there are repeated years in this table and in the model for years where there are multiple ageing error matrices applied within the same year/fleet combination. (*continued*)

year	North Ntrips	North Nfish	North In-putN	North Age-Mat	South Ntrips	South Nfish	South In-putN	South Age-Mat
1998	26	1047	170	C-C	0	0	0	NA
1998	13	637	92	W-S	0	0	0	NA
1999	13	500	82	C-BB	0	0	0	NA
1999	1	35	6	C-S2	0	0	0	NA
1999	12	597	85	W-S	0	0	0	NA
2000	18	822	127	W-S	0	0	0	NA
2001	1	12	3	C-S2	0	0	0	NA
2001	15	729	106	W-S	0	0	0	NA
2002	15	518	86	C-S2	0	0	0	NA
2002	14	693	99	W-S	0	0	0	NA
2003	22	705	119	C-S2	7	96	20	C-BB
2003	26	1100	178	W-S	0	0	0	NA
2004	10	338	57	C-S2	6	153	27	C-BB
2004	23	1103	162	W-S	0	0	0	NA
2005	24	1168	169	W-S	13	269	50	C-BB
2006	44	308	87	C-BB	9	206	37	C-BB
2006	18	894	127	W-S	0	0	0	NA
2007	18	515	89	C-BB	9	175	33	C-BB
2007	22	1099	155	W-S	0	0	0	NA
2008	18	483	85	C-BB	25	395	80	C-BB
2008	19	932	134	W-S	0	0	0	NA
2009	56	537	130	C-BB	3	77	14	C-BB
2009	11	547	78	W-C	0	0	0	NA
2010	45	506	115	C-BB	0	0	0	NA
2010	8	389	56	W-C	0	0	0	NA
2011	54	529	127	C-BB	16	211	45	C-BB
2011	12	643	85	W-BB	0	0	0	NA
2012	59	621	145	C-BB	5	152	26	C-BB
2012	12	599	85	W-BB	0	0	0	NA
2013	77	714	176	C-BB	4	139	23	C-BB
2013	17	840	120	W-BB	0	0	0	NA
2014	42	745	145	C-BB	0	0	0	NA
2014	11	549	78	W-BB	0	0	0	NA
2015	90	718	189	C-BB	0	0	0	NA
2015	15	725	106	W-BB	0	0	0	NA
2016	62	523	134	C-BB	0	0	0	NA

Table 3: Sample sizes of commercial age composition data by year, fleet, and ageing error matrix (Age-Mat) applied to those observations in the model. The AgeMat codes are as follows: C-S1: CAP Surface Pre-1990 (EXCLUDED FROM BASE MODEL), C-S2: CAP Surface, C-C: CAP Combo, C-BB: CAP Break-Burn, W-S: WDFW Surface (EXCLUDED FROM BASE MODEL), W-C: WDFW Combo, W-BB: WDFW Break-Burn. Note that there are repeated years in this table and in the model for years where there are multiple ageing error matrices applied within the same year/fleet combination. (*continued*)

year	North Ntrips	North Nfish	North In-putN	North Age-Mat	South Ntrips	South Nfish	South In-putN	South Age-Mat
2016	9	416	64	W-BB	0	0	0	NA
2017	98	761	203	C-BB	0	0	0	NA
2017	12	585	85	W-BB	0	0	0	NA
2018	88	752	192	C-BB	10	259	46	C-BB
2018	29	744	132	W-BB	0	0	0	NA
2019	92	796	202	C-BB	20	440	81	C-BB
2019	35	681	129	W-BB	0	0	0	NA
2020	56	584	137	C-BB	23	782	131	C-BB
2020	5	59	13	W-BB	0	0	0	NA
2021	52	624	138	C-BB	14	415	71	C-BB
2021	32	438	92	W-BB	0	0	0	NA
2022	65	597	147	C-BB	11	241	44	C-BB
2022	16	515	87	W-BB	0	0	0	NA

Table 4: Sample sizes of Triennial Survey length composition data.

Year	Tows	All Fish	Sexed Fish	Unsexed Fish	Sample Size
1980	1	16	16	0	3
1983	2	30	30	0	6
1986	36	540	540	0	111
1989	141	1419	1415	4	435
1992	116	1015	1015	0	358
1995	145	1369	1369	0	448
1998	236	2624	2594	30	729
2001	254	3016	3012	4	784
2004	239	4676	4675	1	738

Table 5: Sample sizes of WCGBTS length composition data.

Year	Tows	All Fish	Sexed Fish	Unsexed Fish	Sample Size
2003	197	2837	2833	4	608
2004	212	3346	3345	1	655
2005	278	4555	4539	16	859
2006	247	3668	3664	4	763
2007	257	3409	3403	6	794
2008	257	3047	3042	5	794
2009	277	3387	3385	2	855
2010	325	6052	6049	3	1004
2011	320	6176	6172	4	988
2012	295	5372	5366	6	911
2013	218	3445	3440	5	673
2014	332	4822	4805	17	1025
2015	312	4236	4232	4	964
2016	309	4385	4383	2	954
2017	314	4261	4260	1	970
2018	291	3783	3782	1	899
2019	155	1797	1795	2	478
2021	289	3711	3709	2	893
2022	274	3437	3435	2	846

Table 6: Sample sizes of WCGBTS age composition data.

Year	Tows	All Fish	Sexed Fish	Unsexed Fish	Sample Size
2003	173	765	765	0	534
2004	167	723	723	0	516
2005	237	752	751	1	732
2006	236	774	772	2	729
2007	196	690	690	0	605
2008	225	746	745	1	695
2009	258	777	775	2	777
2010	297	801	801	0	801
2011	289	799	798	1	799
2012	269	777	777	0	777
2013	217	843	843	0	670
2014	318	766	766	0	766
2015	291	751	748	3	751
2016	307	893	893	0	893
2017	313	884	884	0	884
2018	291	810	809	1	810
2019	154	621	619	2	475
2021	274	789	789	0	789
2022	271	765	765	0	765

Table 7: Estimated ageing error vectors used in the assessment model for true ages 0–30 read by the Cooperative Ageing Project (CAP) lab. The ages associated with 'CAP Surface Pre-1990' were excluded from the base model. Note that the population age bins extend to age 40, and the largest observed age is 32.

True age	CAP Surface Pre-1990 Mean	CAP Surface Pre-1990 SD	CAP Surface Mean	CAP Surface SD	CAP Combo Mean	CAP Combo SD	CAP BB Mean	CAP BB SD
0.5	0.0	0.0	0.2	0.1	0.5	0.1	0.3	0.2
1.5	0.7	0.0	1.3	0.1	1.4	0.1	1.3	0.2
2.5	2.0	0.1	2.4	0.2	2.4	0.3	2.4	0.2
3.5	3.2	0.2	3.4	0.2	3.3	0.4	3.4	0.3
4.5	4.4	0.3	4.4	0.3	4.3	0.5	4.5	0.4
5.5	5.4	0.4	5.4	0.4	5.2	0.6	5.4	0.4
6.5	6.4	0.5	6.4	0.5	6.2	0.8	6.4	0.5
7.5	7.4	0.6	7.3	0.6	7.1	0.9	7.4	0.6
8.5	8.2	0.7	8.3	0.7	8.1	1.0	8.3	0.7
9.5	9.0	0.8	9.1	0.8	9.0	1.1	9.2	0.8
10.5	9.8	0.9	10.0	1.0	10.0	1.3	10.1	0.9
11.5	10.5	1.1	10.9	1.1	10.9	1.4	10.9	1.0
12.5	11.1	1.2	11.7	1.3	11.9	1.5	11.8	1.2
13.5	11.7	1.3	12.5	1.5	12.8	1.7	12.6	1.3
14.5	12.3	1.5	13.2	1.7	13.8	1.8	13.4	1.5
15.5	12.8	1.7	14.0	1.9	14.7	1.9	14.2	1.6
16.5	13.3	1.8	14.7	2.1	15.7	2.0	14.9	1.8
17.5	13.8	2.0	15.4	2.4	16.6	2.2	15.7	2.0
18.5	14.2	2.2	16.1	2.7	17.6	2.3	16.4	2.2
19.5	14.6	2.4	16.8	3.0	18.5	2.4	17.1	2.5
20.5	15.0	2.6	17.5	3.4	19.5	2.5	17.8	2.7
21.5	15.4	2.8	18.1	3.8	20.4	2.7	18.5	3.0
22.5	15.7	3.1	18.7	4.2	21.4	2.8	19.2	3.3
23.5	16.0	3.3	19.3	4.7	22.3	2.9	19.8	3.6
24.5	16.3	3.6	19.9	5.3	23.3	3.1	20.5	3.9
25.5	16.6	3.9	20.5	5.9	24.2	3.2	21.1	4.3
26.5	16.8	4.2	21.1	6.6	25.2	3.3	21.7	4.7
27.5	17.0	4.5	21.6	7.3	26.1	3.4	22.3	5.1
28.5	17.2	4.8	22.1	8.1	27.1	3.6	22.9	5.6
29.5	17.4	5.2	22.6	9.0	28.0	3.7	23.4	6.1
30.5	17.6	5.5	23.1	10.0	29.0	3.8	24.0	6.7

Table 8: Estimated ageing error vectors used in the assessment model for true ages 0–30 read by the Washington Department of Fish and Wildlife (WDFW) lab. The ages associated with 'WDFW Surface' were excluded from the base model. Note that the population age bins extend to age 40, and the largest observed age is 32.

True age	WDFW Surface Mean	WDFW Surface SD	WDFW Combo Mean	WDFW Combo SD	WDFW BB Mean	WDFW BB SD
0.5	0.1	0.1	0.5	0.1	0.5	0.2
1.5	1.3	0.1	1.5	0.1	1.5	0.2
2.5	2.5	0.2	2.4	0.3	2.5	0.3
3.5	3.6	0.3	3.4	0.4	3.5	0.5
4.5	4.6	0.4	4.4	0.5	4.5	0.6
5.5	5.7	0.5	5.4	0.7	5.5	0.8
6.5	6.7	0.6	6.3	0.8	6.5	0.9
7.5	7.6	0.7	7.3	0.9	7.5	1.1
8.5	8.5	0.8	8.3	1.1	8.6	1.2
9.5	9.4	0.9	9.3	1.2	9.6	1.4
10.5	10.3	1.0	10.3	1.3	10.6	1.5
11.5	11.1	1.1	11.2	1.5	11.6	1.7
12.5	11.9	1.2	12.2	1.6	12.6	1.8
13.5	12.7	1.3	13.2	1.7	13.6	2.0
14.5	13.4	1.4	14.2	1.9	14.6	2.1
15.5	14.1	1.5	15.1	2.0	15.6	2.3
16.5	14.8	1.7	16.1	2.1	16.6	2.4
17.5	15.5	1.8	17.1	2.3	17.6	2.6
18.5	16.1	1.9	18.1	2.4	18.6	2.7
19.5	16.7	2.0	19.0	2.5	19.6	2.9
20.5	17.3	2.1	20.0	2.7	20.6	3.0
21.5	17.9	2.2	21.0	2.8	21.6	3.2
22.5	18.4	2.3	22.0	2.9	22.6	3.3
23.5	19.0	2.4	23.0	3.1	23.6	3.5
24.5	19.5	2.5	23.9	3.2	24.7	3.6
25.5	20.0	2.6	24.9	3.3	25.7	3.8
26.5	20.5	2.7	25.9	3.5	26.7	3.9
27.5	20.9	2.8	26.9	3.6	27.7	4.1
28.5	21.4	2.9	27.8	3.7	28.7	4.2
29.5	21.8	3.0	28.8	3.9	29.7	4.4
30.5	22.2	3.1	29.8	4.0	30.7	4.5

Table 9: Latitude and depth strata used to expand the composition data for the WCGBTS. Note that the boundaries of the U.S. exclusive economic zone, to which survey operations are limited, span a range of latitudes. The latitudinal range of the hauls was 32.00 degrees to 48.46 degrees, so 32 and 49 are chosen to encompass that range.

Strata	Depth lower bound (m)	Depth upper bound (m)	Latitude South	Latitude North
Shallow Southern CA	55	100	32.0	34.5
Shallow Northern CA	55	100	34.5	42.0
Shallow OR	55	100	42.0	46.0
Shallow WA	55	100	46.0	49.0
Middle Southern CA	100	183	32.0	34.5
Middle Northern CA	100	183	34.5	42.0
Middle OR	100	183	42.0	46.0
Middle WA	100	183	46.0	49.0
Deep Southern CA	183	549	32.0	34.5
Deep Northern CA	183	549	34.5	42.0
Deep OR	183	549	42.0	46.0
Deep WA	183	549	46.0	49.0

Table 10: Latitude and depth strata used to expand the composition data for the Triennial Survey.

Strata	Depth lower bound (m)	Depth upper bound (m)	Latitude South	Latitude North
Shallow CA	55	100	37	42
Shallow OR	55	100	42	46
Shallow WA	55	100	46	49
Middle CA	100	183	37	42
Middle OR	100	183	42	46
Middle WA	100	183	46	49
Deep CA	183	350	37	42
Deep OR	183	350	42	46
Deep WA	183	350	46	49

Table 11: Discard rates used in the model for each fleet.

Year	Fleet	North	South	Source
1985	North	0.02		Pikitch
1986	North	0.019		Pikitch
1987	North	0.029		Pikitch
2002	North	0.104	0.038	WCGOP
2003	North	0.044	0.045	WCGOP
2004	North	0.04	0.023	WCGOP
2005	North	0.024	0.011	WCGOP
2006	North	0.039	0.04	WCGOP
2007	North	0.047	0.038	WCGOP
2008	North	0.033	0.015	WCGOP
2009	North	0.147	0.038	WCGOP
2010	North	0.128	0.118	WCGOP
2011	North	0.02	0.021	WCGOP
2012	North	0.012	0.007	WCGOP
2013	North	0.01	0.003	WCGOP
2014	North	0.013	0.003	WCGOP
2015	North	0.003	0.007	WCGOP
2016	North	0.008	0.003	WCGOP
2017	North	0.005	0.004	WCGOP
2018	North	0.004	0.004	WCGOP
2019	North	0.006	0.005	WCGOP
2020	North	0.016	0.005	WCGOP
2021	North	0.008	0.003	WCGOP

Table 12: Specifications and structure of the base and 2019 models

Specification	Base	2019 model
Maximum age	40	40
Sexes	Females, males	Females, males
Population bins	2-78 cm by 2 cm bins	4-78 cm by 2 cm bins
Summary biomass (mt) age	3+	3+
Number of areas	1	1
Number of seasons	1	1
Number of growth patterns	1	1
Start year	1876	1876
End year	2022	2018
Data length bins	12-62 cm by 2 cm bins	12-62 cm by 2 cm bins
Data age bins	1-17 cm by 1 year	1-17 cm by 1 year
Fishing mortality method	Hybrid F	Hybrid F

Table 13: Summary of the estimated parameters in the base and 2019 models

Specification	Base	2019 model	Source of difference
Total	**267**	**304**	
Natural Mortality (M)	2	2	
Growth mean	5	6	Females and males share the L_at_Amin parameter in 2023
Growth variability	4	4	
Stock-recruit	1	2	Steepness now fixed at 0.8
Rec. dev. time series	147	143	Extended by 4 years (2019-2022)
Rec. dev. initial age	31	31	
Rec. dev. forecast	12	12	
Index	1	6	2019 model had 4 catchability parameters related to fishery CPUE (base and power for 2 fleets) and 2 extra SD pars for early and late Triennial vs. 1 in 2023 base
Index time-variation	0	2	2019 model had a change in fishery CPUE catchability in 2004
Size selectivity	16	28	2019 model had separate Winter and Summer fishery fleets
Size selectivity time-variation	24	20	Fewer fishery fleets in 2023 but more parameters are time-varying
Retention	6	12	Fewer fishery fleets in 2023
Retention time-variation	18	36	Fewer fishery fleets in 2023

Table 14: Parameter estimates, estimation phase, parameter bounds, estimation status, estimated standard deviation (SD), prior information [distribution(mean, SD)] used in the base model. Table 1 of 8 showing parameters 1-40.

Label	Value	Phase	Bounds	Status	SD	Prior
NatM_uniform_Fem_GP_1	0.142	2	(0.005, 0.5)	ok	0.0115	lognormal(0.169, 0.310)
L_at_Amin_Fem_GP_1	8.85	3	(5, 45)	ok	0.898	none
L_at_Amax_Fem_GP_1	47.7	3	(35, 80)	ok	0.725	none
VonBert_K_Fem_GP_1	0.193	3	(0.04, 0.5)	ok	0.0113	none
SD_young_Fem_GP_1	1.32	3	(0.5, 15)	ok	0.482	none
SD_old_Fem_GP_1	4.87	4	(0.5, 15)	ok	0.249	none
Wtlen_1_Fem_GP_1	2.04e-06	-3	(-3, 3)	fixed	0	none
Wtlen_2_Fem_GP_1	3.48	-3	(1, 5)	fixed	0	none
Mat50%_Fem_GP_1	35.4	-3	(10, 50)	fixed	0	none
Mat_slope_Fem_GP_1	-0.489	-3	(-3, 3)	fixed	0	none
Eggs_scalar_Fem_GP_1	3.2e-11	-3	(-3, 1)	fixed	0	none
Eggs_exp_len_Fem_GP_1	4.55	-3	(-3, 5)	fixed	0	none
NatM_uniform_Mal_GP_1	0.155	2	(0.005, 0.6)	ok	0.0133	lognormal(0.186, 0.310)
L_at_Amin_Mal_GP_1	0	-3	(0, 45)	fixed	0	none
L_at_Amax_Mal_GP_1	40	3	(35, 80)	ok	0.581	none
VonBert_K_Mal_GP_1	0.246	3	(0.04, 0.5)	ok	0.0147	none
SD_young_Mal_GP_1	1.3	3	(0.5, 15)	ok	0.509	none
SD_old_Mal_GP_1	3.4	4	(0.5, 15)	ok	0.179	none
Wtlen_1_Mal_GP_1	3.04e-06	-3	(-3, 3)	fixed	0	none
Wtlen_2_Mal_GP_1	3.36	-3	(-3, 5)	fixed	0	none
CohortGrowDev	1	-4	(0, 1)	fixed	0	none
FracFemale_GP_1	0.5	-5	(0.3, 0.7)	fixed	0	none
SR_LN(R0)	9.64	1	(5, 20)	ok	0.128	none
SR_BH_steep	0.8	-5	(0.2, 1)	fixed	0	none
SR_sigmaR	0.5	-99	(0, 2)	fixed	0	none
SR_regime	0	-2	(-5, 5)	fixed	0	none
SR_autocorr	0	-99	(0, 0)	fixed	0	none
Early_InitAge_31	3.64e-07	3	(-4, 4)	dev	0.5	normal(0.00, 0.50)
Early_InitAge_30	4.2e-07	3	(-4, 4)	dev	0.5	normal(0.00, 0.50)
Early_InitAge_29	4.84e-07	3	(-4, 4)	dev	0.5	normal(0.00, 0.50)
Early_InitAge_28	5.58e-07	3	(-4, 4)	dev	0.5	normal(0.00, 0.50)
Early_InitAge_27	6.44e-07	3	(-4, 4)	dev	0.5	normal(0.00, 0.50)
Early_InitAge_26	7.42e-07	3	(-4, 4)	dev	0.5	normal(0.00, 0.50)
Early_InitAge_25	8.55e-07	3	(-4, 4)	dev	0.5	normal(0.00, 0.50)
Early_InitAge_24	9.86e-07	3	(-4, 4)	dev	0.5	normal(0.00, 0.50)
Early_InitAge_23	1.14e-06	3	(-4, 4)	dev	0.5	normal(0.00, 0.50)
Early_InitAge_22	1.31e-06	3	(-4, 4)	dev	0.5	normal(0.00, 0.50)
Early_InitAge_21	1.51e-06	3	(-4, 4)	dev	0.5	normal(0.00, 0.50)
Early_InitAge_20	1.73e-06	3	(-4, 4)	dev	0.5	normal(0.00, 0.50)
Early_InitAge_19	2e-06	3	(-4, 4)	dev	0.5	normal(0.00, 0.50)

Table 15: Parameter estimates, estimation phase, parameter bounds, estimation status, estimated standard deviation (SD), prior information [distribution(mean, SD)] used in the base model. Table 2 of 8 showing parameters 41-80.

Label	Value	Phase	Bounds	Status	SD	Prior
Early_InitAge_18	2.29e-06	3	(-4, 4)	dev	0.5	normal(0.00, 0.50)
Early_InitAge_17	2.64e-06	3	(-4, 4)	dev	0.5	normal(0.00, 0.50)
Early_InitAge_16	3.03e-06	3	(-4, 4)	dev	0.5	normal(0.00, 0.50)
Early_InitAge_15	3.47e-06	3	(-4, 4)	dev	0.5	normal(0.00, 0.50)
Early_InitAge_14	3.98e-06	3	(-4, 4)	dev	0.5	normal(0.00, 0.50)
Early_InitAge_13	4.56e-06	3	(-4, 4)	dev	0.5	normal(0.00, 0.50)
Early_InitAge_12	5.21e-06	3	(-4, 4)	dev	0.5	normal(0.00, 0.50)
Early_InitAge_11	5.94e-06	3	(-4, 4)	dev	0.5	normal(0.00, 0.50)
Early_InitAge_10	6.76e-06	3	(-4, 4)	dev	0.5	normal(0.00, 0.50)
Early_InitAge_9	7.67e-06	3	(-4, 4)	dev	0.5	normal(0.00, 0.50)
Early_InitAge_8	8.69e-06	3	(-4, 4)	dev	0.5	normal(0.00, 0.50)
Early_InitAge_7	9.81e-06	3	(-4, 4)	dev	0.5	normal(0.00, 0.50)
Early_InitAge_6	1.1e-05	3	(-4, 4)	dev	0.5	normal(0.00, 0.50)
Early_InitAge_5	1.24e-05	3	(-4, 4)	dev	0.5	normal(0.00, 0.50)
Early_InitAge_4	1.39e-05	3	(-4, 4)	dev	0.5	normal(0.00, 0.50)
Early_InitAge_3	1.56e-05	3	(-4, 4)	dev	0.5	normal(0.00, 0.50)
Early_InitAge_2	1.76e-05	3	(-4, 4)	dev	0.5	normal(0.00, 0.50)
Early_InitAge_1	1.97e-05	3	(-4, 4)	dev	0.5	normal(0.00, 0.50)
Early_RecrDev_1876	2.21e-05	3	(-4, 4)	dev	0.5	normal(0.00, 0.50)
Early_RecrDev_1877	2.48e-05	3	(-4, 4)	dev	0.5	normal(0.00, 0.50)
Early_RecrDev_1878	2.78e-05	3	(-4, 4)	dev	0.5	normal(0.00, 0.50)
Early_RecrDev_1879	3.12e-05	3	(-4, 4)	dev	0.5	normal(0.00, 0.50)
Early_RecrDev_1880	3.5e-05	3	(-4, 4)	dev	0.5	normal(0.00, 0.50)
Early_RecrDev_1881	3.92e-05	3	(-4, 4)	dev	0.5	normal(0.00, 0.50)
Early_RecrDev_1882	4.4e-05	3	(-4, 4)	dev	0.5	normal(0.00, 0.50)
Early_RecrDev_1883	4.93e-05	3	(-4, 4)	dev	0.5	normal(0.00, 0.50)
Early_RecrDev_1884	5.53e-05	3	(-4, 4)	dev	0.5	normal(0.00, 0.50)
Early_RecrDev_1885	6.2e-05	3	(-4, 4)	dev	0.5	normal(0.00, 0.50)
Early_RecrDev_1886	6.94e-05	3	(-4, 4)	dev	0.5	normal(0.00, 0.50)
Early_RecrDev_1887	7.78e-05	3	(-4, 4)	dev	0.5	normal(0.00, 0.50)
Early_RecrDev_1888	8.72e-05	3	(-4, 4)	dev	0.5	normal(0.00, 0.50)
Early_RecrDev_1889	9.77e-05	3	(-4, 4)	dev	0.5	normal(0.00, 0.50)
Early_RecrDev_1890	0.000109	3	(-4, 4)	dev	0.5	normal(0.00, 0.50)
Early_RecrDev_1891	0.000123	3	(-4, 4)	dev	0.5	normal(0.00, 0.50)
Early_RecrDev_1892	0.000137	3	(-4, 4)	dev	0.5	normal(0.00, 0.50)
Early_RecrDev_1893	0.000154	3	(-4, 4)	dev	0.5	normal(0.00, 0.50)
Early_RecrDev_1894	0.000172	3	(-4, 4)	dev	0.5	normal(0.00, 0.50)
Early_RecrDev_1895	0.000193	3	(-4, 4)	dev	0.5	normal(0.00, 0.50)
Early_RecrDev_1896	0.000216	3	(-4, 4)	dev	0.5	normal(0.00, 0.50)
Early_RecrDev_1897	0.000241	3	(-4, 4)	dev	0.5	normal(0.00, 0.50)

Table 16: Parameter estimates, estimation phase, parameter bounds, estimation status, estimated standard deviation (SD), prior information [distribution(mean, SD)] used in the base model. Table 3 of 8 showing parameters 81-120.

Label	Value	Phase	Bounds	Status	SD	Prior
Early_RecrDev_1898	0.00027	3	(-4, 4)	dev	0.5	normal(0.00, 0.50)
Early_RecrDev_1899	0.000302	3	(-4, 4)	dev	0.5	normal(0.00, 0.50)
Early_RecrDev_1900	0.000338	3	(-4, 4)	dev	0.5	normal(0.00, 0.50)
Early_RecrDev_1901	0.000378	3	(-4, 4)	dev	0.5	normal(0.00, 0.50)
Early_RecrDev_1902	0.000423	3	(-4, 4)	dev	0.5	normal(0.00, 0.50)
Early_RecrDev_1903	0.000474	3	(-4, 4)	dev	0.5	normal(0.00, 0.50)
Early_RecrDev_1904	0.00053	3	(-4, 4)	dev	0.5	normal(0.00, 0.50)
Early_RecrDev_1905	0.000593	3	(-4, 4)	dev	0.5	normal(0.00, 0.50)
Early_RecrDev_1906	0.000663	3	(-4, 4)	dev	0.5	normal(0.00, 0.50)
Early_RecrDev_1907	0.000741	3	(-4, 4)	dev	0.5	normal(0.00, 0.50)
Early_RecrDev_1908	0.000829	3	(-4, 4)	dev	0.5	normal(0.00, 0.50)
Early_RecrDev_1909	0.000927	3	(-4, 4)	dev	0.5	normal(0.00, 0.50)
Early_RecrDev_1910	0.00104	3	(-4, 4)	dev	0.5	normal(0.00, 0.50)
Early_RecrDev_1911	0.00116	3	(-4, 4)	dev	0.5	normal(0.00, 0.50)
Early_RecrDev_1912	0.0013	3	(-4, 4)	dev	0.5	normal(0.00, 0.50)
Early_RecrDev_1913	0.00145	3	(-4, 4)	dev	0.5	normal(0.00, 0.50)
Early_RecrDev_1914	0.00162	3	(-4, 4)	dev	0.5	normal(0.00, 0.50)
Early_RecrDev_1915	0.00182	3	(-4, 4)	dev	0.5	normal(0.00, 0.50)
Early_RecrDev_1916	0.00203	3	(-4, 4)	dev	0.5	normal(0.00, 0.50)
Early_RecrDev_1917	0.00226	3	(-4, 4)	dev	0.5	normal(0.00, 0.50)
Early_RecrDev_1918	0.00252	3	(-4, 4)	dev	0.501	normal(0.00, 0.50)
Early_RecrDev_1919	0.00281	3	(-4, 4)	dev	0.501	normal(0.00, 0.50)
Early_RecrDev_1920	0.00314	3	(-4, 4)	dev	0.501	normal(0.00, 0.50)
Early_RecrDev_1921	0.0035	3	(-4, 4)	dev	0.501	normal(0.00, 0.50)
Early_RecrDev_1922	0.00391	3	(-4, 4)	dev	0.501	normal(0.00, 0.50)
Early_RecrDev_1923	0.00438	3	(-4, 4)	dev	0.501	normal(0.00, 0.50)
Early_RecrDev_1924	0.00491	3	(-4, 4)	dev	0.501	normal(0.00, 0.50)
Early_RecrDev_1925	0.00551	3	(-4, 4)	dev	0.501	normal(0.00, 0.50)
Early_RecrDev_1926	0.00621	3	(-4, 4)	dev	0.501	normal(0.00, 0.50)
Early_RecrDev_1927	0.00704	3	(-4, 4)	dev	0.501	normal(0.00, 0.50)
Early_RecrDev_1928	0.00803	3	(-4, 4)	dev	0.501	normal(0.00, 0.50)
Early_RecrDev_1929	0.00926	3	(-4, 4)	dev	0.502	normal(0.00, 0.50)
Early_RecrDev_1930	0.0108	3	(-4, 4)	dev	0.502	normal(0.00, 0.50)
Early_RecrDev_1931	0.0128	3	(-4, 4)	dev	0.502	normal(0.00, 0.50)
Early_RecrDev_1932	0.0152	3	(-4, 4)	dev	0.502	normal(0.00, 0.50)
Early_RecrDev_1933	0.0182	3	(-4, 4)	dev	0.503	normal(0.00, 0.50)
Early_RecrDev_1934	0.0216	3	(-4, 4)	dev	0.503	normal(0.00, 0.50)
Early_RecrDev_1935	0.0246	3	(-4, 4)	dev	0.503	normal(0.00, 0.50)
Early_RecrDev_1936	0.0255	3	(-4, 4)	dev	0.503	normal(0.00, 0.50)
Early_RecrDev_1937	0.021	3	(-4, 4)	dev	0.501	normal(0.00, 0.50)

Table 17: Parameter estimates, estimation phase, parameter bounds, estimation status, estimated standard deviation (SD), prior information [distribution(mean, SD)] used in the base model. Table 4 of 8 showing parameters 121-160.

Label	Value	Phase	Bounds	Status	SD	Prior
Early_RecrDev_1938	0.00642	3	(-4, 4)	dev	0.498	normal(0.00, 0.50)
Early_RecrDev_1939	-0.0233	3	(-4, 4)	dev	0.491	normal(0.00, 0.50)
Early_RecrDev_1940	-0.0702	3	(-4, 4)	dev	0.48	normal(0.00, 0.50)
Early_RecrDev_1941	-0.128	3	(-4, 4)	dev	0.468	normal(0.00, 0.50)
Early_RecrDev_1942	-0.182	3	(-4, 4)	dev	0.457	normal(0.00, 0.50)
Early_RecrDev_1943	-0.206	3	(-4, 4)	dev	0.451	normal(0.00, 0.50)
Early_RecrDev_1944	-0.183	3	(-4, 4)	dev	0.453	normal(0.00, 0.50)
Early_RecrDev_1945	-0.134	3	(-4, 4)	dev	0.463	normal(0.00, 0.50)
Early_RecrDev_1946	-0.127	3	(-4, 4)	dev	0.468	normal(0.00, 0.50)
Early_RecrDev_1947	-0.144	3	(-4, 4)	dev	0.464	normal(0.00, 0.50)
Early_RecrDev_1948	-0.157	3	(-4, 4)	dev	0.46	normal(0.00, 0.50)
Early_RecrDev_1949	-0.153	3	(-4, 4)	dev	0.458	normal(0.00, 0.50)
Early_RecrDev_1950	-0.13	3	(-4, 4)	dev	0.458	normal(0.00, 0.50)
Early_RecrDev_1951	-0.108	3	(-4, 4)	dev	0.46	normal(0.00, 0.50)
Early_RecrDev_1952	-0.113	3	(-4, 4)	dev	0.461	normal(0.00, 0.50)
Early_RecrDev_1953	-0.134	3	(-4, 4)	dev	0.458	normal(0.00, 0.50)
Early_RecrDev_1954	-0.147	3	(-4, 4)	dev	0.456	normal(0.00, 0.50)
Early_RecrDev_1955	-0.176	3	(-4, 4)	dev	0.45	normal(0.00, 0.50)
Early_RecrDev_1956	-0.22	3	(-4, 4)	dev	0.442	normal(0.00, 0.50)
Early_RecrDev_1957	-0.223	3	(-4, 4)	dev	0.438	normal(0.00, 0.50)
Early_RecrDev_1958	-0.0969	3	(-4, 4)	dev	0.449	normal(0.00, 0.50)
Main_RecrDev_1959	0.219	1	(-4, 4)	dev	0.473	normal(0.00, 0.50)
Main_RecrDev_1960	0.431	1	(-4, 4)	dev	0.438	normal(0.00, 0.50)
Main_RecrDev_1961	0.074	1	(-4, 4)	dev	0.443	normal(0.00, 0.50)
Main_RecrDev_1962	-0.0894	1	(-4, 4)	dev	0.416	normal(0.00, 0.50)
Main_RecrDev_1963	0.0116	1	(-4, 4)	dev	0.409	normal(0.00, 0.50)
Main_RecrDev_1964	-0.00914	1	(-4, 4)	dev	0.465	normal(0.00, 0.50)
Main_RecrDev_1965	1.15	1	(-4, 4)	dev	0.368	normal(0.00, 0.50)
Main_RecrDev_1966	0.485	1	(-4, 4)	dev	0.527	normal(0.00, 0.50)
Main_RecrDev_1967	-0.341	1	(-4, 4)	dev	0.406	normal(0.00, 0.50)
Main_RecrDev_1968	-0.578	1	(-4, 4)	dev	0.371	normal(0.00, 0.50)
Main_RecrDev_1969	-0.56	1	(-4, 4)	dev	0.36	normal(0.00, 0.50)
Main_RecrDev_1970	-0.389	1	(-4, 4)	dev	0.356	normal(0.00, 0.50)
Main_RecrDev_1971	-0.259	1	(-4, 4)	dev	0.34	normal(0.00, 0.50)
Main_RecrDev_1972	-0.398	1	(-4, 4)	dev	0.338	normal(0.00, 0.50)
Main_RecrDev_1973	-0.468	1	(-4, 4)	dev	0.329	normal(0.00, 0.50)
Main_RecrDev_1974	-0.306	1	(-4, 4)	dev	0.316	normal(0.00, 0.50)
Main_RecrDev_1975	-0.067	1	(-4, 4)	dev	0.304	normal(0.00, 0.50)
Main_RecrDev_1976	0.154	1	(-4, 4)	dev	0.262	normal(0.00, 0.50)
Main_RecrDev_1977	-0.248	1	(-4, 4)	dev	0.312	normal(0.00, 0.50)

Table 18: Parameter estimates, estimation phase, parameter bounds, estimation status, estimated standard deviation (SD), prior information [distribution(mean, SD)] used in the base model. Table 5 of 8 showing parameters 161-200.

Label	Value	Phase	Bounds	Status	SD	Prior
Main_RecrDev_1978	-0.619	1	(-4, 4)	dev	0.343	normal(0.00, 0.50)
Main_RecrDev_1979	-0.235	1	(-4, 4)	dev	0.318	normal(0.00, 0.50)
Main_RecrDev_1980	-0.0418	1	(-4, 4)	dev	0.312	normal(0.00, 0.50)
Main_RecrDev_1981	-0.166	1	(-4, 4)	dev	0.328	normal(0.00, 0.50)
Main_RecrDev_1982	-0.11	1	(-4, 4)	dev	0.338	normal(0.00, 0.50)
Main_RecrDev_1983	0.456	1	(-4, 4)	dev	0.274	normal(0.00, 0.50)
Main_RecrDev_1984	0.5	1	(-4, 4)	dev	0.278	normal(0.00, 0.50)
Main_RecrDev_1985	0.0523	1	(-4, 4)	dev	0.31	normal(0.00, 0.50)
Main_RecrDev_1986	-0.389	1	(-4, 4)	dev	0.334	normal(0.00, 0.50)
Main_RecrDev_1987	0.0131	1	(-4, 4)	dev	0.298	normal(0.00, 0.50)
Main_RecrDev_1988	0.341	1	(-4, 4)	dev	0.282	normal(0.00, 0.50)
Main_RecrDev_1989	0.416	1	(-4, 4)	dev	0.281	normal(0.00, 0.50)
Main_RecrDev_1990	0.389	1	(-4, 4)	dev	0.312	normal(0.00, 0.50)
Main_RecrDev_1991	0.167	1	(-4, 4)	dev	0.322	normal(0.00, 0.50)
Main_RecrDev_1992	-0.106	1	(-4, 4)	dev	0.346	normal(0.00, 0.50)
Main_RecrDev_1993	0.674	1	(-4, 4)	dev	0.225	normal(0.00, 0.50)
Main_RecrDev_1994	0.314	1	(-4, 4)	dev	0.292	normal(0.00, 0.50)
Main_RecrDev_1995	0.3	1	(-4, 4)	dev	0.251	normal(0.00, 0.50)
Main_RecrDev_1996	0.0475	1	(-4, 4)	dev	0.279	normal(0.00, 0.50)
Main_RecrDev_1997	0.156	1	(-4, 4)	dev	0.25	normal(0.00, 0.50)
Main_RecrDev_1998	0.848	1	(-4, 4)	dev	0.151	normal(0.00, 0.50)
Main_RecrDev_1999	0.39	1	(-4, 4)	dev	0.195	normal(0.00, 0.50)
Main_RecrDev_2000	0.0391	1	(-4, 4)	dev	0.21	normal(0.00, 0.50)
Main_RecrDev_2001	-0.0451	1	(-4, 4)	dev	0.192	normal(0.00, 0.50)
Main_RecrDev_2002	-0.0316	1	(-4, 4)	dev	0.181	normal(0.00, 0.50)
Main_RecrDev_2003	-0.089	1	(-4, 4)	dev	0.188	normal(0.00, 0.50)
Main_RecrDev_2004	0.0924	1	(-4, 4)	dev	0.175	normal(0.00, 0.50)
Main_RecrDev_2005	0.319	1	(-4, 4)	dev	0.175	normal(0.00, 0.50)
Main_RecrDev_2006	1.01	1	(-4, 4)	dev	0.129	normal(0.00, 0.50)
Main_RecrDev_2007	1	1	(-4, 4)	dev	0.15	normal(0.00, 0.50)
Main_RecrDev_2008	1.1	1	(-4, 4)	dev	0.136	normal(0.00, 0.50)
Main_RecrDev_2009	0.298	1	(-4, 4)	dev	0.233	normal(0.00, 0.50)
Main_RecrDev_2010	0.0733	1	(-4, 4)	dev	0.24	normal(0.00, 0.50)
Main_RecrDev_2011	0.0941	1	(-4, 4)	dev	0.224	normal(0.00, 0.50)
Main_RecrDev_2012	0.556	1	(-4, 4)	dev	0.155	normal(0.00, 0.50)
Main_RecrDev_2013	-0.245	1	(-4, 4)	dev	0.274	normal(0.00, 0.50)
Main_RecrDev_2014	0.108	1	(-4, 4)	dev	0.226	normal(0.00, 0.50)
Main_RecrDev_2015	0.0948	1	(-4, 4)	dev	0.229	normal(0.00, 0.50)
Main_RecrDev_2016	-0.31	1	(-4, 4)	dev	0.27	normal(0.00, 0.50)
Main_RecrDev_2017	-0.443	1	(-4, 4)	dev	0.285	normal(0.00, 0.50)

Table 19: Parameter estimates, estimation phase, parameter bounds, estimation status, estimated standard deviation (SD), prior information [distribution(mean, SD)] used in the base model. Table 6 of 8 showing parameters 201-240.

Label	Value	Phase	Bounds	Status	SD	Prior
Main_RecrDev_2018	-0.338	1	(-4, 4)	dev	0.312	normal(0.00, 0.50)
Main_RecrDev_2019	-0.179	1	(-4, 4)	dev	0.363	normal(0.00, 0.50)
Main_RecrDev_2020	-0.151	1	(-4, 4)	dev	0.441	normal(0.00, 0.50)
Late_RecrDev_2021	-0.0379	7	(-4, 4)	dev	0.487	normal(0.00, 0.50)
Late_RecrDev_2022	0	7	(-4, 4)	dev	0.5	normal(0.00, 0.50)
ForeRecr_2023	0	7	(-4, 4)	dev	0.5	normal(0.00, 0.50)
ForeRecr_2024	0	7	(-4, 4)	dev	0.5	normal(0.00, 0.50)
ForeRecr_2025	0	7	(-4, 4)	dev	0.5	normal(0.00, 0.50)
ForeRecr_2026	0	7	(-4, 4)	dev	0.5	normal(0.00, 0.50)
ForeRecr_2027	0	7	(-4, 4)	dev	0.5	normal(0.00, 0.50)
ForeRecr_2028	0	7	(-4, 4)	dev	0.5	normal(0.00, 0.50)
ForeRecr_2029	0	7	(-4, 4)	dev	0.5	normal(0.00, 0.50)
ForeRecr_2030	0	7	(-4, 4)	dev	0.5	normal(0.00, 0.50)
ForeRecr_2031	0	7	(-4, 4)	dev	0.5	normal(0.00, 0.50)
ForeRecr_2032	0	7	(-4, 4)	dev	0.5	normal(0.00, 0.50)
ForeRecr_2033	0	7	(-4, 4)	dev	0.5	normal(0.00, 0.50)
ForeRecr_2034	0	7	(-4, 4)	dev	0.5	normal(0.00, 0.50)
LnQ_base_Triennial(3)	-0.706	-1	(-15, 15)	fixed	0	none
Q_extraSD_Triennial(3)	0.258	5	(0.001, 2)	ok	0.084	none
LnQ_base_WCGBTS(4)	1.39	-1	(-15, 15)	fixed	0	none
Size_DblN_peak_North(1)	61.2	2	(15, 75)	ok	1.66	none
Size_DblN_top_logit_North(1)	-15	-3	(-15, 4)	fixed	0	none
Size_DblN_ascend_se_North(1)	5.26	3	(-4, 12)	ok	0.149	none
Size_DblN_descend_se_North(1)	20	-3	(-2, 20)	fixed	0	none
Size_DblN_start_logit_North(1)	-999	-4	(-1000, 9)	fixed	0	none
Size_DblN_end_logit_North(1)	-999	-4	(-1000, 9)	fixed	0	none
Retain_L_infl_North(1)	28.5	2	(10, 40)	ok	0.545	none
Retain_L_width_North(1)	1.42	4	(0.1, 10)	ok	0.309	none
Retain_L_asymptote_logit_North(1)	9.7	4	(-10, 10)	ok	8.19	none
Retain_L_maleoffset_North(1)	0	-2	(-10, 10)	fixed	0	none
SzSel_Male_Peak_North(1)	-17.7	4	(-25, 15)	ok	1.07	none
SzSel_Male_Ascend_North(1)	-1.71	4	(-15, 15)	ok	0.0954	none
SzSel_Male_Descend_North(1)	0	-4	(-15, 15)	fixed	0	none
SzSel_Male_Final_North(1)	0	-4	(-15, 15)	fixed	0	none
SzSel_Male_Scale_North(1)	1	-4	(-15, 15)	fixed	0	none
Size_DblN_peak_South(2)	54.3	2	(15, 75)	ok	1.78	none
Size_DblN_top_logit_South(2)	-15	-3	(-15, 4)	fixed	0	none
Size_DblN_ascend_se_South(2)	5.97	3	(-4, 12)	ok	0.244	none
Size_DblN_descend_se_South(2)	20	-3	(-2, 20)	fixed	0	none
Size_DblN_start_logit_South(2)	-999	-4	(-1000, 9)	fixed	0	none

Table 20: Parameter estimates, estimation phase, parameter bounds, estimation status, estimated standard deviation (SD), prior information [distribution(mean, SD)] used in the base model. Table 7 of 8 showing parameters 241-280.

Label	Value	Phase	Bounds	Status	SD	Prior
Size_DblN_end_logit_South(2)	-999	-4	(-1000, 9)	fixed	0	none
Retain_L_infl_South(2)	28.2	2	(10, 40)	ok	0.298	none
Retain_L_width_South(2)	1.17	3	(0.1, 10)	ok	0.129	none
Retain_L_asymptote_logit_South(2)	6.66	4	(-10, 10)	ok	1.16	none
Retain_L_maleoffset_South(2)	0	-2	(-10, 10)	fixed	0	none
SzSel_Male_Peak_South(2)	-15.9	4	(-25, 15)	ok	1.23	none
SzSel_Male_Ascend_South(2)	-2.03	4	(-15, 15)	ok	0.209	none
SzSel_Male_Descend_South(2)	0	-4	(-15, 15)	fixed	0	none
SzSel_Male_Final_South(2)	0	-4	(-15, 15)	fixed	0	none
SzSel_Male_Scale_South(2)	1	-4	(-15, 15)	fixed	0	none
Size_DblN_peak_Triennial(3)	35.8	2	(15, 61)	ok	1.63	none
Size_DblN_top_logit_Triennial(3)	-15	-2	(-15, 4)	fixed	0	none
Size_DblN_ascend_se_Triennial(3)	4.52	2	(-4, 12)	ok	0.24	none
Size_DblN_descend_se_Triennial(3)	20	-2	(-2, 20)	fixed	0	none
Size_DblN_start_logit_Triennial(3)	-999	-4	(-1000, 9)	fixed	0	none
Size_DblN_end_logit_Triennial(3)	-999	-4	(-1000, 9)	fixed	0	none
SzSel_Male_Peak_Triennial(3)	-3.32	3	(-15, 15)	ok	1.51	none
SzSel_Male_Ascend_Triennial(3)	-0.232	3	(-15, 15)	ok	0.271	none
SzSel_Male_Descend_Triennial(3)	0	-3	(-15, 15)	fixed	0	none
SzSel_Male_Final_Triennial(3)	0	-3	(-15, 15)	fixed	0	none
SzSel_Male_Scale_Triennial(3)	1	-4	(-15, 15)	fixed	0	none
Size_DblN_peak_WCGBTS(4)	50.5	2	(15, 61)	ok	2.41	none
Size_DblN_top_logit_WCGBTS(4)	-15	-2	(-15, 4)	fixed	0	none
Size_DblN_ascend_se_WCGBTS(4)	5.65	2	(-4, 12)	ok	0.158	none
Size_DblN_descend_se_WCGBTS(4)	20	-2	(-2, 20)	fixed	0	none
Size_DblN_start_logit_WCGBTS(4)	-999	-4	(-1000, 9)	fixed	0	none
Size_DblN_end_logit_WCGBTS(4)	-999	-4	(-1000, 9)	fixed	0	none
SzSel_Male_Peak_WCGBTS(4)	-10.8	3	(-15, 15)	ok	1.77	none
SzSel_Male_Ascend_WCGBTS(4)	-0.845	3	(-15, 15)	ok	0.163	none
SzSel_Male_Descend_WCGBTS(4)	0	-3	(-15, 15)	fixed	0	none
SzSel_Male_Final_WCGBTS(4)	0	-3	(-15, 15)	fixed	0	none
SzSel_Male_Scale_WCGBTS(4)	1	-4	(-15, 15)	fixed	0	none
Size_DblN_peak_North(1)_BLK1repl_1973	61.5	5	(15, 75)	ok	1.53	none
Size_DblN_peak_North(1)_BLK1repl_1983	58.2	5	(15, 75)	ok	1.67	none
Size_DblN_peak_North(1)_BLK1repl_1993	57	5	(15, 75)	ok	1.64	none
Size_DblN_peak_North(1)_BLK1repl_2003	58	5	(15, 75)	ok	1.51	none
Size_DblN_peak_North(1)_BLK1repl_2011	58.3	5	(15, 75)	ok	1.51	none
Size_DblN_peak_North(1)_BLK1repl_2018	58.4	5	(15, 75)	ok	1.65	none
Size_DblN_ascend_se_North(1)_BLK1repl_1973	5.51	6	(-4, 12)	ok	0.101	none
Size_DblN_ascend_se_North(1)_BLK1repl_1983	5.4	6	(-4, 12)	ok	0.12	none

Table 21: Parameter estimates, estimation phase, parameter bounds, estimation status, estimated standard deviation (SD), prior information [distribution(mean, SD)] used in the base model. Table 8 of 8 showing parameters 281-314.

Label	Value	Phase	Bounds	Status	SD	Prior
Size_DblN_ascend_se_North(1)_BLK1repl_1993	5.58	6	(-4, 12)	ok	0.122	none
Size_DblN_ascend_se_North(1)_BLK1repl_2003	5.48	6	(-4, 12)	ok	0.086	none
Size_DblN_ascend_se_North(1)_BLK1repl_2011	5.42	6	(-4, 12)	ok	0.108	none
Size_DblN_ascend_se_North(1)_BLK1repl_2018	5.29	6	(-4, 12)	ok	0.119	none
Retain_L_infl_North(1)_BLK2repl_2002	31.2	5	(10, 40)	ok	0.461	none
Retain_L_infl_North(1)_BLK2repl_2003	30	5	(10, 40)	ok	0.303	none
Retain_L_infl_North(1)_BLK2repl_2009	31.7	5	(10, 40)	ok	0.393	none
Retain_L_infl_North(1)_BLK2repl_2011	27.2	5	(10, 40)	ok	0.612	none
Retain_L_width_North(1)_BLK2repl_2002	0.879	5	(0.1, 10)	ok	0.316	none
Retain_L_width_North(1)_BLK2repl_2003	1.34	5	(0.1, 10)	ok	0.149	none
Retain_L_width_North(1)_BLK2repl_2009	1.72	5	(0.1, 10)	ok	0.263	none
Retain_L_width_North(1)_BLK2repl_2011	1.67	5	(0.1, 10)	ok	0.0824	none
Retain_L_asymptote_logit_North(1)_BLK2repl_2002	9.77	5	(-10, 10)	ok	6.67	none
Retain_L_asymptote_logit_North(1)_BLK2repl_2003	6.2	5	(-10, 10)	ok	0.88	none
Retain_L_asymptote_logit_North(1)_BLK2repl_2009	3.66	5	(-10, 10)	ok	0.472	none
Retain_L_asymptote_logit_North(1)_BLK2repl_2011	7.44	5	(-10, 10)	ok	0.46	none
Size_DblN_peak_South(2)_BLK1repl_1973	50.7	5	(15, 75)	ok	1.76	none
Size_DblN_peak_South(2)_BLK1repl_1983	49	5	(15, 75)	ok	1.64	none
Size_DblN_peak_South(2)_BLK1repl_1993	49.9	5	(15, 75)	ok	1.95	none
Size_DblN_peak_South(2)_BLK1repl_2003	50.9	5	(15, 75)	ok	1.37	none
Size_DblN_peak_South(2)_BLK1repl_2011	50.5	5	(15, 75)	ok	1.36	none
Size_DblN_peak_South(2)_BLK1repl_2018	51.3	5	(15, 75)	ok	1.43	none
Size_DblN_ascend_se_South(2)_BLK1repl_1973	6.25	6	(-4, 12)	ok	0.264	none
Size_DblN_ascend_se_South(2)_BLK1repl_1983	5.26	6	(-4, 12)	ok	0.202	none
Size_DblN_ascend_se_South(2)_BLK1repl_1993	4.94	6	(-4, 12)	ok	0.303	none
Size_DblN_ascend_se_South(2)_BLK1repl_2003	4.98	6	(-4, 12)	ok	0.133	none
Size_DblN_ascend_se_South(2)_BLK1repl_2011	4.97	6	(-4, 12)	ok	0.168	none
Size_DblN_ascend_se_South(2)_BLK1repl_2018	4.92	6	(-4, 12)	ok	0.172	none
Retain_L_infl_South(2)_BLK3repl_2010	30.8	5	(10, 40)	ok	1.26	none
Retain_L_infl_South(2)_BLK3repl_2011	25	5	(10, 40)	ok	1.35	none
Retain_L_width_South(2)_BLK3repl_2010	1.85	5	(0.1, 10)	ok	0.694	none
Retain_L_width_South(2)_BLK3repl_2011	1.62	5	(0.1, 10)	ok	0.165	none
Retain_L_asymptote_logit_South(2)_BLK3repl_2010	9.38	5	(-10, 10)	ok	15.4	none
Retain_L_asymptote_logit_South(2)_BLK3repl_2011	8.19	5	(-10, 10)	ok	1.01	none

Table 22: Time series of population estimates for the base model.

Year	Spawning output (trillions of eggs)	Fraction unfished	Age-3+ biomass (mt)	Dead catch (mt)	Age-0 recruits (1000s)	1-SPR	Exploita-tion rate
1876	22.91	NA	42189	1	15.36	0.000	0.000
1877	22.91	1.000	42189	1	15.36	0.000	0.000
1878	22.91	1.000	42189	1	15.36	0.000	0.000
1879	22.91	1.000	42189	1	15.36	0.000	0.000
1880	22.90	1.000	42102	12	15.36	0.003	0.000
1881	22.90	1.000	42014	22	15.36	0.006	0.001
1882	22.89	0.999	41927	33	15.36	0.008	0.001
1883	22.87	0.998	41840	44	15.36	0.011	0.001
1884	22.85	0.997	41753	54	15.36	0.013	0.001
1885	22.82	0.996	41666	65	15.36	0.016	0.002
1886	22.79	0.995	41579	76	15.36	0.019	0.002
1887	22.76	0.994	41492	86	15.36	0.021	0.002
1888	22.72	0.992	41406	97	15.36	0.024	0.002
1889	22.68	0.990	41319	108	15.35	0.026	0.003
1890	22.64	0.988	41232	118	15.35	0.029	0.003
1891	22.60	0.987	41145	129	15.35	0.032	0.003
1892	22.55	0.984	41059	140	15.35	0.034	0.003
1893	22.50	0.982	40972	150	15.35	0.037	0.004
1894	22.45	0.980	40885	161	15.34	0.040	0.004
1895	22.40	0.978	40798	172	15.34	0.042	0.004
1896	22.35	0.976	40709	183	15.34	0.045	0.004
1897	22.29	0.973	40622	193	15.34	0.047	0.005
1898	22.23	0.971	40535	204	15.34	0.050	0.005
1899	22.18	0.968	40447	214	15.33	0.053	0.005
1900	22.12	0.966	40360	225	15.33	0.055	0.005
1901	22.06	0.963	40272	236	15.33	0.058	0.006
1902	22.00	0.961	40184	246	15.33	0.061	0.006
1903	21.94	0.958	40097	257	15.33	0.063	0.006
1904	21.88	0.955	40009	268	15.32	0.066	0.007
1905	21.82	0.953	39921	278	15.32	0.068	0.007
1906	21.76	0.950	39833	289	15.32	0.071	0.007
1907	21.70	0.947	39744	300	15.32	0.074	0.007
1908	21.64	0.945	39656	310	15.32	0.076	0.008
1909	21.58	0.942	39567	321	15.32	0.079	0.008
1910	21.51	0.939	39479	332	15.32	0.082	0.008
1911	21.45	0.936	39390	342	15.31	0.084	0.009
1912	21.39	0.934	39301	353	15.31	0.087	0.009
1913	21.32	0.931	39213	364	15.31	0.090	0.009
1914	21.26	0.928	39124	374	15.31	0.092	0.009
1915	21.20	0.925	39035	385	15.31	0.095	0.010
1916	21.13	0.923	38983	391	15.31	0.097	0.010

Table 22: Time series of population estimates for the base ... *continued.*

Year	Spawning output (trillions of eggs)	Fraction unfished	Age-3+ biomass (mt)	Dead catch (mt)	Age-0 recruits (1000s)	1-SPR	Exploitation rate
1917	21.07	0.920	37925	532	15.31	0.128	0.013
1918	20.94	0.914	38670	429	15.31	0.106	0.011
1919	20.87	0.911	39365	337	15.31	0.085	0.009
1920	20.86	0.911	40198	233	15.32	0.060	0.006
1921	20.91	0.913	39688	297	15.32	0.075	0.008
1922	20.93	0.914	38665	430	15.33	0.106	0.011
1923	20.87	0.911	38637	432	15.34	0.107	0.011
1924	20.82	0.909	37838	539	15.34	0.131	0.014
1925	20.72	0.904	37851	534	15.35	0.130	0.014
1926	20.62	0.900	37884	528	15.35	0.129	0.014
1927	20.53	0.896	37062	639	15.36	0.154	0.017
1928	20.39	0.890	37119	627	15.37	0.152	0.016
1929	20.27	0.885	36473	716	15.38	0.171	0.019
1930	20.11	0.878	36773	668	15.40	0.162	0.018
1931	19.98	0.872	36911	648	15.42	0.158	0.017
1932	19.89	0.868	37247	605	15.45	0.148	0.016
1933	19.82	0.865	38168	484	15.49	0.120	0.013
1934	19.84	0.866	33407	1193	15.55	0.261	0.032
1935	19.48	0.850	34551	993	15.57	0.227	0.027
1936	19.25	0.840	37027	633	15.56	0.154	0.017
1937	19.23	0.840	34443	1026	15.46	0.230	0.028
1938	19.03	0.831	33582	1136	15.20	0.256	0.031
1939	18.78	0.820	31452	1550	14.72	0.317	0.043
1940	18.35	0.801	32896	1327	14.00	0.272	0.037
1941	18.09	0.790	33947	1183	13.17	0.240	0.034
1942	17.95	0.784	29992	2212	12.46	0.352	0.064
1943	17.36	0.758	28887	2384	12.11	0.385	0.071
1944	16.74	0.731	31104	1629	12.34	0.322	0.050
1945	16.48	0.719	31408	1516	12.91	0.313	0.048
1946	16.25	0.709	25791	2822	12.98	0.477	0.091
1947	15.33	0.669	26735	2240	12.67	0.451	0.076
1948	14.65	0.640	20205	4314	12.44	0.634	0.153
1949	12.91	0.564	21325	3104	12.32	0.604	0.123
1950	11.80	0.515	19977	3495	12.46	0.641	0.149
1951	10.57	0.461	22964	2347	12.55	0.558	0.109
1952	10.01	0.437	22840	2202	12.37	0.561	0.106
1953	9.58	0.418	23043	1957	12.04	0.557	0.097
1954	9.30	0.406	20215	2563	11.81	0.635	0.129
1955	8.76	0.383	20767	2328	11.36	0.620	0.122
1956	8.38	0.366	22608	1876	10.78	0.568	0.101
1957	8.25	0.360	19321	2674	10.71	0.659	0.146
1958	7.77	0.339	19952	2350	12.01	0.641	0.134

Table 22: Time series of population estimates for the base ... *continued.*

Year	Spawning output (trillions of eggs)	Fraction unfished	Age-3+ biomass (mt)	Dead catch (mt)	Age-0 recruits (1000s)	1-SPR	Exploitation rate
1959	7.46	0.326	21545	1907	16.34	0.598	0.113
1960	7.37	0.322	20505	2183	20.13	0.626	0.131
1961	7.15	0.312	18304	2585	13.99	0.686	0.159
1962	6.73	0.294	17609	2731	11.74	0.704	0.172
1963	6.26	0.273	16777	2763	12.79	0.727	0.175
1964	5.87	0.256	18432	2195	12.36	0.682	0.140
1965	5.93	0.259	18808	2148	39.52	0.672	0.134
1966	6.16	0.269	18384	2328	20.38	0.684	0.142
1967	6.36	0.278	19072	2220	8.97	0.665	0.135
1968	6.55	0.286	19479	2174	7.10	0.654	0.120
1969	6.74	0.294	19492	2306	7.26	0.654	0.117
1970	7.09	0.309	18437	2766	8.67	0.682	0.135
1971	7.60	0.332	18466	2925	9.98	0.682	0.143
1972	8.09	0.353	18565	2982	8.75	0.679	0.151
1973	8.27	0.361	17480	3001	8.18	0.703	0.161
1974	7.98	0.349	14984	3691	9.55	0.766	0.215
1975	7.05	0.308	14065	3563	11.86	0.789	0.238
1976	5.96	0.260	14261	2837	14.32	0.783	0.221
1977	5.14	0.224	15118	2332	9.27	0.763	0.204
1978	4.55	0.199	11783	3159	6.21	0.844	0.294
1979	3.62	0.158	9847	3206	8.57	0.885	0.332
1980	2.79	0.122	10193	2594	9.58	0.879	0.306
1981	2.38	0.104	11009	2128	7.99	0.864	0.278
1982	2.26	0.099	9280	2723	8.29	0.903	0.376
1983	1.91	0.083	10139	2276	13.63	0.874	0.356
1984	1.73	0.075	10595	1800	13.62	0.863	0.308
1985	1.66	0.072	9674	1917	8.54	0.882	0.336
1986	1.56	0.068	9680	1831	5.35	0.882	0.316
1987	1.52	0.066	8289	2326	7.87	0.913	0.376
1988	1.38	0.060	8218	2270	10.44	0.915	0.376
1989	1.39	0.061	8251	2253	11.26	0.914	0.397
1990	1.43	0.063	9194	1832	11.11	0.894	0.351
1991	1.49	0.065	8517	2009	9.04	0.908	0.388
1992	1.34	0.059	9293	1631	6.54	0.892	0.320
1993	1.30	0.057	9632	1587	14.05	0.883	0.290
1994	1.39	0.061	10922	1443	10.11	0.853	0.248
1995	1.64	0.071	10634	1727	10.71	0.860	0.281
1996	1.83	0.080	10412	1896	8.71	0.864	0.291
1997	1.90	0.083	10052	2028	9.86	0.873	0.304
1998	1.89	0.083	12059	1524	19.62	0.826	0.225
1999	2.10	0.092	12778	1551	12.93	0.808	0.215
2000	2.36	0.103	11798	1955	9.50	0.832	0.257

Table 22: Time series of population estimates for the base ... *continued.*

Year	Spawning output (trillions of eggs)	Fraction unfished	Age-3+ biomass (mt)	Dead catch (mt)	Age-0 recruits (1000s)	1-SPR	Exploitation rate
2001	2.47	0.108	12153	1911	8.86	0.824	0.232
2002	2.56	0.112	12418	1946	9.08	0.818	0.219
2003	2.72	0.119	12545	2165	8.76	0.820	0.232
2004	2.94	0.128	13559	2038	10.77	0.794	0.215
2005	3.26	0.142	11776	2820	13.95	0.838	0.294
2006	3.19	0.139	11667	2687	27.71	0.840	0.303
2007	2.98	0.130	12027	2317	26.93	0.830	0.280
2008	2.80	0.122	11675	2293	29.08	0.839	0.279
2009	2.60	0.113	12582	1949	12.69	0.818	0.211
2010	2.65	0.116	19302	927	10.21	0.641	0.083
2011	3.42	0.149	21794	951	11.30	0.572	0.065
2012	4.67	0.204	23253	1133	19.48	0.531	0.064
2013	6.30	0.275	19643	2275	9.32	0.632	0.114
2014	7.70	0.336	20526	2425	13.73	0.607	0.116
2015	8.77	0.383	20508	2681	13.83	0.608	0.125
2016	9.32	0.407	20679	2743	9.36	0.603	0.129
2017	9.51	0.415	20070	2946	8.36	0.620	0.141
2018	9.40	0.410	20381	2906	9.43	0.610	0.143
2019	9.17	0.400	20973	2627	11.21	0.593	0.135
2020	8.97	0.392	22675	2100	11.69	0.545	0.112
2021	8.94	0.390	19803	2889	13.31	0.625	0.159
2022	8.42	0.367	18614	3070	13.89	0.658	0.180

Table 23: Data weightings applied to length and age compositions according to the 'Francis' method. 'Obs.' refers to the number of unique composition vectors included in the likelihood. 'N input' and 'N adj.' refer to the sample sizes of those vectors before and after being adjusted by the the weights. 'CAAL' is conditional age-at-length data. The WCGBTS age comps are conditioned on length, so there are more observations with fewer samples per observation.

Type	Fleet	Francis	Obs.	Mean N input	Mean N adj.	Sum N adj.
Length	North	0.278	82	247.3	68.7	5633.6
Length	South	0.136	70	255.0	34.6	2419.0
Length	Triennial	0.290	6	582.0	168.8	1012.5
Length	WCGBTS	0.102	19	838.6	85.3	1621.2
Age	North	0.280	55	108.4	30.3	1668.3
Age	South	0.082	18	47.4	3.9	69.8
CAAL	WCGBTS	0.040	664	22.2	0.9	589.2

Table 24: Estimates of key parameters and derived quantities compared between the base model and the 2019 assessment.

Label	Base model	2019 assessment
Estimates of key parameters		
Recruitment unfished millions	15.357	20.361
Stock-recruit steepness	0.8	0.841
M Female	0.142	0.159
M Male	0.155	0.164
Estimates of derived quantities		
Unfished age 3+ bio 1000 mt	42.198	54.087
Fraction unfished 2019	0.4	0.391
Fraction unfished 2023	0.336	0.3
Fishing intensity 2018	0.61	0.573
Fishing intensity 2022	0.658	0.684
Retained Catch MSY mt	2471	3122
Dead Catch MSY mt	2482	3157
WCGBTS catchability	4.023	2.851
Triennial catchability - early	0.494	0.423
Triennial catchability - late	0.494	0.65

Table 25: Indices sensitivity analyses: differences in negative log-likelihood, estimates of key parameters, and estimates of derived quantities between the base model and several alternative models related to indices (columns). See main text for details on each sensitivity analysis. Red values indicate negative log-likelihoods that were lower (fit better to that component) than the base model. The index and total likelihoods are not comparable for the models that add or subtract data (2004 triennial and fishery CPUE).

Label	Base	Separate Q and selex for late triennial	Allow triennial selex to be dome-shaped	No 2004 triennial index obs.	Extra SD for WCGBTS estimated	Fisheries CPUE included
Diff. in likelihood from base model						
Total	0	-3.953	-3.953	-3.622	-2.006	-42.819
Indices	0	-1.243	-1.243	-3.825	-0.724	-45.256
Length comp	0	-2.987	-2.987	0.032	-0.206	-0.025
Age comp	0	0.222	0.222	0.353	-1.163	0.022
Discard	0	0.027	0.027	-0.048	-0.034	-0.004
Mean body weight	0	0.002	0.002	-0.024	0.007	0.003
Recruitment	0	0.003	0.003	-0.122	0.191	0.003
Parm priors	0	0.023	0.023	0.012	-0.076	2.437
Estimates of key parameters						
Recruitment unfished millions	15.357	15.242	15.242	15.284	15.791	15.362
Stock-recruit steepness	0.8	0.8	0.8	0.8	0.8	0.8
M Female	0.142	0.141	0.141	0.141	0.145	0.142
M Male	0.155	0.154	0.154	0.154	0.158	0.155
Estimates of derived quantities						
Unfished age 3+ bio 1000 mt	42.198	42.392	42.392	42.245	41.63	42.196
B0 trillions of eggs	22.907	23.061	23.061	22.943	22.514	22.905
B2023 trillions of eggs	7.686	7.634	7.634	7.679	7.906	7.685
Fraction unfished 2023	0.336	0.331	0.331	0.335	0.351	0.336
Fishing intensity 2022	0.658	0.661	0.661	0.659	0.646	0.658
Retained Catch MSY mt	2471	2467	2467	2469	2475	2471
Dead Catch MSY mt	2482	2478	2478	2480	2486	2482
OFL mt 2023	3194	3146	3146	3184	3337	3194
WCGBTS catchability	4.023	4.043	4.043	4.035	3.967	4.022

Table 26: Composition data sensitivity analyses: differences in negative log-likelihood, estimates of key parameters, and estimates of derived quantities between the base model and several alternative models related to composition data (columns). See main text for details on each sensitivity analysis. Red values indicate negative log-likelihoods that were lower (fit better to that component) than the base model. The length, age, and total likelihoods are not comparable across models due to differences in weighting and included data.

Label	Base	Dirichlet-multinomial weights	Include early age comps	Exclude early Oregon 'special project' samples
Diff. in likelihood from base model				
Total	0	21782.077	237.47	-21.764
Indices	0	11.059	3.328	0.773
Length comp	0	11662.914	-1.925	-4.132
Age comp	0	10042.121	232.829	-23.206
Discard	0	15.428	0.416	0.823
Mean body weight	0	7.644	-1.187	-0.903
Recruitment	0	20.615	3.769	4.972
Parm priors	0	22.387	0.24	-0.139
Estimates of key parameters				
Recruitment unfished millions	15.357	14.491	13.045	14.858
Stock-recruit steepness	0.8	0.8	0.8	0.8
M Female	0.142	0.139	0.133	0.149
M Male	0.155	0.15	0.148	0.161
Estimates of derived quantities				
Unfished age 3+ bio 1000 mt	42.198	43.772	38.899	36.078
B0 trillions of eggs	22.907	25.309	21.164	18.962
B2023 trillions of eggs	7.686	11.862	8.564	6.997
Fraction unfished 2023	0.336	0.469	0.405	0.369
Fishing intensity 2022	0.658	0.6	0.628	0.651
Retained Catch MSY mt	2471	2332	2332	2253
Dead Catch MSY mt	2482	2344	2345	2266
OFL mt 2023	3194	4002	3547	3236
WCGBTS catchability	4.023	2.493	3.275	5.291

Table 27: Biology sensitivity analyses: differences in negative log-likelihood, estimates of key parameters, and estimates of derived quantities between the base model and several alternative models related to biology (columns). See main text for details on each sensitivity analysis. Red values indicate negative log-likelihoods that were lower (fit better to that component) than the base model. Sensitivity to using the 2019 fecundity is represented in the bridging analysis.

Label	Base	2019 weight-length	2019 maturity	Est. age-0 frac. female	Frac. female + no sex offset
Diff. in likelihood from base model					
Total	0	-1.038	-1.42	-5.558	29.95
Indices	0	0.005	-0.088	0.125	-0.368
Length comp	0	-0.458	-0.019	-2.129	32.72
Age comp	0	-0.022	-0.46	-2.817	-6.108
Discard	0	0.004	-0.007	-0.136	0.261
Mean body weight	0	-0.563	-0.009	0.087	-0.408
Recruitment	0	-0.003	-0.943	-1.465	3.497
Parm priors	0	-0.002	0.108	0.777	0.362
Estimates of key parameters					
Recruitment unfished millions	15.357	15.4	14.563	14.439	14.292
Stock-recruit steepness	0.8	0.8	0.8	0.8	0.8
M Female	0.142	0.142	0.138	0.161	0.128
M Male	0.155	0.155	0.151	0.118	0.146
Estimates of derived quantities					
Unfished age 3+ bio 1000 mt	42.198	42.188	42.178	41.684	46.839
B0 trillions of eggs	22.907	22.937	24.199	20.146	27.264
B2023 trillions of eggs	7.686	7.697	8.255	7.401	8.587
Fraction unfished 2023	0.336	0.336	0.341	0.367	0.315
Fishing intensity 2022	0.658	0.658	0.648	0.629	0.683
Retained Catch MSY mt	2471	2471	2458	2447	2437
Dead Catch MSY mt	2482	2482	2469	2458	2449
OFL mt 2023	3194	3195	3356	3564	2906
WCGBTS catchability	4.023	4.021	4.039	4.174	2.988

Table 28: Recruitment and environmental index sensitivity analyses: differences in negative log-likelihood, estimates of key parameters, and estimates of derived quantities between the base model and several alternative models related to recruitment and environmental index (columns). See main text for details on each sensitivity analysis. Red values indicate negative log-likelihoods that were lower (fit better to that component) than the base model. The indices and total likelihoods are not comparable for the environmental index model due to the additional data.

Label	Base	Environ-mental index	Zero-centered recdevs	All recdevs in 'main' period
Diff. in likelihood from base model				
Total	0	-26.69	1.073	0
Indices	0	-45.28	0.229	0
Length comp	0	10.116	0.188	0
Age comp	0	10.155	0.693	0
Discard	0	0.57	0.018	0
Mean body weight	0	0.419	0.014	0
Recruitment	0	-2.412	0.082	0.003
Parm priors	0	-0.255	-0.15	0
Estimates of key parameters				
Recruitment unfished millions	15.357	16.983	17.8	15.357
Stock-recruit steepness	0.8	0.8	0.8	0.8
M Female	0.142	0.155	0.148	0.142
M Male	0.155	0.17	0.162	0.155
Estimates of derived quantities				
Unfished age 3+ bio 1000 mt	42.198	39.014	44.569	42.198
B0 trillions of eggs thousand mt	0.023	0.021	0.024	0.023
B2023 trillions of eggs thousand mt	0.008	0.009	0.008	0.008
Fraction unfished 2023	0.336	0.415	0.325	0.336
Fishing intensity 2022	0.658	0.609	0.642	0.658
Retained Catch MSY mt	2471	2488	2720	2471
Dead Catch MSY mt	2482	2499	2732	2482
OFL mt 2023	3194	4101	3406	3194
WCGBTS catchability	4.023	4.053	4.021	4.023

Table 29: The trans-boundary nature of the stock sensitivity analyses: differences in negative log-likelihood, estimates of key parameters, and estimates of derived quantities between the base model and several alternative models related to the trans-boundary nature of the stock (columns). See main text for details on each sensitivity analysis. Red values indicate negative log-likelihoods that were lower (fit better to that component) than the base model. The indices and total likelihoods are not comparable for the models that include the Canadian index.

Label	Base	Canadian index added	Canadian catches added	Canadian catches and index added
Diff. in likelihood from base model				
Total	0	-7.55	3.593	-4.324
Indices	0	-7.494	1.389	-6.396
Length comp	0	-0.079	0.446	0.301
Age comp	0	0.087	-0.041	-0.01
Discard	0	0.012	0.095	0.102
Mean body weight	0	-0.002	0.024	0.023
Recruitment	0	-0.07	1.857	1.832
Parm priors	0	-0.003	-0.176	-0.175
Estimates of key parameters				
Recruitment unfished millions	15.357	15.407	19.487	19.517
Stock-recruit steepness	0.8	0.8	0.8	0.8
M Female	0.142	0.142	0.149	0.149
M Male	0.155	0.155	0.164	0.164
Estimates of derived quantities				
Unfished age 3+ bio 1000 mt	42.198	42.283	47.88	48.026
B0 trillions of eggs thousand mt	0.023	0.023	0.026	0.026
B2023 trillions of eggs thousand mt	0.008	0.008	0.01	0.01
Fraction unfished 2023	0.336	0.34	0.391	0.396
Fishing intensity 2022	0.658	0.654	0.626	0.623
Retained Catch MSY mt	2471	2477	2948	2955
Dead Catch MSY mt	2482	2488	2960	2967
OFL mt 2023	3194	3254	4447	4519
WCGBTS catchability	4.023	4.003	3.198	3.186

Table 30: Projections of estimated OFL (mt), ABC (mt), resulting ACLs (mt) based on the 25-5 rule and applied buffers, and estimated spawning output in trillions of eggs, and spawning output relative to unfished for 2025-2034, with assumed removals in 2023 and 2024 based on recommended values from the Groundfish Management Team.

Year	Adopted OFL (mt)	Adopted ABC (mt)	Adopted ACL (mt)	Assumed catch (mt)	OFL (mt)	Buffer	ABC	ACL	Spawn. Output	Frac. Un-fished
2023	3763	3485	3485	3485	-	-	-	-	7.69	0.336
2024	3563	3285	3285	3285	-	-	-	-	6.70	0.293
2025	-	-	-	-	2518	0.935	2354	2354	5.85	0.255
2026	-	-	-	-	2424	0.930	2255	2238	5.56	0.243
2027	-	-	-	-	2422	0.926	2242	2217	5.48	0.239
2028	-	-	-	-	2475	0.922	2282	2263	5.55	0.242
2029	-	-	-	-	2549	0.917	2337	2334	5.69	0.248
2030	-	-	-	-	2618	0.913	2390	2390	5.85	0.255
2031	-	-	-	-	2672	0.909	2429	2429	5.99	0.261
2032	-	-	-	-	2709	0.904	2449	2449	6.09	0.266
2033	-	-	-	-	2733	0.900	2460	2460	6.16	0.269
2034	-	-	-	-	2749	0.896	2463	2463	6.20	0.271

Table 31: Decision table with 10-year projections. 'Mgmt' refers to the three management scenarios (A) the default harvest control rule $P^* = 0.45$, (B) harvest control rule with a lower $P^* = 0.40$. In each case the 2023 and 2024 catches are fixed at the ACLs which have been set for that year with estimated fleet allocation provided by the GMT. The alternative states of nature ('Low', 'Base', and 'High' as discussed in the text) are provided in the columns, with Spawning Output ('Spawn', in trillions of eggs) and Fraction of unfished ('Frac') provided for each state.

Mgmt	Year	Catch	Low Spawn M=0.072	Low Frac M=0.072	Base Spawn M=0.142	Base Frac M=0.142	High Spawn M=0.219	High Frac M=0.219
A	2023	3485	6.86	0.195	7.69	0.336	8.53	0.528
	2024	3285	6.03	0.172	6.70	0.292	7.41	0.458
	2025	2354	5.27	0.150	5.85	0.255	6.49	0.401
	2026	2238	4.97	0.141	5.56	0.243	6.17	0.382
	2027	2217	4.83	0.137	5.48	0.239	6.08	0.376
	2028	2263	4.78	0.136	5.55	0.242	6.14	0.380
	2029	2334	4.79	0.136	5.69	0.248	6.28	0.388
	2030	2390	4.80	0.137	5.85	0.255	6.43	0.398
	2031	2429	4.79	0.136	5.99	0.261	6.55	0.405
	2032	2449	4.75	0.135	6.09	0.266	6.62	0.409
	2033	2460	4.68	0.133	6.16	0.269	6.67	0.412
	2034	2463	4.59	0.131	6.20	0.271	6.69	0.414
B	2023	3485	6.86	0.195	7.69	0.336	8.53	0.528
	2024	3285	6.03	0.172	6.70	0.292	7.41	0.458
	2025	2198	5.27	0.150	5.85	0.255	6.49	0.401
	2026	2117	5.05	0.144	5.63	0.246	6.24	0.386
	2027	2115	4.96	0.141	5.61	0.245	6.19	0.383
	2028	2169	4.96	0.141	5.72	0.250	6.29	0.389
	2029	2226	5.01	0.143	5.90	0.258	6.46	0.400
	2030	2279	5.07	0.144	6.09	0.266	6.63	0.410
	2031	2318	5.12	0.146	6.27	0.274	6.77	0.419
	2032	2345	5.13	0.146	6.41	0.280	6.88	0.425
	2033	2356	5.12	0.146	6.52	0.285	6.94	0.429
	2034	2360	5.08	0.145	6.60	0.288	6.98	0.432

8 Figures
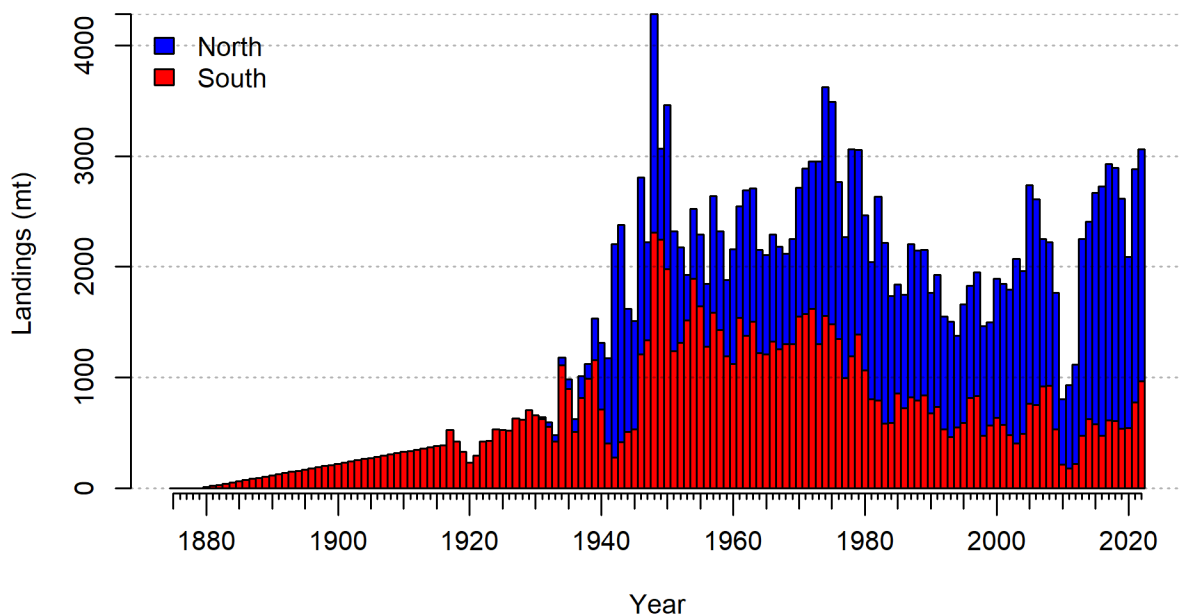
8.1 Data
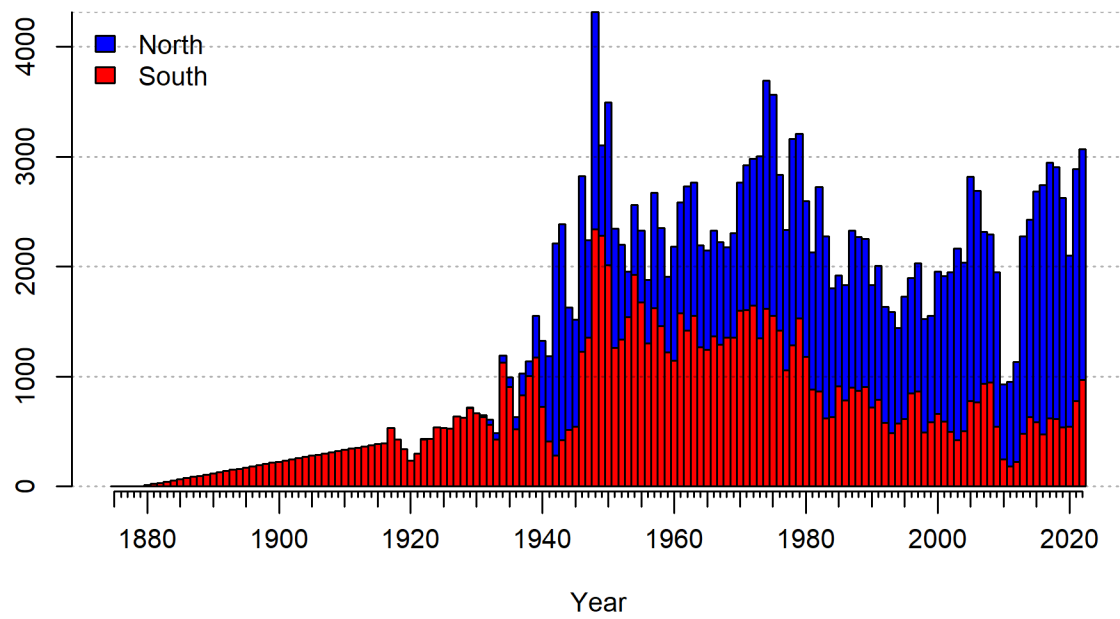
Figure 1: Map of the U.S. West Coast Exclusive Economic Zone within which the assessment is focused. The dashed line and colors delineate the two fishing fleets represented in the model: North (blue) and South (red).
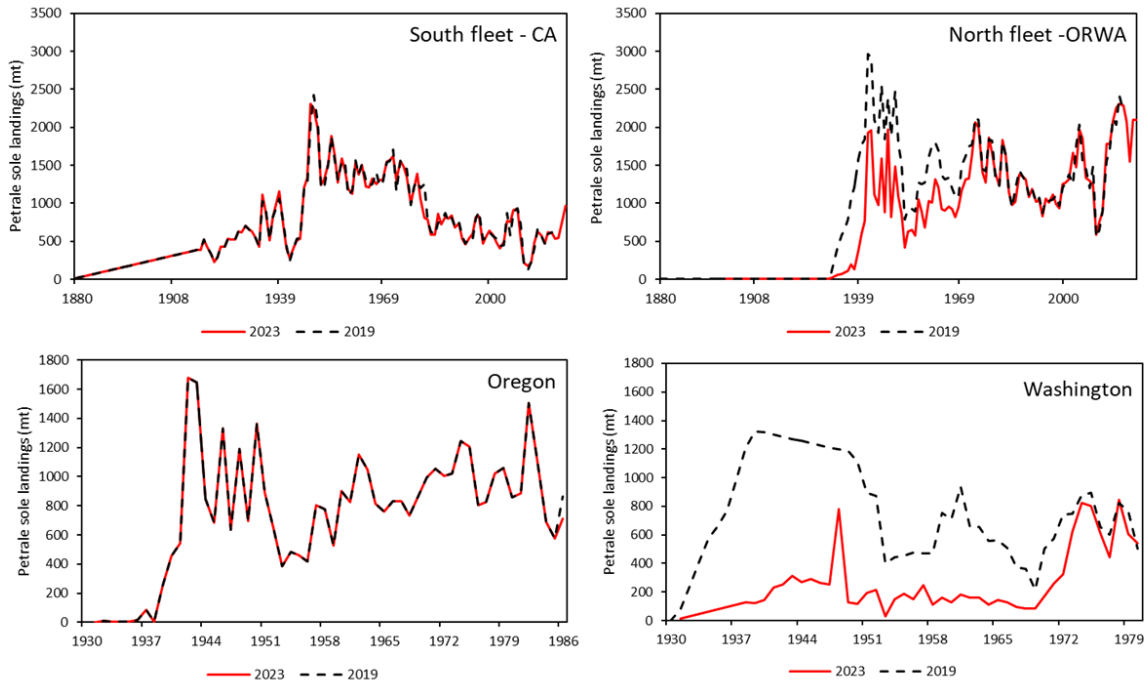
Figure 2: Data presence by year for each fleet, where circle area is relative within a data type. Circles are proportional to total catch for catches; to precision for indices, discards, and mean body weight observations; and to total sample size for compositions.
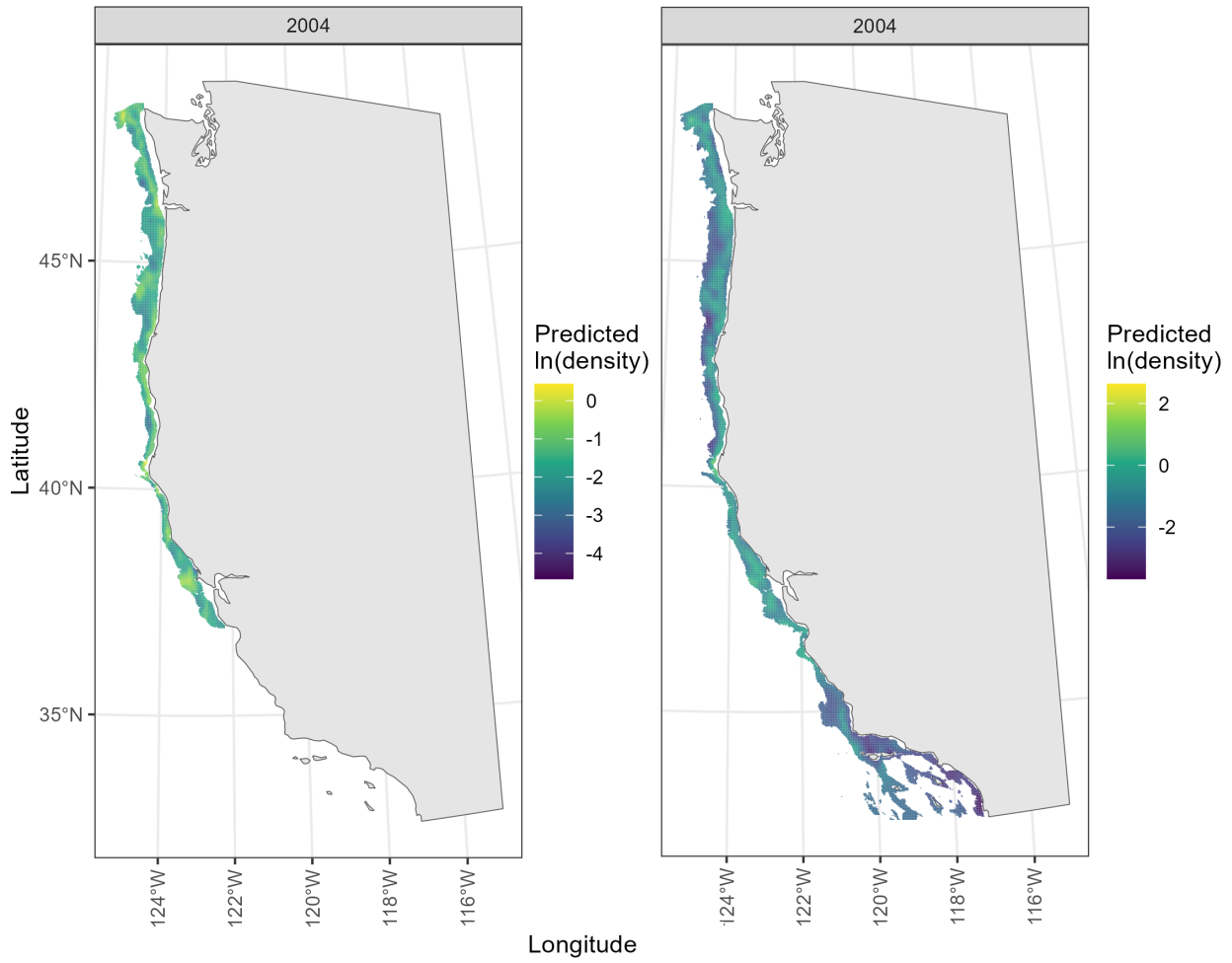
Figure 3: Landings (mt) by fleet used in the base model.

Figure 4: Landings plus dead discards (mt) by fleet as estimated in the base model.
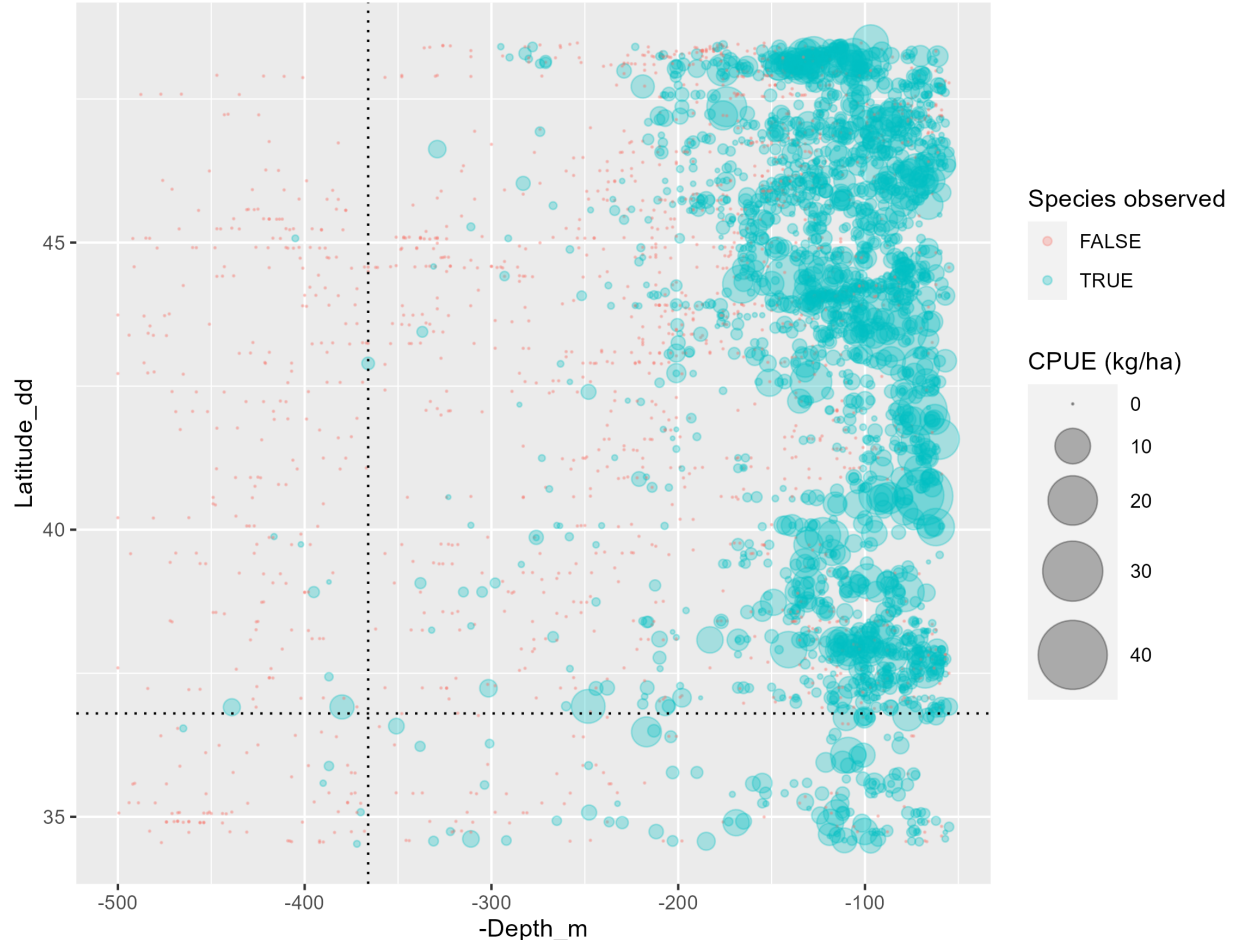
Figure 5: Comparison of landings used in this assessment (red line) with landings used in 2019 assessment (dashed black line) by state and fleet. Please see section on Historical landings for details.
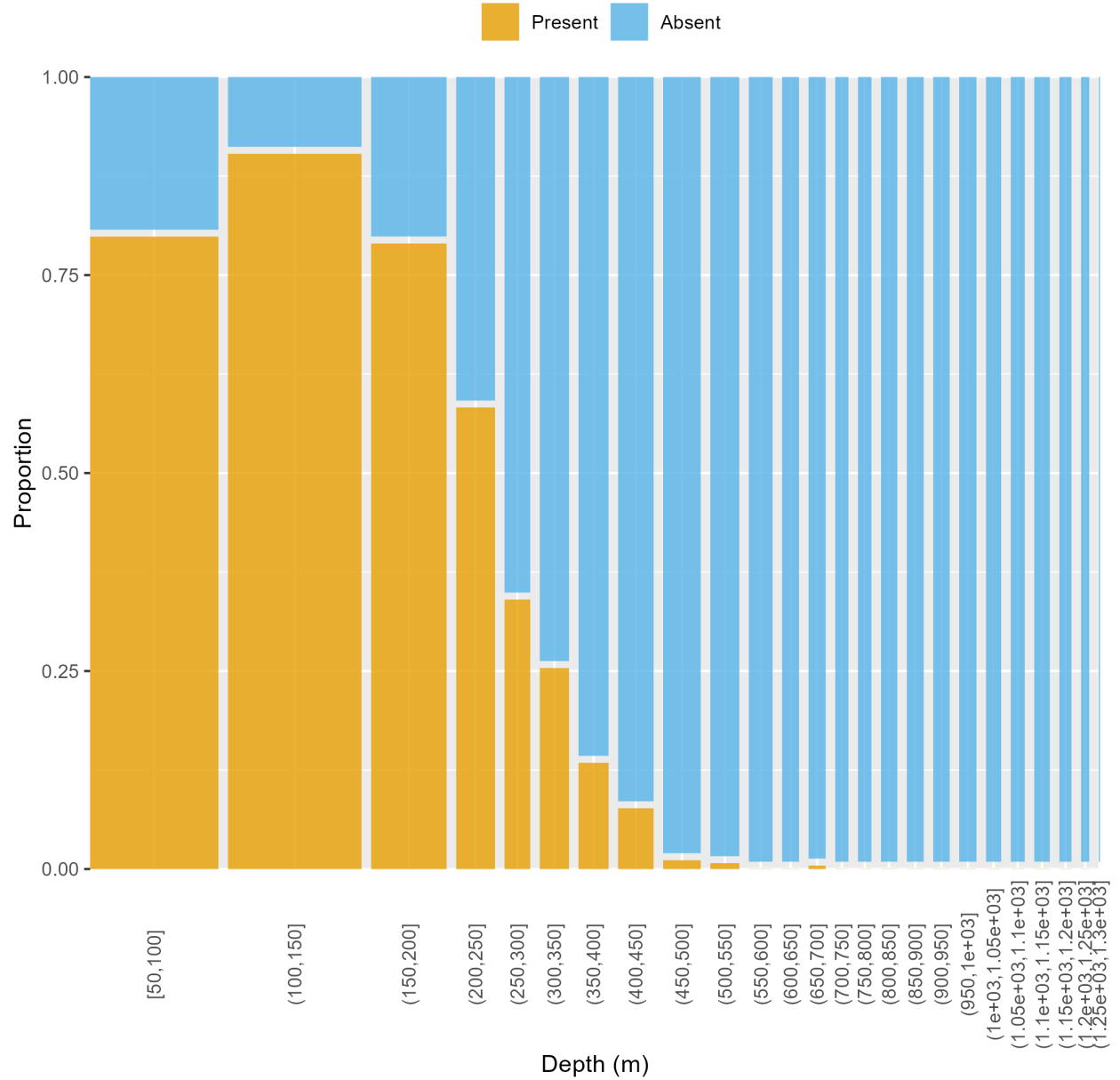
Figure 6: Predicted density from the geostatistical standardization of the Triennial Survey (left) and the West Coast Groundfish Bottom Trawl Survey (WCGBTS, right) in 2004, the one year in which both surveys were conducted. Density is on a log scale and the colors correspond to different scales as shown in the two legends.
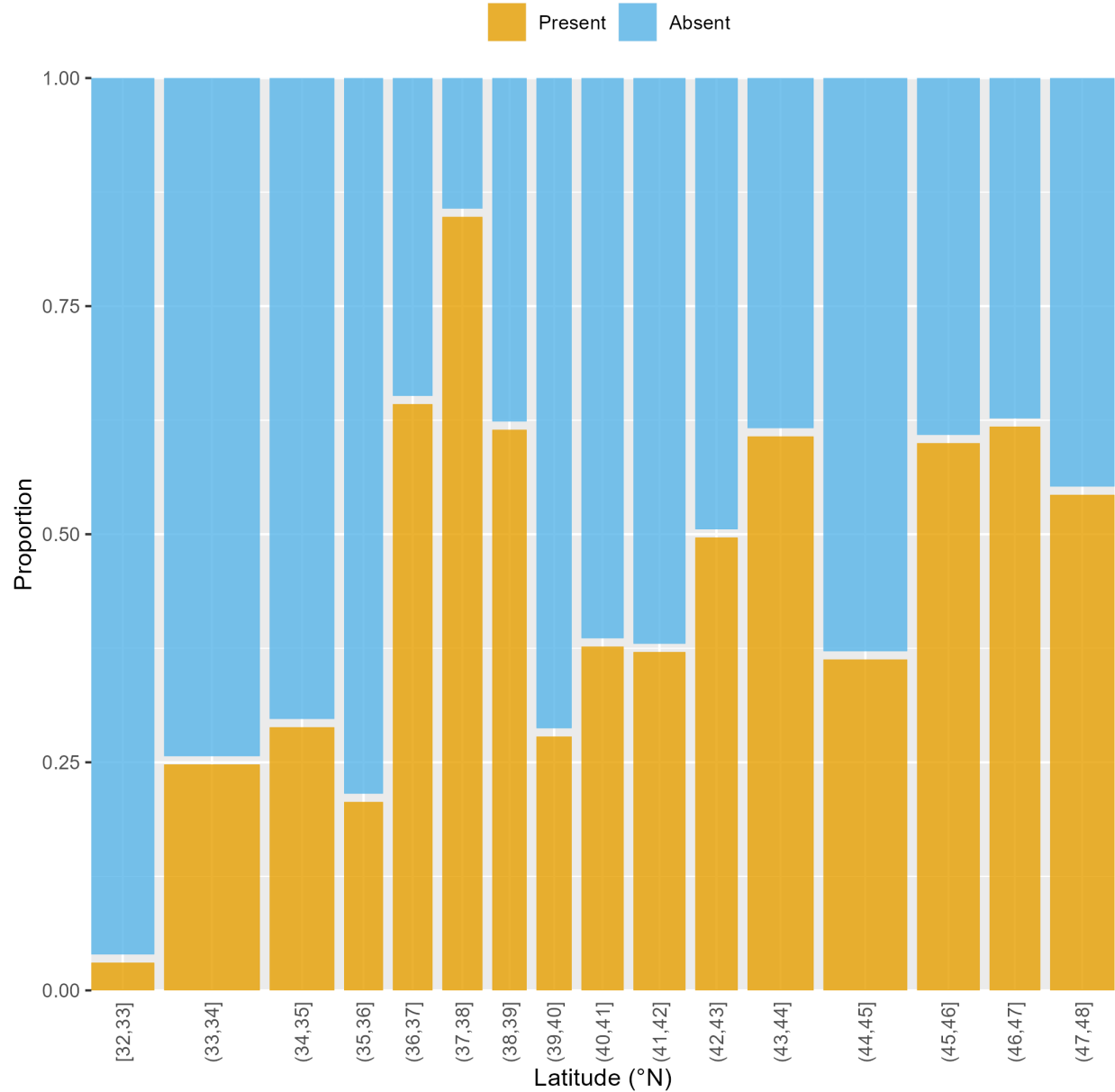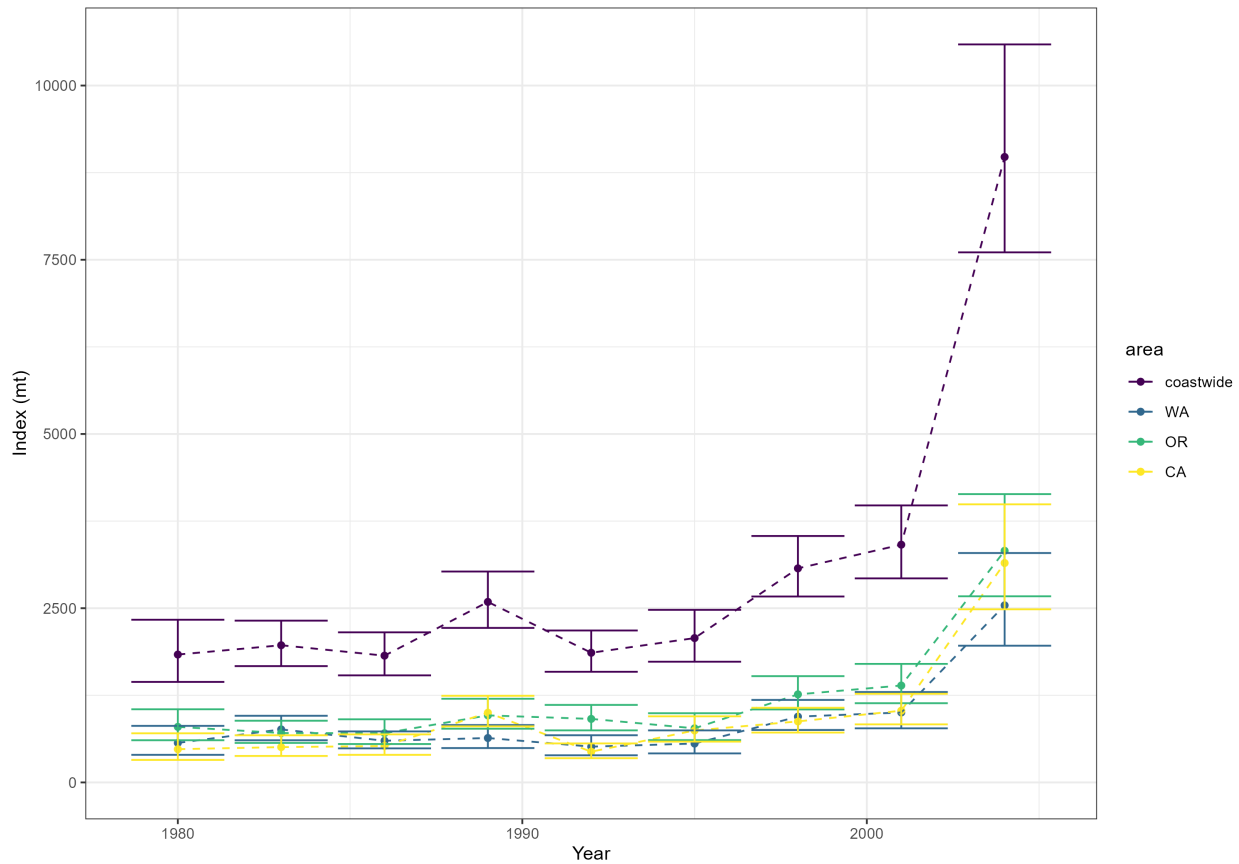
Figure 7: Distribution of petrale catch rates in the Triennial survey. The dashed lines represent the 366 m and 37 degree limits of the early years of the survey which were used to truncate the data to provide a consistent spatial coverage for the index standardization and length composition data.
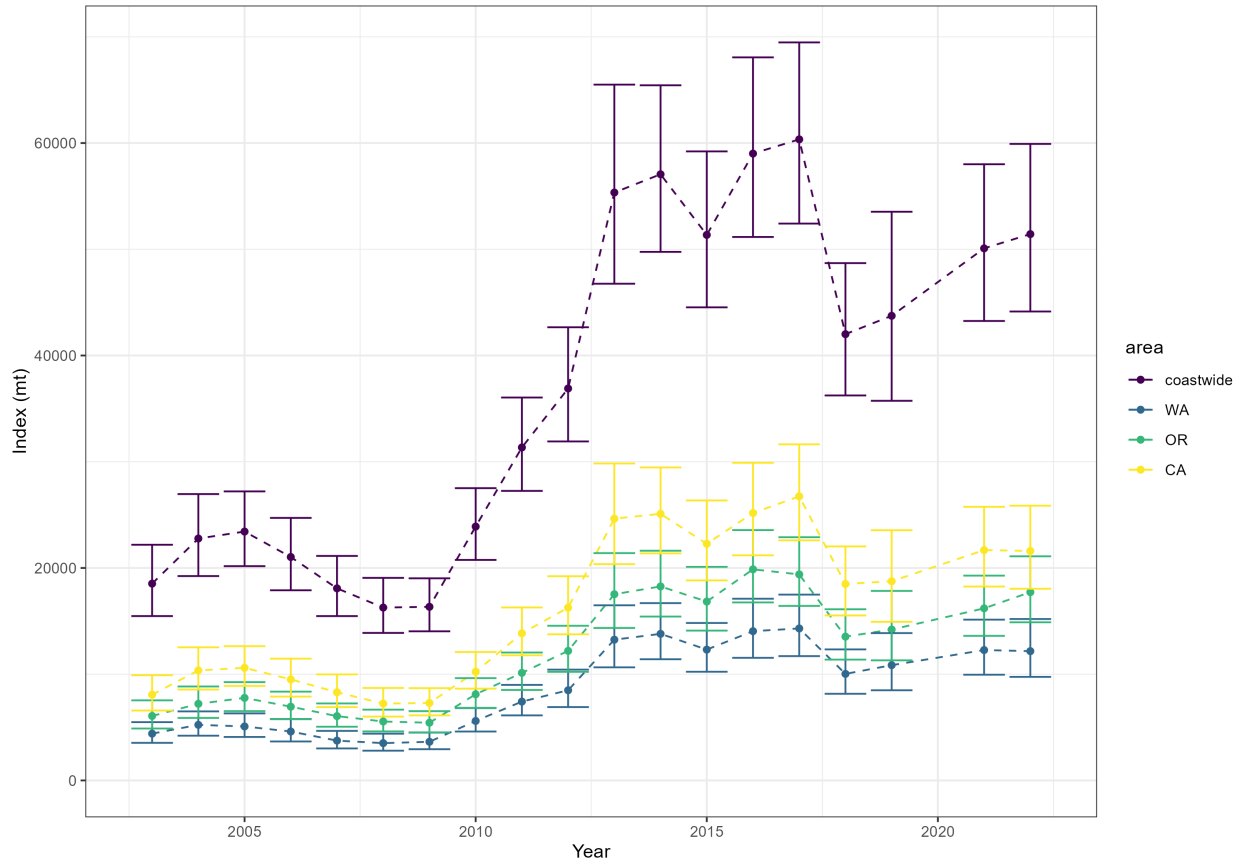
Figure 8: Presence/absence of petrale sole by depth in the WCGBTS. Bar widths are proportional to the number of hauls in that bin. Values are aggregated across all years of the survey.

Figure 9: Presence/absence of petrale sole by latitude in the WCGBTS. Bar widths are proportional to the number of hauls in that bin. Values are aggregated across all years of the survey.

Figure 10: Estimated coastwide index from the geostatistical standardization of the Triennial Survey. The subset of the biomass estimated within the waters off each state is shown as well.
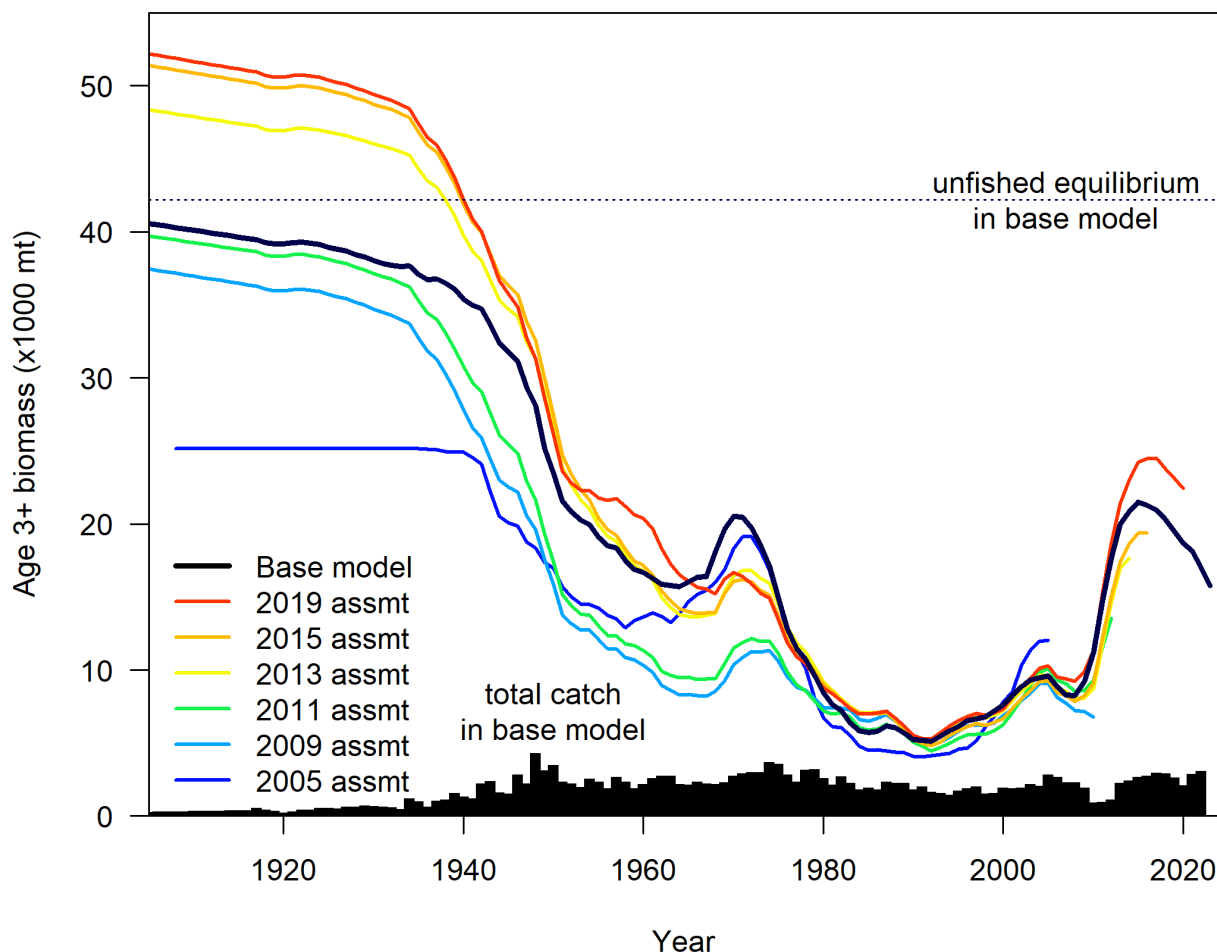
Figure 11: Estimated coastwide index from the geostatistical standardization of the WCGBTS. The subset of the biomass estimated within the waters off each state is shown as well.
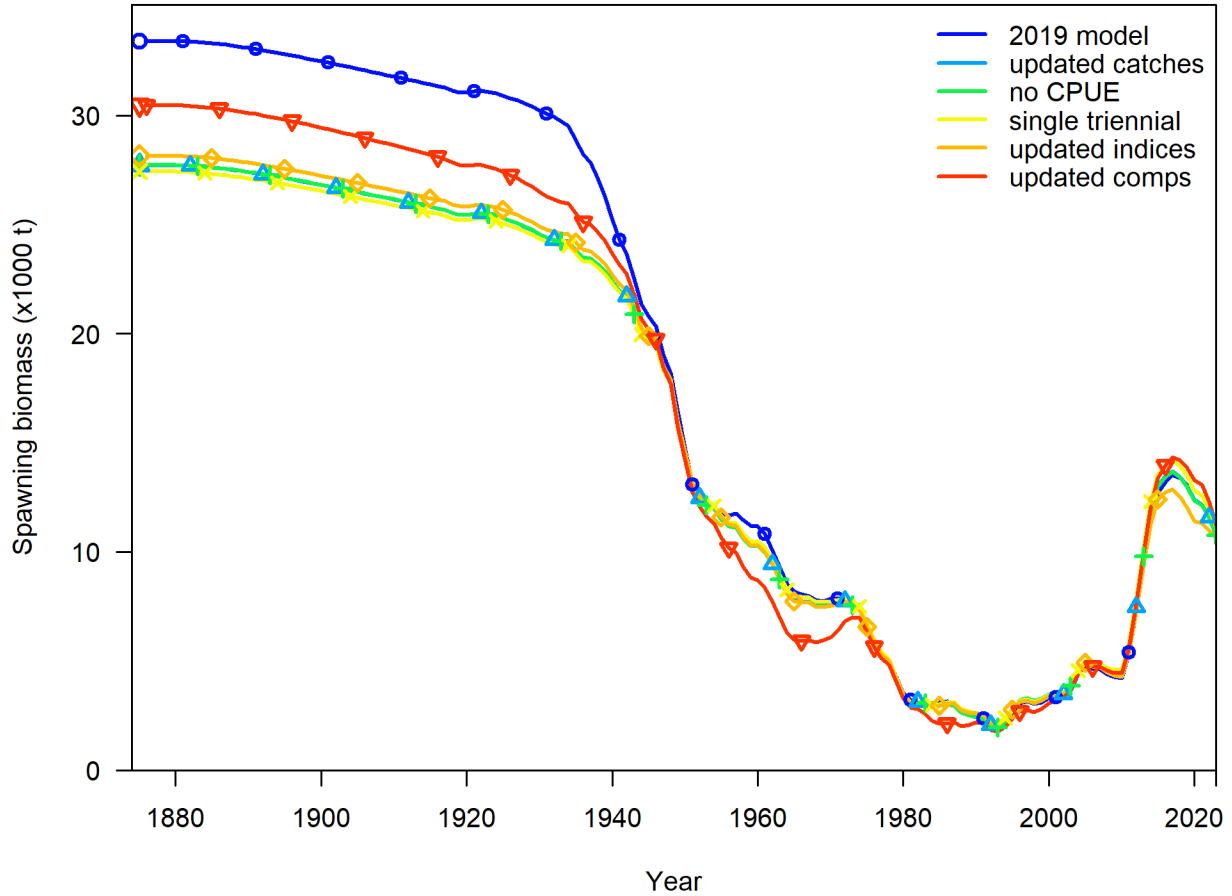
Figure 12: Photos from the largest recorded petrale sole catch on the WCGBTS: 8390 kg from a 15-minute tow on 23 September 2021. The photos were taken by John Buchanan on board the F/V Noah's Ark. The location was 123.9581 W, 38.92528 N with average haul depth of 310 m.
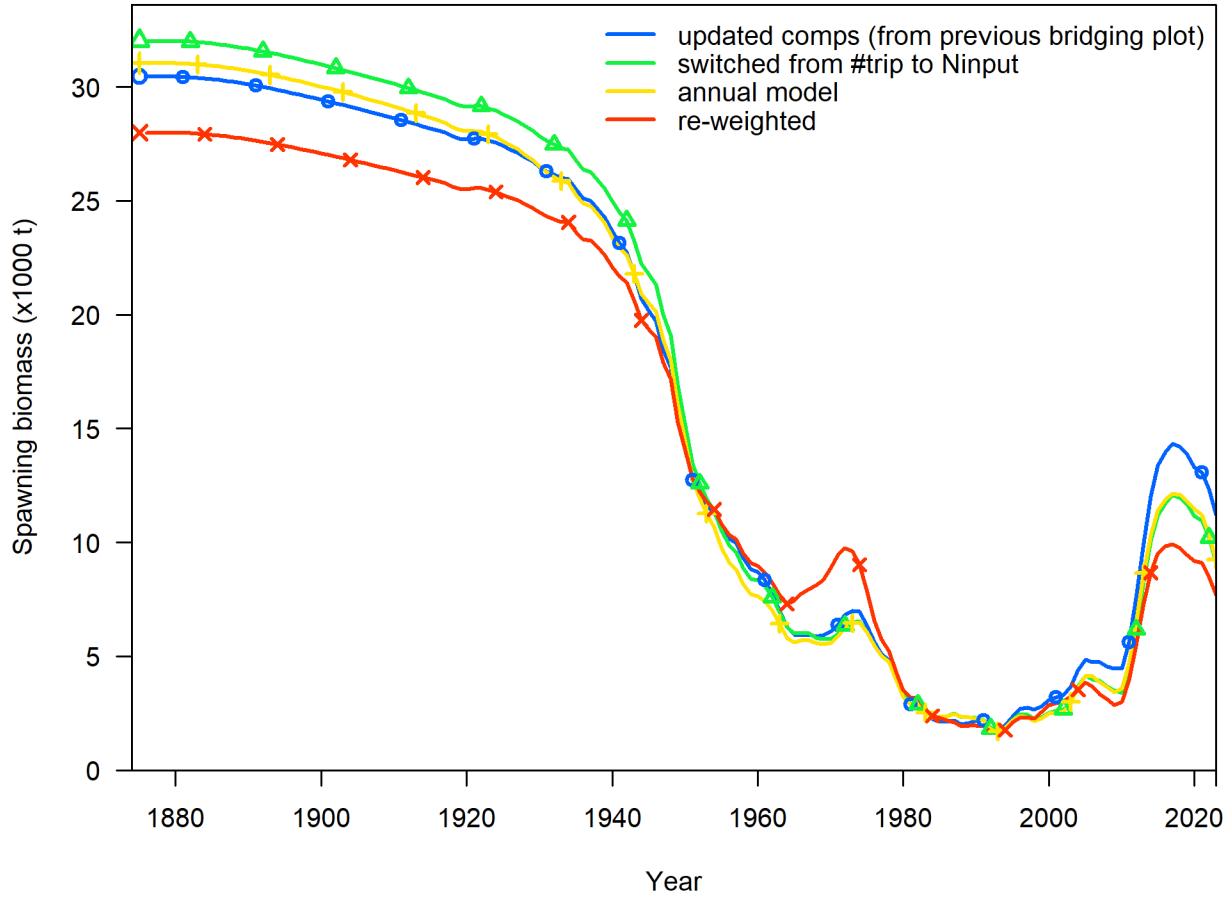
8.2 Model Results
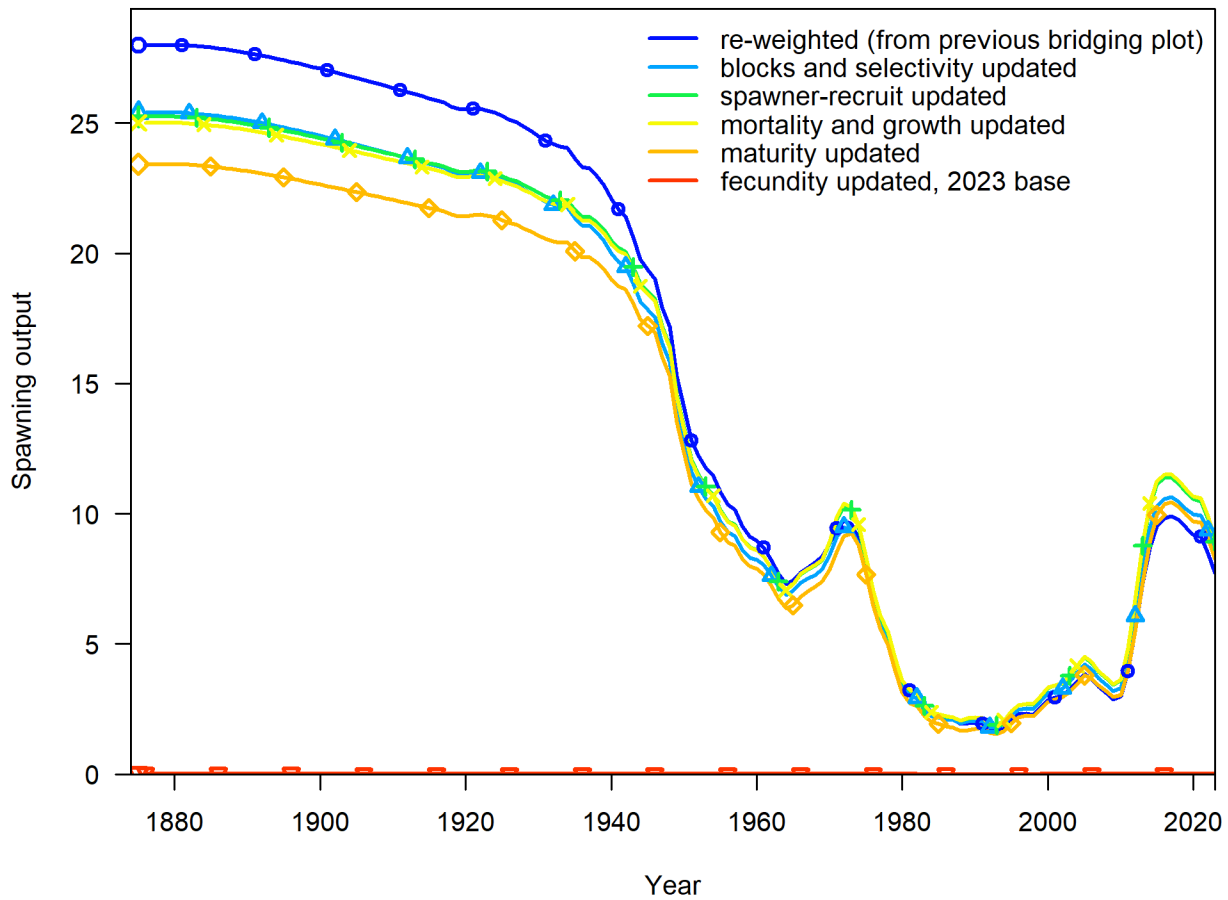
Figure 13: Comparison of biomass time series (colored lines) across recent assessments. Units are estimated biomass of females and males ages 3 and older. Total mortality from the base model (black bars) is included as well. Spawning biomass is not comparable across these assessments because the inclusion of a fecundity relationship starting in 2023 which results in spawning output in units of eggs.
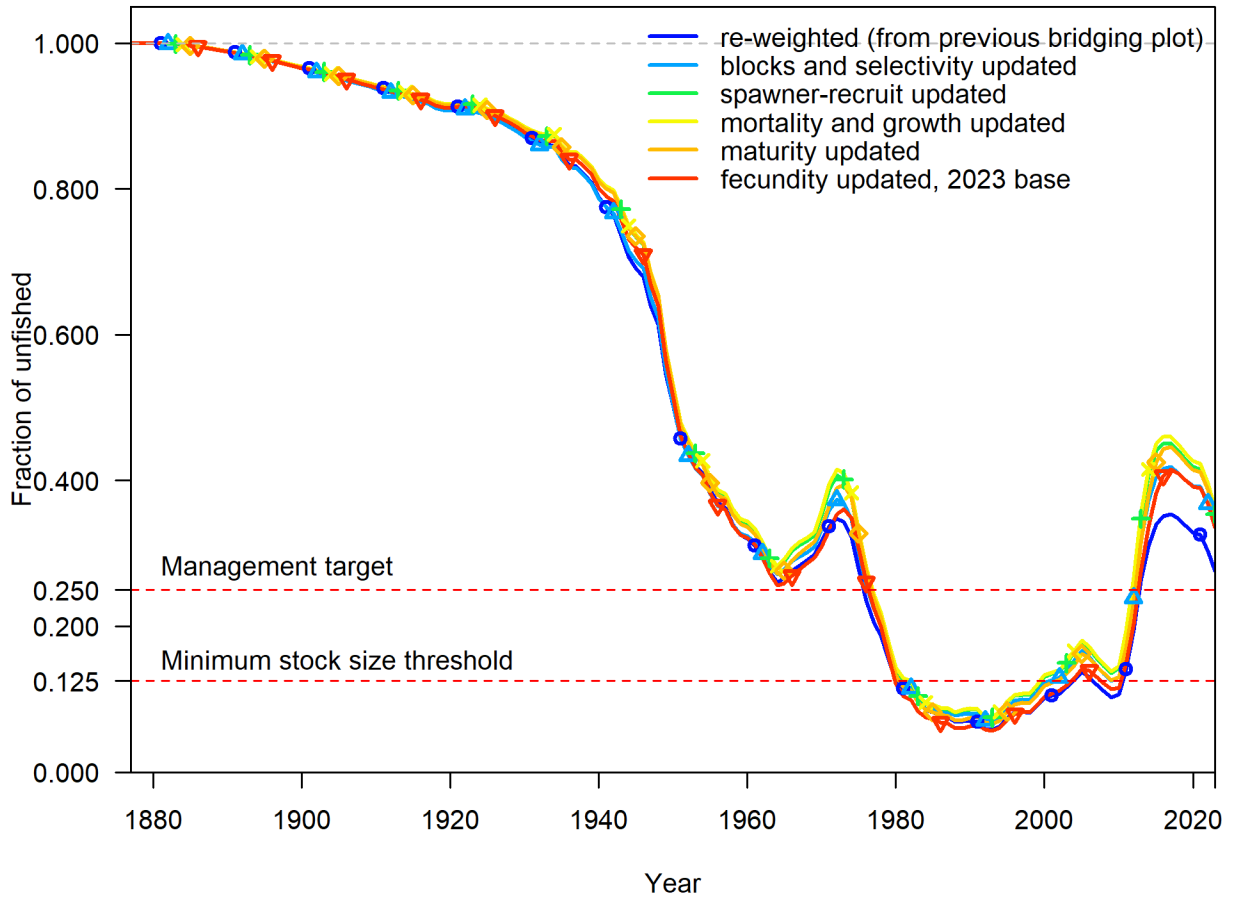
Figure 14: Time series of estimated spawning biomass (1,000s of mt) for the 2019 assessment model and bridging steps 1 to 5. The changes are cumulative.
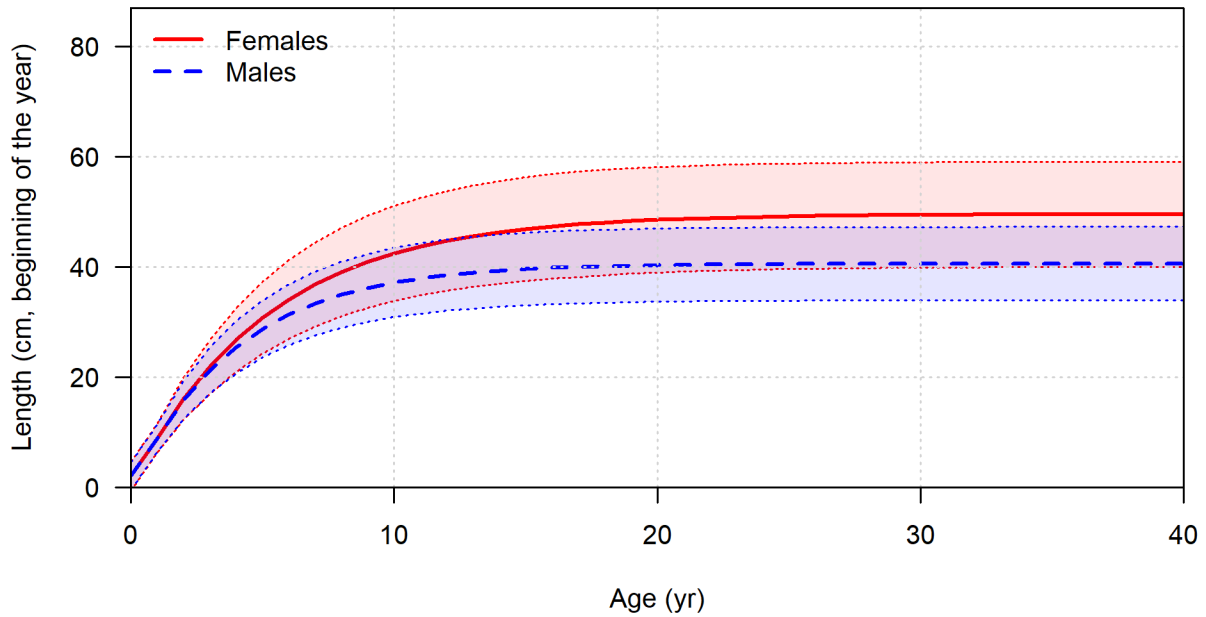
Figure 15: Time series of estimated spawning biomass (1,000s of mt) for bridging steps 5 to 8. The changes are cumulative.
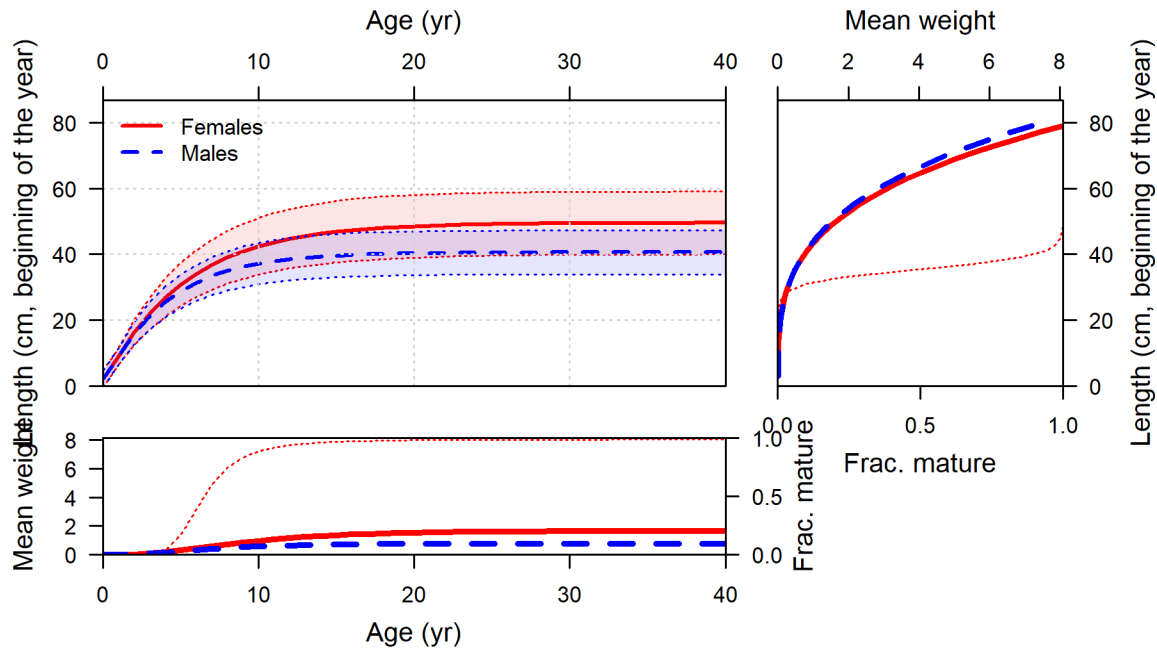
Figure 16: Time series of estimated spawning biomass (1,000s of mt) for briding steps 8 to 13, where the final step is the 2023 base model. The change in fecundity associated with the final step (2023 base, red line) changes the units of spawning output to trillions of eggs so the values are not comparable. The changes are cumulative.
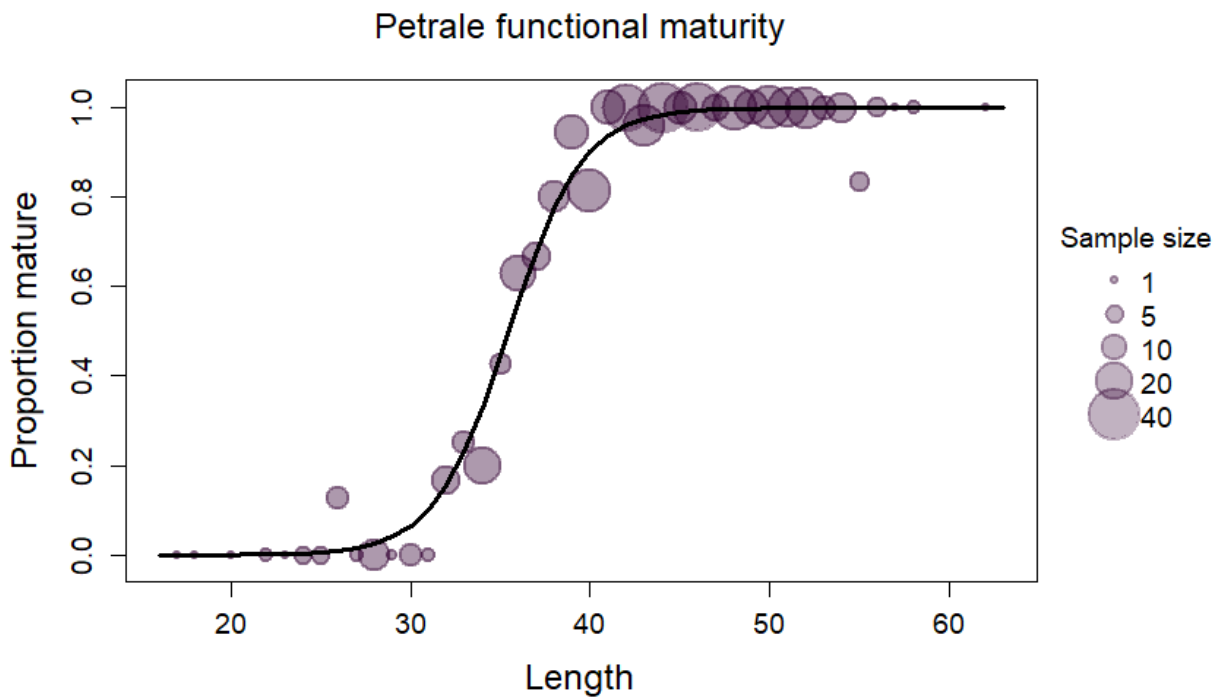
Figure 17: Time series of fraction of unfished spawning output for briding steps 8 to 13, where the final step is the 2023 base model. The changes are cumulative.
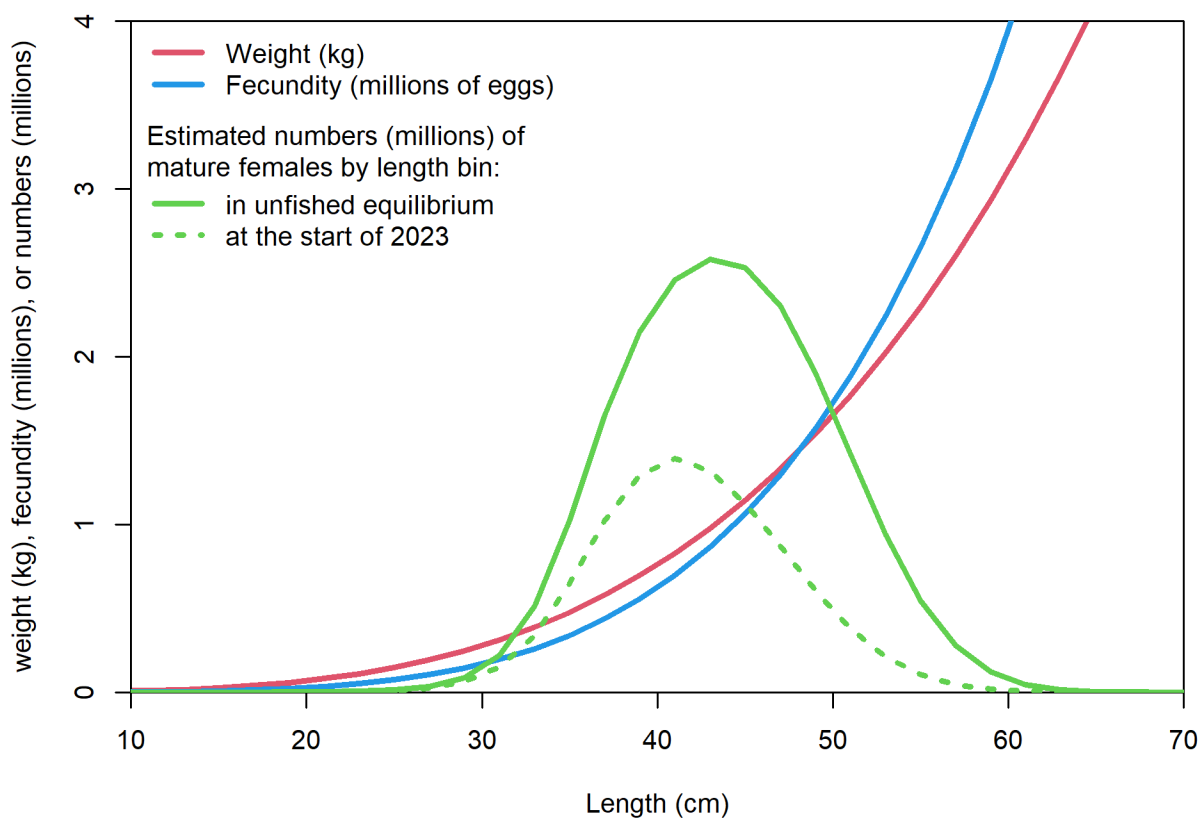
Figure 18: Model estimated length-at-age in the beginning of the year. Shaded area indicates 95 percent distribution of length-at-age around the estimated growth curve.
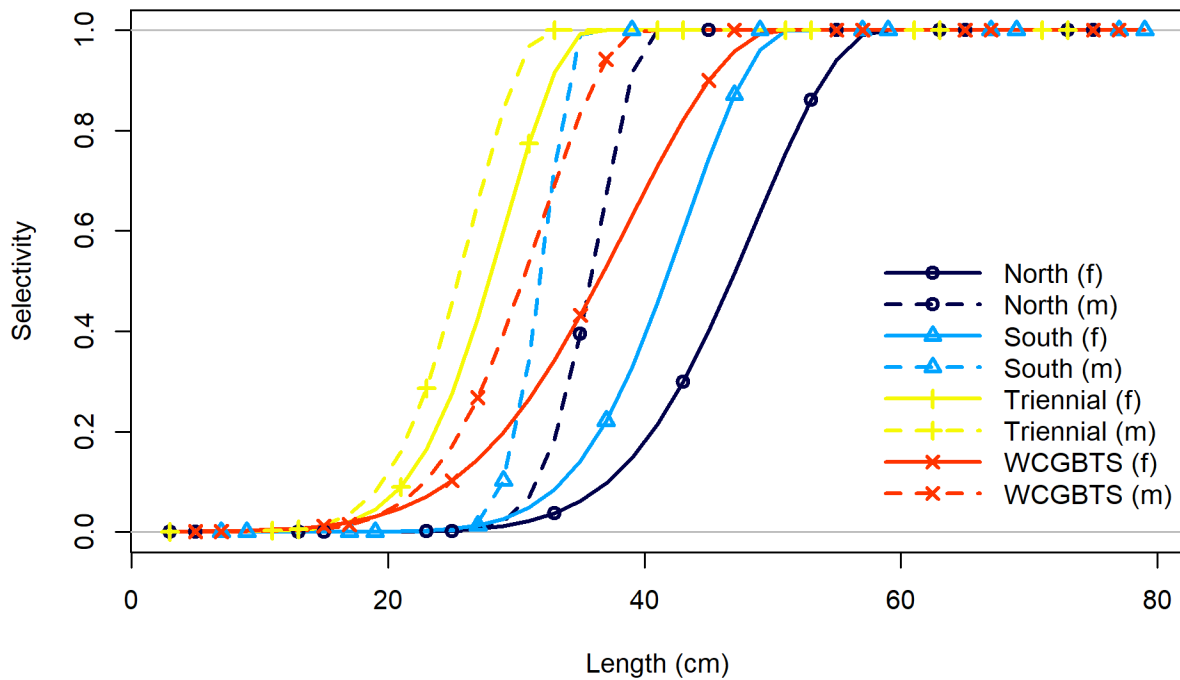
Figure 19: Relationship between growth, maturity, and weight. Length at age is in the top-left panel with weight (thick lines) and maturity (thin lines) shown in top-right and lower-left panels.
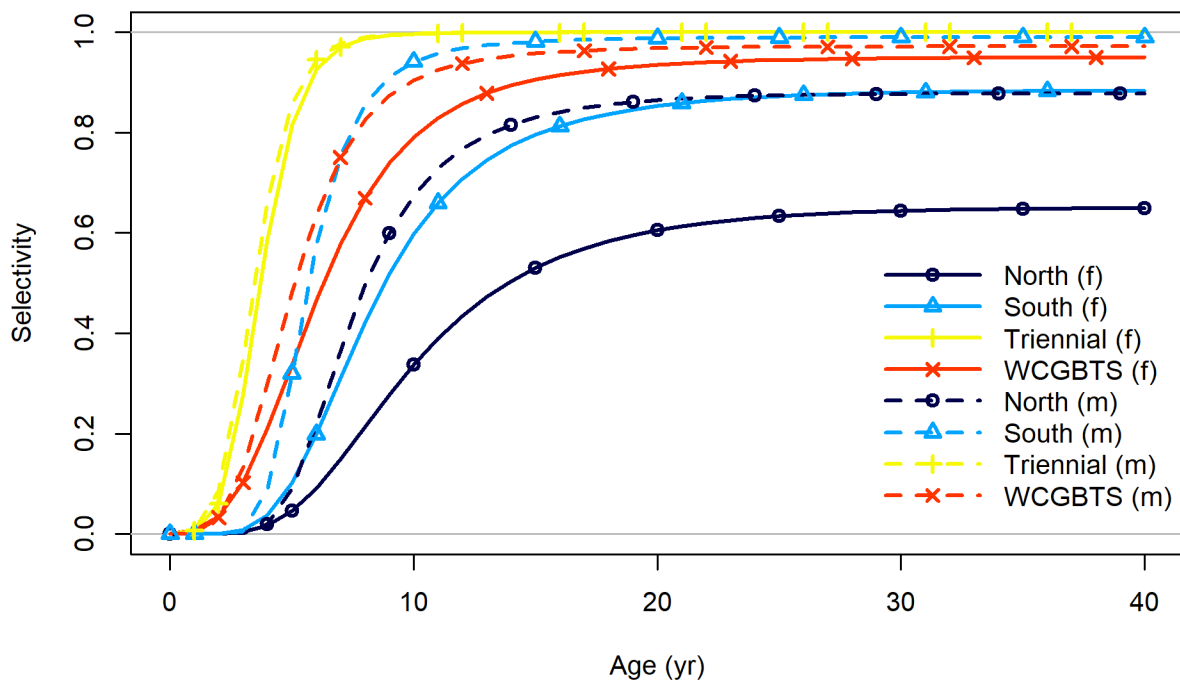
Figure 20: Maturity ogive showing fit to observed fraction mature within each length bin.
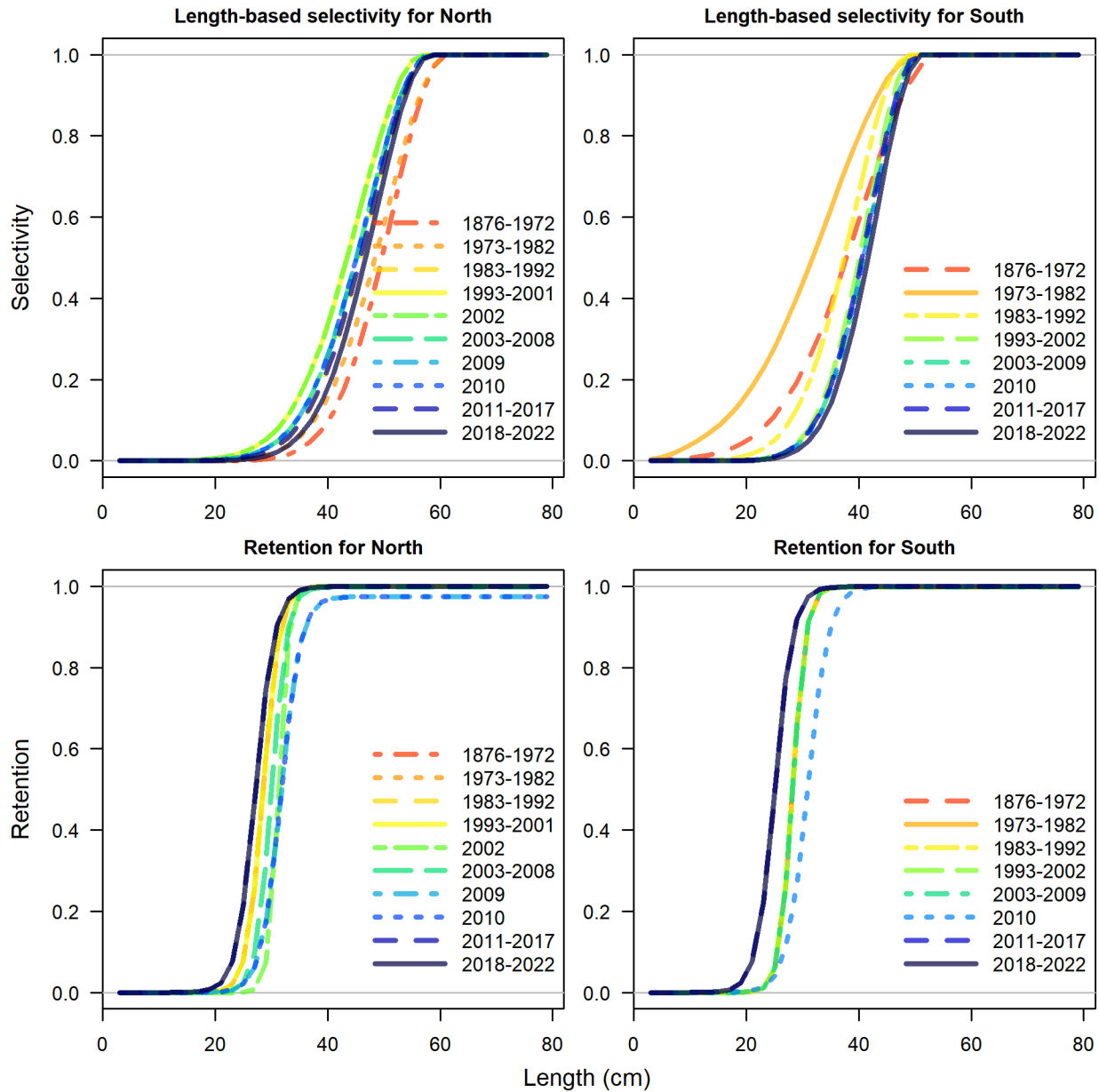
Figure 21: Fecundity relationship relative to body weight at length for females. The distribution of estimated numbers of mature females in unfished equilibrium and at the start of 2023 is shown for comparison. The population size bins extend to 78 cm, but the number of individuals beyond 70cm is negligible.
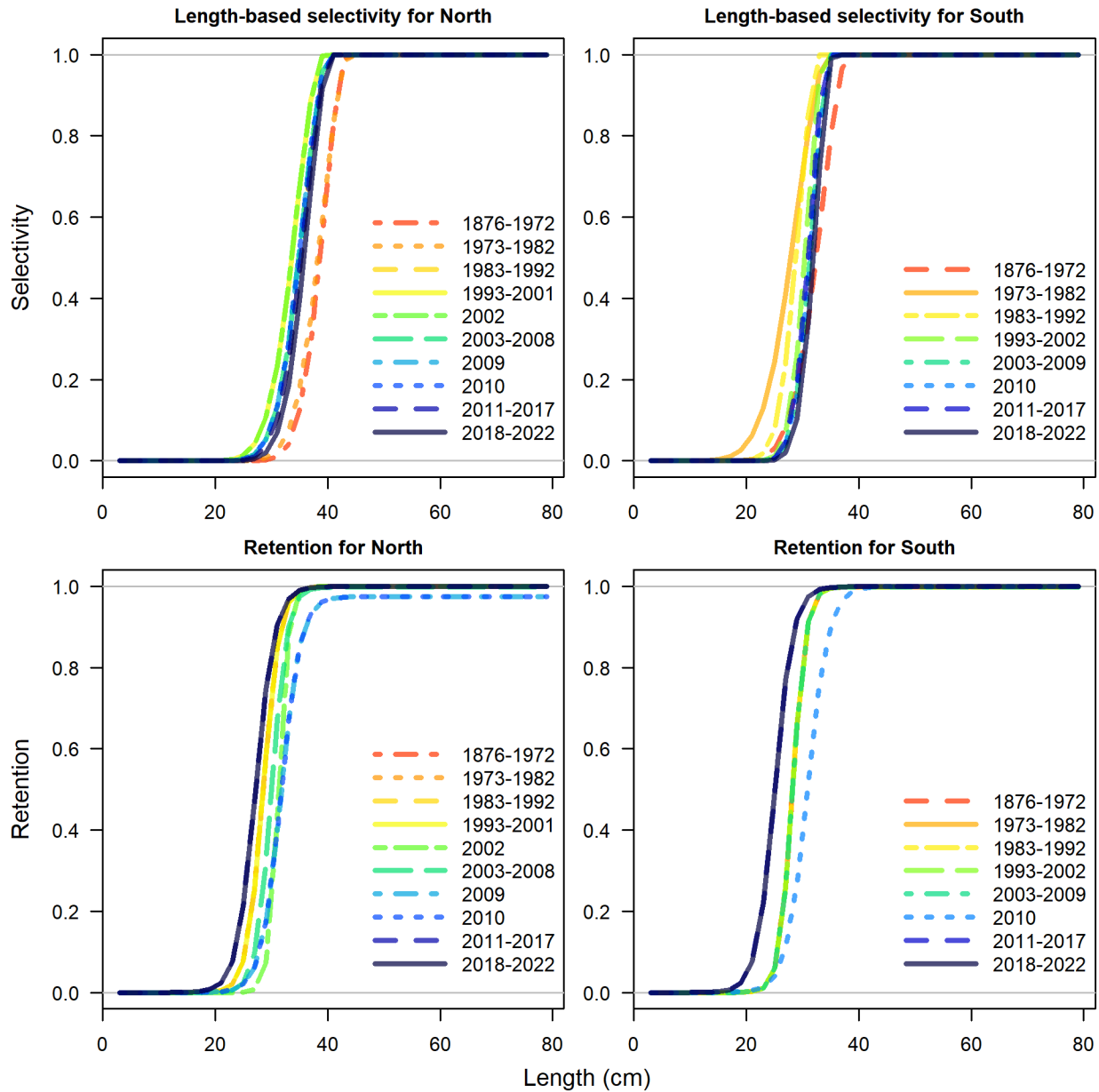
Figure 22: Ending-year selectivity at length for multiple fleets. Solid lines are female selectivity, dashed are male.
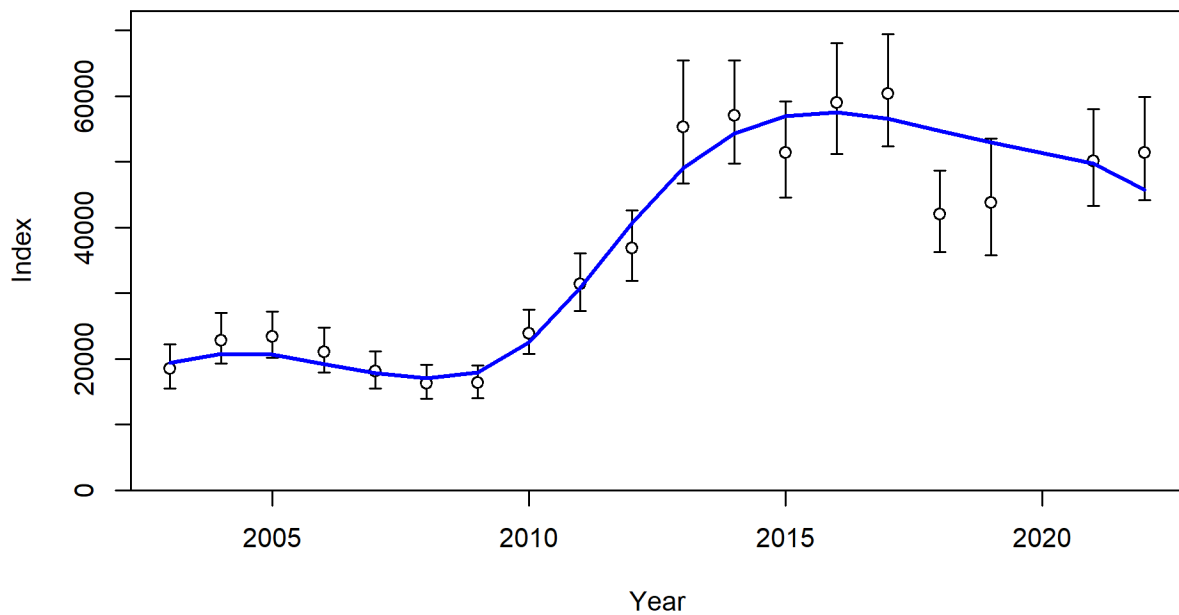
Figure 23: Ending-year selectivity at age derived from selectivity at length (solid female, dashed male).
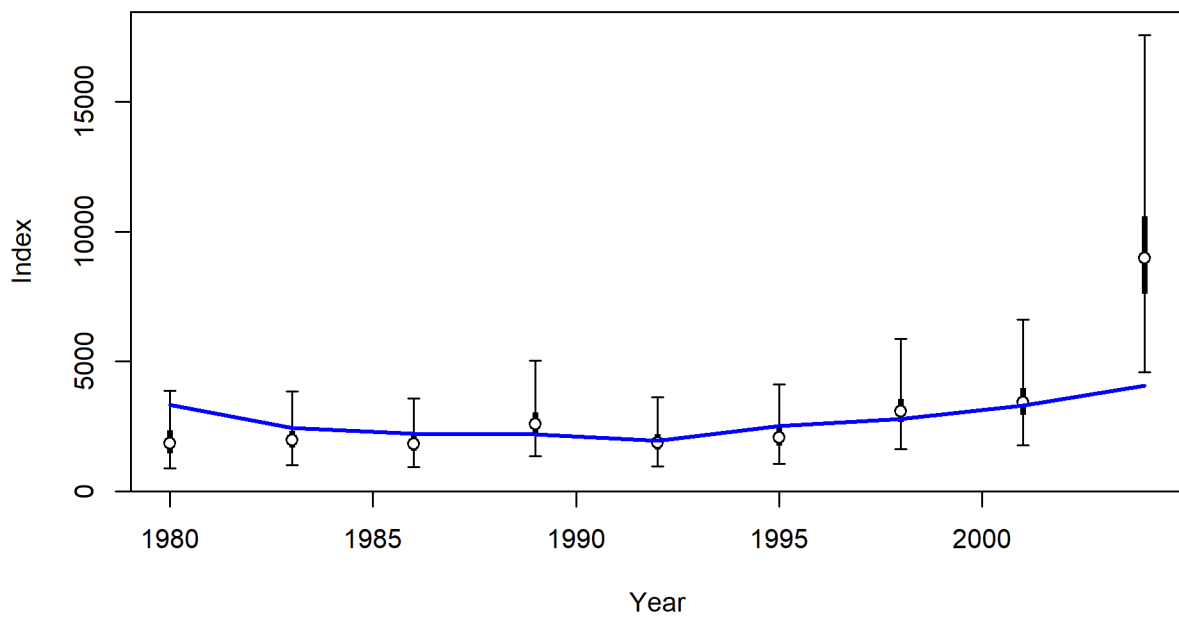
Figure 24: Time-varying female selectivity (top) and retention (bottom) for the fishing fleets. Retention is the same for females and males. Note: the legend shows the time periods in which there are blocks on either retention or discards even if they don't apply in each case.
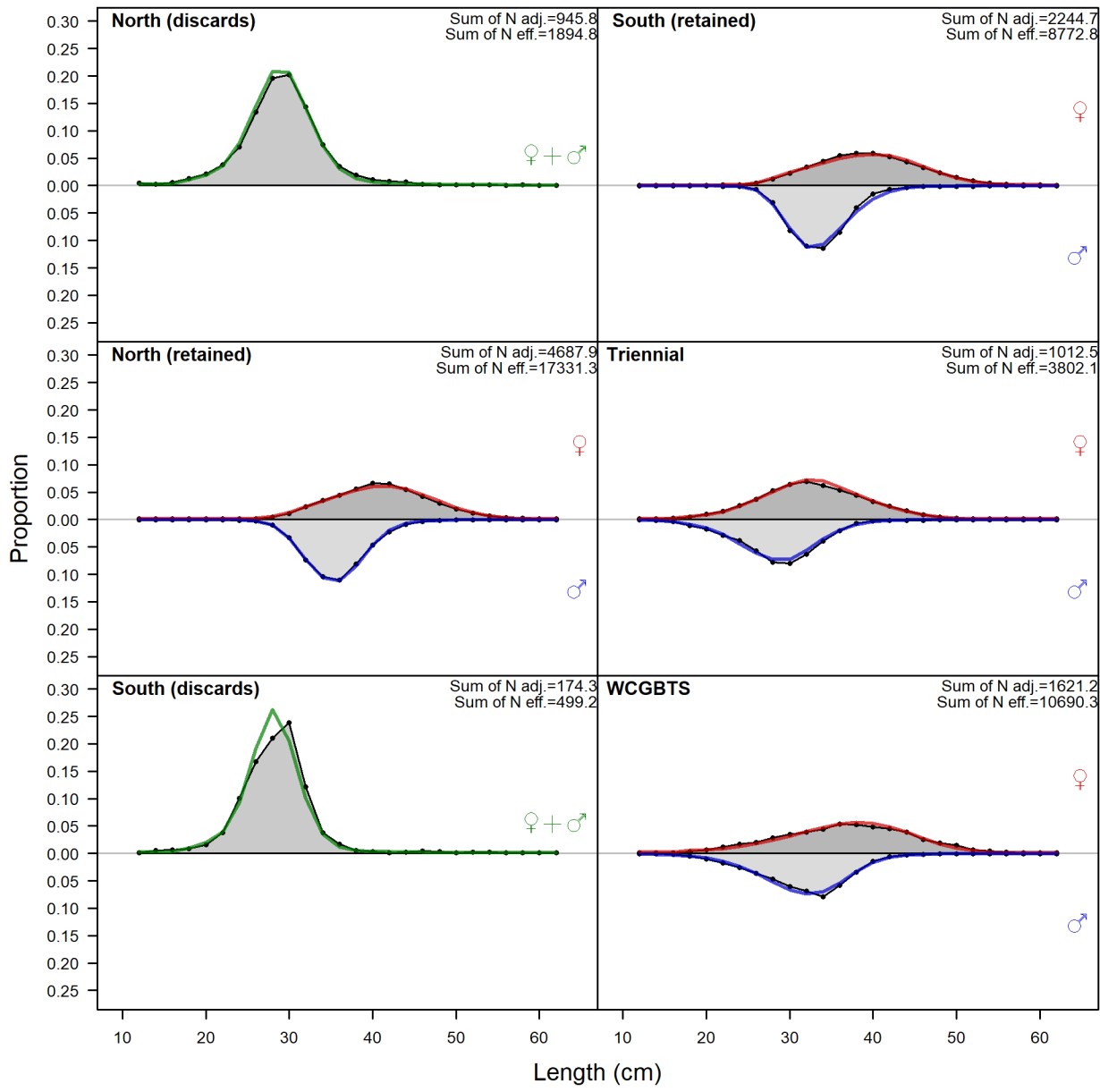
Figure 25: Time-varying male selectivity (top) and retention (bottom) for the fishing fleets. Retention is the same for females and males. Note: the legend shows the time periods in which there are blocks on either retention or discards even if they don't apply in each case.
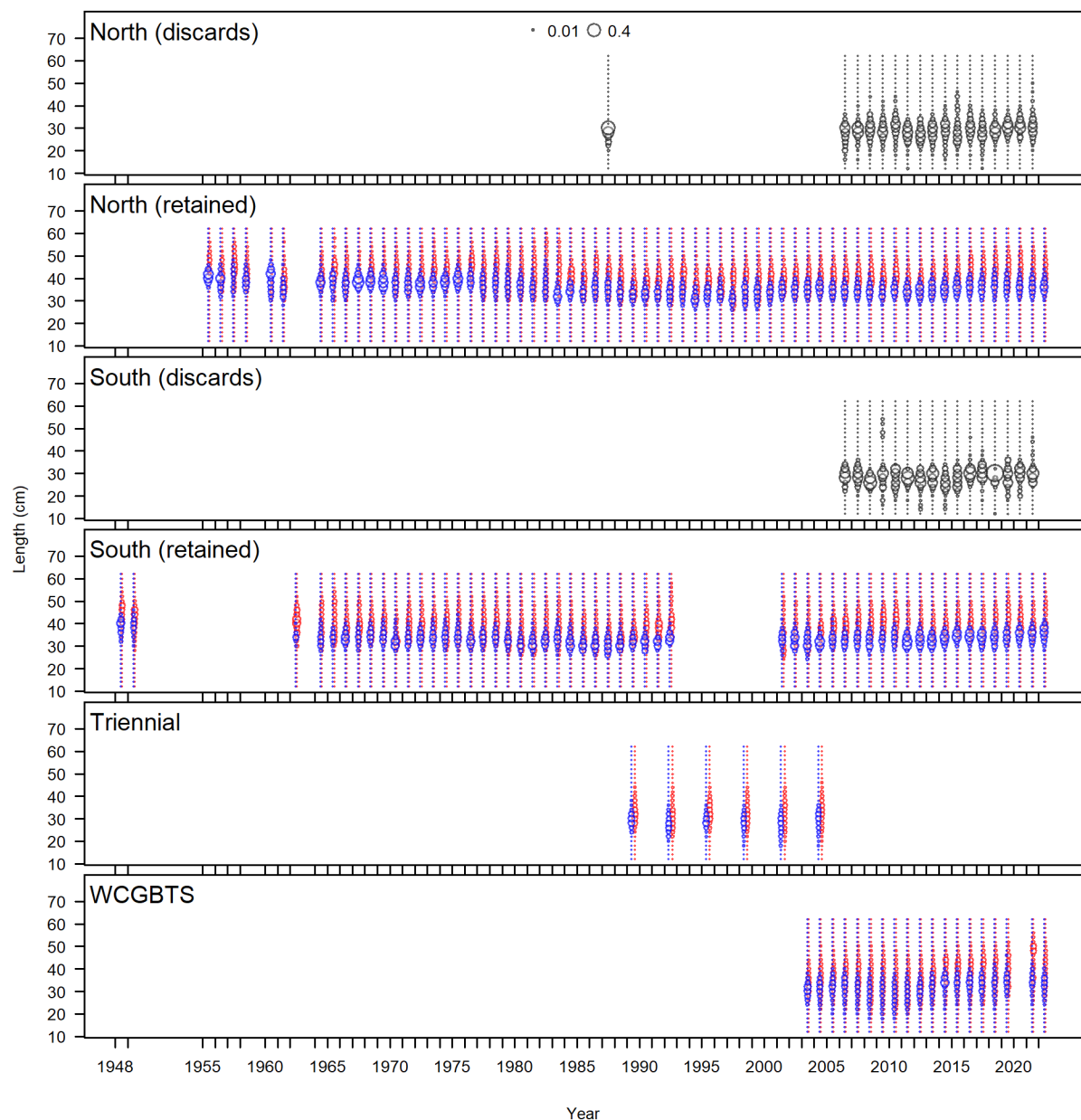
Figure 26: Fit to index data for WCGBTS. Lines indicate 95% uncertainty interval around index values based on the model assumption of lognormal error.
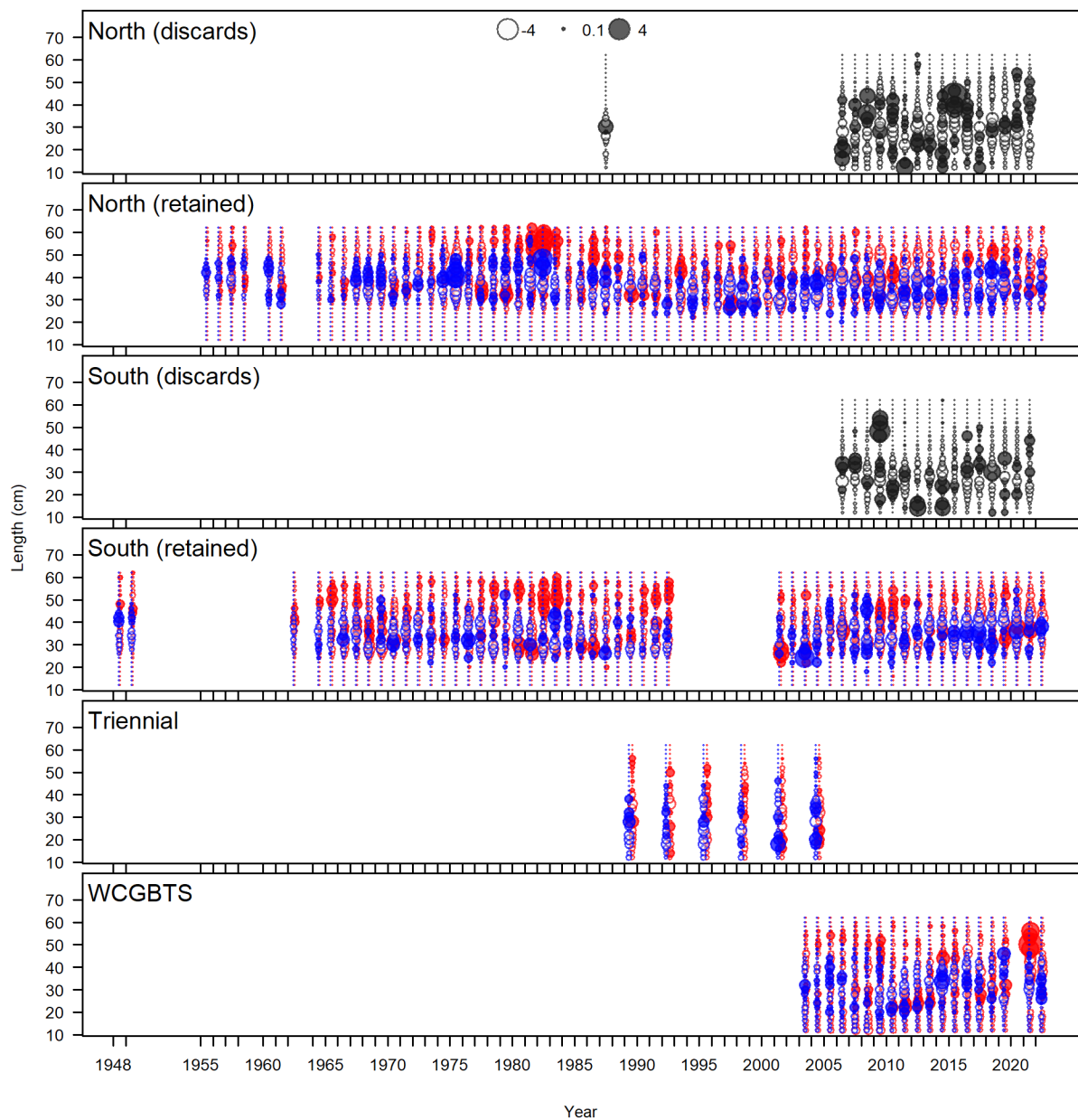
Figure 27: Fit to index data for the Triennial survey. Lines indicate 95% uncertainty interval around index values based on the model assumption of lognormal error with and without estimated additional uncertainty parameter.
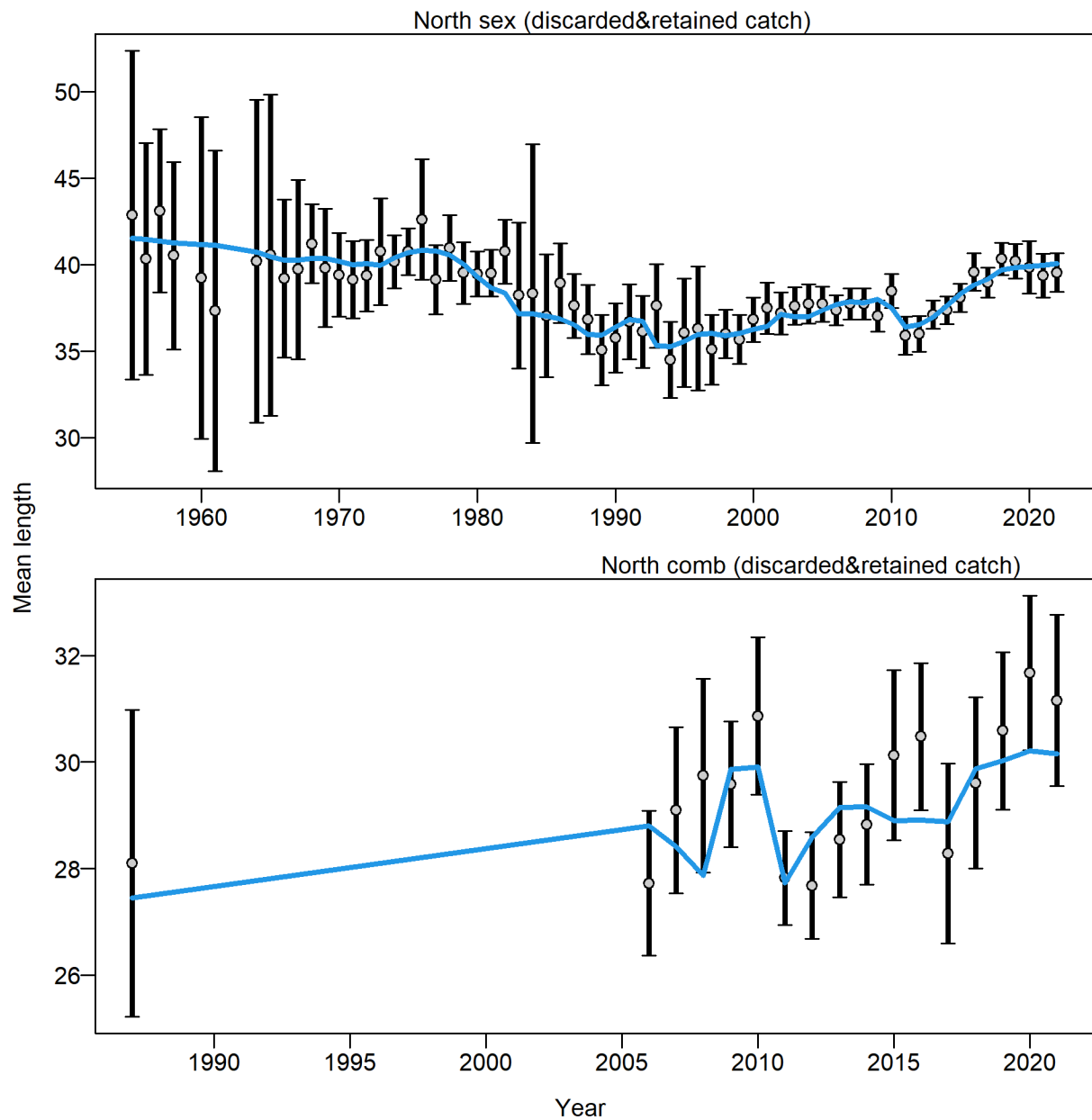
Figure 28: Length composition aggregated across years by fleet with the model estimated fit to the data by sex (red female and blue male).
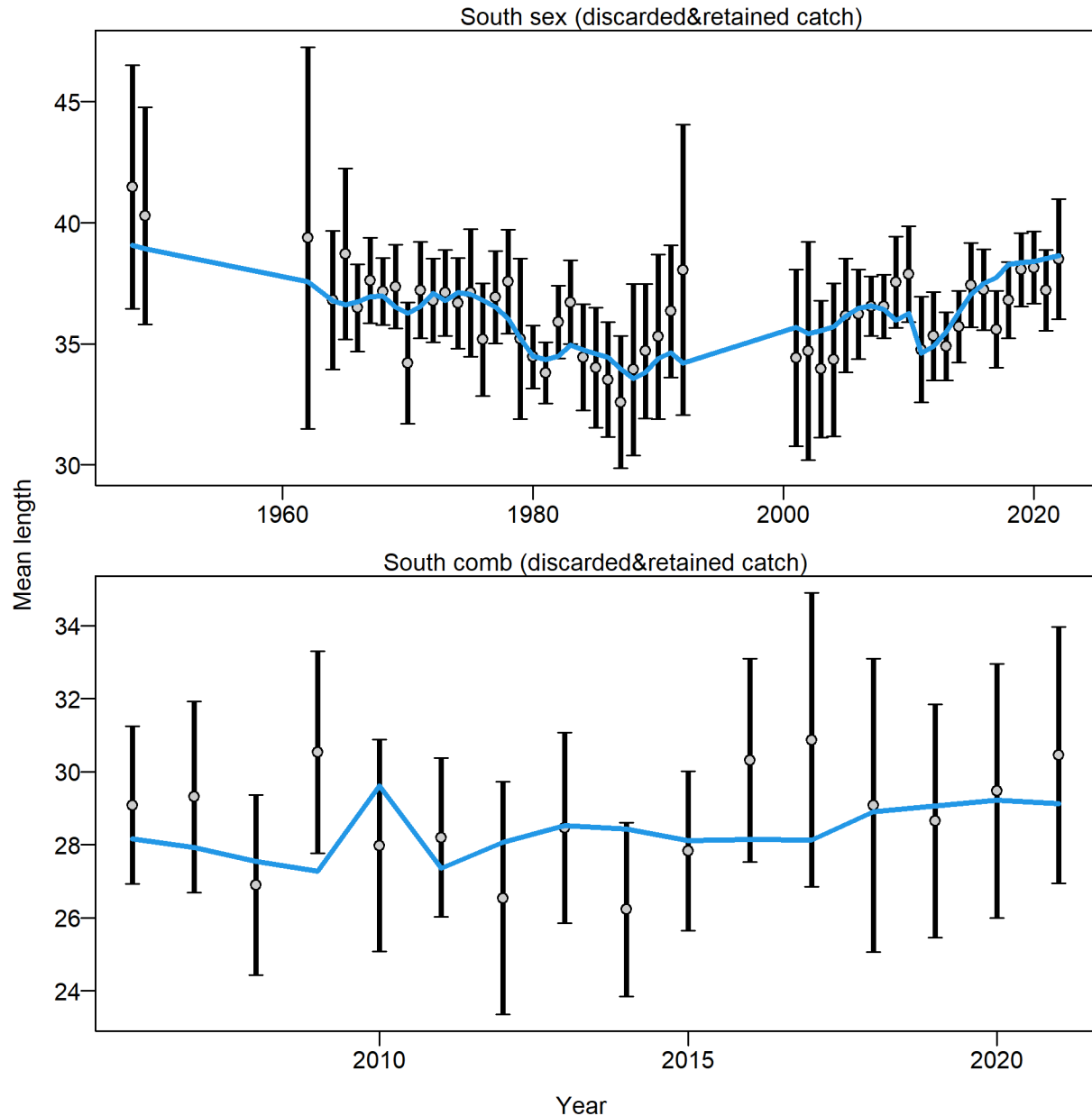
Figure 29: Length composition data for all fleets (red female, blue male, grey unsexed).
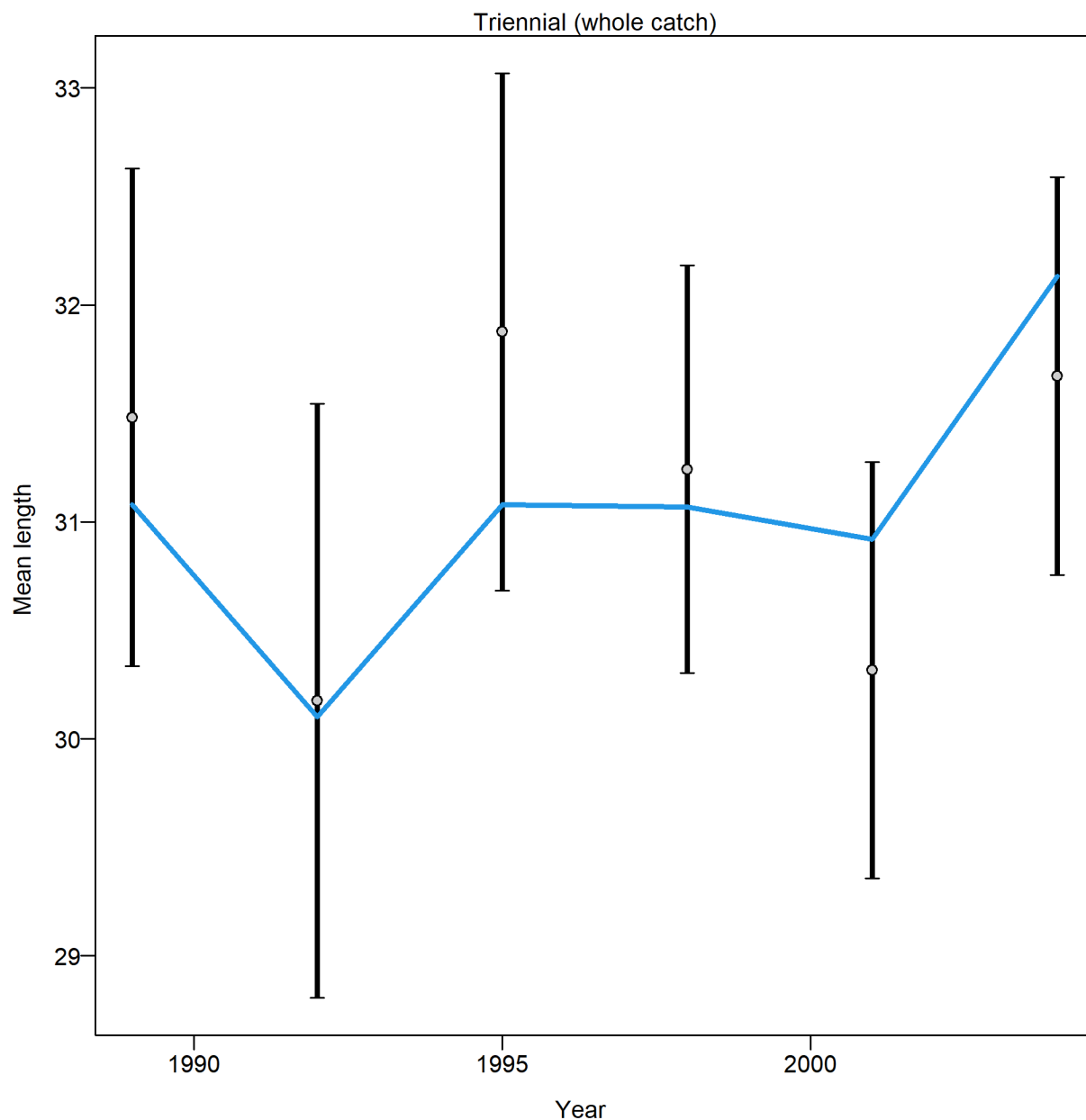
Figure 30: Pearson residuals for fit to length composition data for all fleets (red female, blue male, grey unsexed). Closed bubbles are positive residuals (observed > expected) and open bubbles are negative residuals (observed < expected).
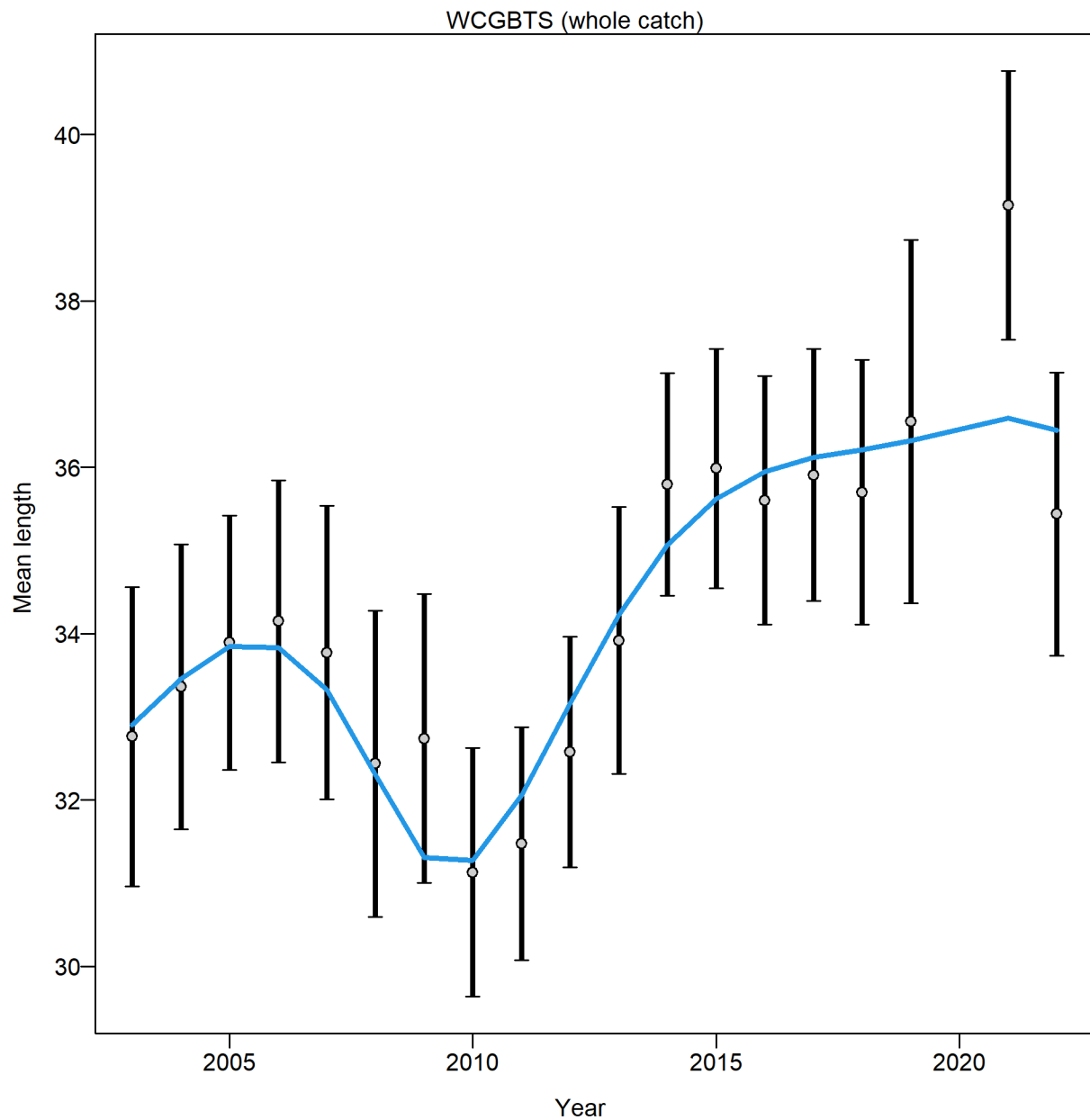
Figure 31: Mean lengths calculated from the observed (black) and expected (blue) length compositions from the North fleet. Retained catch is shown in the top and discards on the bottom (NOTE: the figure title indicates that discards and retained are shown in both plots, but this is incorrect.). 95% intervals for the observations are based on the adjusted input sample sizes.
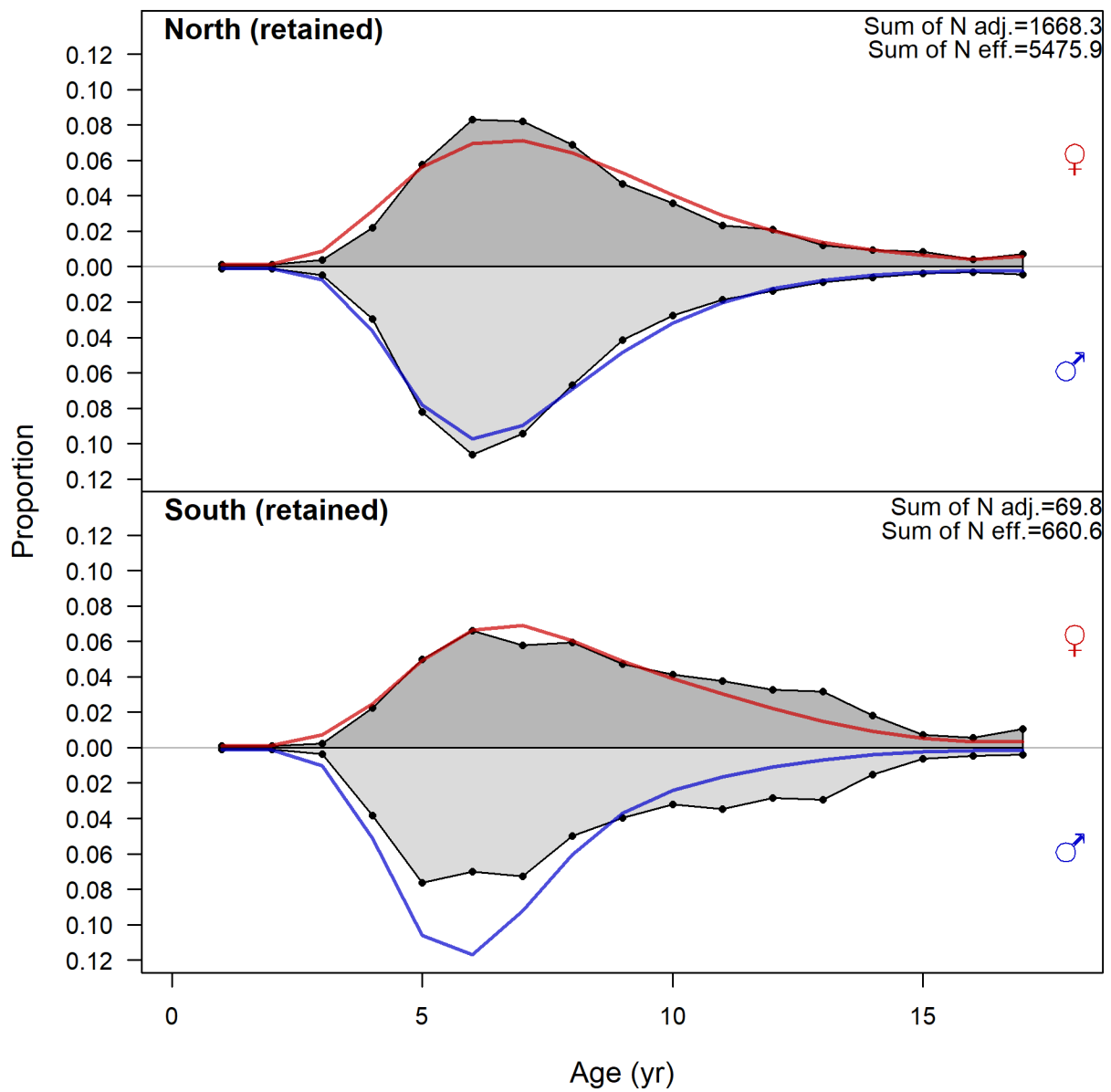
Figure 32: Mean lengths calculated from the observed (black) and expected (blue) length compositions from the South fleet. Retained catch is shown in the top and discards on the bottom. (NOTE: the figure title indicates that discards and retained are shown in both plots, but this is incorrect.) 95% intervals for the observations are based on the adjusted input sample sizes.
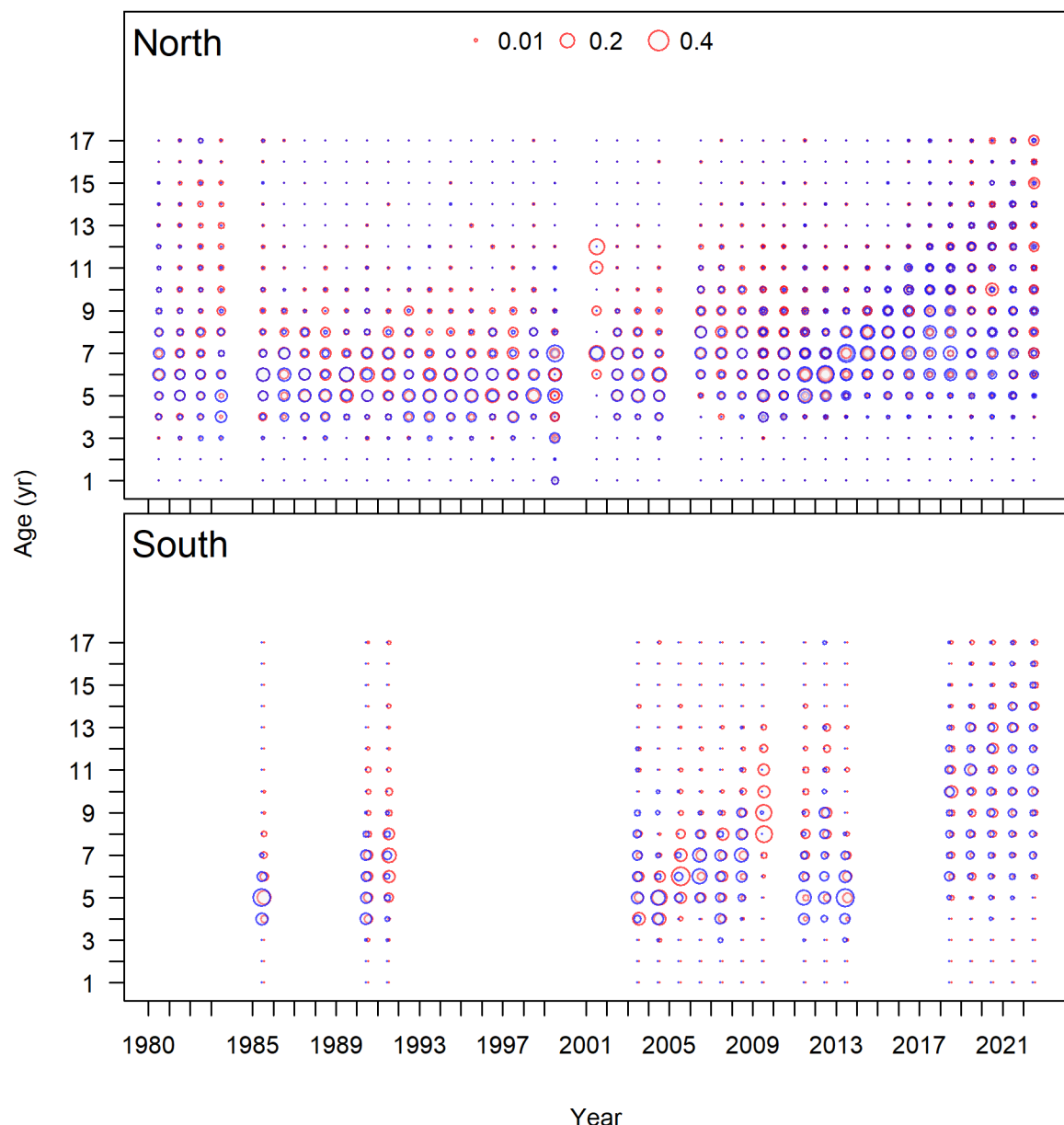
Figure 33: Mean lengths calculated from the observed (black) and expected (blue) length compositions from the Triennial Survey. 95% intervals for the observations are based on the adjusted input sample sizes.
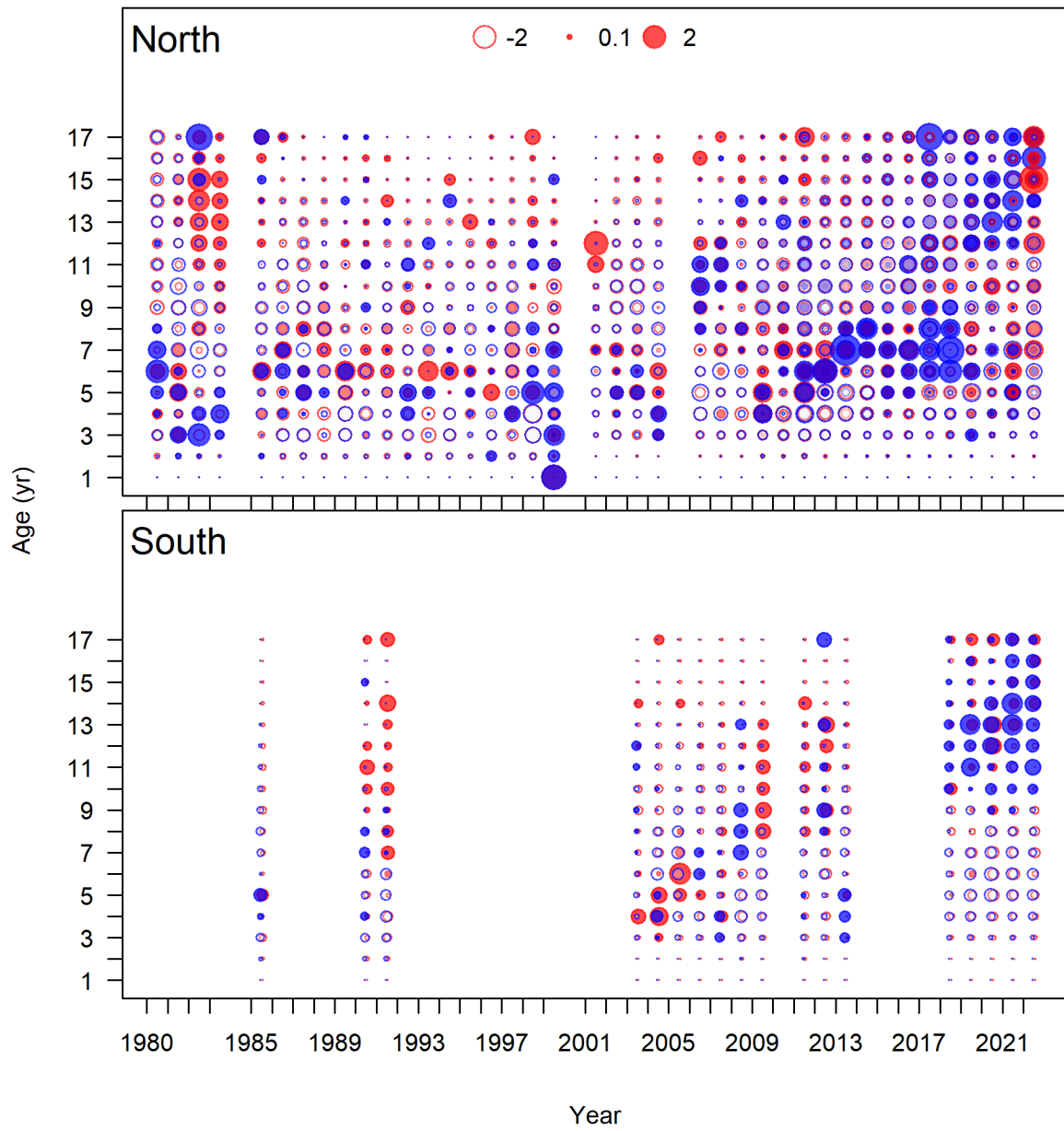
Figure 34: Mean lengths calculated from the observed (black) and expected (blue) length compositions from the WCGBTS. 95% intervals for the observations are based on the adjusted input sample sizes.
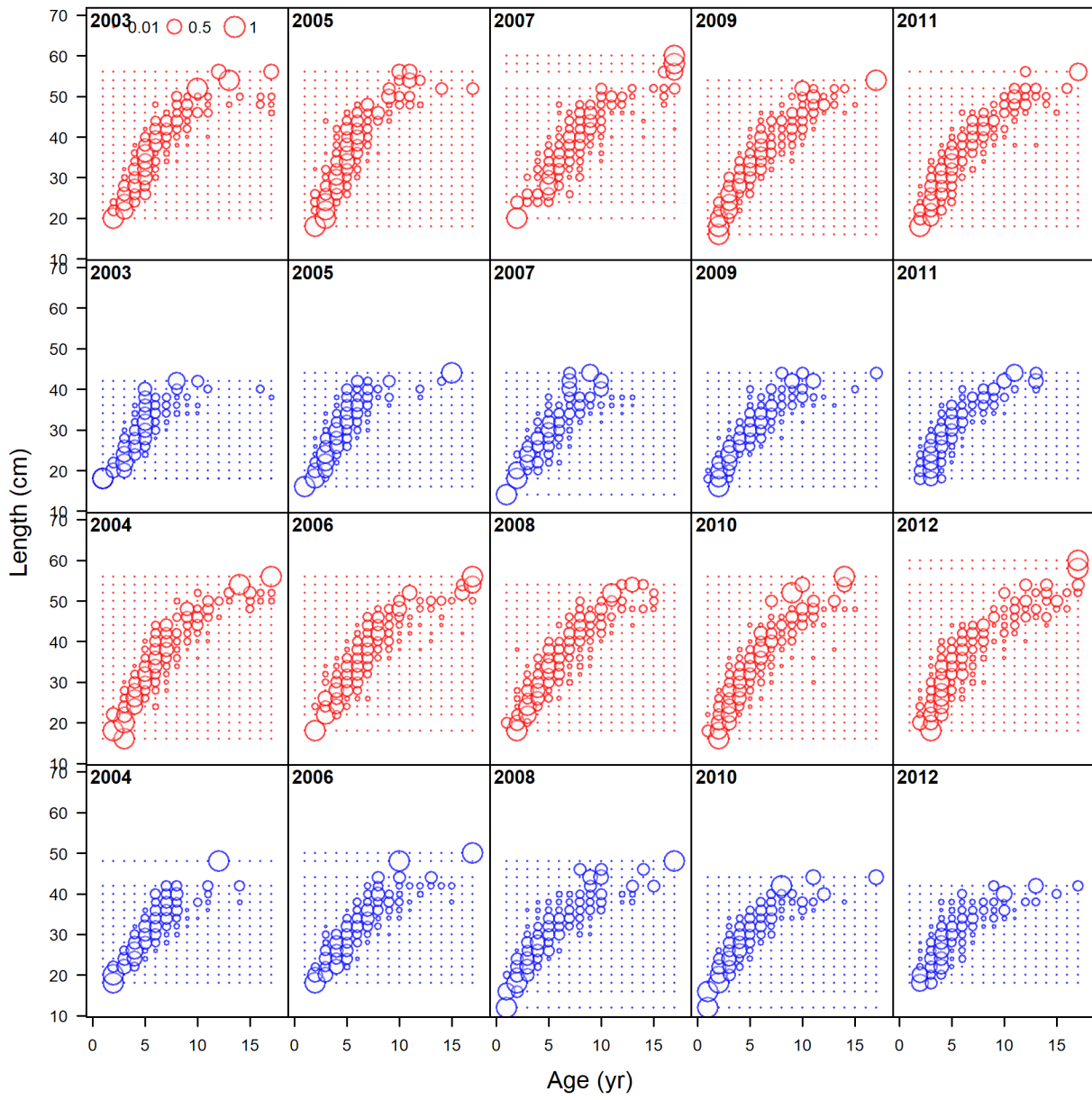
Figure 35: Age composition data aggregated across time by fleet and sex (red female and blue male).
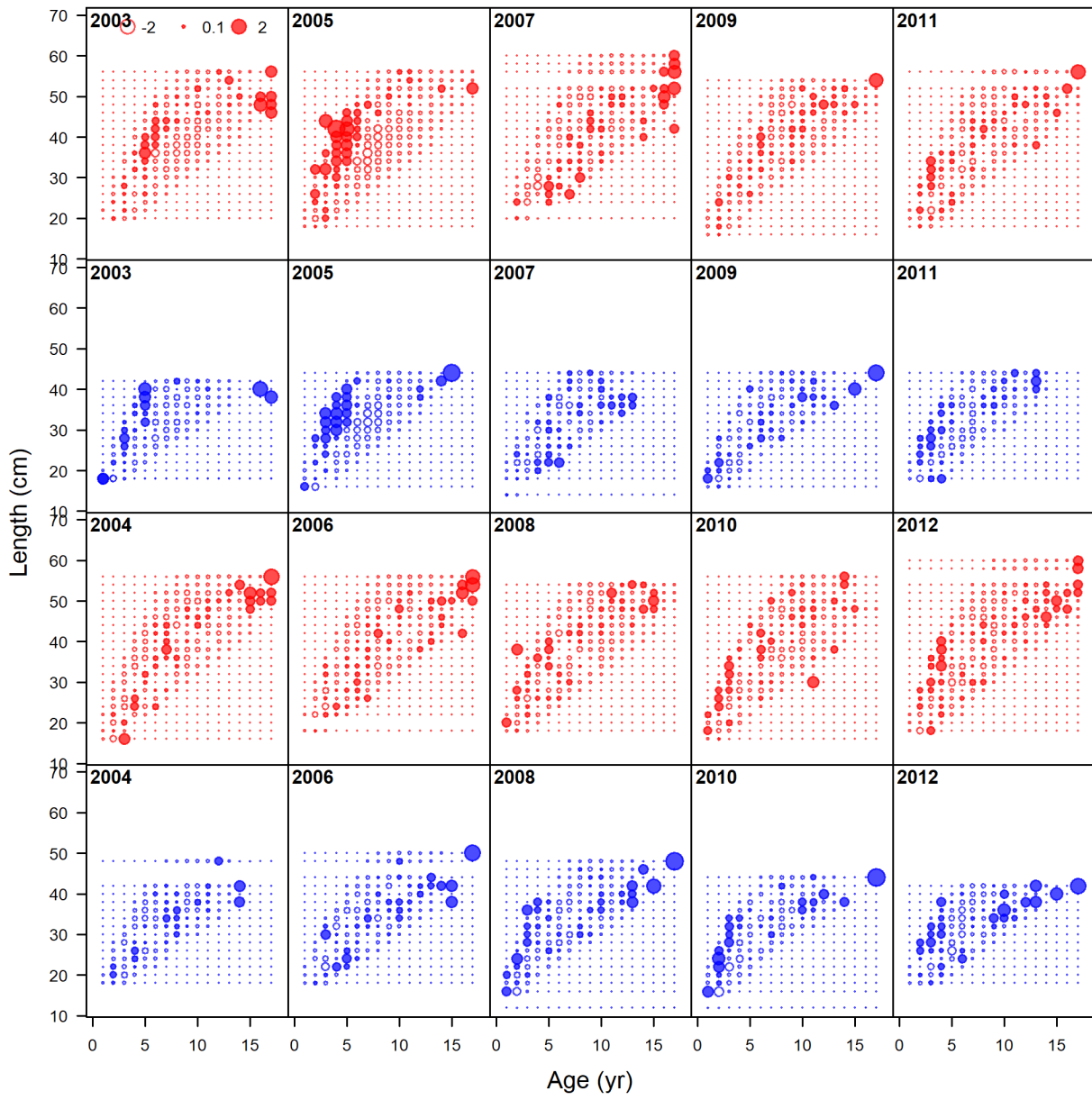
Figure 36: Age composition data for all fleets (red female, blue male).
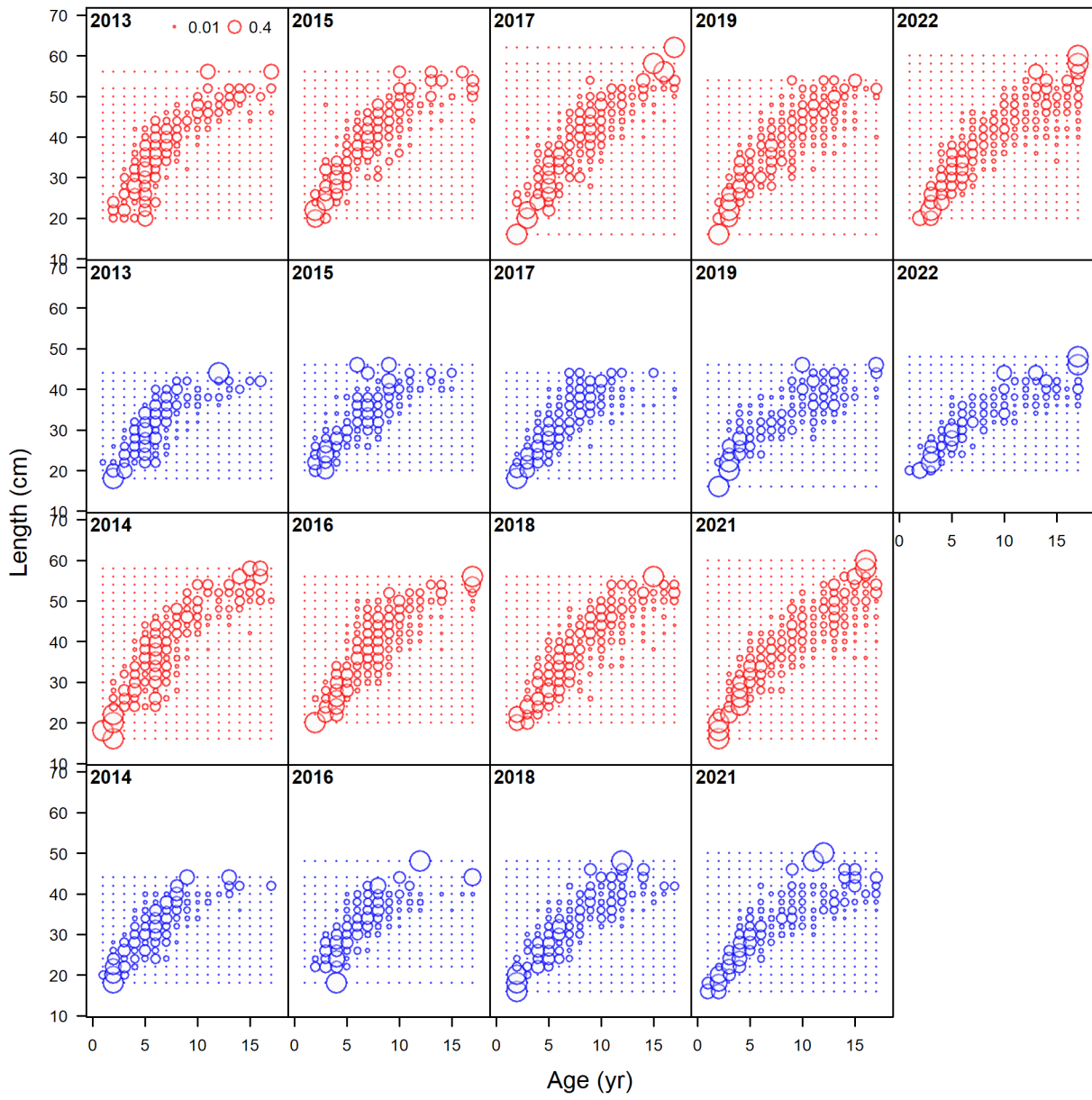
Figure 37: Pearson residuals for fit to age composition data for all fleets (red female, blue male). Closed bubbles are positive residuals (observed > expected) and open bubbles are negative residuals (observed < expected).
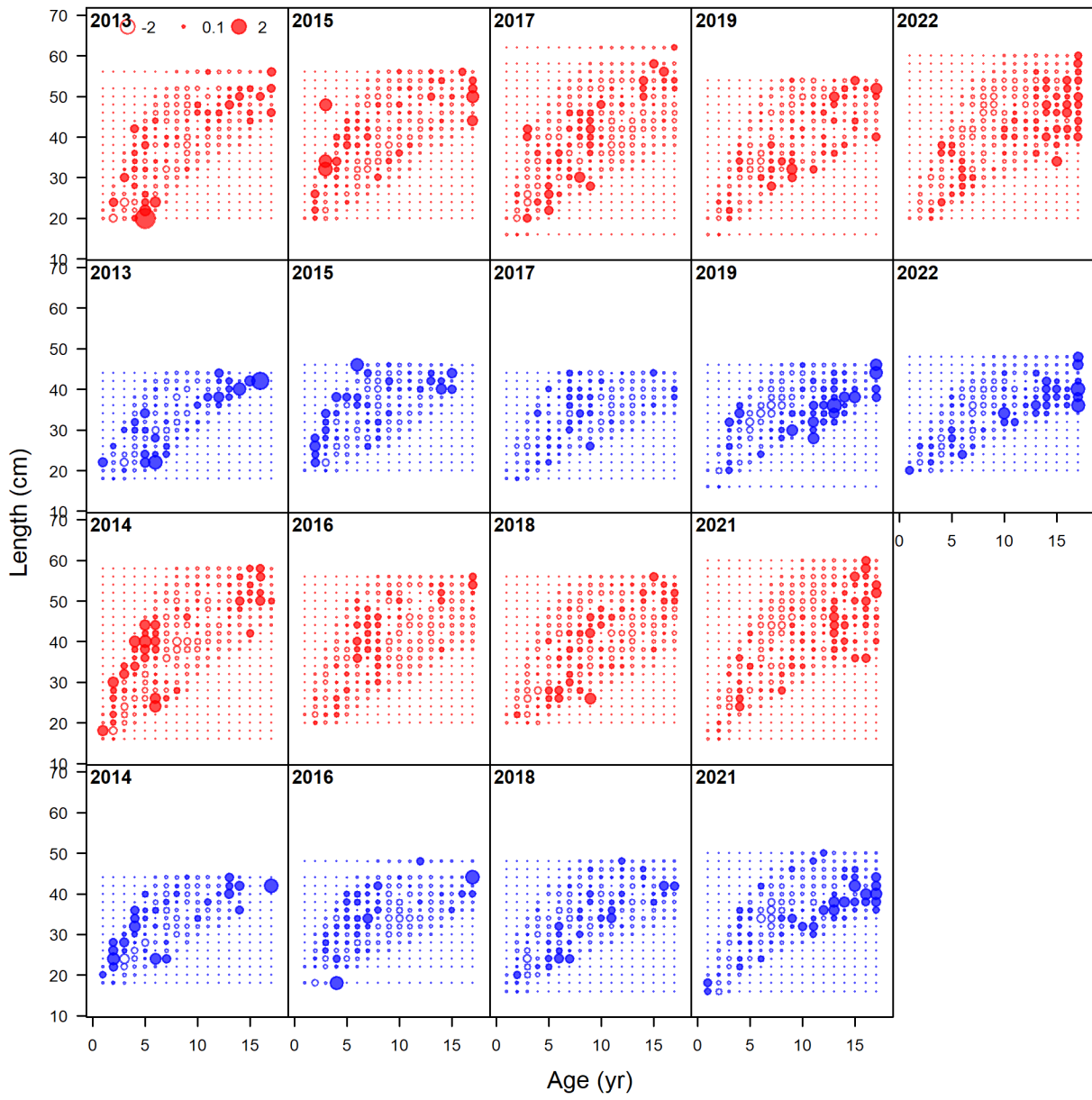
Figure 38: Conditional age-at-length data from WCGBTS (data plot 1 of 2, interleaved with the residual plots to facilitate flipping back and forth).

Figure 39: Pearson residuals for conditional age-at-length data from WCGBTS (residual plot 1 of 2, interleaved with the data plots to facilitate flipping back and forth).

113

Figure 40: Conditional age-at-length data from WCGBTS (data plot 2 of 2, interleaved with the residual plots to facilitate flipping back and forth).

Figure 41: Pearson residuals for conditional age-at-length data from WCGBTS (residual plot 2 of 2, interleaved with the data plots to facilitate flipping back and forth).
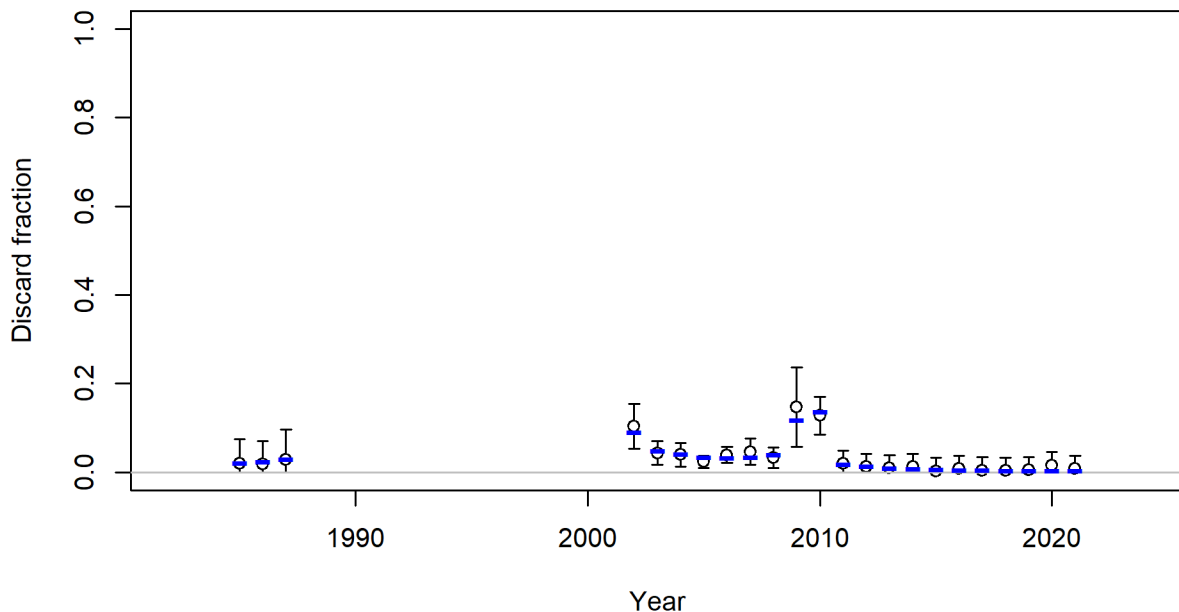
Figure 42: Discard fraction for the North fishery with 95% intervals (black) with fit of expected value (blue).
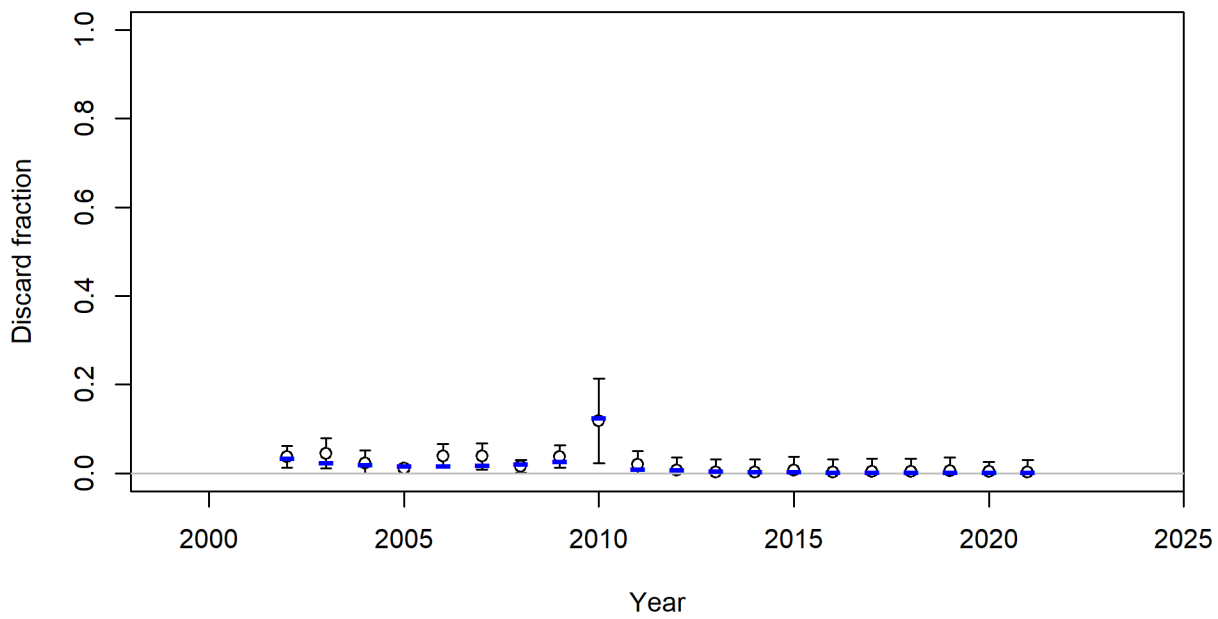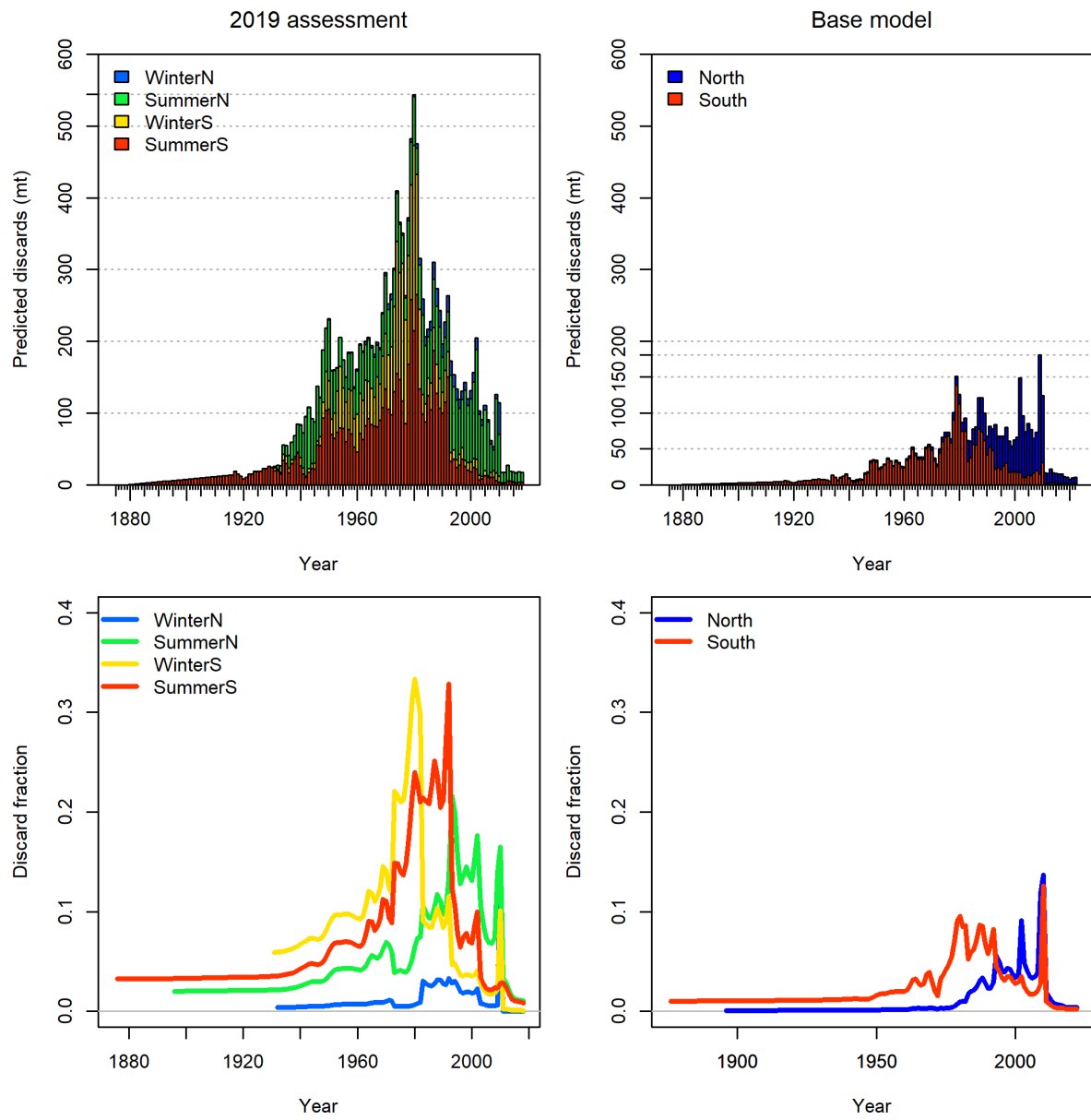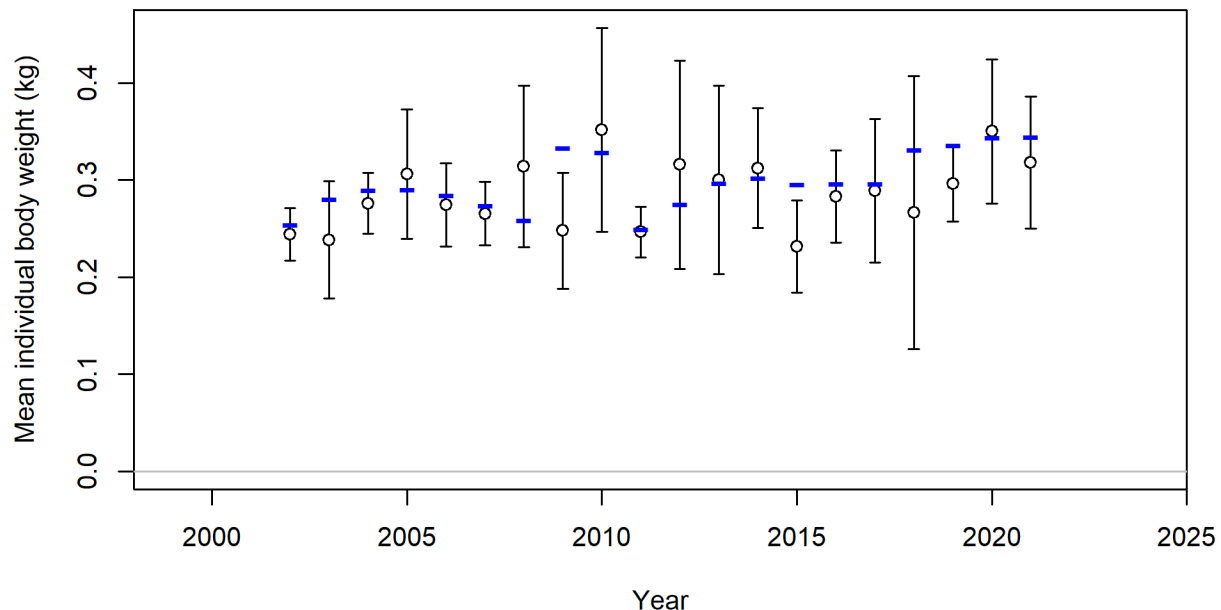
Figure 43: Discard fraction for the South fishery with 95% intervals (black) with fit of expected value (blue).

116
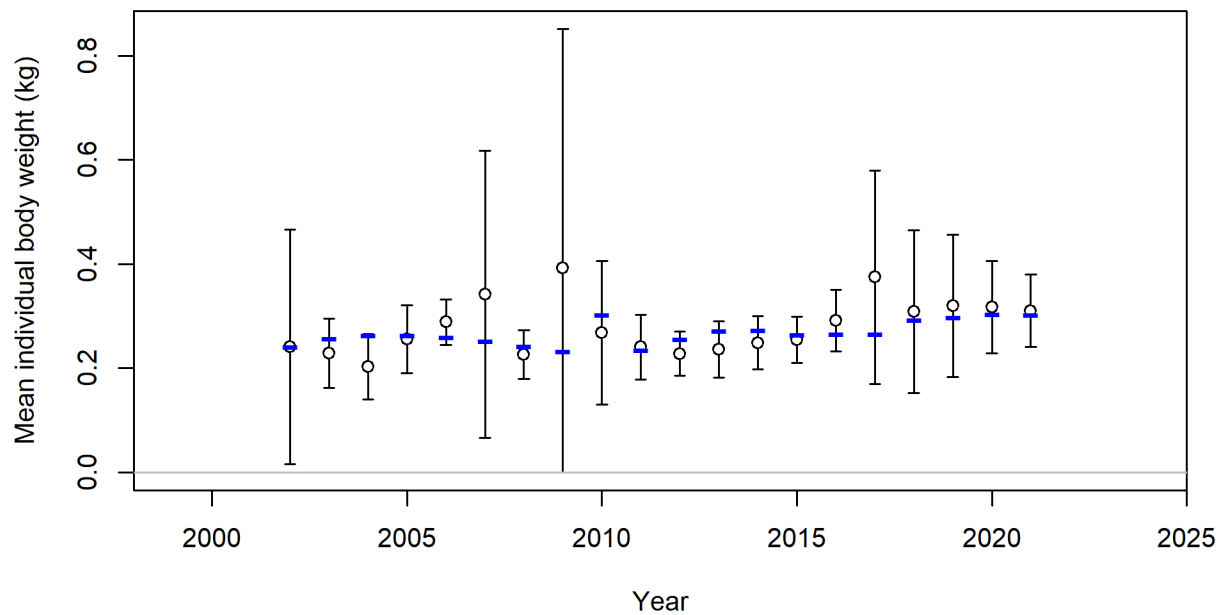
Figure 44: Estimated total discards (top) and discard fractions (bottom) for each fleet in the 2019 assessment (left) and base model (right).
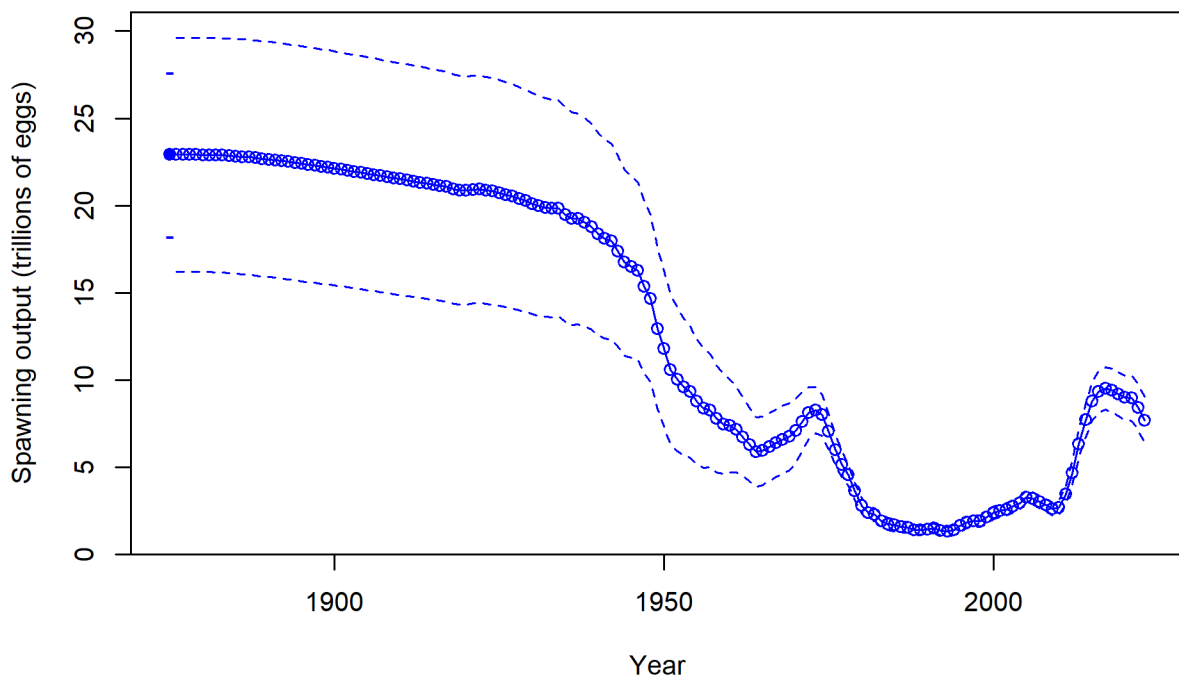
Figure 45: Mean individual body weight of the discards for the North fishery with 95% intervals (black) with fit of expected value (blue).
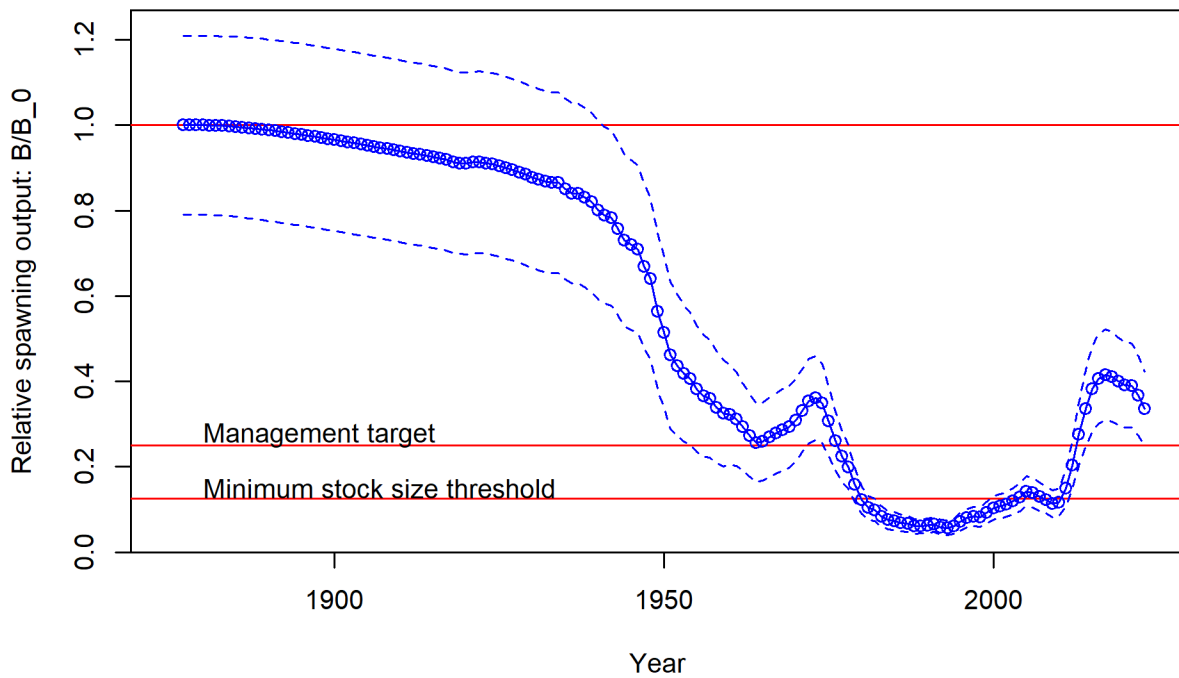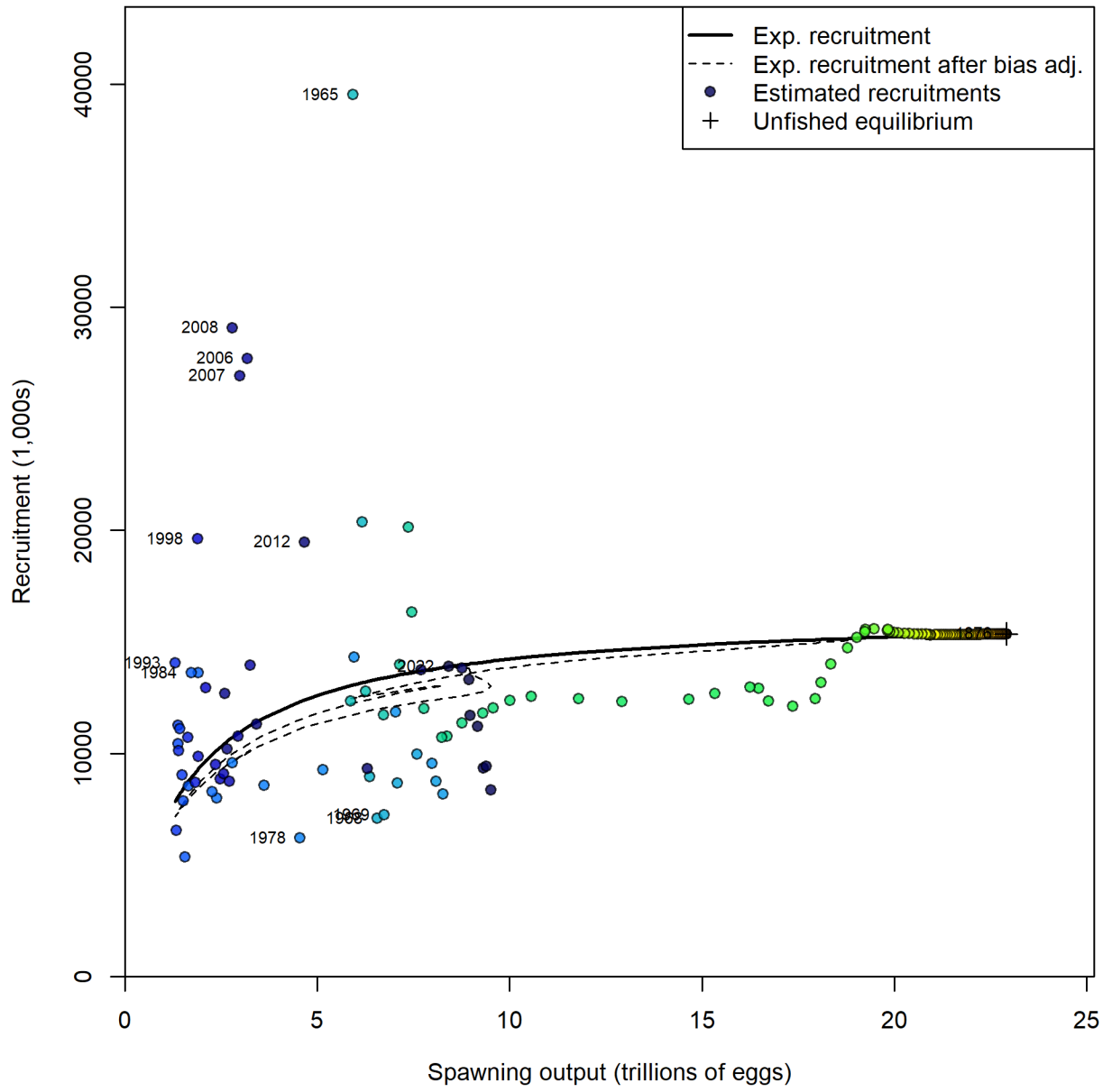
Figure 46: Mean individual body weight of the discards for the South fishery with 95% intervals (black) with fit of expected value (blue).
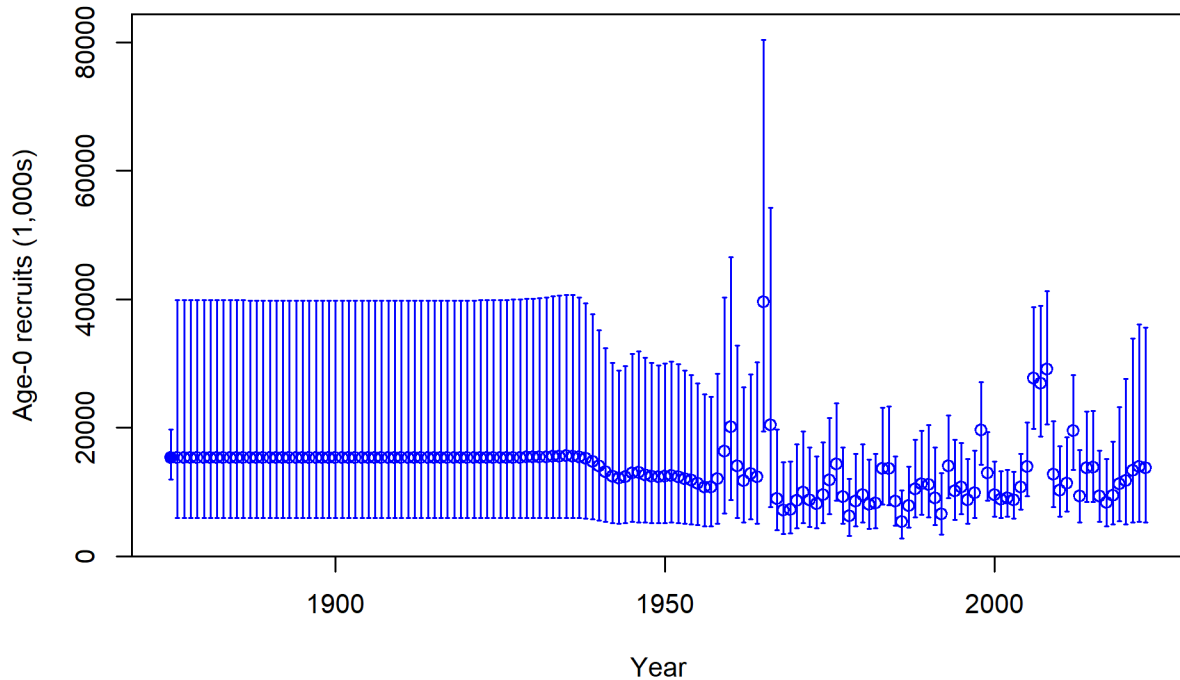
Figure 47: Estimated time series of female spawning output (in trillions of eggs) with approximate 95% asymptotic intervals.
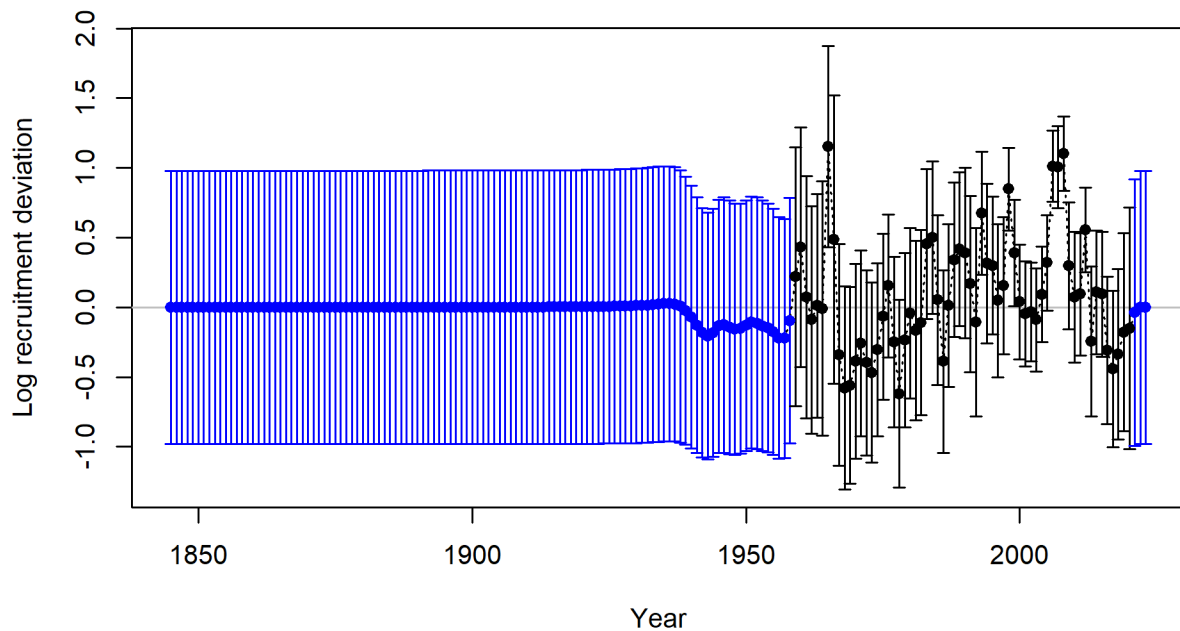
Figure 48: Estimated time series of relative spawning output with approximate 95% asymptotic intervals.
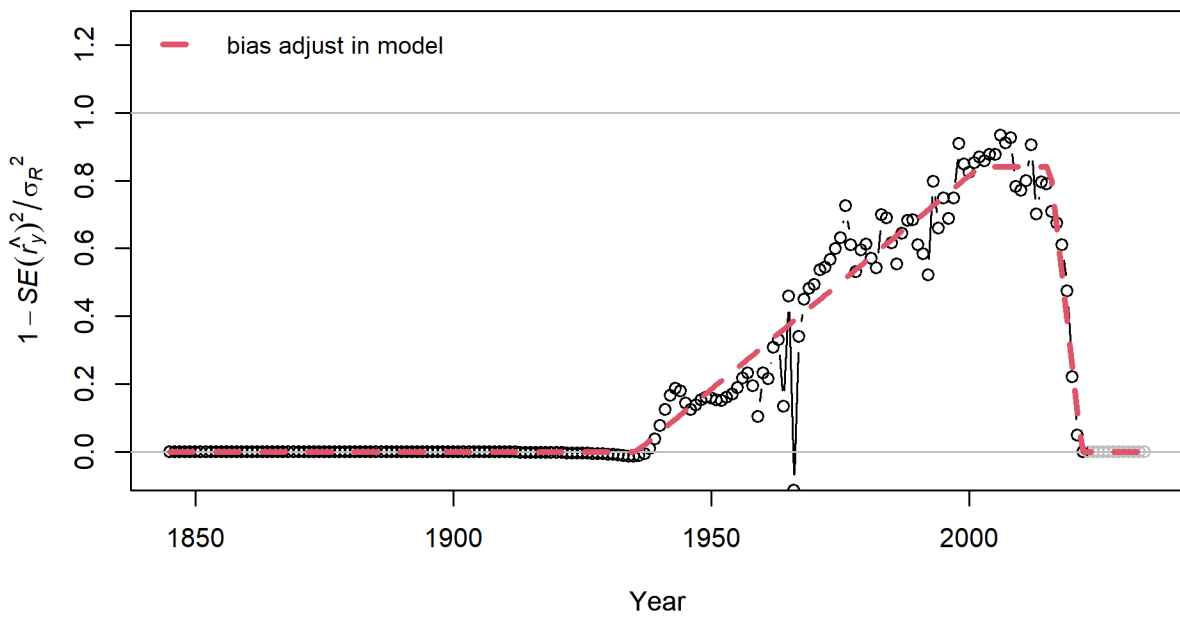
Figure 49: Stock-recruit curve. Labels indicate first, last, and years with (log) deviations > 0.5. Point colors indicate year, with warmer colors indicating earlier years and cooler colors in showing later years.
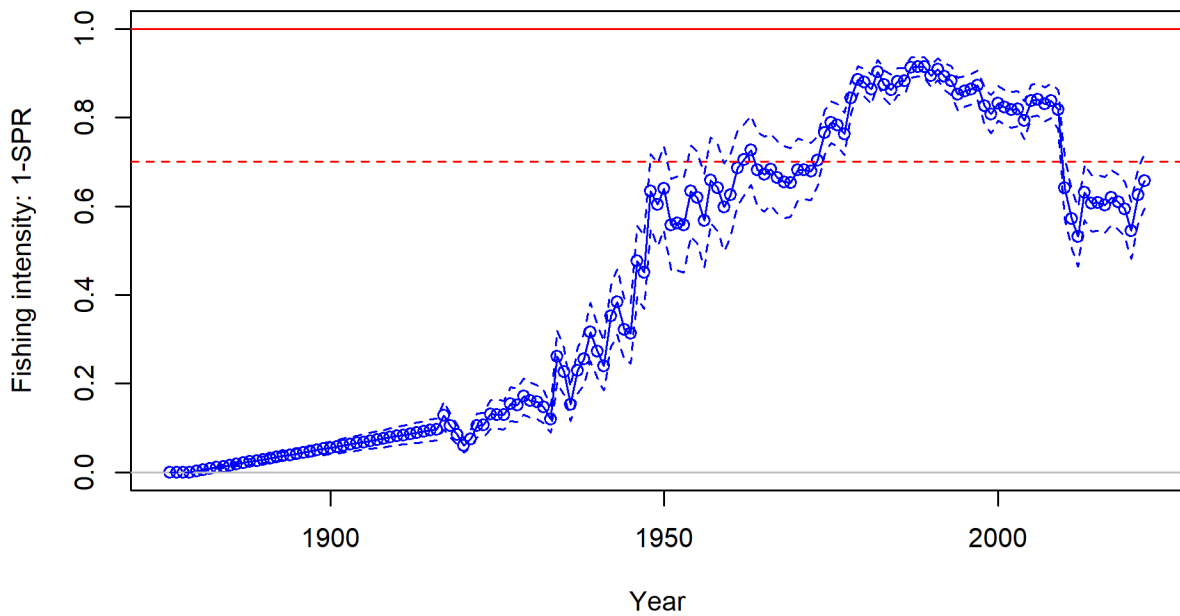
Figure 50: Estimated time series of age-0 recruits (1,000s) with approximate 95% asymptotic intervals.
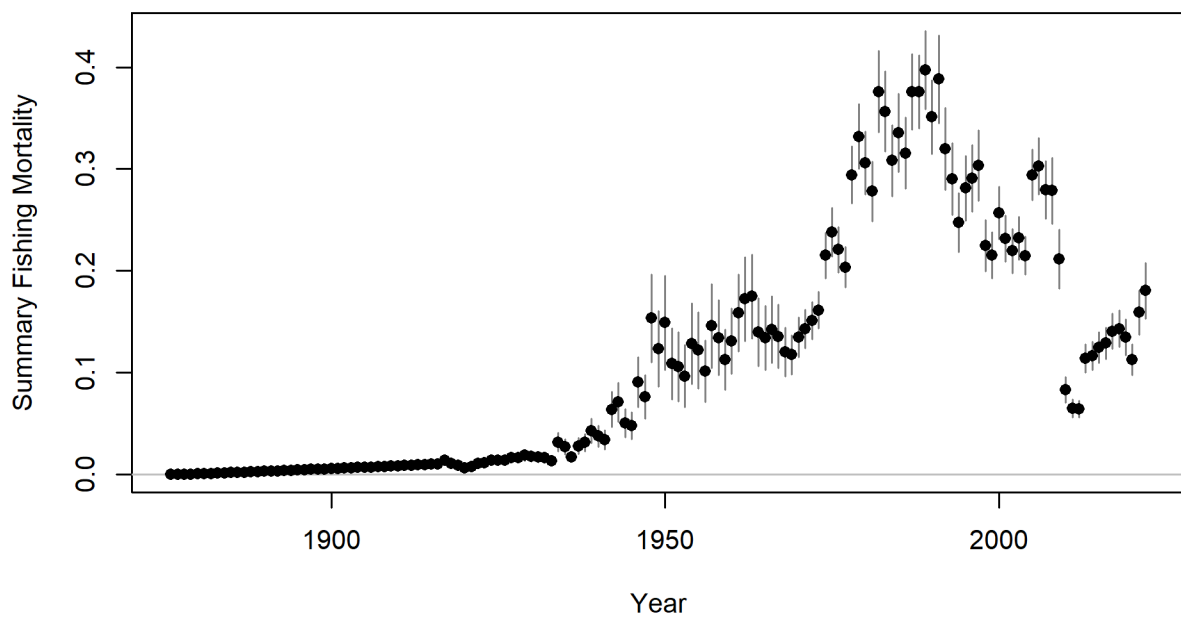
Figure 51: Estimated time series of recruitment deviations with approximate 95% asymptotic intervals. The black color indicates the 'main' recruitment period.
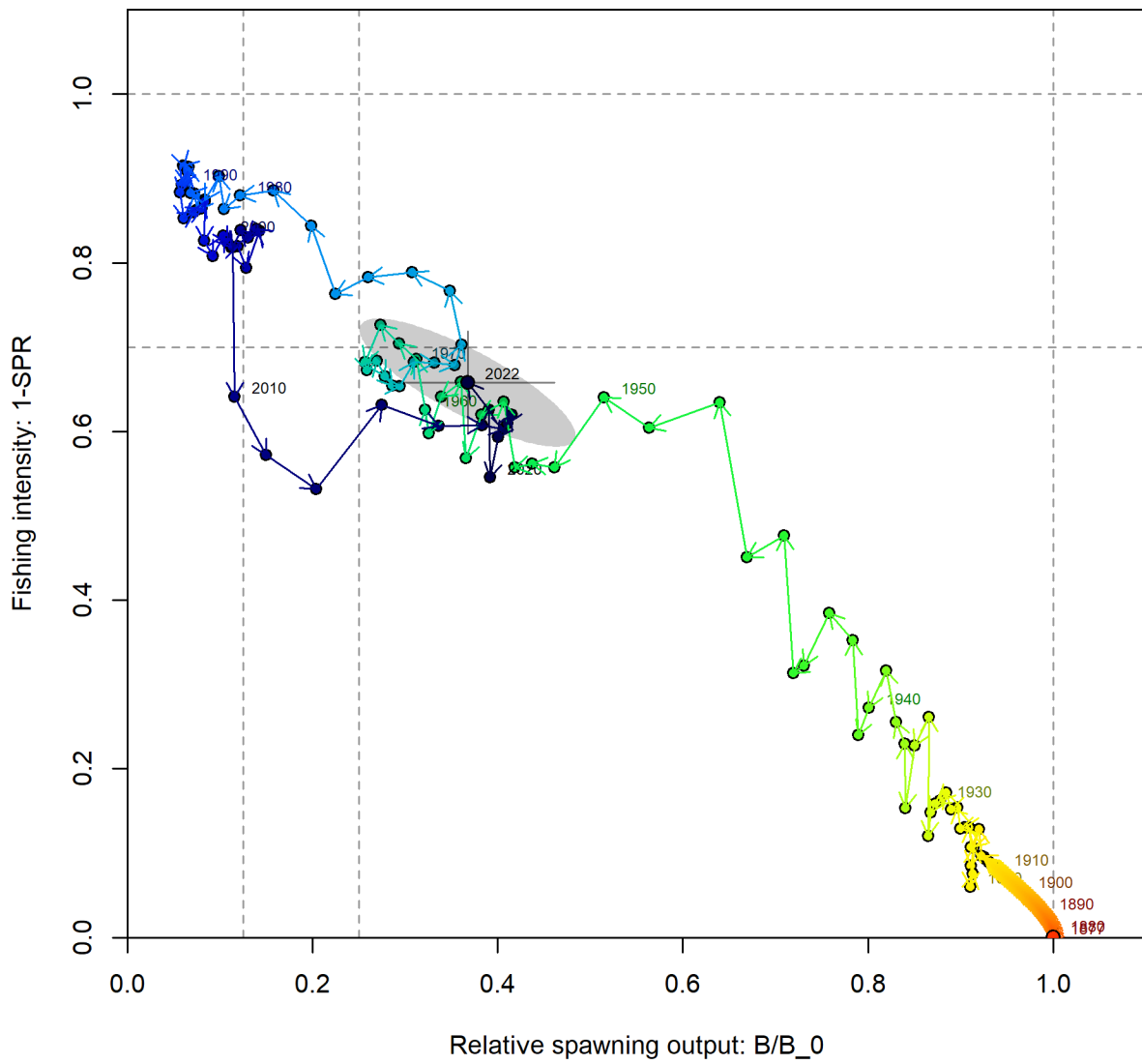
Figure 52: Bias adjustment applied to the recruitment deviations (red line). Points are transformed variances relative to $\sigma_R = 0.5$.
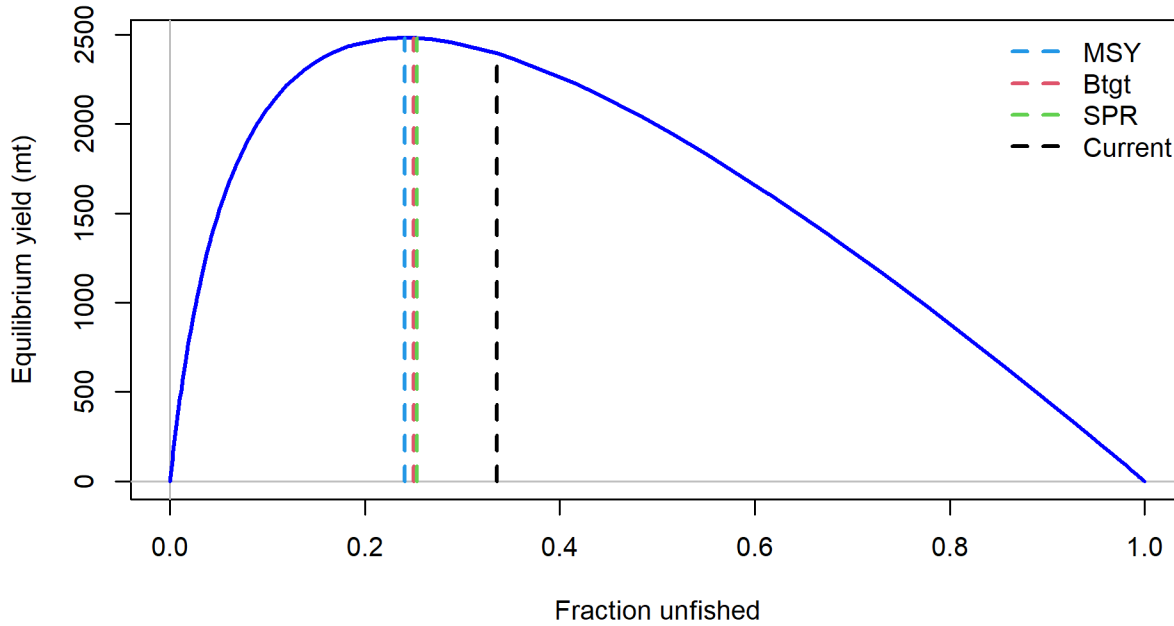
Figure 53: Estimated time series of the fishing intensity (1 - SPR), where SPR is the spawning potential ratio, with approximate 95% asymptotic intervals. The horizontal line at 0.7 corresponds to SPR = 0.3, the management reference point for petrale sole. The horizontal line at 1.0 corresponds to SPR = 0 (all spawning fish removed from the population).
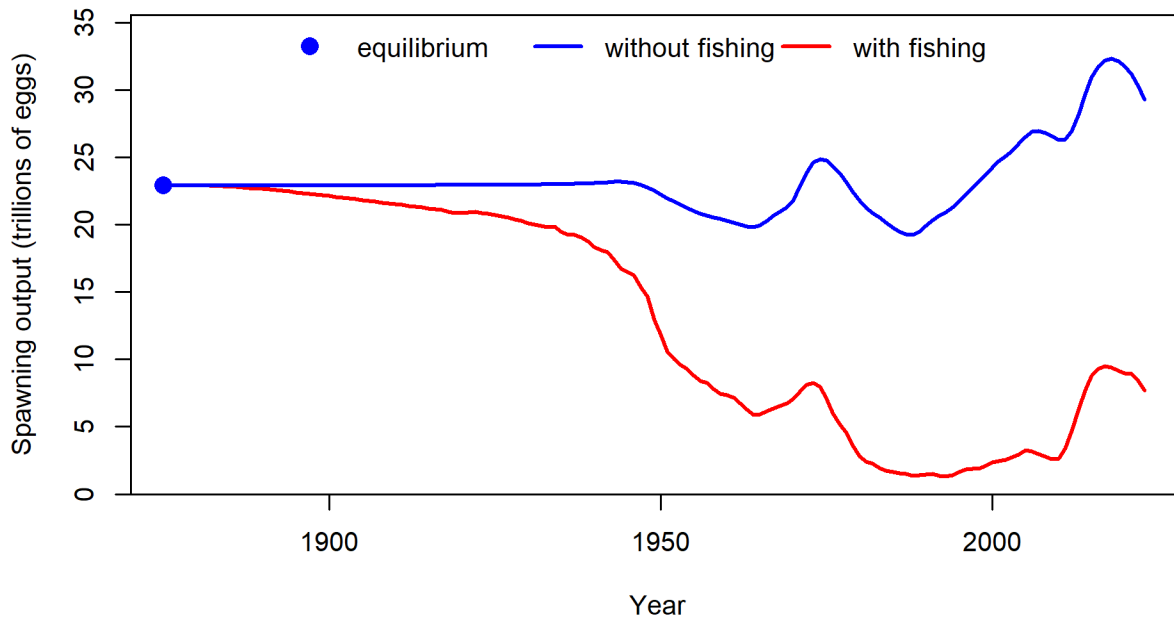
Figure 54: Estimated time series of the exploitation rate (total catch / age 3+ biomass) with approximate 95% asymptotic intervals.
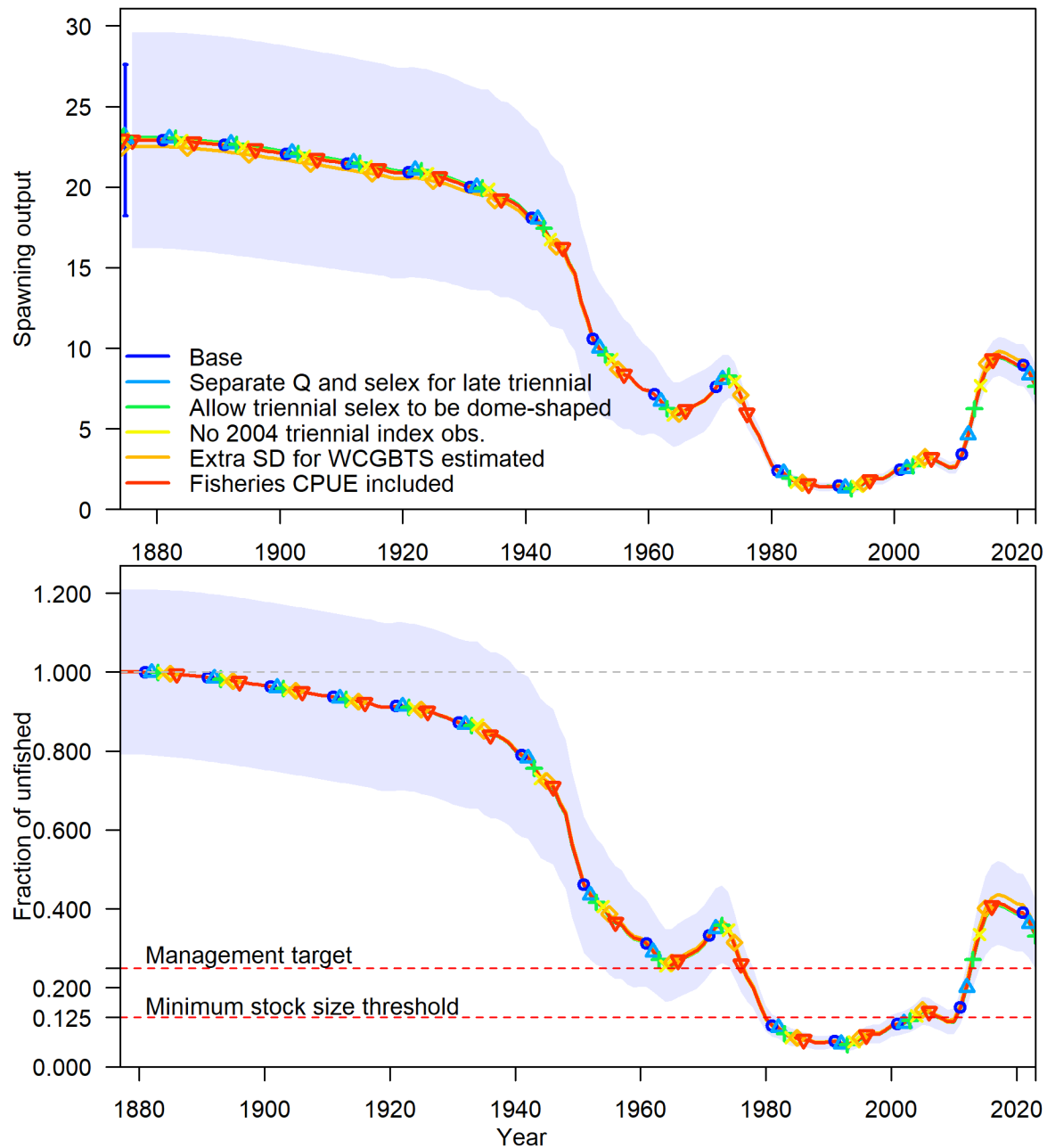
Figure 55: Phase plot of biomass ratio vs. SPR ratio. Each point represents the biomass ratio at the start of the year and the relative fishing intensity in that same year. Warmer colors (red) represent early years and colder colors (blue) represent recent years. Lines through the final point show 95% intervals based on the asymptotic uncertainty for each dimension. The shaded ellipse is a 95% region which accounts for the estimated correlation between the two quantities: -0.824. .
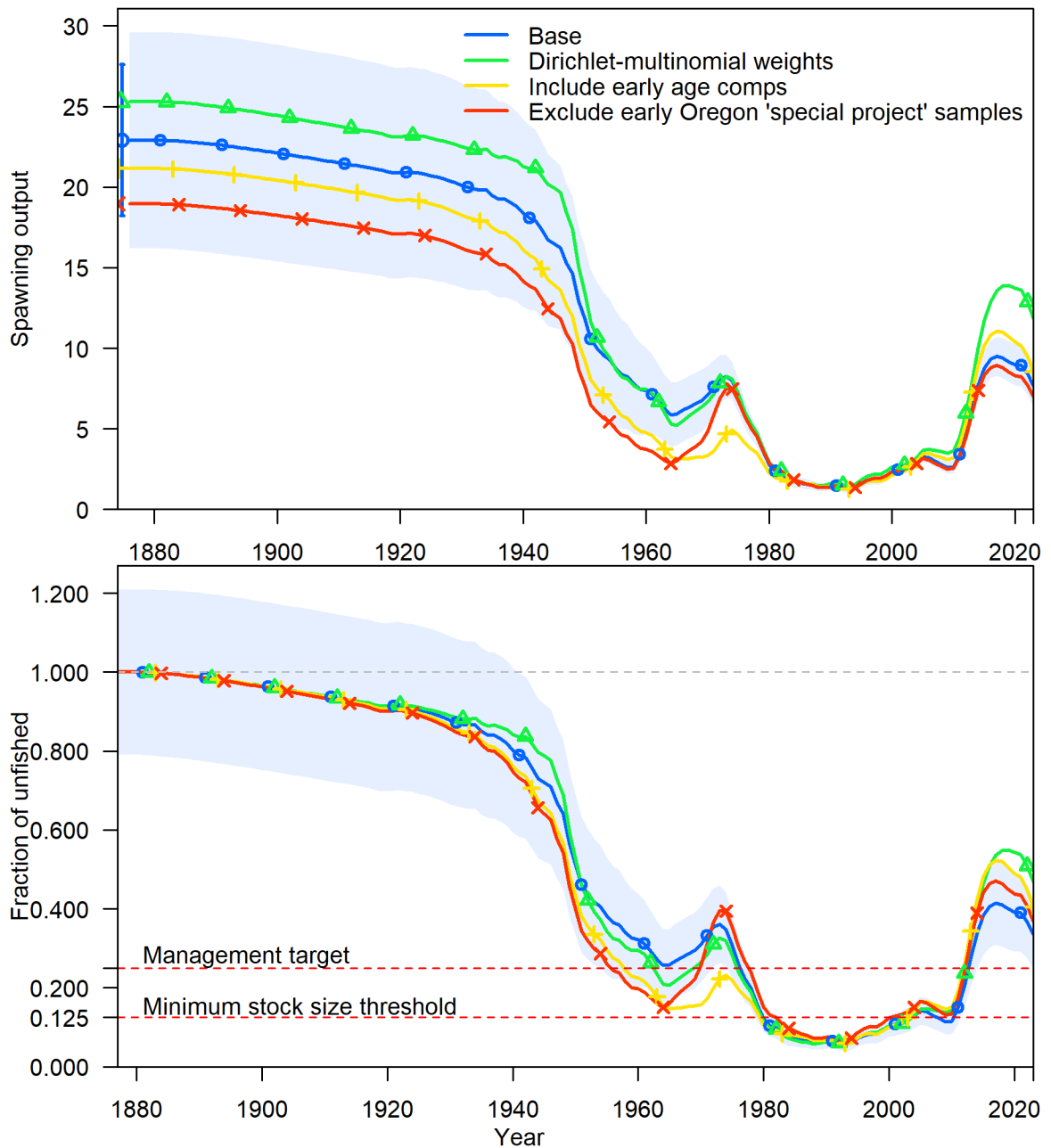
Figure 56: Equilibrium yield curve for the base case model. Values are based on the most recent fishery selectivities and retention curves and with steepness fixed at 0.80.
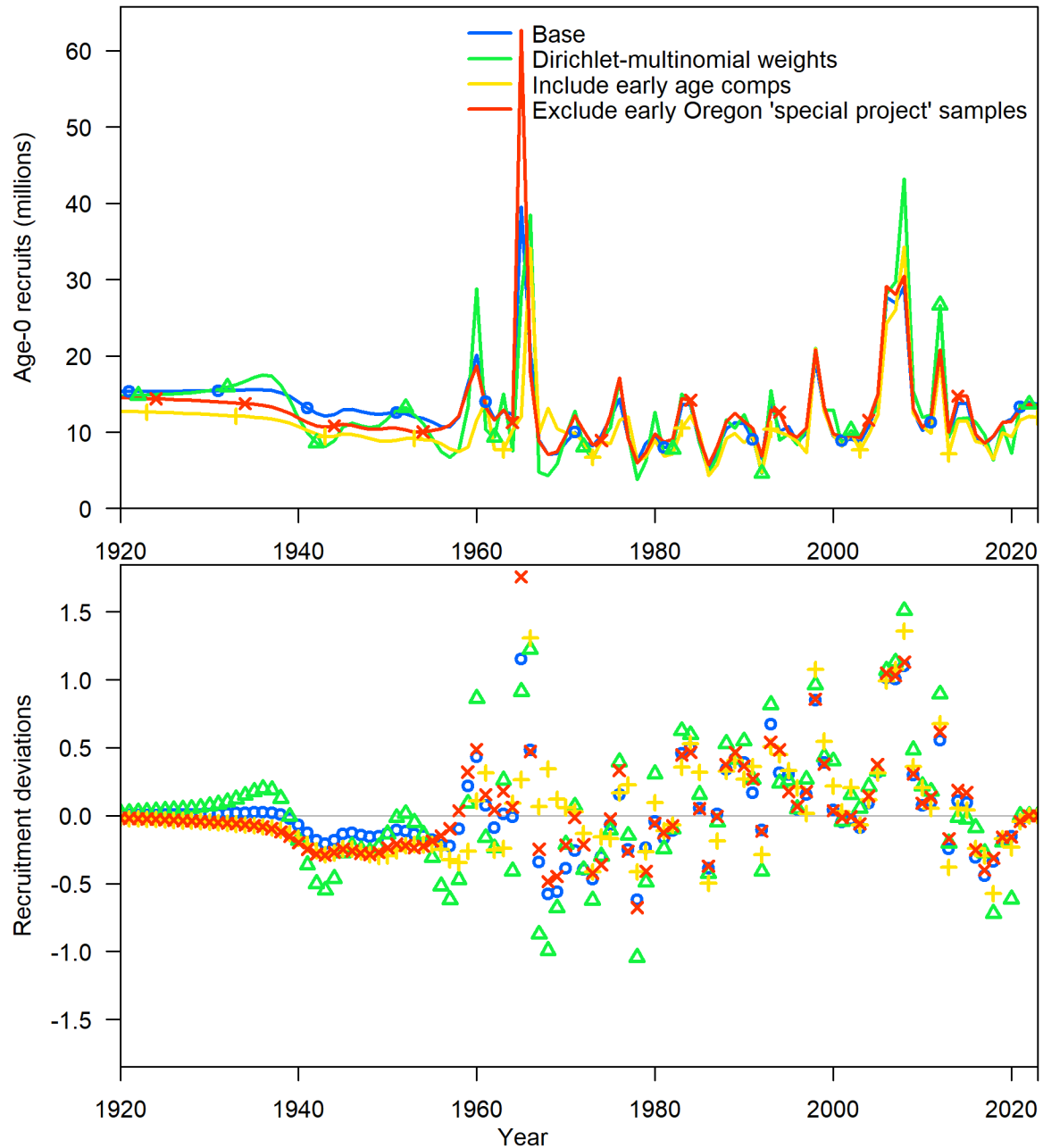
Figure 57: Dynamic B0 plot. The lower line shows the time series of estimated spawning output in the presence of fishing mortality. The upper line shows the time series that could occur under the same dynamics (including deviations in recruitment), but without fishing. The point at the left represents the unfished equilibrium.
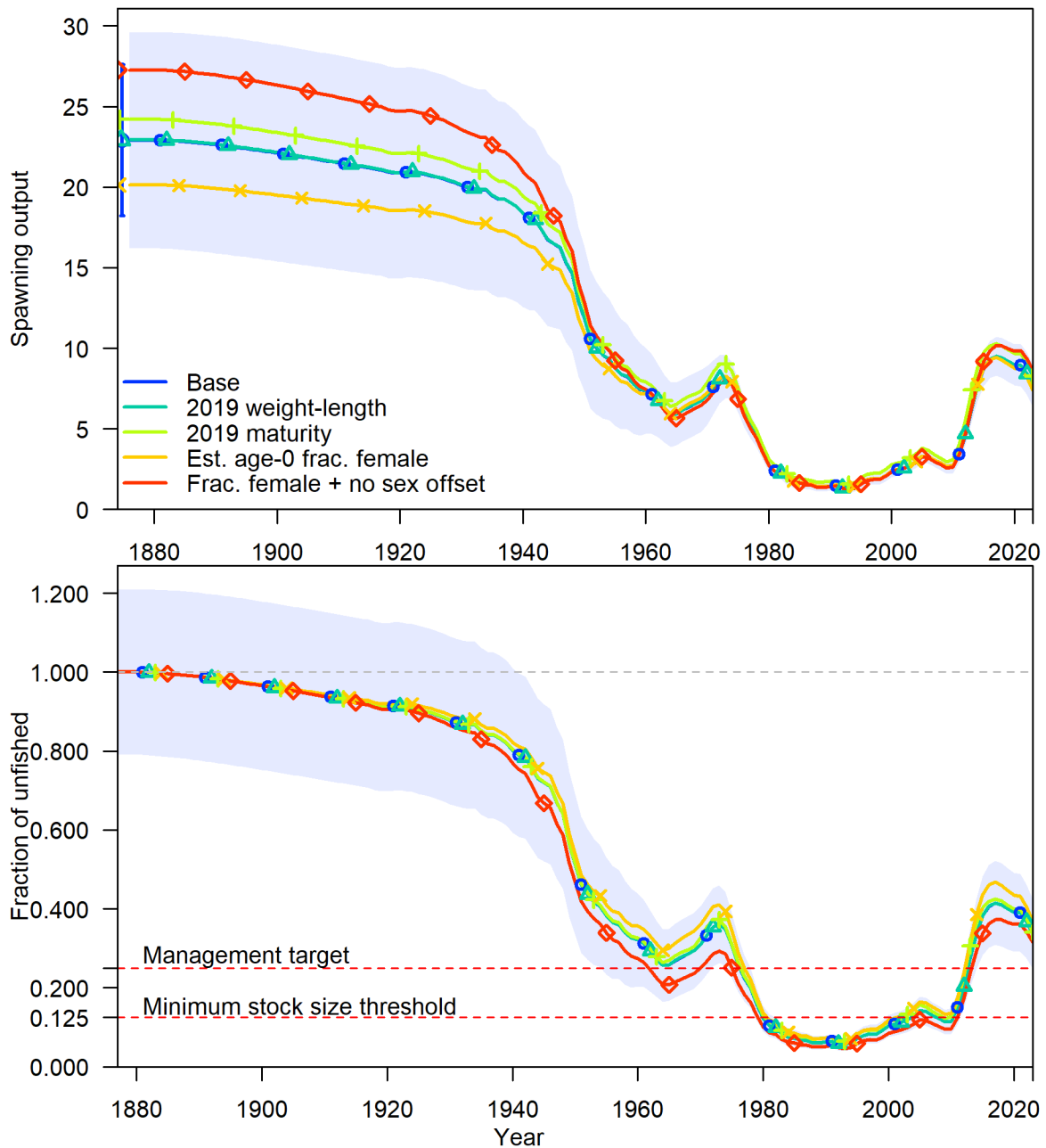
Figure 58: Time series of spawning output (trillions of eggs, top) and fraction of unfished (bottom) for the sensitivity analyses related to index data.
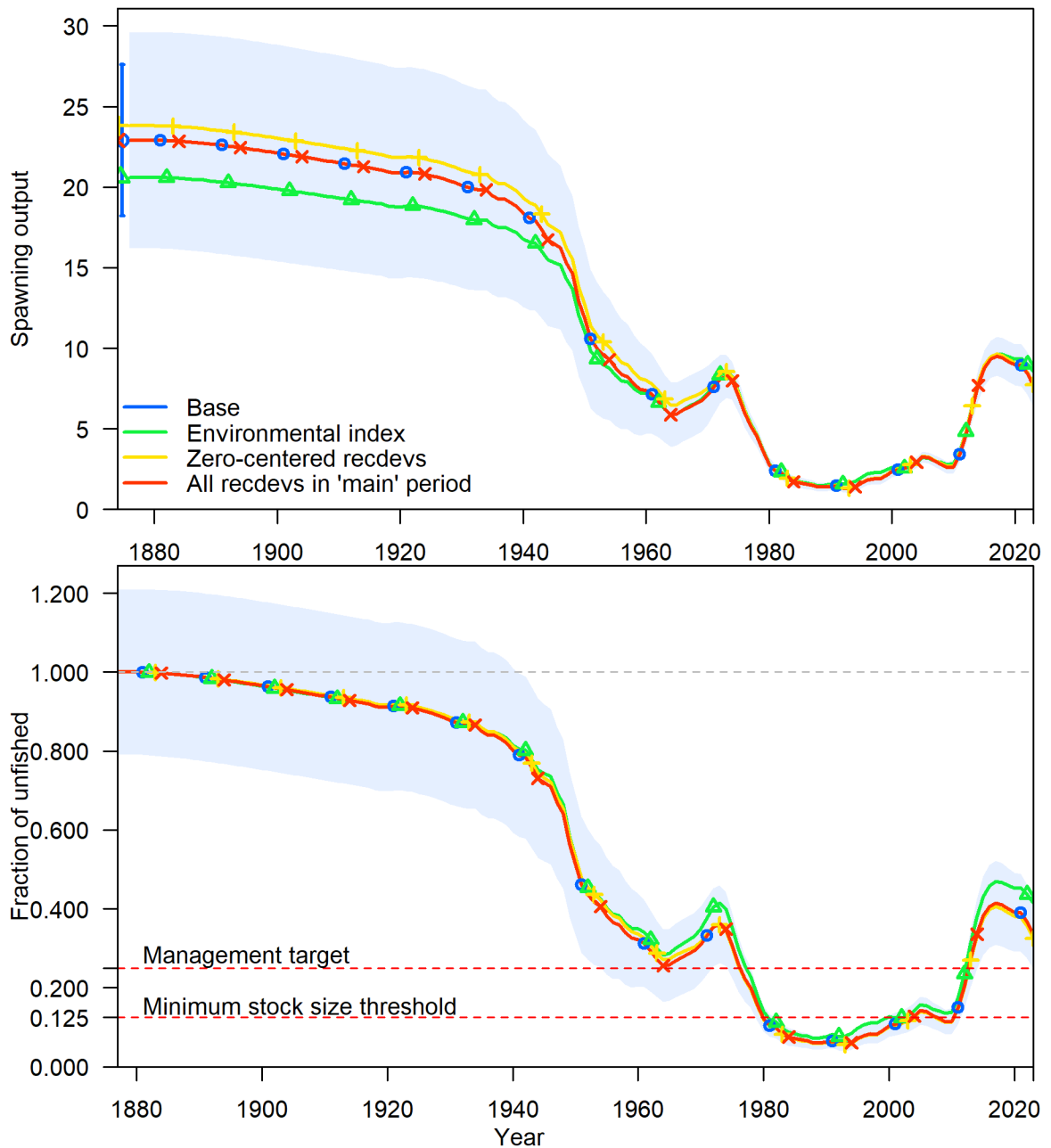
Figure 59: Time series of spawning output (trillions of eggs, top) and fraction of unfished (bottom) for the sensitivity analyses related to composition data.
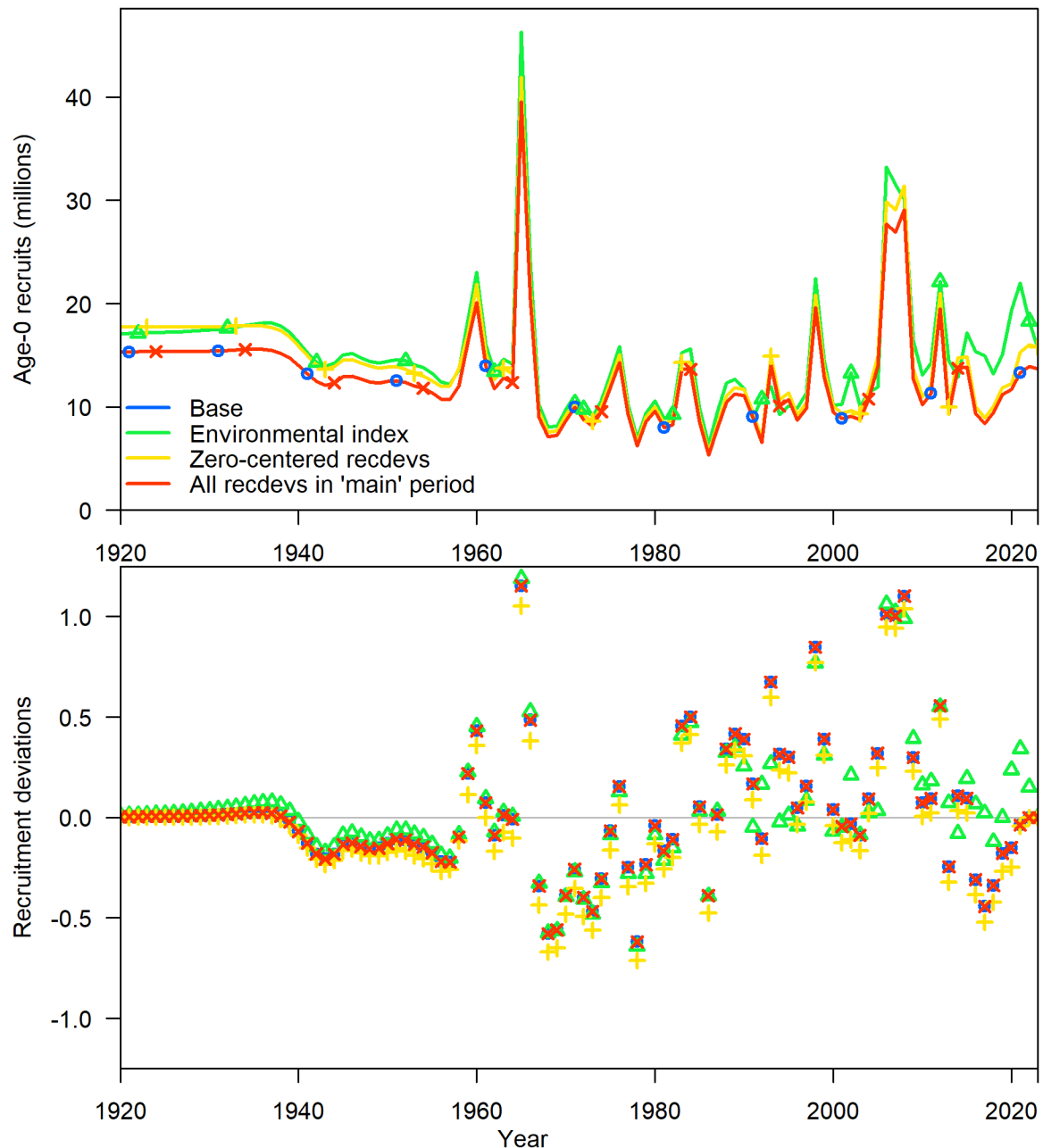
Figure 60: Time series of recruitment (top) and recruitment deviations (bottom) for the sensitivity analyses related to composition data.
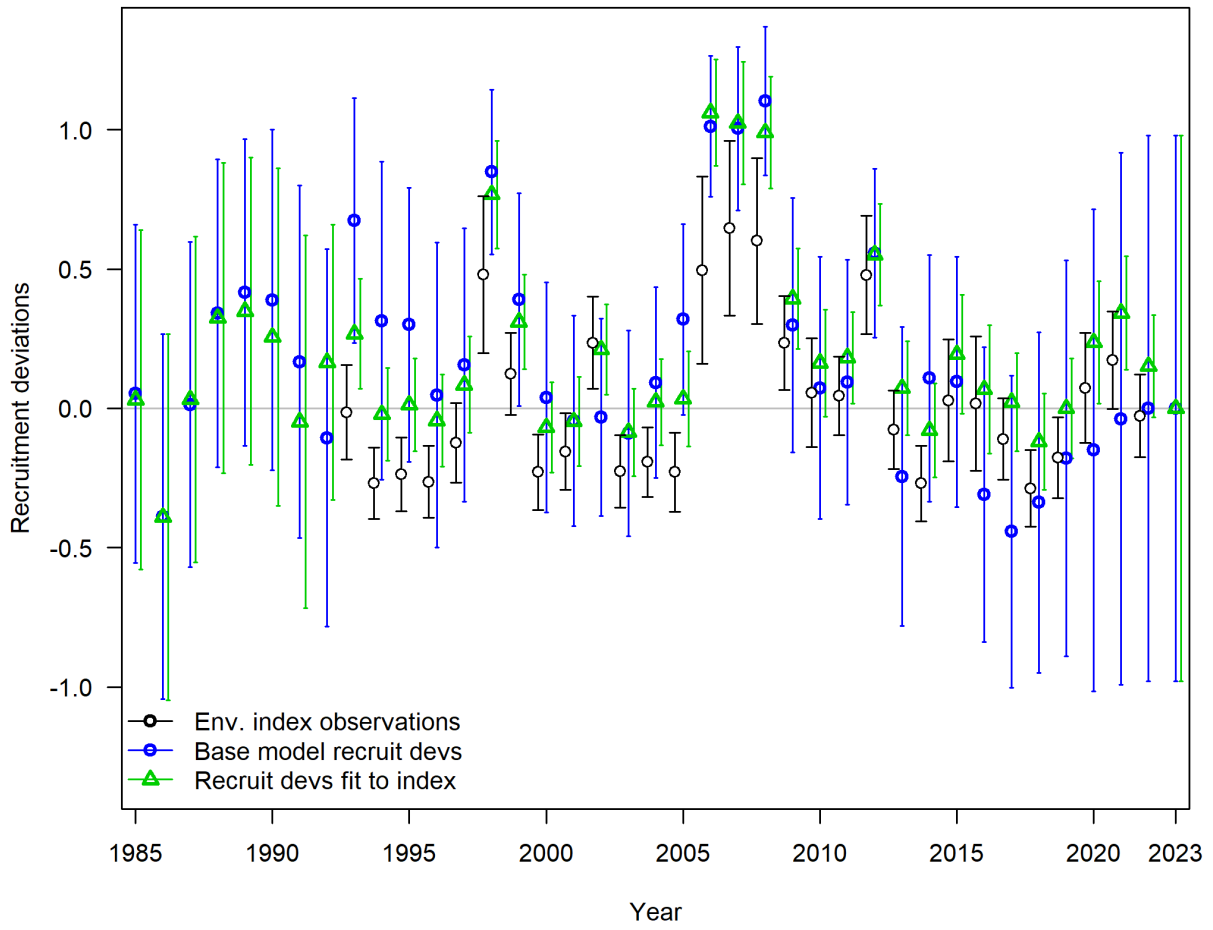
Figure 61: Time series of spawning output (trillions of eggs, top) and fraction of unfished (bottom) for the sensitivity analyses related to biology.
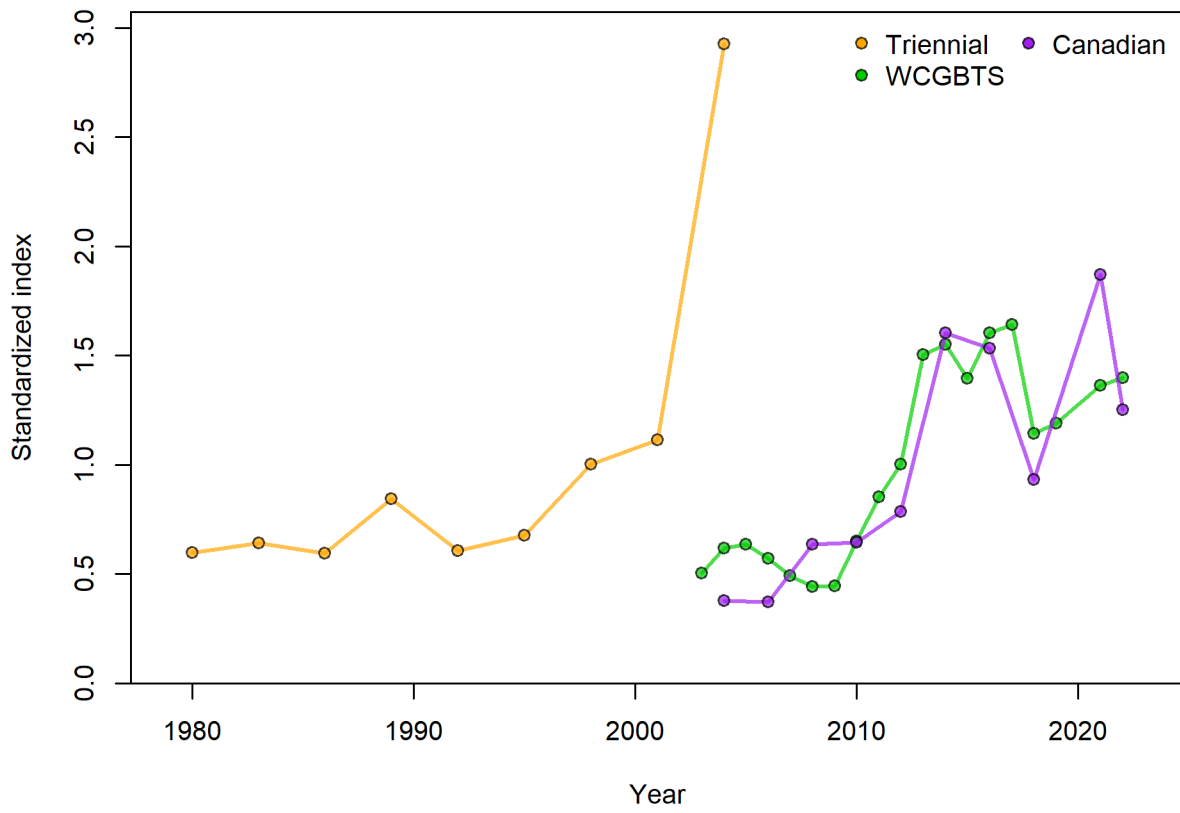
Figure 62: Time series of spawning output (trillions of eggs, top) and fraction of unfished (bottom) for the sensitivity analyses related to recruitment.
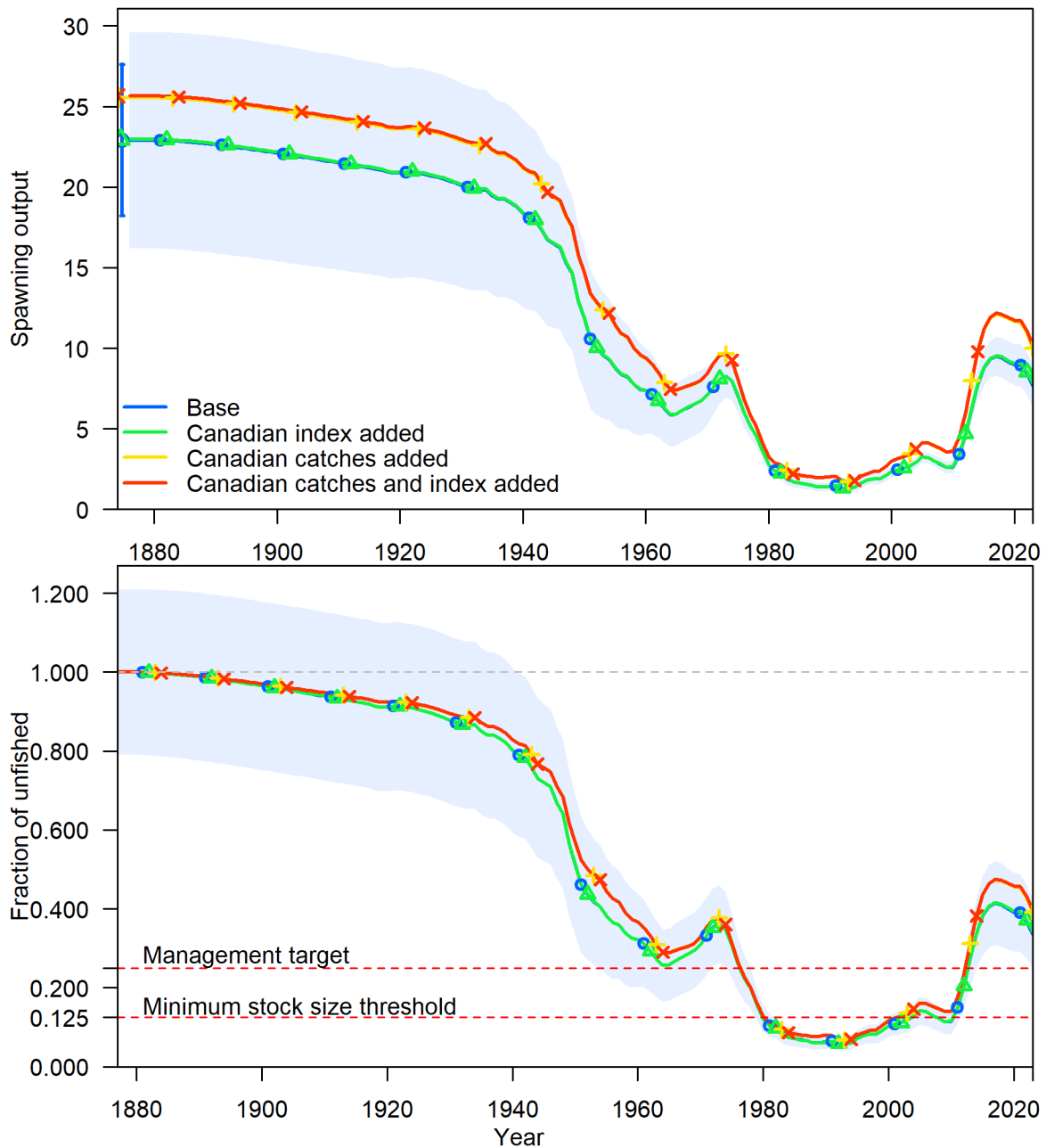
Figure 63: Time series of recruitment (top) and recruitment deviations (bottom) for the sensitivity analyses related to recruitment.
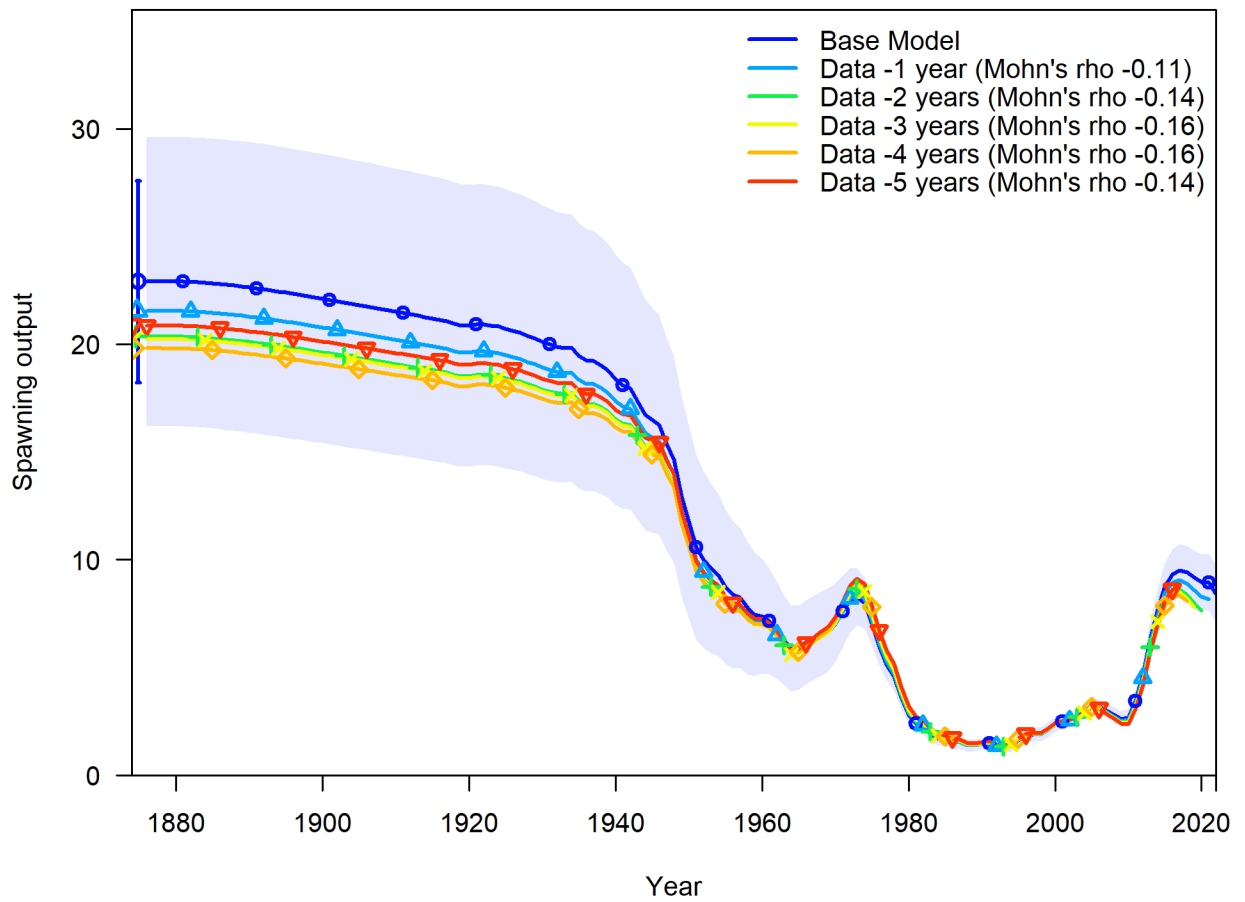
Figure 64: Environmental index of recruitment used in the sensitivity analysis (black points) shown with estimated recruitment deviations from the base model (blue) and from the sensitivity analysis in which the environmental index was included (green). The black intervals show the input uncertainty associated with the index while the blue and green intervals show the uncertainty associated with the estimated recruitment deviation parameters. The 2023 recruitment deviation is not informed by any observations so estimated at zero with uncertainty associated with $\sigma_R = 0.5$.
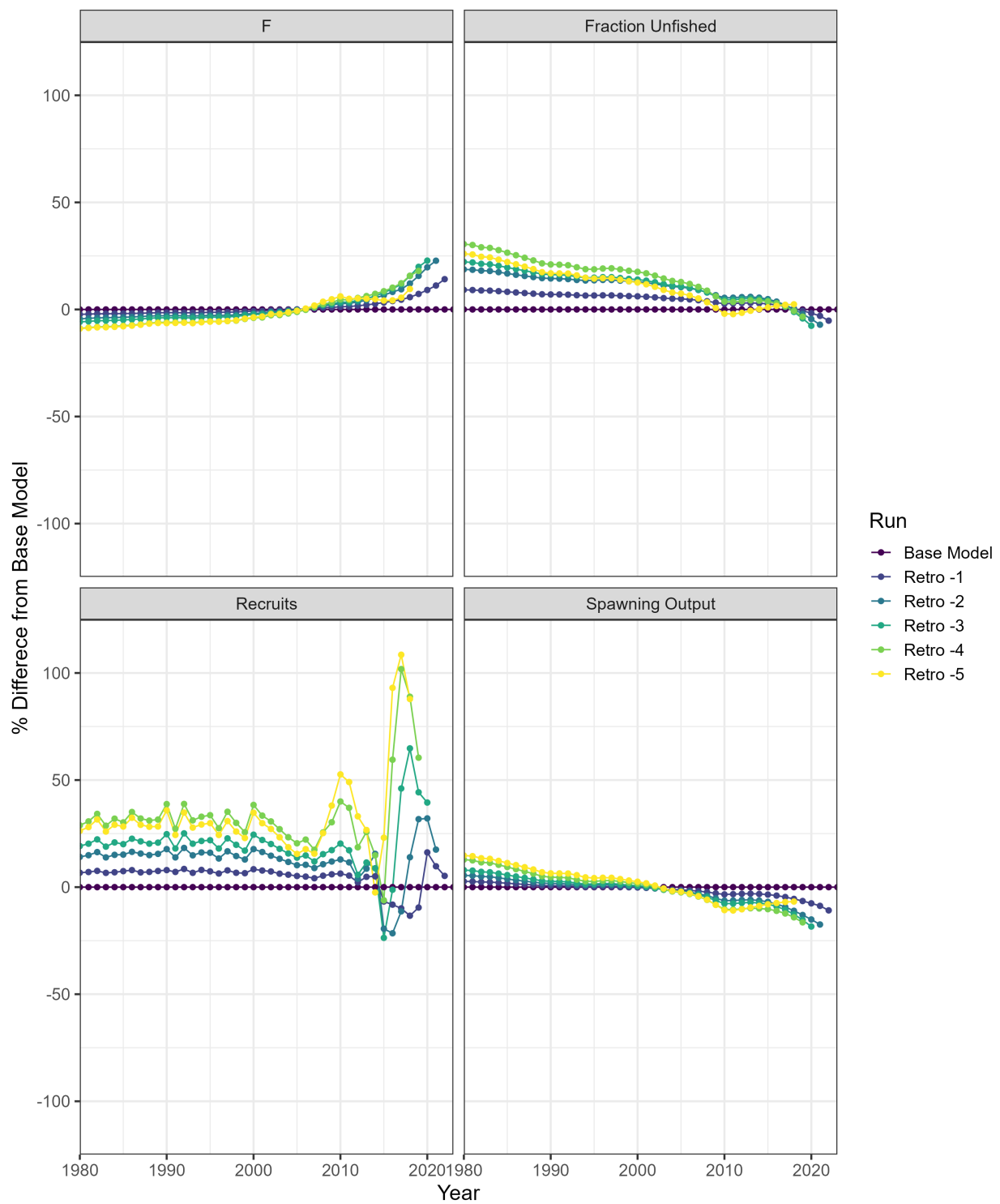
Figure 65: Standardized indices showing comparison of the WCGBTS and Canadian indices as well as the Triennial index.
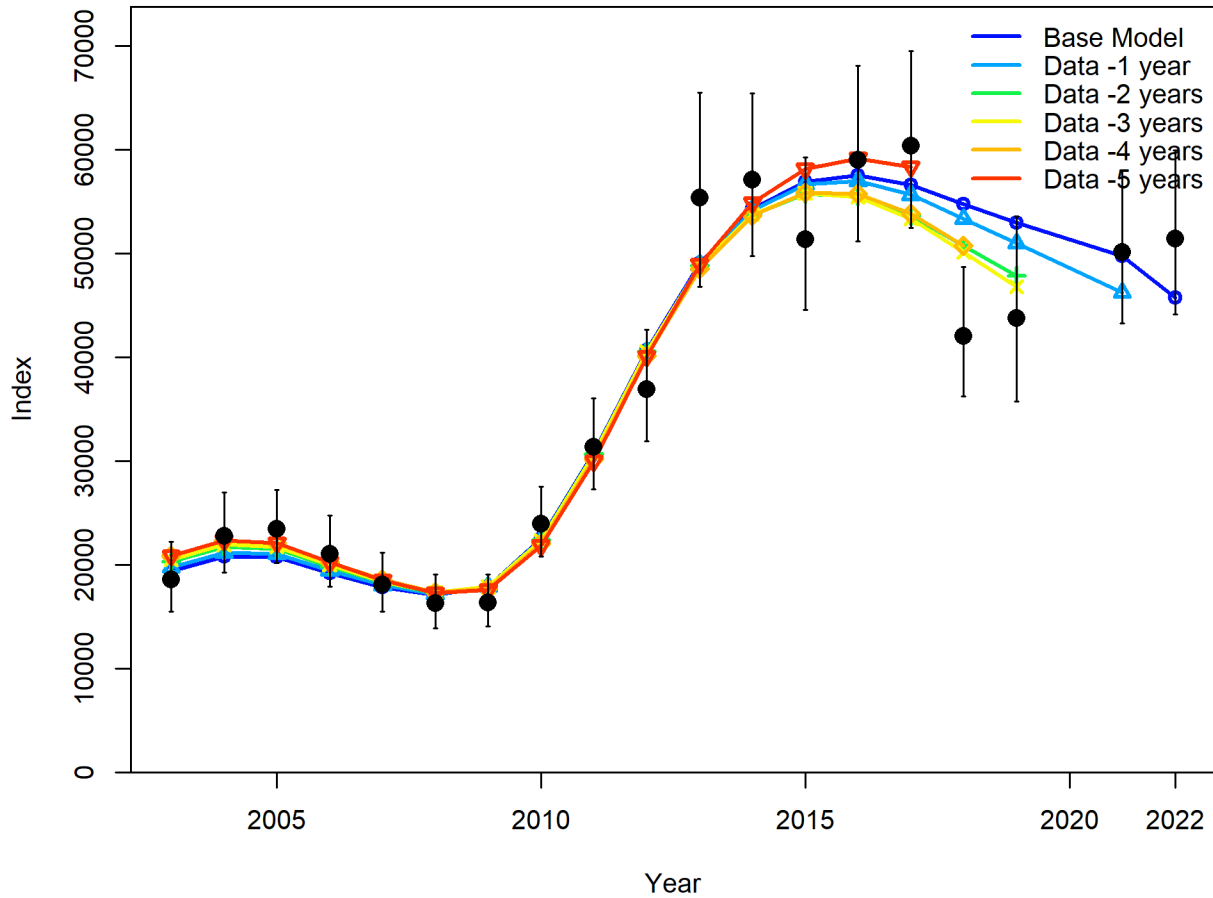
Figure 66: Time series of spawning output (trillions of eggs, top) and fraction of unfished (bottom) for the sensitivity analyses related to data from Canada.
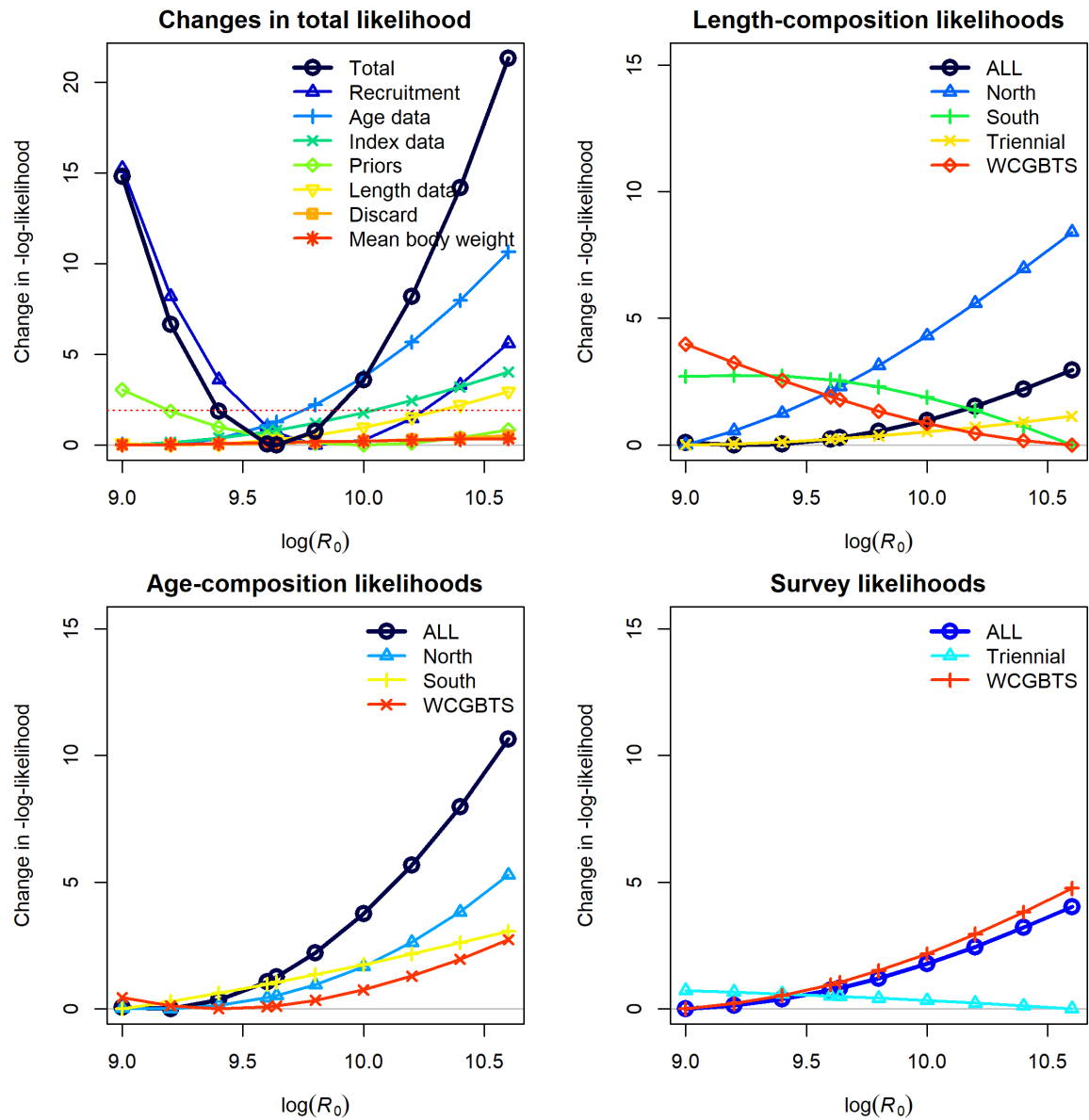
Figure 67: Retrospective results: change in the estimate of spawning output when the most recent 5 years of data area removed sequentially. The Mohn's rho values are averages across the respective number of peels in each case. See equation (2) in Hurtado-Ferro et al. for additional details.
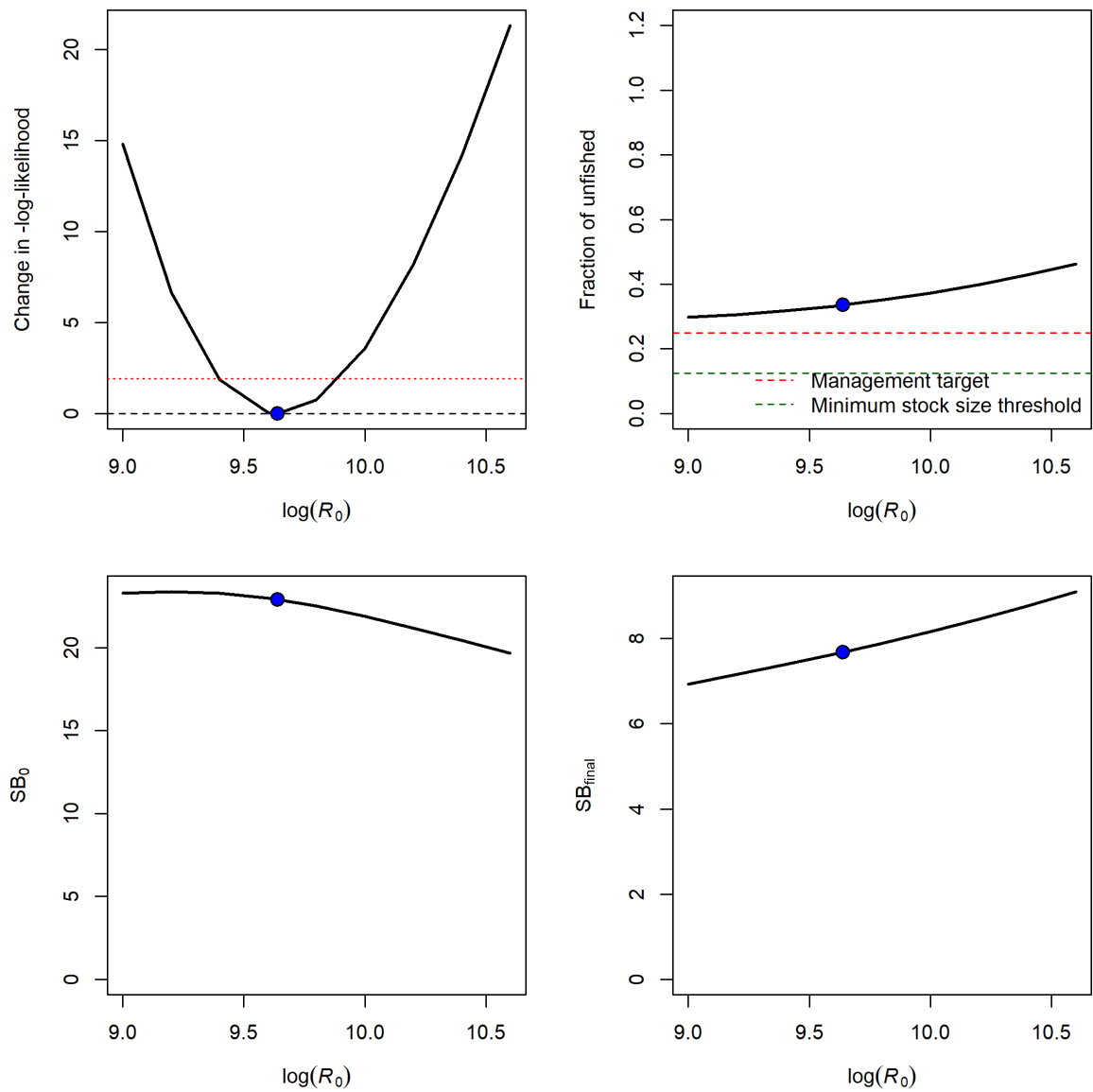
Figure 68: Retrospective results: percent change from the base model for exploitation rate (F), fraction unfished, recruitment, and spawning output.
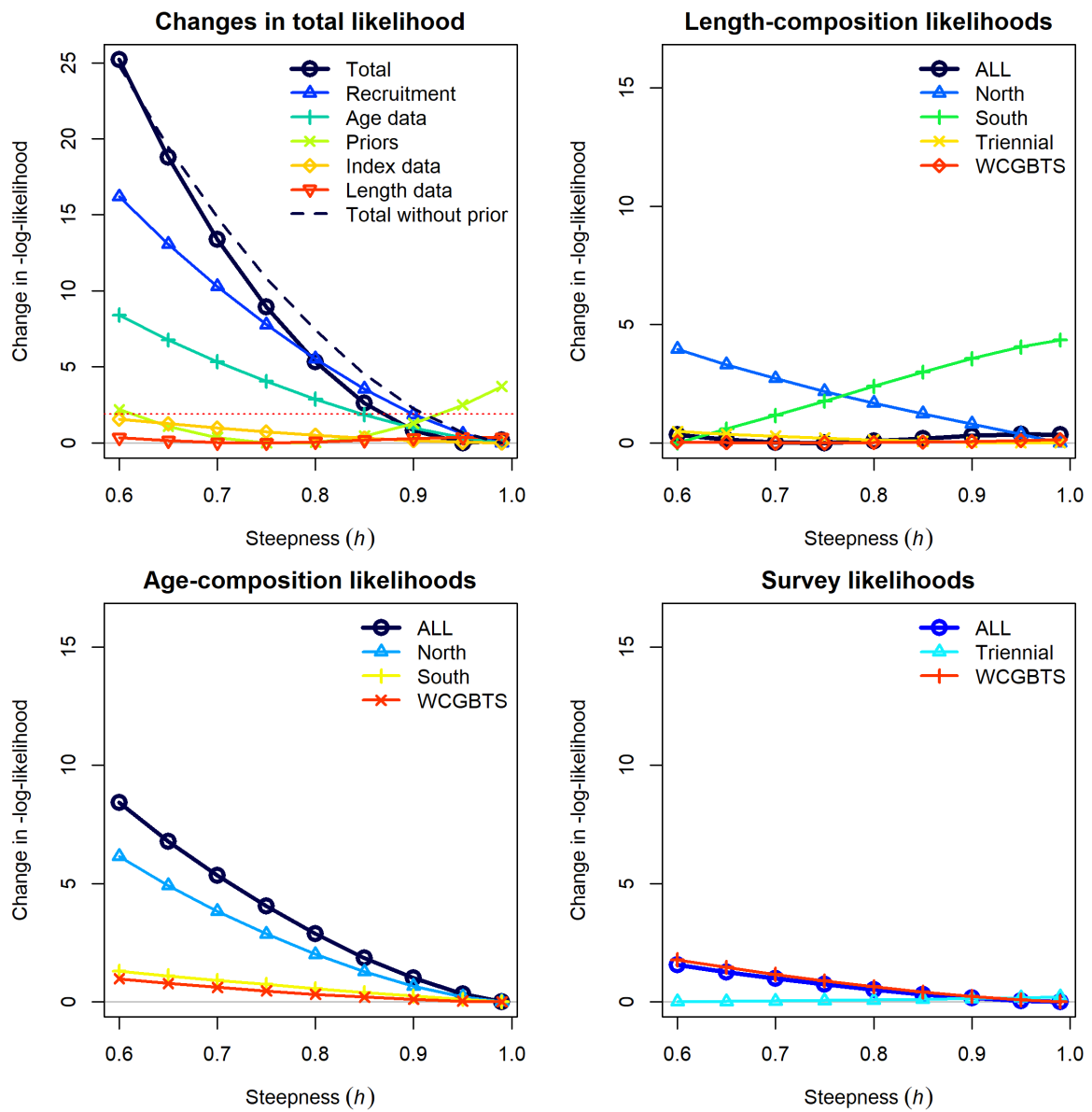
Figure 69: Retrospective results: change in the fit to the WCGBTS index when the most recent 5 years of data area removed sequentially.
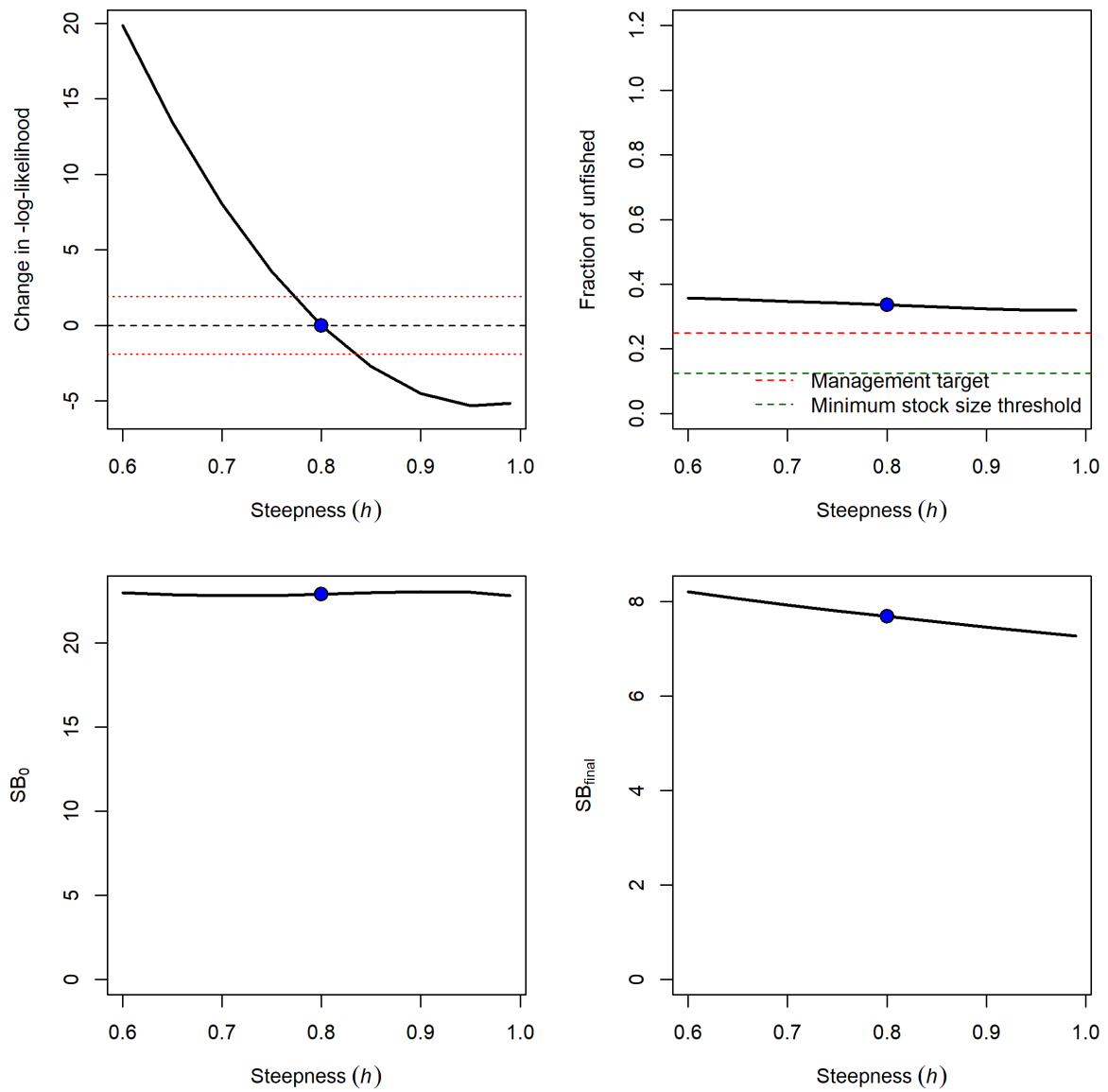
Figure 70: Change in the negative log-likelihood across a range of log(R_0) values.

Figure 71: Change in quantities of interest related to spawning output across a range of $\log(R\_0)$ values: Fraction of unfished spawning output in 2023 (top-right), Spawning output in 2023 (bottom-right), and Unfished equilibrium spawning output (bottom-left). These are shown along with the change in total negative log-likelihood (top-left, matches previous figure).
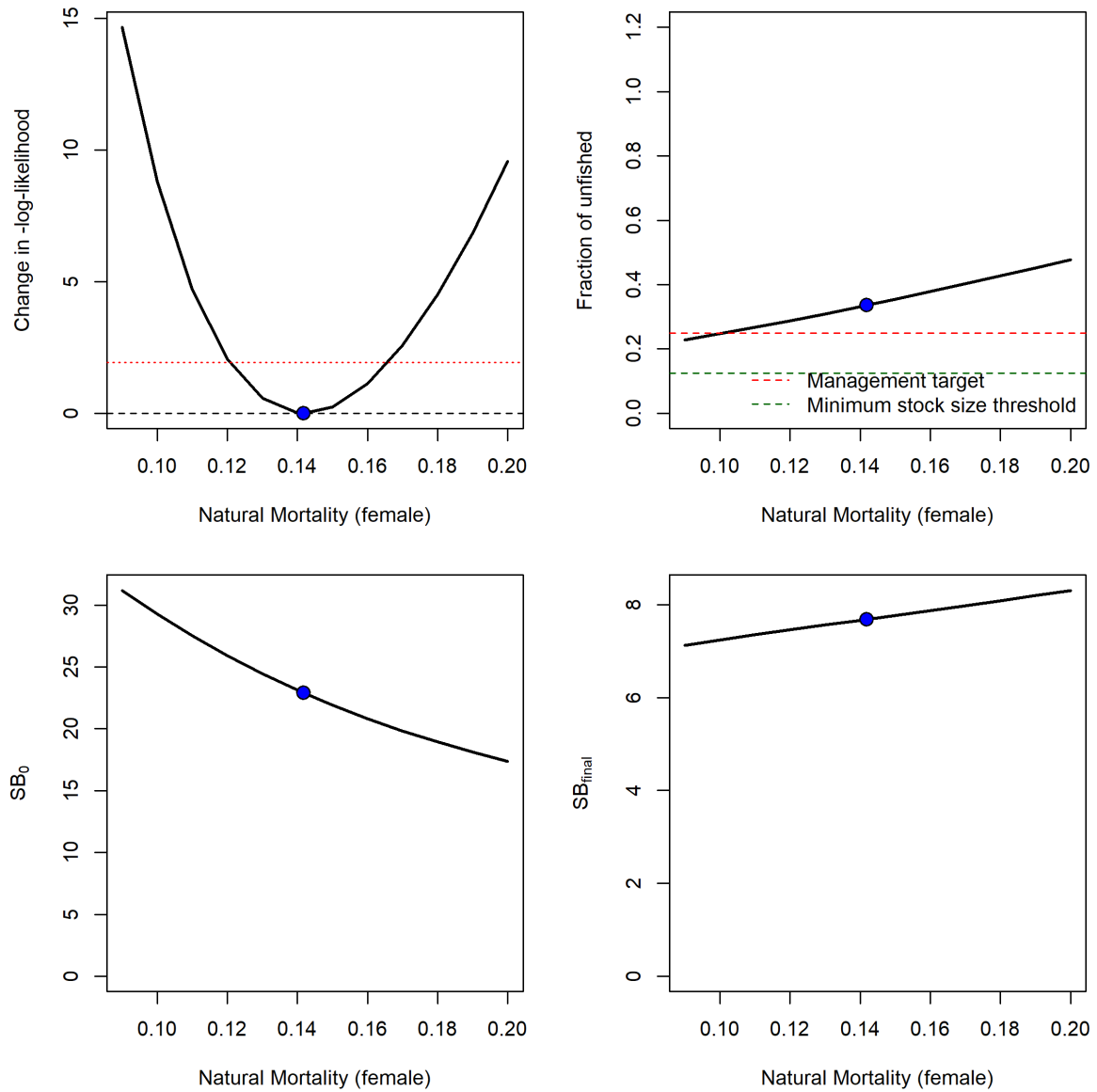
Figure 72: Change in the negative log-likelihood across a range of steepness (h) values.
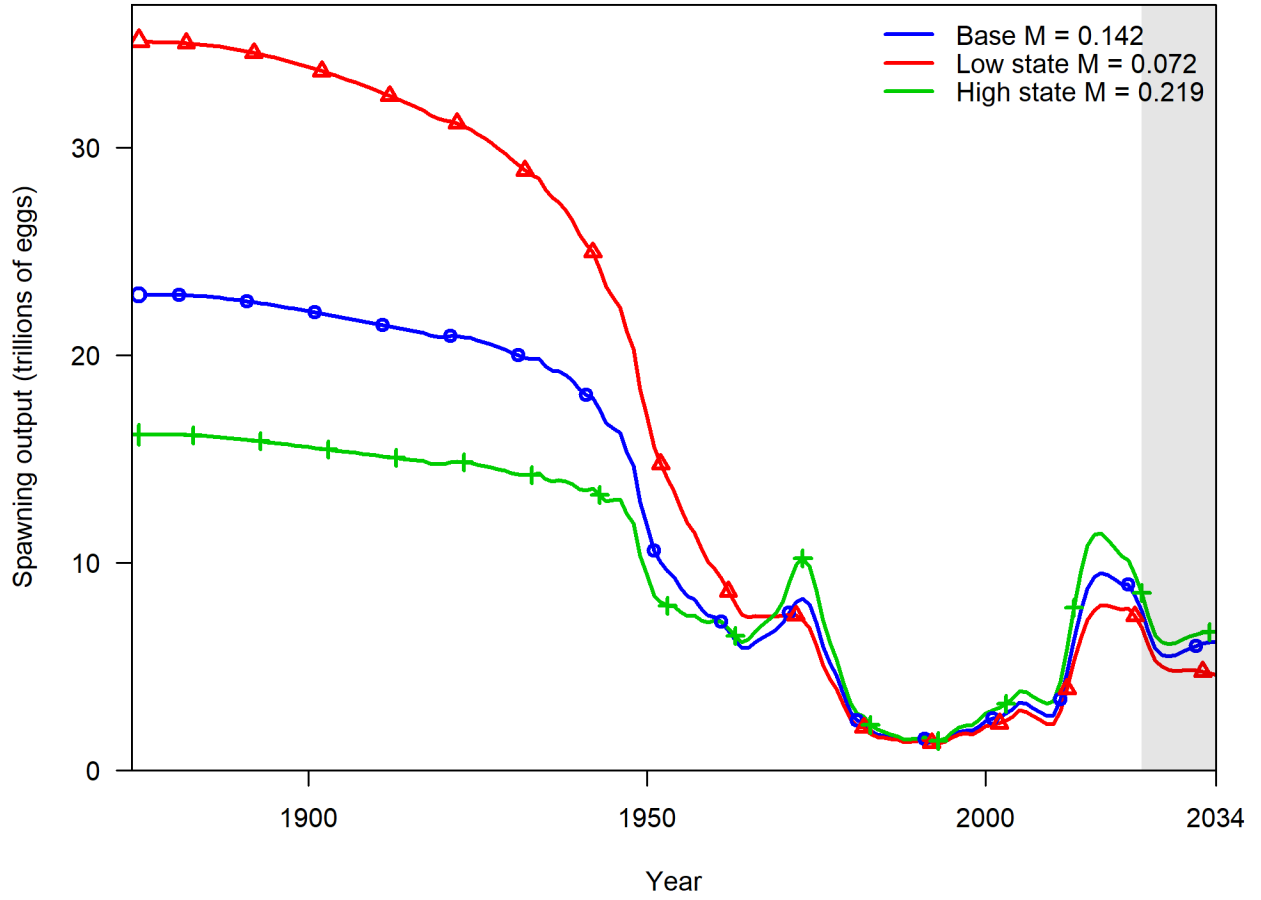
Figure 73: Change in quantities of interest related to spawning output across a range of steepness (h) values: Fraction of unfished spawning output in 2023 (top-right), Spawning output in 2023 (bottom-right), and Unfished equilibrium spawning output (bottom-left). These are shown along with the change in total negative log-likelihood (top-left, matches previous figure).
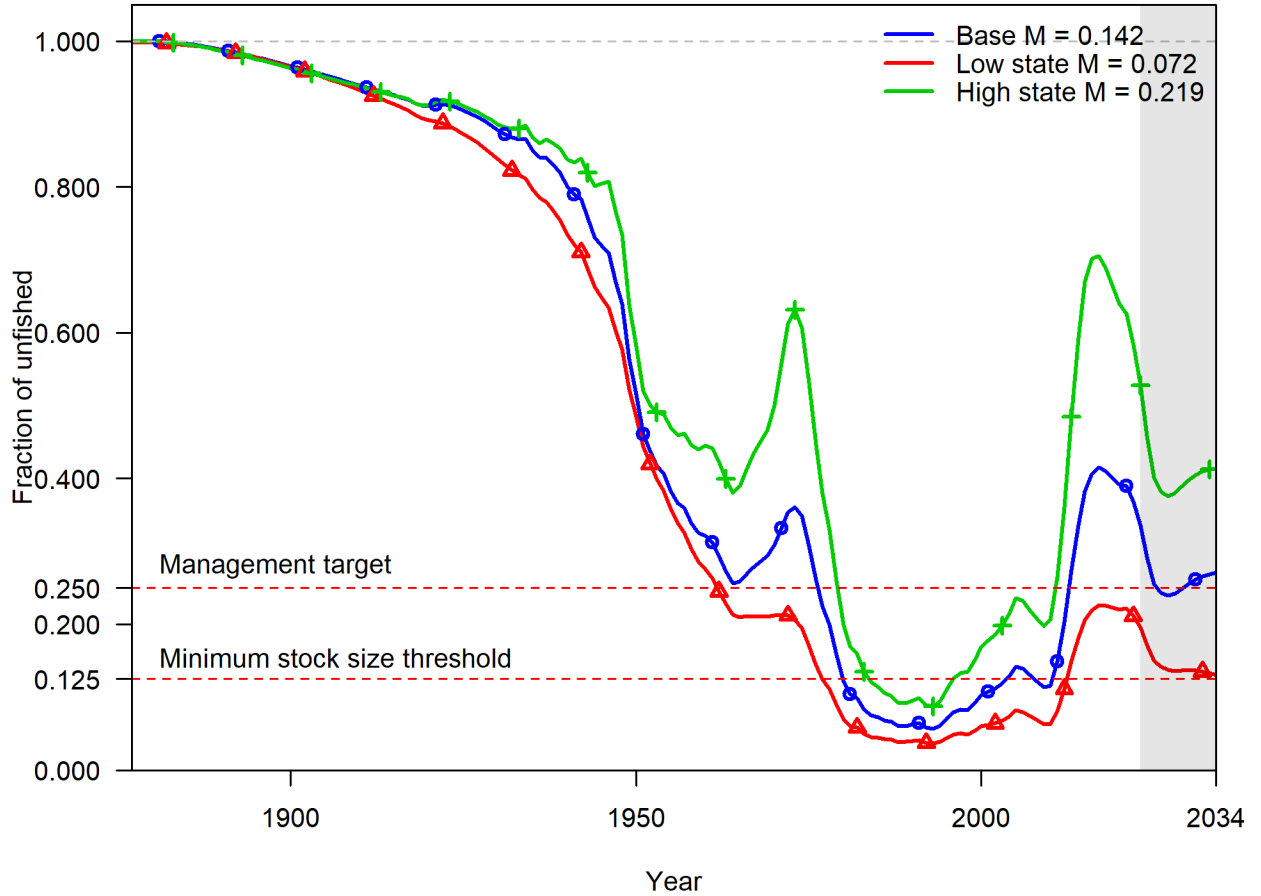
Figure 74: Change in the negative log-likelihood across a range of female natural mortality (M) values.

Figure 75: Change in quantities of interest related to spawning output across a range of female natural mortality (M) values: Fraction of unfished spawning output in 2023 (top-right), Spawning output in 2023 (bottom-right), and Unfished equilibrium spawning output (bottom-left). These are shown along with the change in total negative log-likelihood (top-left, matches previous figure).

Figure 76: Spawning output time series and projections for the base model and states of nature using the default harvest control rule as shown in the decision table.

Figure 77: Fraction unfished time series and projections for the base model and states of nature using the default harvest control rule as shown in the decision table.

A Environmental indices of petrale recruitment, and estimates of the abundance spatial distribution of juveniles

Nick Tolimieri

A.1 Prior ROMS based indicators of petrale recriutment

Haltuch et al. (2020) examined the relationship between recruitment deviations from the 2019 petrale assessment (Wetzel 2019b) and oceanographic drivers based on model output from a Regional Ocean Modeling System (ROMS) model for the California Current Ecosystem (Neveu et al. 2016). Potential drivers were selected based a conceptual life history model, which was used to generate life-stage-specific and spatio-temporally-specific mechanistic hypotheses regarding oceanographic variables that might likely influence survival at each life stage. The study area encompassed the region from 40 to 48°N in the California Current Ecosystem with individual predictors limited by depth or distance from shore (Table A.1). Model selection resulted in a single model in which four oceanographic variables explained 73% of the variation in in the recruitment deviations. Recruitment deviations were:

(1) positively correlated with degree days during the female precondition period (DDpre),

(2) positively correlated with mixed-layer depth during the egg stage (MLDegg),

(3) negatively correlated with cross-shelf transport during the larval stage (CSTlarv), and

(4) negatively correlated with cross-shelf transport during the benthic juvenile stage (CSTbjuv).

These results suggested that ROMS output might be useful as the basis for an environmental index of recruitment for petrale to allow for better model precision and near-term forecasting. However, while the ROMS model used by Haltuch et al. (2020) was consistent in structure and inputs for 1980-2010, the ROMS model was updated beginning in 2011 producing potential discontinuities in the ROMS predictions and the identified drivers from the earlier 1980-2010 time period.

Here, outputs from the updated ROMS model for 2011-2022 were compared to the 1980-2010 mode looking for discontinuities in ROMS time series used in Haltuch et al. (2020) with a focus on the the four predictors identified as important in that work. The conceptual life-history model and abbreviation for terms are shown in Table A.1.

Table A.1: Conceptual life-history model for petrale, including abbreviation of ROMS term. Reproduced from Haltuch et al. (2019). DD = degree days; T = temperature; MLD = mixed-layer depth, LST = longshore transport, CST = cross-shelf transport; pre = female preconditioning stage; egg = egg stage, larv = larval stage, pjuv = pelagic juveniles, bjuv = benthic juveniles.

Life stage	Year	Stage duration	Stage depth	Abbrv.	Hypothesis	ROMS variable
Precon-dition-ing	Year 0 May–October		Bottom depths of 50–200 m	DDpre	Higher bottom water temperatures increases food demand resulting in lower egg production, egg quality, or probability of spawning and lowers recruitment (likely a bell-shaped relationship)	Mean bottom water temperature (°C, 4 days)
Spawn-ing	Year 1 Novem-ber–March		Bottom depths of 250–500 m	Tpre.a	Bottom water temperature acts as a spawning cue with fish less likely to spawn at high temperature resulting in lower recruitment	Mean bottom water temperature (°C, 4 days)
				Tpre.b	Water column temperature acts as a spawning cue with fish less likely to spawn at high temperature resulting in lower recruitment	Mean water column temperature (°C, 4 days)
Egg, surface	Year 1 Novem-ber–April	6–14 days	Water column from surface to MLD	MLDegg	Eggs are buoyant so mixed-layer depth limits how far they rise in the water column affecting later transport	Mean mixed-layer depth (m)
				LSTegg1	Transport in the water column above the MLD to settlement habitat affects recruitment	Mean long-shore transport between the surface and MLD (m/s, 4 days cumulative)
				CSTegg	Transport in the water column above the MLD to settlement habitat affects recruitment (aka Advection reduces recruitment while retention enhances recruitment)	Mean cross-shelf transport between the surface and MLD (m/s, 4 days cumulative)
				DDegg1	Growth/Predation hypothesis: growth rate is faster in warm water leading to reduced time vulnerable to predators	Degree days in the water column calculated from mean water column temperature between the surface and MLD (days,

Table A.1: Conceptual life-history model for petrale, including abbreviation of ROMS term. Reproduced from Haltuch et al. (2019). DD = degree days; T = temperature; MLD = mixed-layer depth, LST = longshore transport, CST = cross-shelf transport; pre = female preconditioning stage; egg = egg stage, larv = larval stage, pjuv = pelagic juveniles, bjuv = benthic juveniles. (*continued*)

Life stage	Year	Stage duration	Stage depth	Abbrv.	Hypothesis	ROMS variable
Egg, sinking	Year 1 November–April	6–14 days	Water column from MLD to 400 m	LSTegg2	Transport in the water column to settlement habitat affects recruitment (aka Advection reduces recruitment while retention enhances recruitment)	Mean long-shore transport from the MLD to 400 m (m/s, 4 days cumulative)
				CSTegg2	Transport in the water column to settlement habitat affects recruitment	Mean cross-shelf transport from the MLD to 400 m (m/s, 4 days cumulative)
				DDegg2	Growth/Predation hypothesis: growth rate is faster in warm water leading to reduced time vulnerable to predators	Degree days in the water column calculated from mean water column temperature between the MLD and 400 m (days, 4 days)
Larvae (both yolk sack and feeding)	Year 1 December - May	~5 months for all pelagic stages	Water column from 0–50 m	LST-larv	North to south transport in the water column brings northern zooplankton and	Mean long-shore transport in the water column at 50–150 km offshore (m/s, 4 days cumulative)
				CST-larv	Transport in the water column to settlement habitat affects recruitment (aka Advection reduces recruitment while retention enhances recruitment)	Mean cross-shelf transport in the water column at 50– 150 km offshore (m/s, 4 days cumulative)
				DDlarv	Growth/Predation hypothesis: growth rate is faster in warm water leading to reduced time vulnerable to predators	Degree days in the water column calculated from mean water column temperature at 50 – 150 km offshore (days, 4 days)
Pelagic juveniles (feeding pelagics)	Year 1 March–June	~5 months for all pelagic stages	Water column from 0 to 150 m	LST-pjuv	North to south transport brings northern zooplankton and leads to higher survival and recruitment, Transport to settle- ment habitat affects recruitment	Mean long-shore transport in the water column at 80– 120 km offshore (m/s, 4 days cumulative)

Table A.1: Conceptual life-history model for petrale, including abbreviation of ROMS term. Reproduced from Haltuch et al. (2019). DD = degree days; T = temperature; MLD = mixed-layer depth, LST = longshore transport, CST = cross-shelf transport; pre = female preconditioning stage; egg = egg stage, larv = larval stage, pjuv = pelagic juveniles, bjuv = benthic juveniles. (*continued*)

Life stage	Year	Stage duration	Stage depth	Abbrv.	Hypothesis	ROMS variable
				CST-pjuv	Transport in the water column to settlement habitat affects recruitment (aka Advection reduces recruitment while retention enhances recruitment)	Mean cross-shelf transport in the water column at 80–120 km offshore (m/s, 4 days cumulative)
				DDpjuv	Growth/Predation hypothesis: growth rate is faster in warm water leading to reduced time vulnerable to predators	Degree days in the water column calculated from mean water column temperature at 80–120 km offshore (days, 4 days)
Benthic Juvenile (Age-0)	Year 1 April–October		Bottom depths from 50–150 m AND 150–500 m	LSTb-juv	Bottom water transport to settlement habitat affects recruitment (Advection reduces recruitment while retention enhances recruitment)	Mean long-shore transport at bottom depths of 50–150 m and 150–500 m (m/s, 4 days cumulative); Two depth ranges are considered due to uncertainty regarding juvenile distributions
				CSTb-juv	Bottom water transport to settle-ment habitat affects recruitment (aka Advection reduces recruitment while retention enhances recruitment)	Mean cross-shelf transport at bottom depths of 50–150 m and 150–500 m (m/s, 4 days cu-mulative); Two depth ranges are considered due to uncertainty regarding juvenile distributions

A.1.1 ROMS outputs

Visual comparison of the 1980-2010 and the 2011-2022 ROMS outputs show distinct discontinuities between the two time periods in multiple time series (Fig. A.1). In particular, DDpre and MLDegg (from the original recruitment analysis) both show distinction changes in scale and trend across the 2010/2011 boundary. The cross-shelf transport time series from the original model (CSTlarv and CSTbjuv.a) are not as distinct but do suggest some discontinuity between ROMS models. Other parameters also show rapid changes, such as the longshore transport terms for the egg stage (LSTegg and LSTegg2) as well as the temperature terms. In some cases, the 2014-2016 marine heatwave may have influenced the 2011+ outputs (and thus be real), but

this effect is unlikely the case for many of the terms that jump sharply from 2010 to 2011.

There are multiple possibilities for how an individual ROMS time series may change over the 2010/2011 boundary and how those changes might impact the ROMS-recruitment model from Haltuch et al. (2020). There might be no change in the extracted ROMS variable such that the relationship between the ROMS predictor and petrale recruitment deviations remains the same. That is, there is no change in the intercept, slope, or variance (Fig. A.2c). This outcome would be ideal because the current ROMS-recruitment model could be used unchanged with updated ROMS time series. The overall relationship might stay the same but variability in the ROMS parameter mighty change due to new observed model inputs leading to more correct estimates (Fig. A.2b). Essentially, the variance increase (or decreases) from 2011+ due to change in the ROMS model structure, including new or different time series of observed data, but the slope and intercept remain the same. This outcome could be modeled by allowing the variance to change across the 2010/2011 boundary.

Additionally, the absolute value of the ROMS variable might change (e.g., water column temperature is warmer than previously modeled), but the overall relationship (slope) remains the same but with a different y-intercept (Fig. A.2c). Here, one could add a time-period term to the model to account for different intercepts in the two blocks of time.

Finally, the relationship between the ROMS predictor and recruitment deviations might actually change (Fig. A.2d). While one could include an interaction term in the model, this case represents the least desired outcome, as it is difficult to interpret the meaning of the interaction. Relationships between environmental variables and biological outcomes are often non-linear, with performance decreasing both above and below a species optimum (e.g., growth and temperature relationships for fish). Obviously, there can also be some combination of b-d, or the relationship can just breakdown completely.

A.1.2 Refitting the Haltuch et al. (2020) model
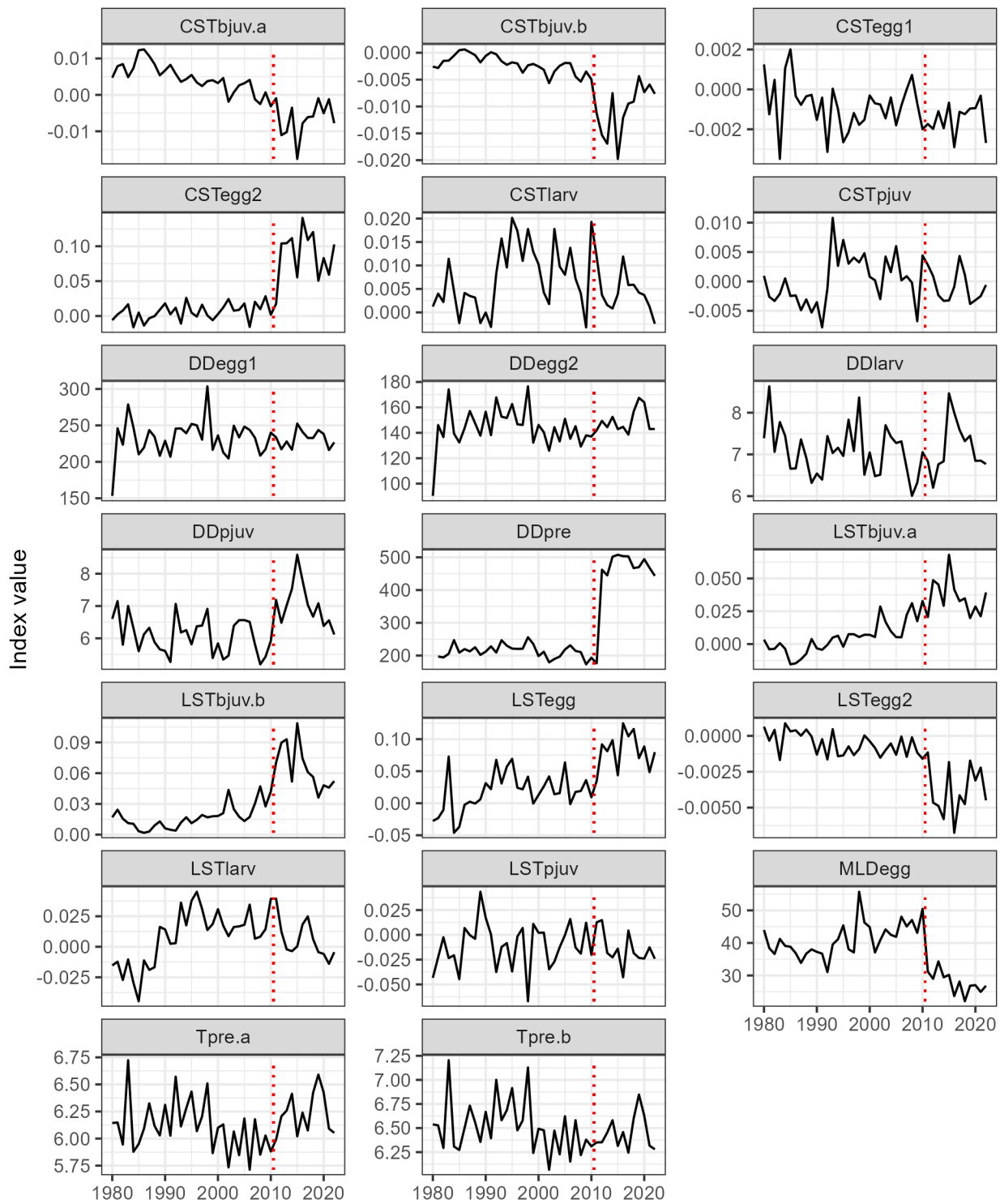
To examine the impact of updating the ROMS model on the ROMS-recruitment relationship, the ROMS time series were updated (following Haltuch et al. (2020)) to include the new 2011+ ROMS outputs. The full ROMS time series were then fit against recruitment deviations from the 2019 petrale stock assessment (Wetzel 2019b). The best-fit model from Haltuch et al. (2020) was used as the base model:

Recruitment Deviations ~ DDpre + MLDegg + CSTlarv + CSTbjuv.a
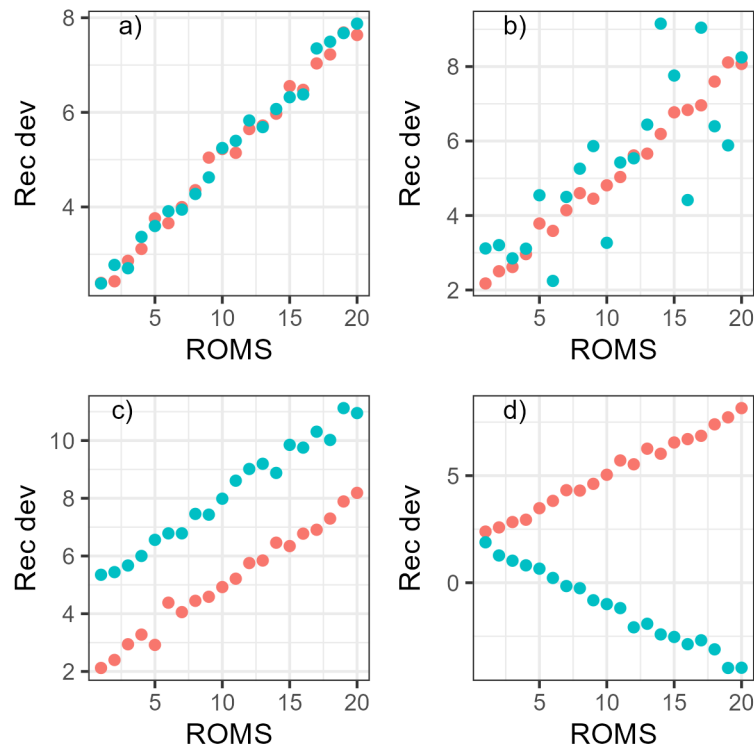
Recruitment deviations ran from 1981-2018 because some parameters were averaged over the winter and included data from two calendar years (i.e., Dec 2010 in the 2011 time series), and the first year with all predictors is 1981. The year 2011 was excluded from the analysis because some of the averaged ROMS variables would include data from both ROMS time periods and there were obvious step changes in some variables.

In addition to the base model, the following model structures were also investigated. These structures included the base model, plus:

(1) different intercepts by period (1981-2010 vs, 2012-2018)
(2) different variance by period

Figure A.1: ROMS predictors used in the original 1980-2010 analysis but updated to include 2011-2022 outputs. DD = degree days, CST = cross-shelf transport, LST = long-shore transport, MLD = mixed layer depth, pre = prespawning, egg = egg stage, larv = larval stage, pjuv = pelagic juveniles, bjuv = benthic juveniles. 'a' and 'b' suffixes indicate drivers with the same time period but different depth ranges due to differences in the literature. Dotted red line indicates the 2010/2011 switch in model outputs.

Figure A.2: Hypothetical relationships between ROMS predictors and petrale recruitment deviations across the 2010/,2011 boundary. a) the relationship is the same, b) a change in variance of the ROMS predictor, c) a change in the intercept, and d) a change in the slope. Colors represent different time periods.

(3) interactions between Period and the four terms in the original best-fit model (un

(4) the model with interactions back-fit to remove non-significant interaction terms.

(5) a separate four-factor generalized additive model (GAM) was also included to better visualize non-linear relationships between the ROMS predictors and petrale recruitment deviations.

For the linear models, the model including the interaction terms but with some interactions removed had the lowest AIC and fewest coefficients (Table A.2) and was chosen as the most parsimonious model (Burnham and Anderson 1998).

Table A.2: Model fitting criteria for the ROMS-recruitment model fits. Bold indicates the best-fit model based on delta AIC < 2.0 and the fewest parameters.

Model	AIC	Parameters	Delta AIC
All interactions	-1.882	10	0.000
GAM	-0.979	37	0.903
Back-fit with interactions	**-0.514**	**8**	**1.368**
Period	19.980	6	21.862
Orginal best-fit	22.843	5	24.725
Different variances	30.276	8	32.158

For 1981-2018, the best-fit model included Period and two interactions (Back-fit with interactions) because it had a ΔAIC < 2.0 and the fewest parameters:
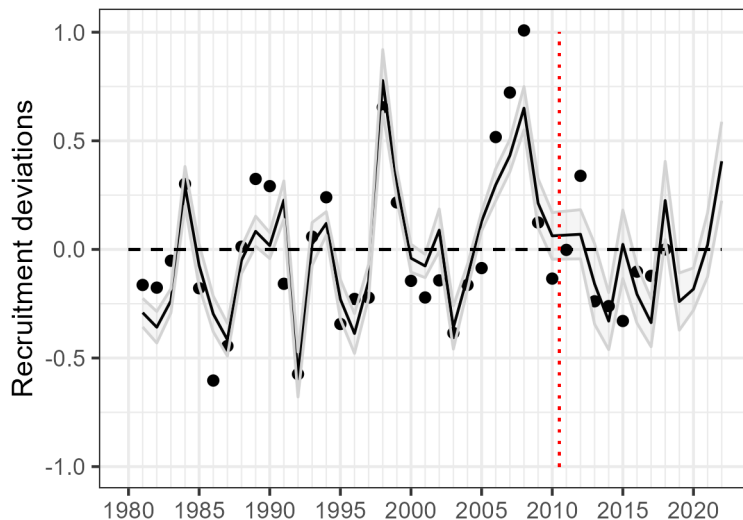
*Recruitment Deviations ~ Period + DDpre + MLDegg + CSTlarv + CSTbjuv.a + DDpre*Period + MLDegg-*Period*

This model explained slightly less variance ($r^2 = 0.71$) than the original 1980-2010 model ($r^2 = 0.73$), but had 7 parameters (excluding the intercept) and 37 data points (1981:2010, 2012-2018), or just over five points per predictor term. Examination of the model coefficients (Table A.3) indicates that the relationships between recruitment deviations and DDpre and MLDegg changed across the 2010/2011 boundary from positive to negative.

Overall the model fit to the data was good and captured a decline in recruitment later in the time series (Fig. A.3). Forecasting through 2022 (latest ROMS output availability), suggested high recruitment in 2022. This model also over-predicted recruitment in 2015 during the 2014-2016 marine heatwave.

Table A.3: Parameter estimates from the best-fit model including combined ROMS time series from 1981-2018. Model $r^2 = 0.71, p < 0.001$.
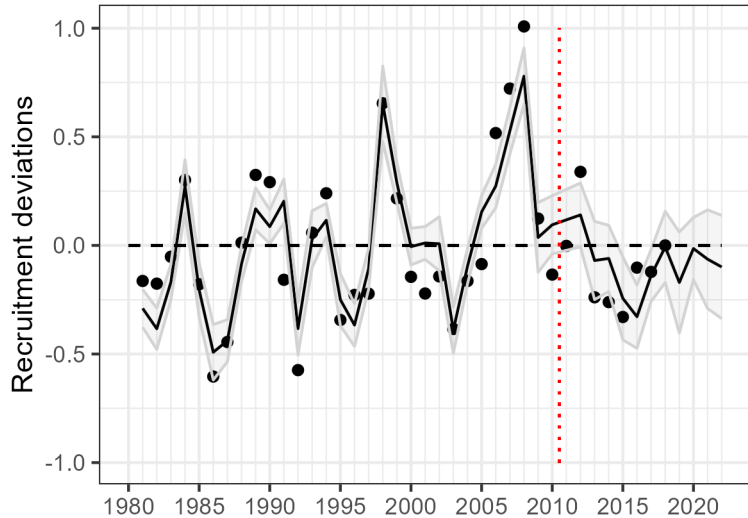
Model	Estimate	SE	t-value	p-value
Intercept	3.862	1.984	1.946	0.061
Period (before)	-7.605	2.073	-3.669	0.001
DDpre	-0.005	0.004	-1.308	0.201
MLDegg	-0.067	0.023	-2.874	0.008
CSTlarv	-38.082	7.108	-5.358	0.000
CSTbjuv	-38.795	11.695	-3.317	0.002
DDpre x Period	0.016	0.004	3.637	0.001
MLDegg x Period	0.112	0.025	4.505	0.000

Figure A.3: Model fit for ROMS predictors to the recruitment deviations for 1981-2018. Black line = model prediction including forecast to 2019-2022. Points are the recruitment deviations from the 2019 petrale stock assessment. Error envelopes indicate 1.0 s.e.

As noted earlier, the interaction makes it somewhat difficult to draw conclusions on the credibility of the model - especially given the large discontinuities in the ROMS outputs and the change in slope of some of the relationships. Therefore, the four-factor GAM output was examined to better understand the relationships between the ROMS predictors and recruitment deviations. The four-factor GAM explained about 65% of the variance in petrale recruitment deviations (Fig. A.4, $r^2 = 0.67$). While the fit is slightly lower than the linear model, the GAM did not over-predict the more or less average 2018 recruitment deviation, while slightly over-predicting several lower recruitment deviations earlier in the time series. In particular, the GAM model caught the low recruitment in 2015 but under predicted recruitment in 2016.

For CSTlarv the new data fall within the same range as the 1980-2010 models, although there may be a slight

Figure A.4: GAM model fit to the recruitment deviations for 1981-2018. Black line = model prediction including forecast to 2019-2022. Points are the recruitment deviations from the 2019 petrale stock assessment. Error envelopes indicate 1.0 s.e.

change in the slope (Fig. A.5). CSTbjuv appearsnon-linear but largely due to one data point (Fig. A.5). Nevertheless, the newer values are all lower than the earlier period with the exception of one point.

Likewise, for MLD, the newer ROMS model predicts a shallower MLD and there appears to be a shift in the slope of the relationship (Fig. A.5). With a continuous time series, one might reasonably interpret this non-linear relationship as reasonable, but given that the shift is associated with two different models, it seems more likely that the pattern is an artifact of the model discontinuity.

A.1.3   Other models
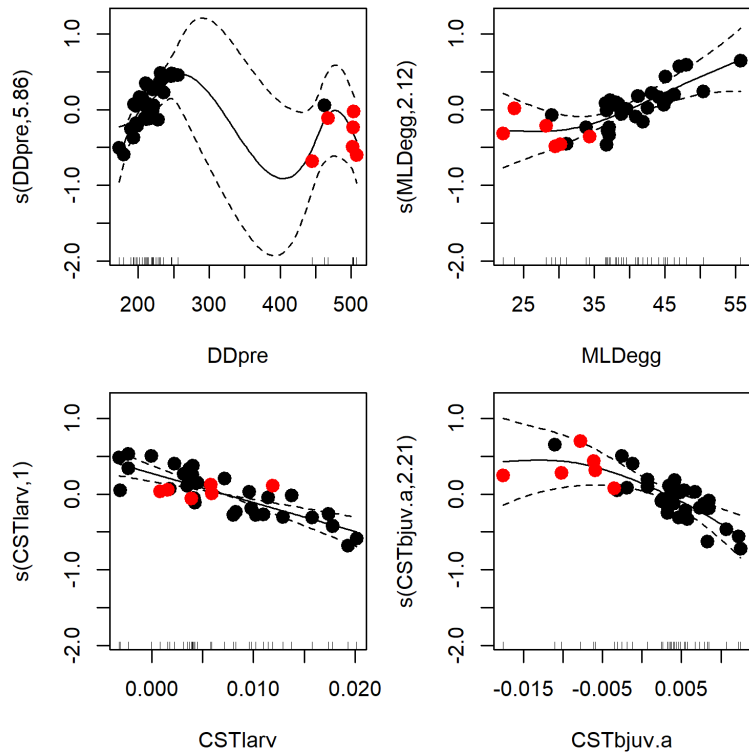
For DDpre, the 2011+ data are much "warmer" and in a different part of the graph, with the exception of one earlier period data point for DDpre (Fig. A.5). For DDpre, the convex shape of the relationship would make some sense if there were no obvious shifts in temperature between time periods. Temperature typically impacts growth and survival for many fishes with an optimal temperature and declining performance in either warmer or colder waters. However, given the discontinuity between with the 2011+ data being warmer (Fig. A.1), it seem more likely that this result is an artifact of the different ROMS models and not a biological one.

A.2   Replacing ROMS predictors with observed variables

Because of the difficulties with the updated ROMS outputs, we also examined replacing specific ROMS predictors with observed variables or variables derived from observations, like the cumulative upwelling index.

A.2.1   West Coast Groundfish Bottom Trawl Survey (WCGBTS) bottom temperature data

In addition to bottom trawls for groundfish biomass and biological data, the WCGBTS (Keller et al. 2017) collects environmental data like bottom temperature. The survey time series begins in 2003, covers

Figure A.5: Smooths from the four-factor GAM. Black points are 1981-2010. Red points are 2012-2018. Numbers in parentheses on the y-axis are the estimated degrees of freedom where edf = 1.0 suggests a linear relationship.

approximately 50 - 1200 m, and is conducted from May to October. This time period overlaps with the preconditioning period for petrale sole (Haltuch et al. 2020) suggesting that directly observed bottom temperature might be used to replace the DDpre term from the ROMS model.

Bottom temperature (btemp) from the WCGBTS was averaged for each year for May - October and then lagged one year to match the pre-conditioning year (btemp_pre). This lagging sets the available observed time series at 2004-2022. Degree days was also calculated as bottom temperature minus the reference temperature of 3.5 °C and averaged for each year. Normally one would sum degree days, but it was averaged here due varying samples sizes each year and multiple observations each year. Estimated this way degree days (btemp_DDpre) is essentially the same as btemp_pre but 3.5 degrees °C lower. The resulting time series are shown in Figure A.6 along with DDpre and Tpre.a from the ROMS output for comparison. Interestingly, there were no significant correlations between the ROMS predictors and observed bottom temperature data whether compared across 2004-2022 or when separated by time period (2004-2010, 2011-2022) (Fig. A.6).

A.2.2 Cumulative upwelling index (CUTI)

The negative correlation with cross-shelf transport during the larval and benthic juvenile stages seen by Haltuch et al. (2020) indicates that recruitment is better when there is offshore transport in surface waters. This condition implies that better recruitment may correlate with upwelling either due to some transport-related interaction or better productivity during upwelling conditions leading to better feeding conditions. Therefore, CUTI was examined as a potential replacement for CSTlarv and CSTbjuv.a by averaging daily values for December-May and April-October, respectively (Fig. A.7).

Cross-shelf transport and CUTI were correlated during the larval stage (Fig. A.8a, r = -0.68, p < 0.001), but not during the benthic juvenile stage Fig. A.8b, r = 0.01, p = 0.972).

A.2.3 Fitting new models
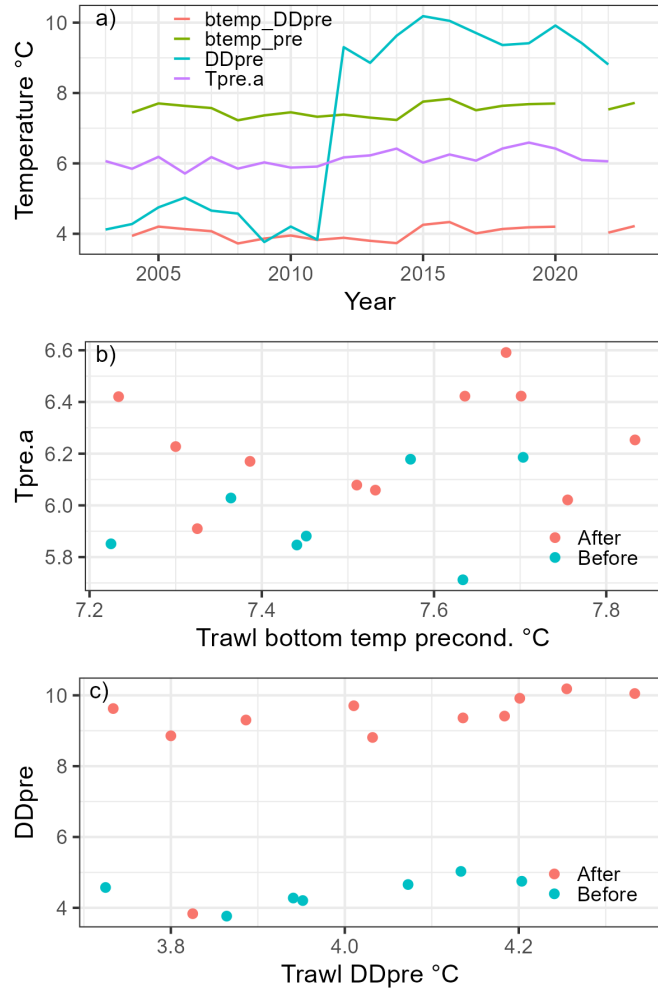
Although correlations between the ROMS variables in the best-fit model from Haltuch et al. (2020) and observed ocean temperature and the CUTI time series were weak, these new variables were used to fit the following model:

Recruitment deviations = btemp_pre + cuti_larv + cuti_juv
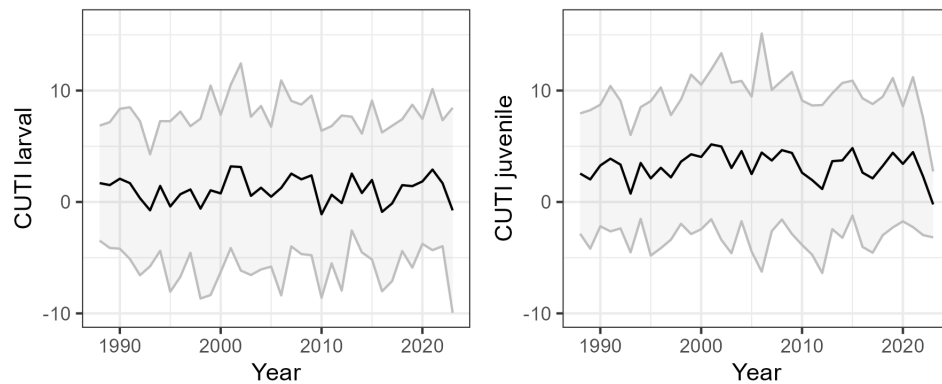
This model explained only 12% of the variance and was non-significant (p = 0.7). The model did capture some trends in recruitment deviations (Fig. A.9) but missed both high and low recruitment events, suggesting that while it might be improved, but the relationship does not seem valuable at present.

A.2.4 Basin scale predictors
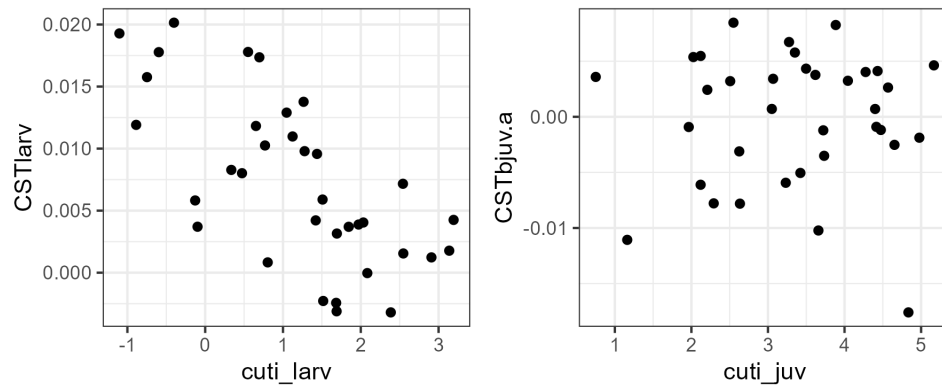
The Ecosystem Status Report from the California Current Integrated Ecosystem Assessment reports several basin-scale indicators as indicative of environmental conditions along the west coast of the USA (Harvey 2022). These indicators include the Ocean Niño Index (ONI), Pacific Decadal Oscillation (PDO) index, and the North Pacific Gyre Oscillation (NPGO) index. These indicators were tested here to determine whether they could be used as the basis of an environmental index of petrale recruitment. The Coastal Upwelling Transport Index (CUTI) was also included as a measure of large scale cross-shelf transport for the basin. Indices were averaged for the spring (April-June) and summer (July-Sept). The ONI, PDO, and NPGO were
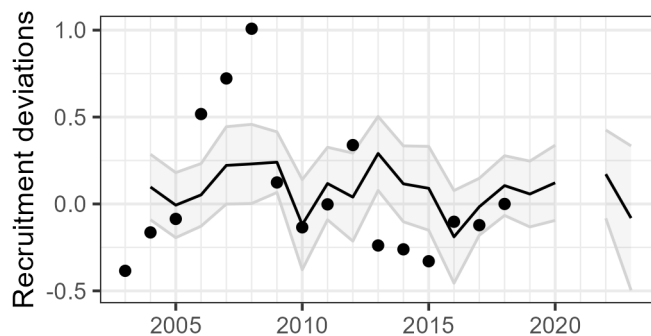
Figure A.6: Relationships between observed temperature from the trawl survey (WCGBTS) and modeled ROMS variables. (a) time series of observed bottom temperature during the preconditioning period (btemp_pre), observed degree days during the preconditioning period (btemp_DDpre), DDpre, and Tpre.a, (b) correlation between Tre.a and trawl bottom temperature, and (c) correlation between DDpre and trawl bottom temperature. There were no significant correlations between observed bottom temperature data and modeled ROMS variables whether tested across both time periods (2004-2022, extent of the trawl data) or separated by ROMS time periods (2004-2010 and 2011-2022, $p > 0.05$ in all cases).

Figure A.7: Cumulative upwelling indices (CUTI) calculated for the larval and benthic juvenile stages. Error envelopes indicate 1.0 s.d.
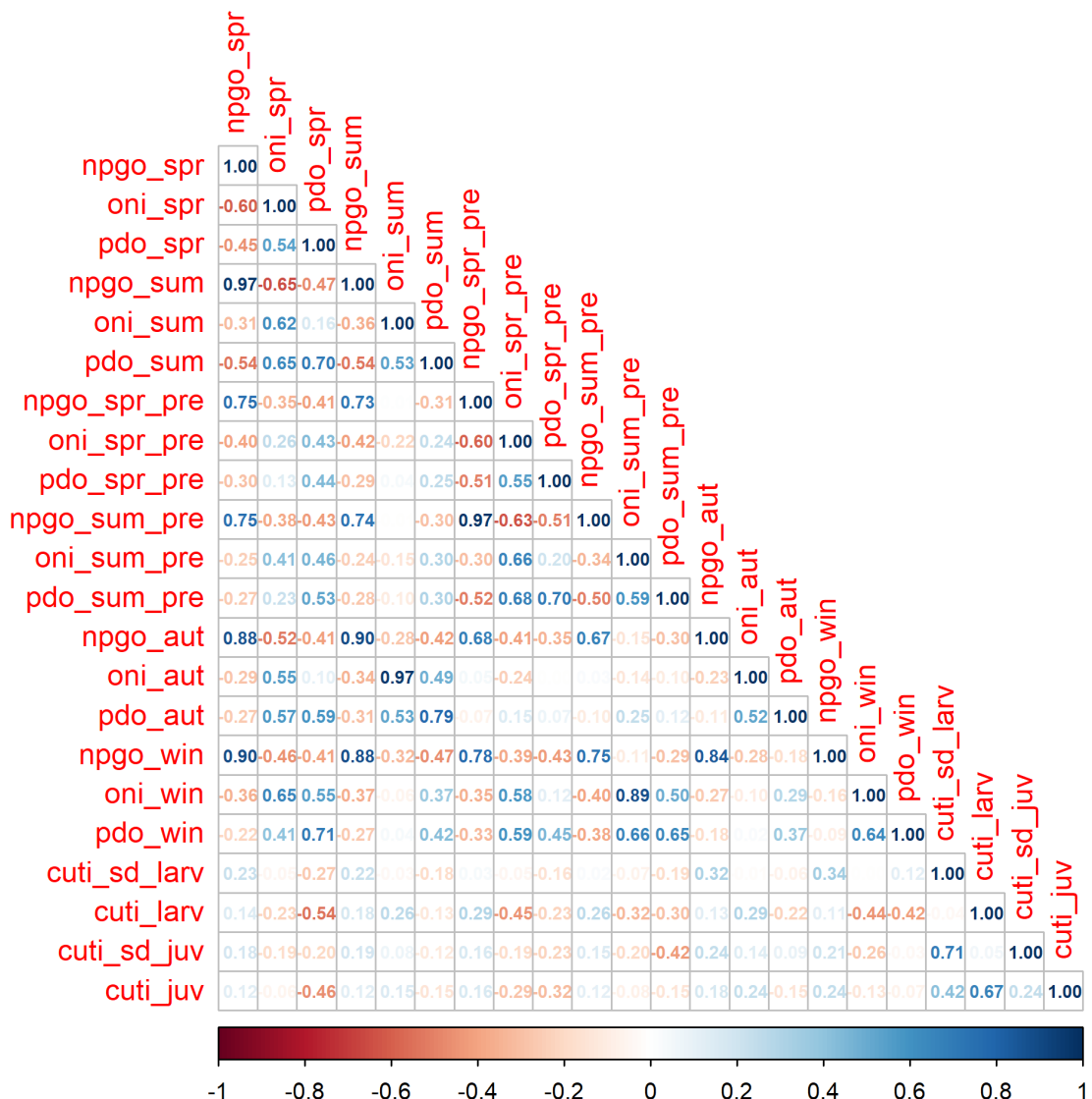
Figure A.8: Relationships between CUTI and ROMS variables.

Figure A.9: Model fit for the bottom-temperature and CUTI predictors. Points are the recruitment deviations from the 2019 stock assessment; line is the predicted fit with standard error. Note that there is no prediction for 2021 because there was no bottom trawl temperature data in 2020, which was necessary for calculating btemp_pre.

also lagged to the pre-conditioning year for females because prior analyses (Haltuch et al. 2020) suggested that climate in the form of degree days was important during the pre-conditioning period (May-October).

Model selection (delta AIC < 2.0 and fewest parameters, Burnham and Anderson (1998)) was then used to select the best-fit model with the restriction that no model could have more than five predictor variables. Predictors that were correlated (r > 0.75) were excluded from the same model. For example, spring and summer NPGO indices were highly correlated and excluded from the same model (Fig. A.10). See Tolimieri et al. (2018) and Haltuch et al. (2020) for more detail on overall methodology.

Figure A.10: Correlations among basin-scale predictors.

Table A.4: Model selection parameters and coefficients for the models with delta AIC < 2.0. NPGO/npgo = Northern Pacific Gyre Oscillation; ONI/oni = Ocean Nino Index, PDO/pdo = Pacific decadal oscillation; spr = spring; sum = summer; pre = female precoditioning year. The best-fit model is shown in bold.

Intercept	cuti_larv	npgo_aut	npgo_spr_pre	npgo_sum	npgo_sum_pre	oni_aut	oni_spr_pre	pdo_aut	pdo_spr	pdo_spr_pre	pdo_sum_pre	pdo_win	R2	AICc	delta	weight
0.16			-0.28	0.15			-0.29	-0.24		0.14			0.60	12.87	0.00	0.08
0.09			-0.25	0.17			-0.21	-0.2	0.14				0.60	13.05	0.18	0.08
0.09			-0.42	0.15	0.26			-0.2	0.13				0.60	13.39	0.52	0.06
0.08			-0.19	0.17				-0.21	0.12				0.55	13.69	0.82	0.06
0.07			-0.24	0.18			-0.12				-0.13		0.54	13.82	0.94	0.05
0.02			-0.17	0.17			-0.1		0.11		-0.15		0.59	13.87	1.00	0.05
-0.01	0.08		-0.28	0.19			-0.12				-0.11		0.59	13.96	1.09	0.05
-0.04	0.1		-0.50	0.17	0.28		-0.14						0.59	14.00	1.12	0.05
0.13			-0.27	0.18				-0.2					0.49	14.15	1.27	0.04
0.06			-0.19	0.16			-0.11			0.1	-0.19		0.59	14.20	1.32	0.04
0.01		0.14	-0.14				-0.14		0.14		-0.15		0.59	14.21	1.33	0.04
0.09			-0.24	0.16			-0.1	-0.15					0.54	14.25	1.38	0.04
0.07			-0.20	0.18				-0.14	0.13		-0.11		0.58	14.40	1.53	0.04
0.17			-0.22		-0.1		-0.41	-0.29		0.18			0.58	14.51	1.64	0.04
0.03			-0.17	0.21					0.14		-0.17		0.53	14.57	1.70	0.04
-0.04	0.1	0.14	-0.53		0.33		-0.18						0.58	14.59	1.71	0.04
0.15			-0.48	0.17	0.24			-0.19					0.53	14.60	1.72	0.04
-0.06	0.09		-0.24	0.18			-0.14						0.53	14.60	1.73	0.04
0.06			-0.27	0.22		0.08	-0.16				-0.11		0.58	14.64	1.77	0.03
0.11			-0.30	0.16		-0.18	-0.1	-0.14					0.58	14.66	1.79	0.03
0.13			-0.22	0.17				-0.15		0.13	-0.15		0.58	14.73	1.86	0.03
0.15			-0.33	0.18			-0.17	-0.19					0.53	14.84	1.97	0.03

Model selection produced a large number of similarly weighted models. There were 22 models with an AICc < 2.0 (Table A.4). AICc weights for these models were low and relatively similar. Most models included the NPGO during the pre-conditioning spring (npgo_spr_pre), NPGO during the summer of recruitment (npgo_sum), and PDO in the spring of the recruitment year (pdo_spring), while other terms occurred in some model but not all. Because it had the fewest terms and these terms were consistent across all models, the following model was chosen as the best-fit for the basin-scale parameters:

Recruitment deviations ~ npgo_spr_pre + npgo_sum + pdo_spr

Petrale recruitment deviations were negatively correlated with the NPGO in the pre-condition spring and with the PDO in the spring of the age-0 year. Recruitment was positively correlated with the NPGO in the summer of the recruitment year (Table A.5).
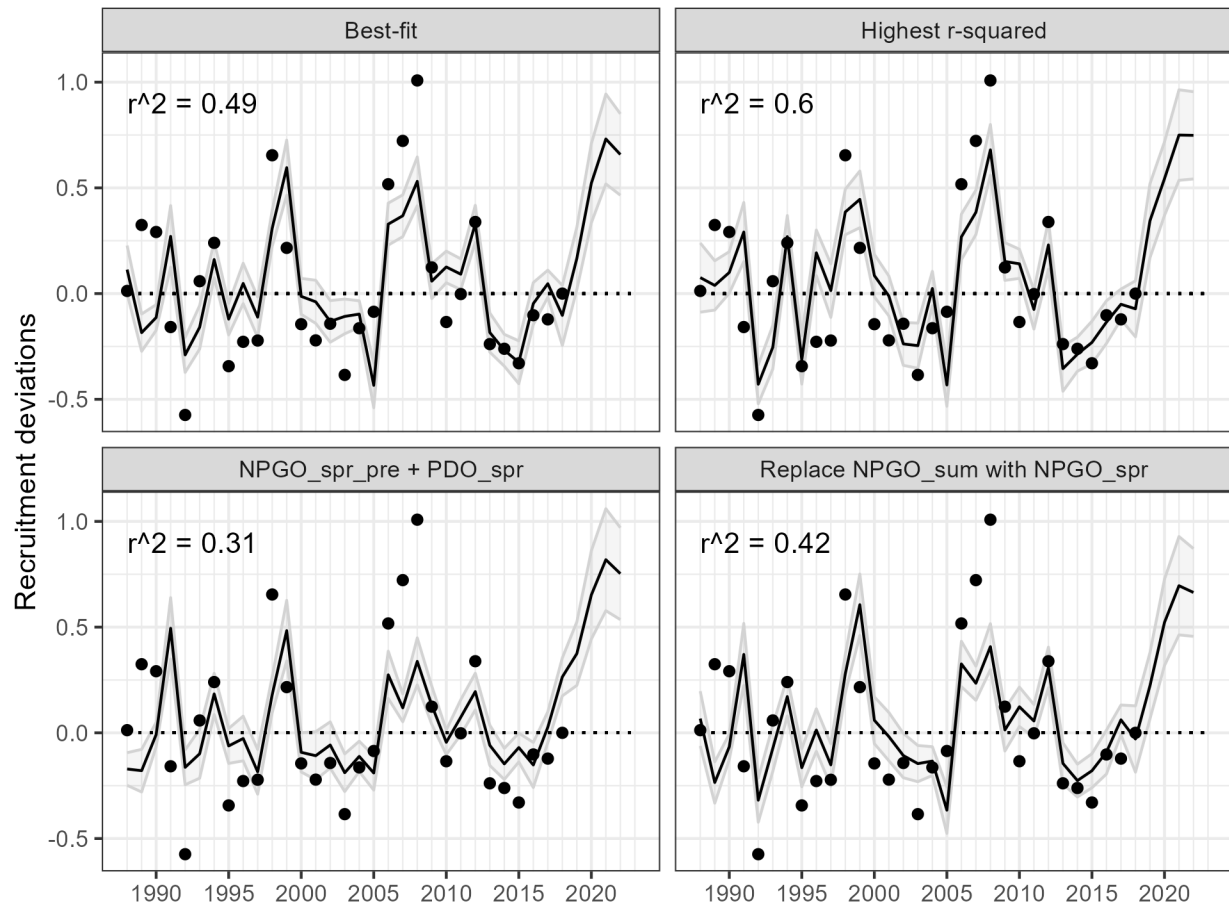
Table A.5: Parameter estimates from the best-fit model using basin scale predictors: ONI, PDO, NGPO, and CUTI. Model $r^2 = 0.49, p < 0.001$. NPGO/npgo = Nothern Pacific Gyre Ossilation; PDO/pdo = Pacific decadal oscillation; spr = spring; sum = summer; pre = female precoditioning year.

Model	Estimate	SE	t-value	p-value
Intercept	0.134	0.058	2.332	0.027
npgo_spr_pre	-0.268	0.065	-4.150	0.000
npgo_sum	0.182	0.059	3.107	0.004
pdo_spr	-0.201	0.070	-2.859	0.008

This basin-scale predictors model explained 49% of the variation in recruitment deviations ($r^2 = 0.49$, p < 0.001, Fig. A.11). The model under-estimated highs and lows in petrale recruitment and predicted increases in recruitment later in the time series. While basin-scale predictors lack direct mechanistic explanations (compared to the ROMS predictors) and there are always concerns about the non-stationarity of relationships between the basin-scale indicators and physical processes, this model does track recruitment well.

For comparison, the predictions and fit for the model with the highest r^2 (and delta AIC < 2.0) are also shown in Figure A.11. This model explained about 11% more variance (Table A.4) and did a better job of matching the higher and lower recruitment (as one would expect from a model with more terms). These results suggest that the three-term model is generally good at capturing variation in petrale recruitment but that other drivers impact the more extreme recruitment that the base mode either over or under predicts.

From a stock assessment context, the inclusion of the npgo_sum term (Table A.5) is a problem since the index would be available until the end of September at the earliest, causing the index to be a year behind the assessment. Removing the npgo_sum (and npgo_spr) term explained less variance but the model was also significant ($r^2 = 0.31$, p = 0.006)(Fig. A.11). However, the spring and summer NPGO are highly correlated (r = 0.97, Fig. A.10). Therefore, the best-fit model was re-run replacing npgo_sum with npgo_spr. This model explained slightly less variation in recruitment than the best-fit model but performed well overall ($r^2 = 0.42$, p = 0.002) (Fig. A.11).

Figure A.11: Model fits for different models using the basin-scale predictors. NPGO = North Pacific Gyre Oscillation; PDO = Pacific Decadal Oscillation; spr = April=June; sum = July-September; pre = pre-conditioning year. Line is the predicted fit with standard error; Points are the recruitment deviations; dotted line indicates the zero recruitment deviation for reference.

A.3 Copernicus Marine Environment Monitoring Service (CMEMS) Oceanographic Products

Given the difficulties with the combined ROMS analyses across 2010/2011, we also investigated alternative oceanographic model products produced by Copernicus Marine Environment Monitoring Service (CMEMS) (https://marine.copernicus.eu/) and Mercator Ocean International (MOI) (https://www.mercator-ocean.eu/) to test if this modelling framework could be used to produce an environmental index of petrale recruitment.

We combined two CMEMS products: the Global Ocean Reanalysis and Simulation (GLORYS12V1: GLOBAL_MULTIYEAR_PHY_001_030, https://doi.org/10.48670/moi-000211) (Fernandez and Lellouche 2018; Jean-Michel et al. 2021; Drevillon et al. 2022) and the Copernicus Marine global analysis and forecast (CMGAF, GLOBAL_ANALYSISFORECAST_PHY_001_024; https://doi.org/10.48670/moi-00016) (Le Galloudec et al. 2022). The data are served by the Copernicus Marine Service (https://marine.copernicus.eu/). When downloaded the data covered: GLORYS: 1993-01-01 to 2020-10-31 and CMGAF: 2020-11-01 to 2023-06-01. Note both the reanalysis and the analysis and forecast walk forward in time. For the CMGAF, time series are updated at regular intervals beginning with a daily forecast and hindcast simulation, and a weekly 'hindcast-best analysis' with data assimilation through -15 days (Le Galloudec et al. 2022).

Overall the CMEMS analysis followed Tolimieri et al. (2018) and Haltuch et al. (2020). More specifically, data for water column temperature, bottom temperature, and mixed-layer depth were downloaded as daily values for 40-48 °N and processed as follows for each life-history-stage predictor:

1. Subsetted data by bottom depth, mixed-layer depth, and distance from shore as relevant (see Table A.1)
2. Calculated the daily average
3. Subsetted #2 by the relevant time periods (months in Table A.1)
4. Calculated the annual average (or sum for degree days) for 1993-2023 for that potential predictor
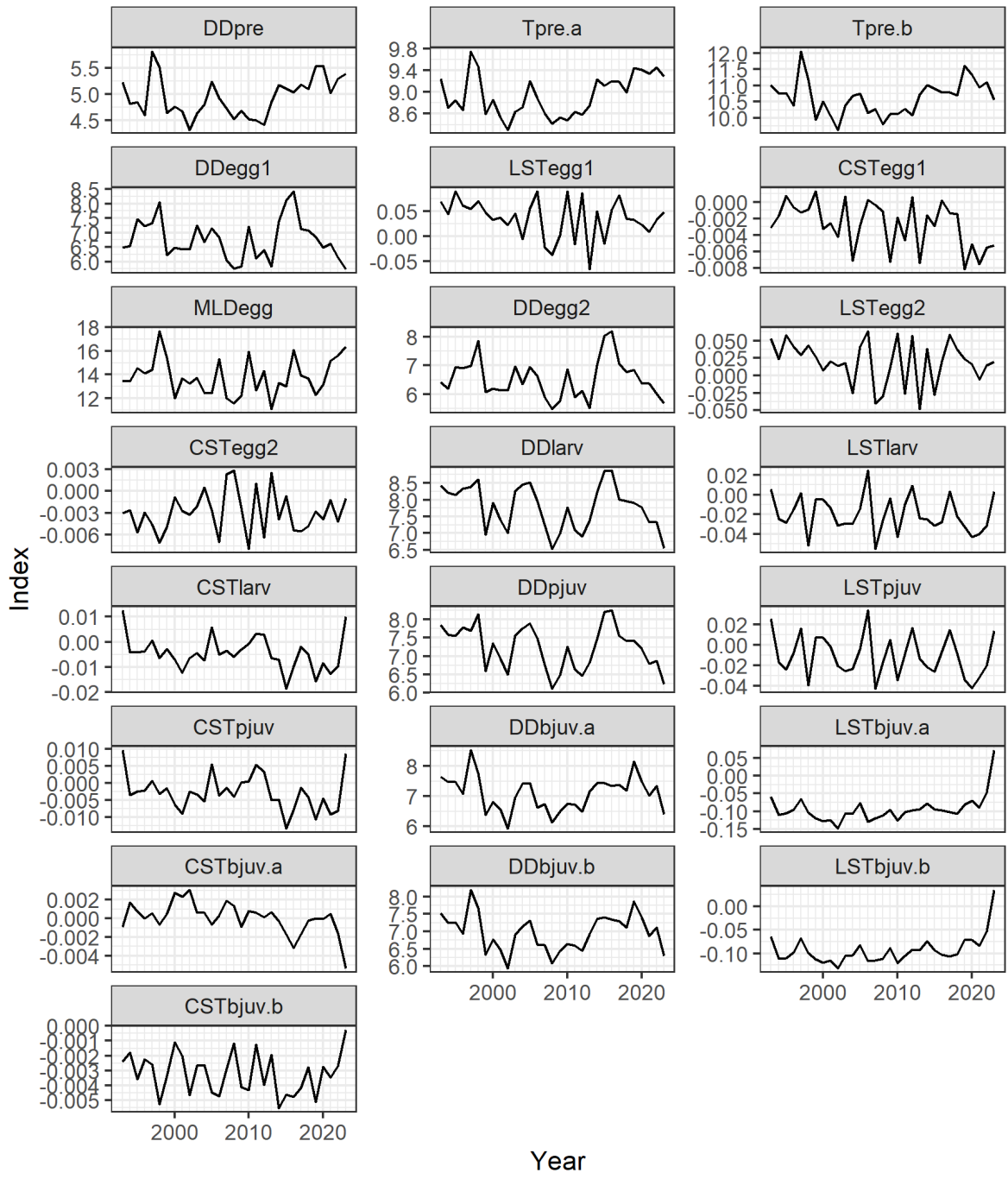
For transport variables, monthly means from the CMEMS models were used to reduce processing time but followed the same overall model selection process as as above. Overall, the combined CMEMS time series did not show obvious break points from 2020 to 2021 (Fig. A.12).

Model selection followed Tolimieri et al. (2018) and Haltuch et al. (2020). Briefly, CMEMS predictors were pre-screened for correlations among variables and non-linear relationships with petrale recruitment deviations. Correlated predictors (r >= 0.75, Fig. @ref(fig: glorys-correlations)) were excluded from the same model. Non-linearity for individual terms was evaluated by comparing the linear model to a model including both the linear and quadratic forms of the predictor. If the AICc of the quadratic form was lower, we included the quadratic form as a potential predictor as well, but required that the linear term appear in models that included the quadratic from.
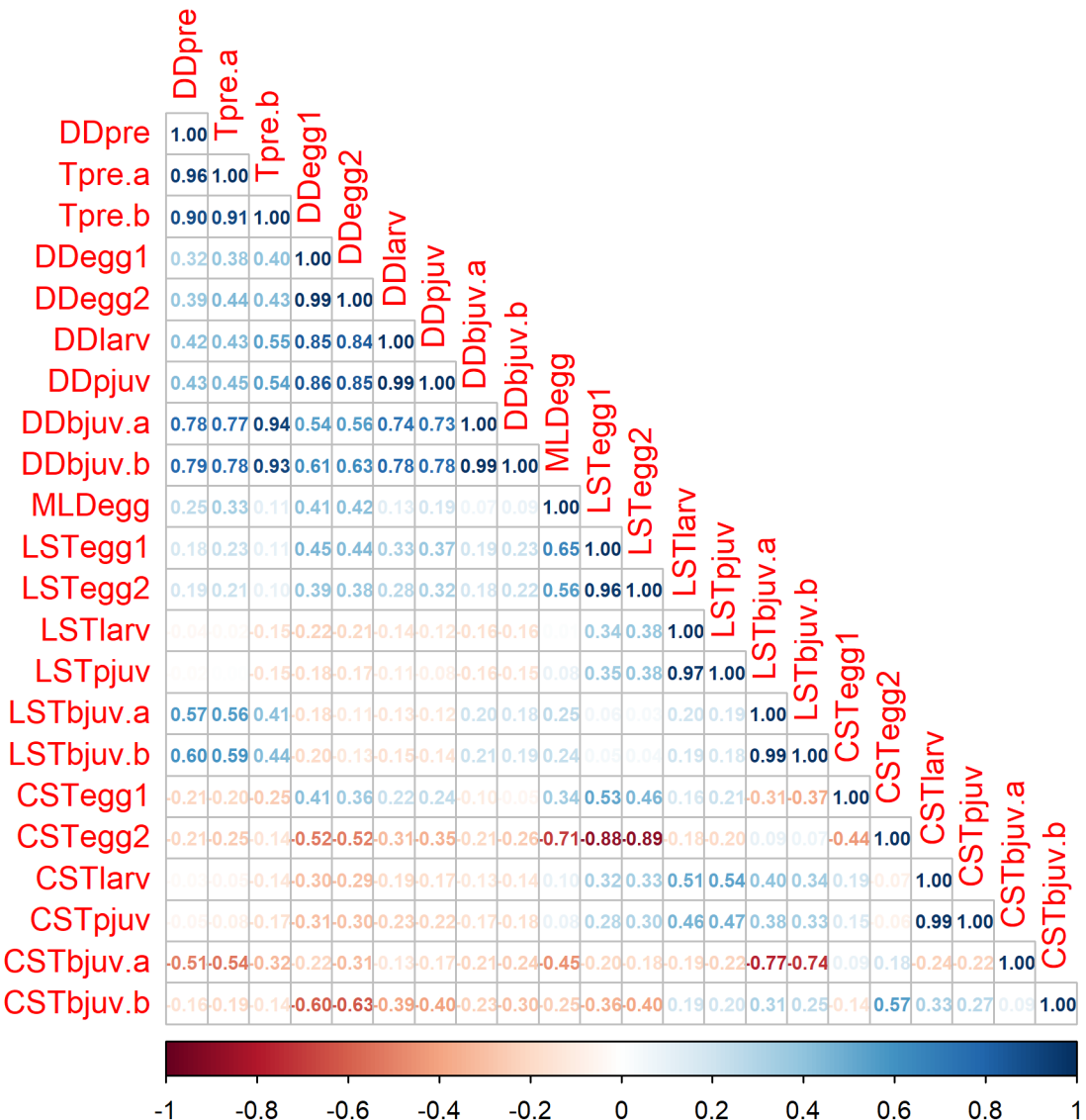
Model selection was carried out using the 'dredge' function in the MuMIn package in R (R Core Team (2023), Bartoń (2023)). Candidate models were evaluated based on their delta AIC and number of predictors.

A.3.1 Results

Only two candidate models had delta AICc values of 4.0 or less; only one model had a delta AICc of less than 2.0. (Table A.6). The best-fit model included degree days during the pelagic juvenile period (DDpjuv)

**Figure A.12:** Time series of processed CMEMS indicators used in the model fitting.
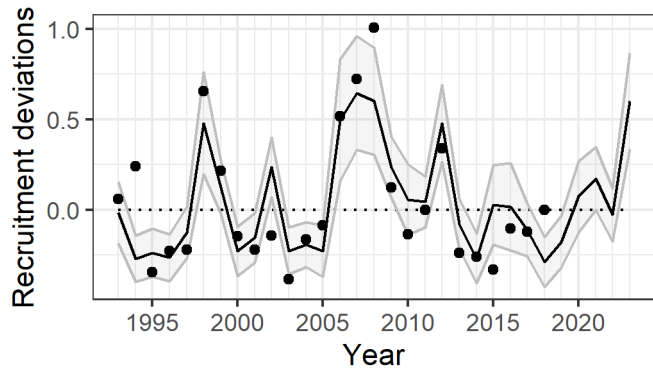
Figure A.13: Correlations between CMEMS time series. DD = degree days, T = temperature, MLD = mixed-layer depth, LST = longshore transport, CST = cross-shelf transport, pre = female precondition period prior to spawning, egg = egg stage, larv = larval stage, pjuv = pelagic juveniles, bjuv = benthic juveniles.

in both its linear and quadratic form, and long-shore transport (LSTlarv) in the larval stage (Table A.6).

Table A.6: Terms and coefficients for the candidate models with a delta AIC value of 4.0 or less. DD = degree days; LST = longshore transport, larv = larval stage, pjuv = pelagic juveniles.

Int	DDpjuv	DDpjuv2	LST-larv	LST-larv2	LST-pjuv	LST-pjuv2	r^2	AICc	delta	weight
24.859	-6.683	0.446	15.776	474.695	NA	NA	0.683	6.014	0.000	0.87
26.754	-7.212	0.480	NA	NA	5.958	471.358	0.633	9.820	3.805	0.13

This best-fit model explained 68% of the variance in the petrale recruitment deviations from 1993-2018 (Fig A.14) and generally captured the peaks and lows in the recruitment deviations well. Predictions of potential petrale recruitment through 2023 are included in Figure A.14. However, the model did over-predict recruitment in 2015 during the large marine heatwave off the us west coast. When predicted through 2023, this index suggests strong incoming recruitment equivalent to historical highs during the 2006-2008 period.
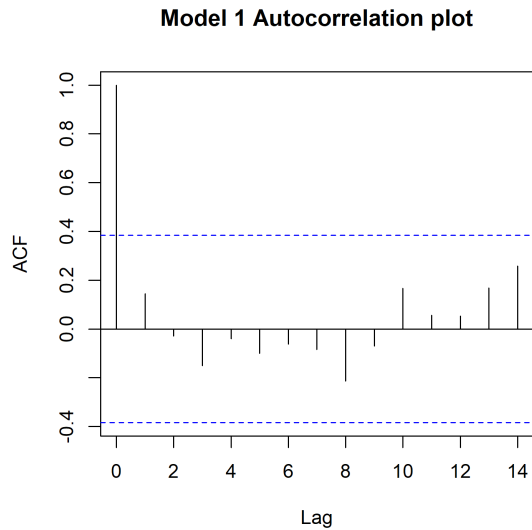

Figure A.14: Relationship between recruitment deviations from the 2019 assessment and the MOI index for 1993-2018 and predictions for 2019-2023. Points are the recruitment deviations from the assessment; solid like is the MOI environemental index of recruitment, and grey envelope represents 95 confidence intervals.

A.3.2   Model diagnostics and testing

Model diagnostics and testing followed Tolimieri et al. (2018) and Haltuch et al. (2020). Model testing was carried out to determine how stable the best-fit model was to both individual years and the precision of the estimates of recruitment deviations. Tests included:

1. Boot-strap analysis on the best-fit model was used to estimate bias
2. Jackknife analysis on the best-fit model was used to determine the impact of individual years on the model fit.
3. Refit the best-fit model using data for 1993-2013 and then predict 2014-2018.
4. Recruitment deviations were re-sampled 1000 times from a log-normal distribution to evaluate the impact of the precision of these estimates on the fit of the best-fit model.
5. Individual years were jackknifed and then the entire model selection process was rerun to determine the impact of individual years on the selection of the predictors in the best-fit model.
6. Recruitment deviations were re-sampled 100 times and the entire model selection process rerun to evaluate the impact of the precision of these estimates on the predictors included in the best-fit model.

A.3.2.1 Diagnostics for the best-fit model There was no obvious autocorrelation in the residuals (Fig. A.15). Diagnostic plots did suggest some under-prediction when recruitment deviations were high (Fig. A.16.


Figure A.15: Autocorrelation plot for the best-fit model.
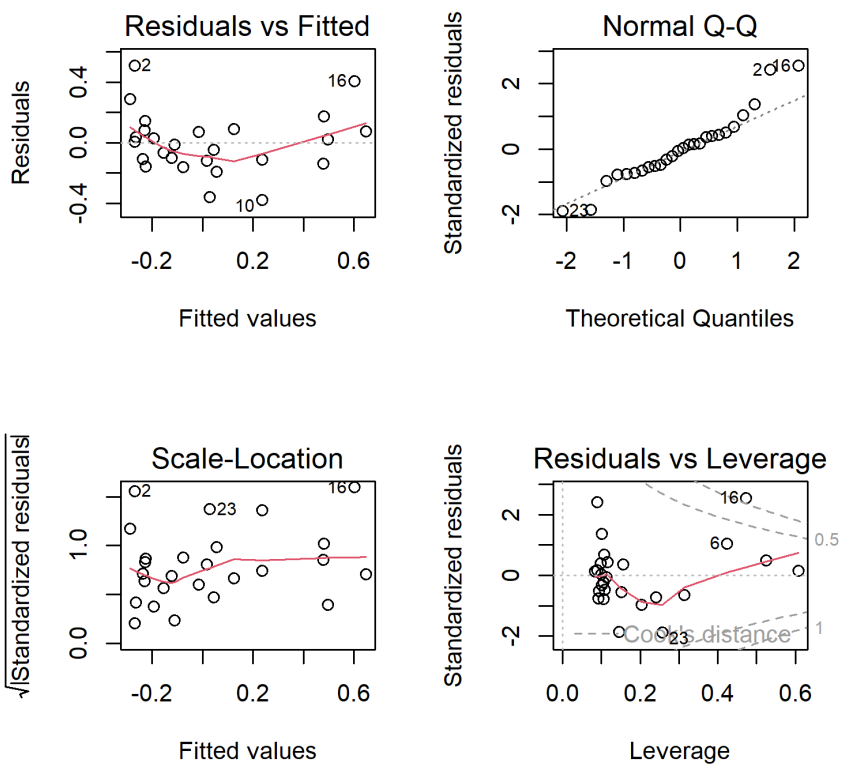
A.3.2.2 Model testing Bias (estimated from bootstrap analysis with 1000 bootstraps) was generally low (Table A.7) at around 5-15% of the scaled coefficient with the exception of LSTlarv, which had a small impact overall on the model relationship (standardized coefficient of -0.028.

Table A.7: Standardized coefficients and estimates of bias from 1000 bootstraps. DD = degree days; LST = longshore transport, larv = larval stage, pjuv = pelagic juveniles.
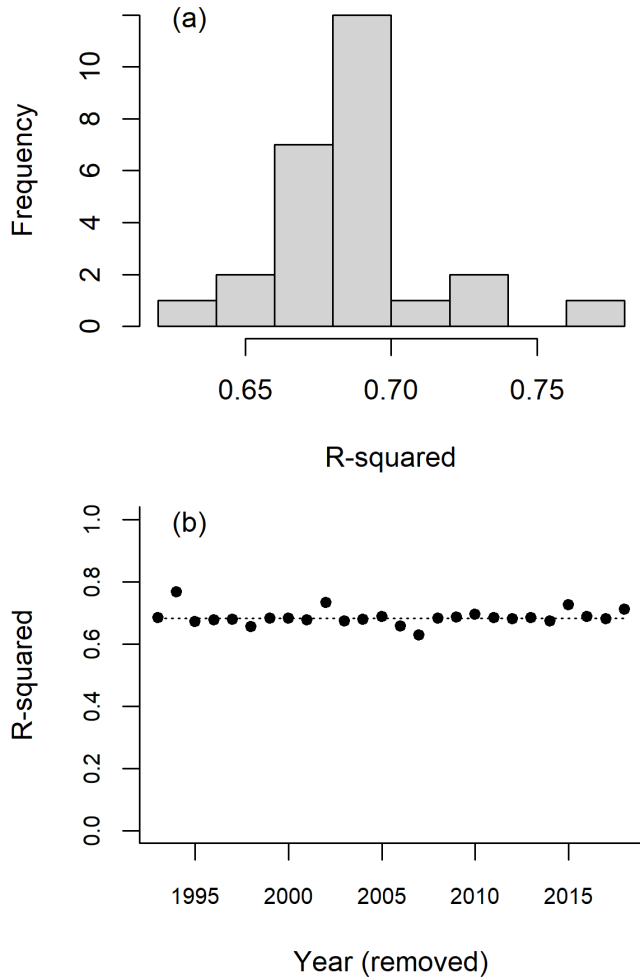
Predictor	Coefficient	Bias	SE	Std Coef	Std Bias	Std SE
tercept	24.859	-1.930	11.363	-0.288	0.016	0.074
DDpjuv	-6.683	0.506	3.134	-0.096	0.015	0.060
LSTlarv	15.776	-0.448	4.352	-0.028	0.011	0.051
DDpjuv^2	0.446	-0.033	0.215	0.163	-0.014	0.076
LSTlarv^2	474.695	-27.744	124.598	0.167	-0.010	0.052

Jackknifing the best-fit model by year (removing individual years and refitting the best-fit model) did not show strong effects of individual years on the fit of the model (Fig. A.17) with the majority of r^2 values falling between 0.65 and 0.70.
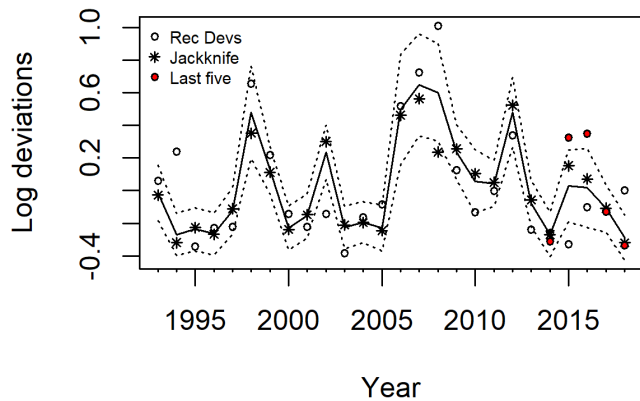
Predictions of individuals years from the jackknife analysis fell largely along the same trend as for the best-fit model and within the 95% confidence limits (Fig. A.18). Prediction 2014 to 2018 based on refitting the best-fit model to data for 1993-2013 captured the last five years relatively well, although estimates for 2015 and 2016 were high (Fig. A.18).

**Figure A.16:** Diagnostic plots for the best-fit model.

Figure A.17: Results of jackknife re-fitting of the best-fit model to evaluate the impact of individual years on the model fit.


Figure A.18: Fit of the best-fit model to the recruitment deviations from the 2019 petrale asessment. Solid line is the predicted fit and dashed lines are the 95% confidence limits. Open circles are the log recruitment deviations from the 2019 assessment. Stars are predicted values from jackknife analysis removing individual years one at a time. Red points are predictions from fitting best-fit model to 1993-2013 and then predicting 2014-2018.

To examine the impact of the precision of the estimate of recruitment deviations on the fit of the best-fit model, recruitment deviations were re-sampled from a log-normal distribution using the estimate and standard error for each year and the model refit. This procedure was completed 1000 times. The performance of the best-fit model was fairly stable (Table A.8). The mean r^2 for the across all 1000 iterations was $r^2 = 0.567$ with a lower 95% quantile of $r^2 = -6.602$.

Table A.8: Results of resampling recruitment deviations and refitting the best fit model 1000 times. Best-fit = best-fit model; Mean = mean values over the 1000 refits, median = median values over the 1000 refits; and 2.5 and 97.5 confidence intervals. DD = degree days; LST = longshore transport, larv = larval stage, pjuv = pelagic juveniles.

Term	r^2	Int	DDpjuv	DDpjuv^2	LST-larv	LSTlarv^2	p
Best-fit	0.683	24.859	-6.683	0.446	15.776	474.695	0.000
Mean	0.567	24.572	-6.602	0.440	15.791	474.485	0.005
Median	0.573	24.554	-6.596	0.441	15.781	475.272	0.001
2.5%	0.385	11.931	-9.792	0.194	10.321	367.356	0.000
97.5%	0.737	35.892	-3.061	0.662	21.215	576.199	0.031

Jackknifing years and re-running the entire model selection process also produced stable results (Table A.9). DDpjuv and LSTlarv occurred in the 23 and 24 (0 respectively) of the top model across the 100 jackknifes. CSTegg1 and DDegg1 each occurred in three models, while MLDegg and its quadratic form occurred in two.

Table A.9: Result of jackknifing individual years and re-running the model selection process. The results are the number of times a predictor appeared in the model with the lowest AICc in each iteration of the re-selection. DD = degree days; T = temperature; MLD = mixed-layer depth, LST = longshore transport, CST = cross-shelf transport; egg = egg stage, larv = larval stage, pjuv = pelagic juveniles.

Predictor	Number
CSTegg1	3
DDegg1	3
DDpjuv	23
DDpjuv^2	23
LSTlarv	24
LSTlarv^2	24
MLDegg	2
MLDegg^2	2

A similar analysis was conducted in which recruitment deviations were re-sample from a log-normal distribution and the entire model selection process was rerun to determine how the variability in recruitment estimates might impact the overall model selection process. LSTlarv and DDpjuv and their quadratic terms were included in at least 79% of the refits (Table A.10). The two linear terms alone appeared in 90% (LSTlarv) and 85% (DDpjuv) of models, providing strong support for stability these terms in relation to the precision of estimates of recruitment deviations.

Table A.10: Result of resampling recruitment deviations and completing the model selection process 100 times. The results are the number of times a predictor appeared in the model with the lowest AICc from each re-dredging iteration. DD = degree days; T = temperature; MLD = mixed-layer depth, LST = longshore transport, CST = cross-shelf transport; pre = female preconditioning stage; egg = egg stage, larv = larval stage, pjuv = pelagic juveniles, bjuv = benthic juveniles.
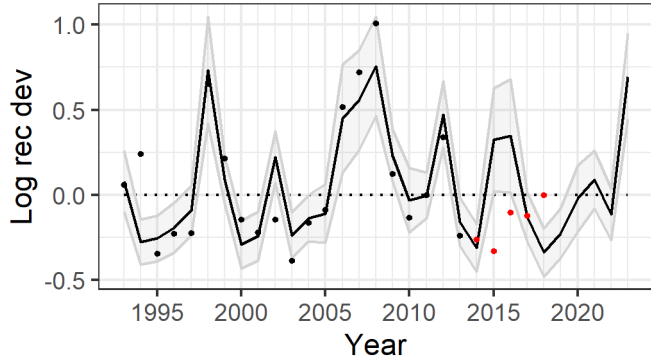
Predictor	No. models	No jackknifes
CSTbjuv.a	6	4
CSTbjuv.b	1	1
CSTegg1	59	33
CSTegg2	6	5
CSTlarv	1	1
CSTpjuv	1	1
DDbjuv.a	2	2
DDbjuv.b	1	1
DDegg1	48	39
DDegg2	18	18
DDlarv	26	22
DDpjuv	85	61
DDpre	7	6
$CSTegg2^2$	6	5
$DDpjuv^2$	79	56
$LSTlarv^2$	87	68
$LSTpjuv^2$	26	26
$MLDegg^2$	45	27
LSTbjuv.a	0	0
LSTbjuv.b	1	1
LSTegg1	1	1
LSTegg2	0	0
LSTlarv	90	69
LSTpjuv	31	30
MLDegg	45	27
Tpre.a	7	4
Tpre.b	8	5

Finally, the data were subset to 1993-2013 and the entire model selection process was re-run. The resulting best-fit model included the same terms as for the full analysis. This 1993-2013 model was then used to predict petrale recruitment deviations through 2023. The overall fit of the model though 2013 was high ($r^2 = 0.78$) (Fig. A.19). However, like the best-fit model, it over-predicted recruitment for 2015 and 2016 during the height of the marine heatwave, suggesting that some fundamental dynamics may have shifted during this period.

A.4 Distribution and abundance of juvenile petrale

Tolimieri et al. (2020) used spatio-temporal models to examine the distribution and abundance of 13 species of juvenile fishes along the West Coast. Those results are updated here following Tolimieri et al. (2020) but using the 'sdmTMB' package (Anderson et al. 2022a) for R instead of the 'VAST' package (Thorson 2019).

Data come from the West Coast Groundfish Bottom Trawl Survey (WCGBTS)(Keller et al. 2017) for
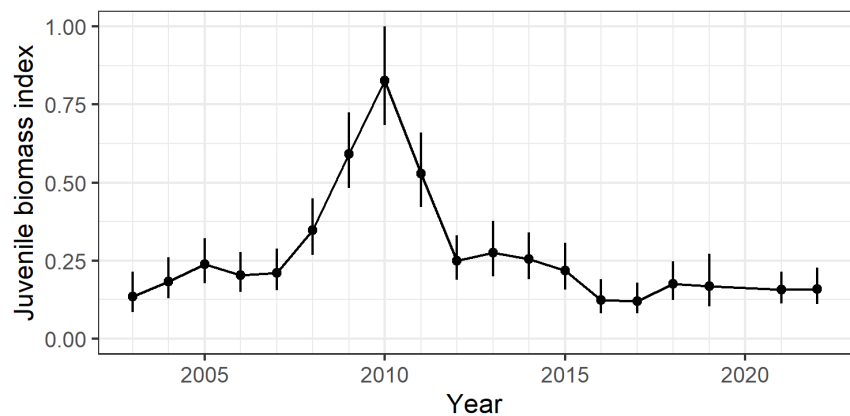
Figure A.19: Fit of the best-fit model from the 1993-2013 analysis and predictions through 2023. Black line is the model prediction with 95% confidence limits. Black points are the recruitment deviations used in the model development; red points are future recruitments.

2003-2022. There are no data for 2020 as COVID restrictions prevented the survey from being completed. The individual biomass data contain estimates of age, length, and biomass for subsamples of each haul and occasionally data for the entire haul when catch is low. There is length information (cm total length) for all individuals in the subsample but many individual fishes lack weight or age data due to time-constraints in the field. To expand the subsample, the following procedure was followed:
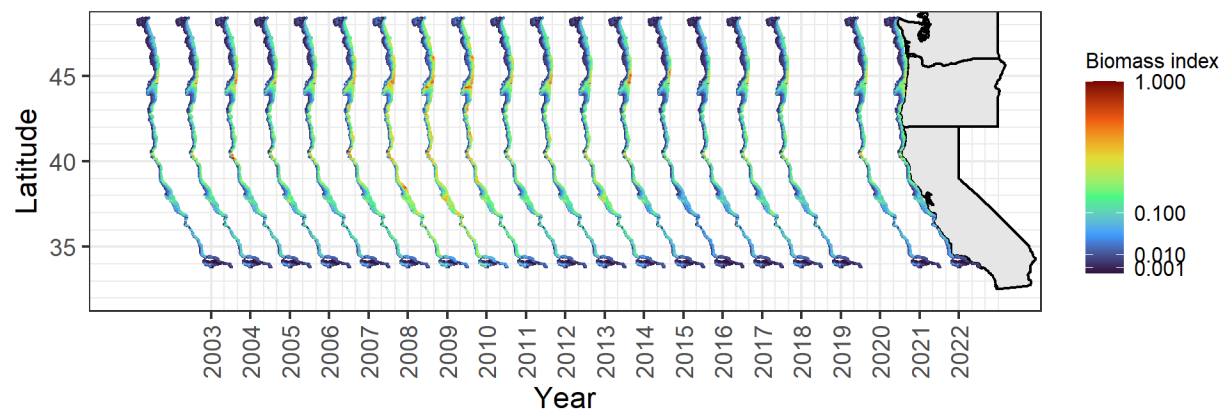
1. Missing weights for individuals in the subsample were estimated by first estimating the length-weight relationship from existing data and using this relationship to estimate the missing weights.

2. Individual fish were allocated to age classes following Tolimieri et al. (2020) by using length-age relationships from the WCGBTS data to determine age-class maximum lengths. See Tolimieri et al. (2020) for more detail. The maximum lengths used here were taken from Tolimieri et al. (2020). Maximum length was 21 cm total length, and depth ranged from 50-200 m. Based on otolith analyses, these fish would be age-1 and age-2 fishes. Thus, these results do not represent recruitment but juvenile abundance several years later.

3. The proportional biomass of juveniles in each subsamble was calculated and used to estimate the total biomass of juvenile fishes in the full trawl.

The juvenile biomass index was low in recent years (Fig. A.20), which does not match up with the predictions of recruitment from the basin-scale models. Observed modeled recruitment deviations from the 2019 assessment and the observed juvenile biomass in the trawl survey do not align either. Juvenile abundance for petrale was highest in the 2008-2011 time period (Fig. A.20) with high densities just south of 45°N and moderate abundance to the south until about 37 °N. This period of high abundance followed several strong recruitment events from 2006-2008 (Fig. A.14) suggesting a 2-3 year delay between recruitment events and when they are observed in the trawl survey, which is consistent with the age of the fishes in the trawl survey. This delay would also function to reduce the correlation between the recruitment deviations from the assessment and observed abundance of agee-1 and age-2 petrale since the index in Figure A.20 integrates several age classes.

Age-1 and age-2 petrale were widely distributed from 35 to 46 °N during the period of high abundance from 2008-2011 (Fig. A.21). Abundance was highest around the bank system at approximately 44 °N, even in years of lower abundance.

**Figure A.20:** Index of juvenile abudance from the species distribution modeling.

Figure A.21: Distribution juvenile petrale sole along the West Coast from 2003-2022 from the species distribution modeling.